



2015

## SELECTIVE TRIPODAL TITANIUM SILSESQUIOXANE CATALYSTS FOR THE EPOXIDATION OF UNACTIVATED OLEFINS

Sarah M. Peak

University of Kentucky, [speak0@yahoo.com](mailto:speak0@yahoo.com)

[Right click to open a feedback form in a new tab to let us know how this document benefits you.](#)

---

### Recommended Citation

Peak, Sarah M., "SELECTIVE TRIPODAL TITANIUM SILSESQUIOXANE CATALYSTS FOR THE EPOXIDATION OF UNACTIVATED OLEFINS" (2015). *Theses and Dissertations--Chemistry*. 52.

[https://uknowledge.uky.edu/chemistry\\_etds/52](https://uknowledge.uky.edu/chemistry_etds/52)

This Doctoral Dissertation is brought to you for free and open access by the Chemistry at UKnowledge. It has been accepted for inclusion in Theses and Dissertations--Chemistry by an authorized administrator of UKnowledge. For more information, please contact [UKnowledge@lsv.uky.edu](mailto:UKnowledge@lsv.uky.edu).

## **STUDENT AGREEMENT:**

I represent that my thesis or dissertation and abstract are my original work. Proper attribution has been given to all outside sources. I understand that I am solely responsible for obtaining any needed copyright permissions. I have obtained needed written permission statement(s) from the owner(s) of each third-party copyrighted matter to be included in my work, allowing electronic distribution (if such use is not permitted by the fair use doctrine) which will be submitted to UKnowledge as Additional File.

I hereby grant to The University of Kentucky and its agents the irrevocable, non-exclusive, and royalty-free license to archive and make accessible my work in whole or in part in all forms of media, now or hereafter known. I agree that the document mentioned above may be made available immediately for worldwide access unless an embargo applies.

I retain all other ownership rights to the copyright of my work. I also retain the right to use in future works (such as articles or books) all or part of my work. I understand that I am free to register the copyright to my work.

## **REVIEW, APPROVAL AND ACCEPTANCE**

The document mentioned above has been reviewed and accepted by the student's advisor, on behalf of the advisory committee, and by the Director of Graduate Studies (DGS), on behalf of the program; we verify that this is the final, approved version of the student's thesis including all changes required by the advisory committee. The undersigned agree to abide by the statements above.

Sarah M. Peak, Student

Dr. Folami Ladipo, Major Professor

Dr. Dong-Sheng Yang, Director of Graduate Studies

SELECTIVE TRIPODAL TITANIUM SILSESQUIOXANE CATALYSTS FOR THE  
EPOXIDATION OF UNACTIVATED OLEFINS

---

DISSERTATION

---

A dissertation submitted in partial fulfillment of the  
requirements for the degree of Doctor of Philosophy in the  
College of Arts and Sciences  
at the University of Kentucky

By  
Sarah Michelle Peak

Lexington, Kentucky

Director: Dr. Folami Ladipo, Professor of Chemistry

Lexington, Kentucky

2015

Copyright © Sarah Michelle Peak

## ABSTRACT OF DISSERTATION

### SELECTIVE TRIPODAL TITANIUM SILSESQUIOXANE CATALYSTS FOR THE EPOXIDATION OF UNACTIVATED OLEFINS

Regiomic mixture of  $\text{HMe}_2\text{Si}(\text{CH}_2)_3(i\text{-Bu})_6\text{Si}_7\text{O}_9(\text{OH})_3$  (**6**), containing a Si-H group in one of the ligands of the silsesquioxane, was tethered onto a vinyl terminated hyperbranched poly(siloxysilane) polymer via a hydrosilation reaction to generate extremely active catalysts, **P1-8** and **c-P1-8**. The synthesis of **6**, in good yield, was accomplished via hydrosilation of  $\text{CH}_2=\text{CHCH}_2(i\text{-Bu})_7\text{Si}_8\text{O}_{12}$  (**1**) to generate  $\text{CMe}_2\text{Si}(\text{CH}_2)_3(i\text{-Bu})_7\text{Si}_8\text{O}_{12}$  (**3**) followed by the reduction of **3** with  $\text{LiAlH}_4$  to afford  $\text{HMe}_2\text{Si}(\text{CH}_2)_3(i\text{-Bu})_7\text{Si}_8\text{O}_{12}$  (**4**) where the base-catalyzed excision of one framework silicon was employed to generate a regiomic mixture of **6**.

$[\text{Ti}(\text{NMe}_2)\{\text{Et}_3\text{Si}(\text{CH}_2)_3(i\text{-Bu})_6\text{Si}_7\text{O}_{12}\}]$  (**7**),  $[\text{Ti}(\text{NMe}_2)\{\text{HMe}_2\text{Si}(\text{CH}_2)_3(i\text{-Bu})_6\text{Si}_7\text{O}_{12}\}]$  (**8**),  $[\text{Ti}(\text{NMe}_2)\{(i\text{-C}_4\text{H}_9)_7\text{Si}_7\text{O}_{12}\}]$  (**9**) and  $[\text{Ti}(\text{NMe}_2)\{(c\text{-C}_6\text{H}_{11})_7\text{Si}_7\text{O}_{12}\}]$  (**10**) were synthesized via protonolysis of  $\text{Ti}(\text{NMe}_2)_4$  with one equivalent of the trisilanol precursor in order to determine if the presence of isomers would be intrinsically different as compared to the uniformly substituted catalysts. Isomers **8** and **9**, demonstrated lower activity as compared to the uniformly substituted catalysts **9** and **10**, however the isomers still exhibited extremely high catalytic activity for the epoxidation of 1-octene using *tert*-butyl hydroperoxide (TBHP) relative to titanium catalysts used in industry. Additionally, **9**, **10**, **P1-8** and **c-P1-8** were very selective catalysts for the epoxidation of various olefins such as terminal (1-octene), cyclic (cyclohexene or 1-methylcyclohexene), and more demanding olefins (limonene or  $\alpha$ -pinene) employing TBHP as the oxidant. Furthermore, **P1-8** and **c-P1-8** were recyclable with minimal loss of titanium however the catalysts could also be repaired if a loss in activity was observed.

Preliminary epoxidation reactions employing **P1-8** and **c-P1-8** along with hydrogen peroxide ( $\text{H}_2\text{O}_2$ ) as the oxidant were also explored using different solvents. **P1-8** degraded quickly due to the hydrolysis of the titanium from the large amount of water present in the reaction mixture however **c-P1-8** showed activity for the epoxidation of cyclohexene. Finally, regiomic mixture of  $\text{Ti}(\text{NMe}_2)(\text{HS}(\text{CH}_2)_3(i\text{-C}_4\text{H}_9)_6\text{Si}_7\text{O}_{12})$  (**13**), was tethered onto gold nanoparticles

for the conversion of propene to propylene oxide using molecular hydrogen and oxygen. While the catalysts showed low activity under our reaction conditions, numerous improvements can be investigated in order to improve upon the catalysts.

Keywords: Olefin epoxidation; Titanium silsesquioxane; Gold nanoparticles; Heterogeneous catalysis; Immobilized catalysts; Non-activated alkenes

Sarah Peak

July, 21, 2015

SELECTIVE TRIPODAL TITANIUM SILSESQUIOXANE CATALYSTS FOR THE  
EPOXIDATION OF UNACTIVATED OLEFINS

By

Sarah Peak

Dr. Folami Ladipo  
Director of Dissertation

Dr. Dong-Sheng Yang  
Director of Graduate Studies

July 21, 2015

FOR MY FAMILY

## ACKNOWLEDGEMENTS

I would like to take this opportunity express my gratitude to multiple people who have encouraged, aided, and supported me while I have been in graduate school. First and foremost would be my advisor, Dr. Folami Ladipo, who has guided me taught me how to think critically about solutions and not accepting things at face-value. Additionally, Dr. Mark Crocker has been invaluable to my research by allowing me to test my epoxidation trials on the equipment at CAER and providing solid practical advice about my research. I would also like to thank my additional committee members, Drs. Watson and Knuston for all their support over the course of my stay at the University of Kentucky. Thank you to Tonya Morgan who ran the majority of the GC data for me. Her work was instrumental to the research described herein. In addition, I would like to thank Mr. John Layton for his assistance with NMR spectroscopy as well as Dr. Anne LaPointe for her assistance with GPC.

My family and friends also deserves my deepest heartfelt thanks for all their support, love, encouragement, and patience given to me while at UK. Without my family, I would not have been able to accomplish this research and wouldn't be the person I am today. They have taught me that hard-work eventually pays off and that if you are going to start something, you have to finish it to the best of your ability. I cannot express how grateful I am for my families support.

I also need to thank all my colleagues at the University of Kentucky. They have aided me tremendously by encouraging my research endeavors, engaging in discussions that allowed me to think deeper about subjects, as well as borrowing equipment and/or chemicals which were needed for my research. In particular I would like to thank Dr. Anitha Gowda who was a great friend and colleague in Dr. Ladipo's lab when I first arrived at UK as well as Daudi Saang'onoyo who joined our group recently.

Finally, I would like to thank my previous professors who have taught me to believe in myself and shoot for the stars. First off, thank you to my advisor



from Eastern Kentucky University, Dr. Nathan Tice, who encouraged me in my endeavors and even recommended Dr. Ladipo's group to me. I would also be remiss if I didn't not mention my professors at Georgetown College, Drs. Campbell, Fraley and Wiseman who lit a fire in me for my passion for chemistry. They made the subject come to life and have taught me more than they will ever know. It is because of these professors that I am able to write this dissertation and achieve my goals.

Lastly, I would like to thank the National Science Foundation who supported this work through a grant under CHE - 1058097.

## TABLE OF CONTENTS

Chapter	Page
Acknowledgement.....	iii
List of Tables.....	x
List of Figures.....	xiii
List of Schemes.....	xxi
1. Introduction .....	1
1.1 Importance .....	1
1.2 Synthetic Methods .....	5
1.3 Catalytic Pathways.....	8
1.4 Objective and Dissertation Outline.....	23
2. Selective epoxidation of 1-octene with tert-butyl hydroperoxide catalyzed by tripodal titanium silsesquioxane complexes grafted onto hyperbranched poly(siloxysilane) matrices	
2.1 Introduction .....	26
2.2 Experimental.....	28
2.2.1 Materials and methods.....	28
2.2.2 Catalyst Preparation .....	30
2.2.2.1 Synthesis of $\text{Et}_3\text{Si}(\text{CH}_2)_3(i\text{-C}_4\text{H}_9)_7\text{Si}_8\text{O}_{12}$ ( <b>2</b> ) .....	30
2.2.2.2 Synthesis of $\text{ClMe}_2\text{Si}(\text{CH}_2)_3(i\text{-C}_4\text{H}_9)_7\text{Si}_8\text{O}_{12}$ ( <b>3</b> ).....	31
2.2.2.3 Synthesis of $\text{HMe}_2\text{Si}(\text{CH}_2)_3(i\text{-C}_4\text{H}_9)_7\text{Si}_8\text{O}_{12}$ ( <b>4</b> ). .....	31
2.2.2.4 Synthesis of $\text{Et}_3\text{Si}(\text{CH}_2)_3(i\text{-C}_4\text{H}_9)_6\text{Si}_7\text{O}_9(\text{OH})_3$ ( <b>5</b> ). ....	32
2.2.2.5 Synthesis of $\text{HMe}_2\text{Si}(\text{CH}_2)_3(i\text{-C}_4\text{H}_9)_6\text{Si}_7\text{O}_9(\text{OH})_3$ ( <b>6</b> ). 33	33
2.2.2.6 Synthesis of $[\text{Ti}(\text{NMe}_2)\{\text{Et}_3\text{Si}(\text{CH}_2)_3(i\text{-C}_4\text{H}_9)_6\text{Si}_7\text{O}_{12}\}]$ ( <b>7</b> ).....	33
2.2.2.7 Synthesis of $[\text{Ti}(\text{NMe}_2)\{\text{HMe}_2\text{Si}(\text{CH}_2)_3(i\text{-C}_4\text{H}_9)_6\text{Si}_7\text{O}_{12}\}]$ ( <b>8</b> ).....	34
2.2.2.8 Synthesis of <b>P1-6</b> (Grafting <b>6</b> onto <b>P1</b> ).....	35
2.2.2.9 Synthesis of <b>c-P1-6</b> .....	35

2.2.2.10 Synthesis of titanium silsesquioxane material <b>P1-8</b> ..	36
2.2.2.11 Synthesis of titanium silsesquioxane material <b>c-P1-8</b> ..	36
2.2.3 Procedure for catalytic alkene epoxidation.....	37
2.2.3.1 Epoxidation of 1-octene with <i>t</i> -butyl hydroperoxide (TBHP) catalyzed by titanium silsesquioxanes <b>7-10</b> ....	37
2.2.3.2 Epoxidation of 1-Octene with <i>t</i> -butyl hydroperoxide (TBHP) catalyzed by titanium silsesquioxane materials <b>P1-8</b> and <b>c-P1-8</b> .....	37
2.2.3.3 <b>c-P1-8</b> -catalyzed epoxidation of 1-octene with <i>t</i> -butyl hydroperoxide (TBHP) in the presence of added <i>t</i> -butanol .....	38
2.2.4 Catalyst recyclability studies .....	38
2.2.5 Catalyst Repair .....	38
2.3 Results/Discussion.....	38
2.3.1 Preparation and characterization of trisilanolisobutyl-POSS ligands .....	38
2.3.2 Preparation and characterization of tripodal titanium silsesquioxane complexes .....	43
2.3.3 Covalent grafting of tripodal titanium silsesquioxane complexes to hyperbranched polysiloxysilane matrices.....	46
2.3.4 Alkene Epoxidation activity .....	50
2.3.4.1 Alkene Epoxidation activity of tripodal titanium silsesquioxane complexes .....	50
2.3.4.2 Alkene Epoxidation activity of tripodal titanium silsesquioxane materials .....	53
2.3.4.3 Titanium leaching and catalyst recyclability studies	56
2.4 Conclusion .....	58

3. Immobilized tripodal titanium silsesquioxanes onto a hyperbranched poly(siloxysilane) polymer for the epoxidation of hindered olefins using TBHP as oxidant	
3.1 Introduction .....	59
3.2 Experimental .....	60
3.2.1 Synthesis of <b>c-P1-6</b> .....	62
3.2.2 Synthesis of titanium silsesquioxane material <b>P1-8</b> .....	63
3.2.3 Synthesis of titanium silsesquioxane material <b>c-P1-8</b> .....	63
3.2.4 Epoxidation trials.....	63
3.2.4.1 Trials for various olefins .....	63
3.2.4.2 Analysis for determination of apparent activation energy .....	64
3.2.4.3 Recyclability of <b>NCP-9</b> and <b>CP-9</b> .....	64
3.3 Results/Discussion .....	64
3.3.1 Preparation of catalysts.....	64
3.3.2 Alkene Epoxidation activity .....	67
3.3.2.1 Homogeneous tripodal titanium catalysts using a 20:1 olefin/TBHP ratio .....	67
3.3.2.2 Homogeneous tripodal titanium catalysts using a 1:1 olefin/TBHP ratio .....	73
3.3.2.3 Immobilized tripodal titanium catalysts using a 20:1 olefin/TBHP ratio .....	80
3.3.2.4 Immobilized tripodal titanium catalysts using a 1:1 olefin/TBHP ratio .....	87
3.3.3 Recyclability of <b>P1-8</b> and <b>c-P1-8</b> with limonene .....	92
3.3.4 Epoxidation of 1-octene .....	94
3.4 Conclusion .....	95

4. Immobilized tripodal titanium silsesquioxanes onto a hyperbranched poly(siloxysilane) polymer for the epoxidation of cyclohexene using H <sub>2</sub> O <sub>2</sub> as oxidant	
4.1 Introduction .....	97
4.2 Results/Discussion.....	102
4.2.1 Synthesis <b>P1-8</b> and <b>c-P1-8</b> .....	102
4.2.2 Epoxidation of Cyclohexene.....	104
4.3 Conclusion .....	112
5. Immobilization of tripodal titanium silsesquioxanes onto gold-on-silica for the direct epoxidation of propylene	
5.1 Introduction .....	114
5.2 Experimental.....	127
5.2.1 General Considerations .....	127
5.2.2 Reactor Setup .....	128
5.2.3 Synthesis .....	131
5.2.3.1 Synthesis of (HS(CH <sub>2</sub> ) <sub>3</sub> ( <i>i</i> -C <sub>4</sub> H <sub>9</sub> ) <sub>6</sub> Si <sub>7</sub> O <sub>9</sub> (OH) <sub>3</sub> ( <b>12</b> )...	131
5.2.3.2 Synthesis of {Ti(NMe <sub>2</sub> )(HS(CH <sub>2</sub> ) <sub>3</sub> )( <i>i</i> -C <sub>4</sub> H <sub>9</sub> ) <sub>6</sub> Si <sub>7</sub> O <sub>12</sub> ) } ( <b>13</b> ).....	132
5.2.3.3 Synthesis of {Ti(OPr <sup><i>i</i></sup> )(HS(CH <sub>2</sub> ) <sub>3</sub> )( <i>i</i> -C <sub>4</sub> H <sub>9</sub> ) <sub>6</sub> Si <sub>7</sub> O <sub>12</sub> ) } ( <b>14</b> ).....	132
5.2.3.4 Au/SiO <sub>2</sub> .....	133
5.2.3.5 Tethering of {Ti(NMe <sub>2</sub> )(HS(CH <sub>2</sub> ) <sub>3</sub> )( <i>i</i> -C <sub>4</sub> H <sub>9</sub> ) <sub>6</sub> Si <sub>7</sub> O <sub>12</sub> ) } ( <b>13</b> ) onto Au/SiO <sub>2</sub> ( <b>13-Au/SiO<sub>2</sub></b> ) .....	133
5.2.3.6 Tethering of {Ti(OPr <sup><i>i</i></sup> )(HS(CH <sub>2</sub> ) <sub>3</sub> )( <i>i</i> -C <sub>4</sub> H <sub>9</sub> ) <sub>6</sub> Si <sub>7</sub> O <sub>12</sub> ) } ( <b>14</b> ) onto Au/SiO <sub>2</sub> ( <b>14-Au/SiO<sub>2</sub></b> ) .....	133
5.2.3.7 Impregnation of [Ti(OPr <sup><i>i</i></sup> ){( <i>c</i> -C <sub>6</sub> H <sub>11</sub> ) <sub>7</sub> Si <sub>7</sub> O <sub>12</sub> }] ( <b>15</b> ) onto Au/SiO <sub>2</sub> ( <b>15-Au</b> ).....	134
5.2.4 Epoxidation Trials .....	134
5.3 Results and Discussion.....	134
5.3.1 Grafting of tripodal Ti POSS onto Au/SiO <sub>2</sub> supports .....	134

5.3.2 Epoxidation Trials .....	138
5.4 Conclusion .....	144
6. Future Works.....	147
Appendix .....	151
List of References .....	183
Vita.....	191

## LIST OF TABLES

Table	Page
Chapter 1	
1.1. Epoxides used in the fragrance industry.....	4
1.2. Examples of various metal catalysts.....	9
1.3. Examples of olefins used in Sharpless asymmetric epoxidation.....	14
1.4. Ti containing catalysts for the epoxidation of 1-octene .....	19
Chapter 2	
2.1. Epoxidation of 1-octene with TBHP catalyzed by titanium silsesquioxane complexes and related materials .....	52
2.2. Epoxidation of 1-octene with TBHP catalyzed by titanium silsesquioxane materials <b>P1-8</b> and <b>c-P1-8</b> . .....	55
2.3. Catalyst recyclability, retardation, and reparability studies <sup>a</sup> . .....	57
Chapter 3	
3.1. Catalytic activity of tripodal titanium catalysts ( <b>9</b> and <b>10</b> ) for epoxidation of cyclohexene employing a 20:1 olefin:TBHP ratio .....	69
3.2. Catalytic activity of tripodal titanium catalysts ( <b>9</b> and <b>10</b> ) for epoxidation of 1-methylcyclohexene employing a 20:1 olefin:TBHP ratio.....	70
3.3. Catalytic activity of tripodal titanium catalysts ( <b>9</b> and <b>10</b> ) for epoxidation of limonene employing a 20:1 olefin:TBHP ratio.....	71

3.4. Catalytic activity of tripodal titanium catalysts ( <b>9</b> and <b>10</b> ) for epoxidation of $\alpha$ -pinene employing a 20:1 olefin:TBHP ratio.....	73
3.5. Catalytic activity of tripodal titanium catalysts ( <b>9</b> and <b>10</b> ) for epoxidation of cyclohexene employing a 1:1 olefin:TBHP ratio .....	75
3.6. Catalytic activity of tripodal titanium catalyst ( <b>10</b> ) for epoxidation of 1-methylcyclohexene employing a 1:1 olefin:TBHP ratio.....	76
3.7. Catalytic activity of tripodal titanium catalyst ( <b>10</b> ) for epoxidation of limonene employing a 1:1 olefin:TBHP ratio .....	78
3.8. Catalytic activity of tripodal titanium catalyst ( <b>10</b> ) for epoxidation of $\alpha$ -pinene employing a 1:1 olefin:TBHP ratio .....	79
3.9. Catalytic activity of immobilized tripodal titanium catalysts ( <b>P1-8</b> and <b>c-P1-8</b> ) for epoxidation of cyclohexene employing a 20:1 olefin:TBHP ratio .....	81
3.10. Catalytic activity of immobilized tripodal titanium catalysts ( <b>P1-8</b> and <b>c-P1-8</b> ) for epoxidation of 1-methylcyclohexene employing a 20:1 olefin:TBHP ratio.....	82
3.11. Catalytic activity of immobilized tripodal titanium catalysts ( <b>P1-8</b> and <b>c-P1-8</b> ) for epoxidation of limonene employing a 20:1 olefin:TBHP ratio .....	84
3.12. Catalytic activity of immobilized tripodal titanium catalysts ( <b>P1-8</b> and <b>c-P1-8</b> ) for epoxidation of $\alpha$ -pinene employing a 20:1 olefin:TBHP ratio.....	86
3.13. Catalytic activity of immobilized tripodal titanium catalyst ( <b>P1-8</b> ) for epoxidation of cyclohexene employing a 1:1 olefin:TBHP ratio .....	88



3.14. Catalytic activity of immobilized tripodal titanium catalyst ( <b>P1-8</b> ) for epoxidation of 1-methylcyclohexene employing a 1:1 olefin:TBHP ratio..	89
3.15. Catalytic activity of immobilized tripodal titanium catalyst ( <b>P1-8</b> ) for epoxidation of limonene employing a 1:1 olefin:TBHP ratio.....	91
3.10. Recyclability of <b>NCP-9</b> and <b>CP-9</b> with limonene .....	93

#### Chapter 4

4.1. Catalytic activity of immobilized tripodal titanium ( <b>c-P1-8</b> ) for epoxidation of cyclohexene employing a 20:1 olefin:H <sub>2</sub> O <sub>2</sub> ratio .....	106
4.2. Catalytic activity of immobilized tripodal titanium ( <b>c-P1-8</b> ) for epoxidation of cyclohexene employing a 20:1 olefin:H <sub>2</sub> O <sub>2</sub> ratio with anhydrous Na <sub>2</sub> SO <sub>4</sub> .....	108
4.3. Catalytic activity of immobilized tripodal titanium ( <b>c-P1-8</b> ) for epoxidation of cyclohexene employing a 20:1 olefin:H <sub>2</sub> O <sub>2</sub> ratio with TEAB .....	109

#### Chapter 5

5.1. Epoxidation Results .....	140
--------------------------------	-----

## LIST OF FIGURES

Figure	Page
Chapter 1	
1.1. Bisphenol A epoxy resin .....	1
1.2. Epoxide Structure .....	2
1.3. (a)- fosfomicin and (b)- cytochalasin E .....	2
1.4. Examples of Compounds used in fragrance industry .....	3
1.5. Jacobsen's catalyst .....	15
1.6. Generalized, Condensed structure of titania silica supports .....	16
1.7. Possible structures in heterogeneous titanosilicates: (a) tetrapodal, (b) tripodal, and (c) bipodal .....	17
1.8. Structure of Polyhedral Oligomeric Silsesquioxanes (POSS) .....	18
1.9. CpTi[( <i>c</i> -C <sub>5</sub> H <sub>9</sub> ) <sub>7</sub> Si <sub>7</sub> O <sub>12</sub> ] which was immobilized on silica support .....	21
1.10. Tripodal Ti POSS tethered onto a linear polymer .....	22
Chapter 2	
2.1. <sup>1</sup> H NMR spectra corresponding to titrations of Ti(NMe <sub>2</sub> ) <sub>4</sub> with sub-equimolar amounts of <b>6</b> . (Ti(NMe <sub>2</sub> ) <sub>4</sub> : <b>6</b> ratios: <i>a</i> = 2.2:1; <i>b</i> = 2:1; <i>c</i> = 1.8:1; <i>d</i> = 1.6:1; <i>e</i> = 1.4:1; <i>f</i> = 1.2:1) .....	46
2.2. Pseudo-first order rate plots for the epoxidation of 1-octene with TBHP catalyzed by titanium silsesquioxane complexes: <b>▲9</b> , <b>◇ 10</b> , <b>■ 7</b> and <b>×8</b> ...	52

2.3. TBHP conversion as a function of time for the epoxidation of 1-octene catalyzed by ▲ <b>P1-8</b> , □ <b>c-P1-8</b> (preswelled for 4 h), and ◇ <b>c-P1-8</b> (reaction conditions: T = 80 °C, TBHP = 0.55 mmol, 1-octene (20 g), 0.05 mmol Ti for <b>P1-8</b> and 0.02 mmol Ti for <b>c-P1-8</b> ) .....	55
---	----

### Chapter 3

3.1. Structure of Ti[(c-C <sub>5</sub> H <sub>9</sub> ) <sub>7</sub> Si <sub>7</sub> O <sub>11</sub> (OSiMe <sub>2</sub> CHCH <sub>2</sub> ) <sub>2</sub> .....	72
3.2. Reaction profile for the epoxidation of 1-methylcyclohexene (■) and limonene (◇) employing <b>10</b> as the catalyst.....	74
3.3. Reaction Profile for the epoxidation of limonene employing <b>P1-8</b> (◇) or <b>c-P1-8</b> (■) as catalyst.....	85
3.4. Determination of apparent activation energy ■= <b>P1-8</b> and ◇= <b>c-P1-8</b> .....	95

### Chapter 4

4.1. Silsesquioxane gels developed <sup>1</sup> .....	99
4.2. Tripodal Ti POSS tethered onto a linear polymer .....	100

### Chapter 5

5.1. Au nanoparticles formed with impregnation (a) or DP (b).....	121
5.2. Bidentate peroxo species formed with Au/TiO <sub>2</sub> .....	123
5.3. Schematic representation of isolated Ti sites in heterogeneous materials (a)	

and propene epoxidation with Au dispersed on titanasilicates (b). .....	124
5.4. Reactor setup .....	129
5.5. Column held within the oven.....	130
5.6. Size distribution of Au/SiO <sub>2</sub> nanoparticles air-cooled after calcination step ....	
.....	135
5.7. TEM micrographs of Au/SiO <sub>2</sub> nanoparticles air-cooled after calcination step .	
.....	135
5.8. Size distribution of Au/SiO <sub>2</sub> nanoparticles N <sub>2</sub> -cooled after calcination step ....	
.....	136
5.9. TEM micrographs of Au/SiO <sub>2</sub> nanoparticles N <sub>2</sub> -cooled after calcination step .	
.....	136
5.10. Size distribution of silylated Au/SiO <sub>2</sub> nanoparticles air-cooled after calcination step.....	141
5.11. TEM micrographs of silylated Au/SiO <sub>2</sub> nanoparticles air-cooled after calcination step.....	142
5.12. Size distribution of silylated Au/SiO <sub>2</sub> nanoparticles N <sub>2</sub> -cooled after calcination step.....	142
5.13. TEM micrographs of silylated Au/SiO <sub>2</sub> nanoparticles N <sub>2</sub> -cooled after calcination step.....	143

## Chapter 6

6.1. Tripodal titanium silsesquioxane.....	149
--	-----

### Appendix

A.1. UV-Vis of [Ti(NMe <sub>2</sub> ){Et <sub>3</sub> Si(CH <sub>2</sub> ) <sub>3</sub> ( <i>i</i> -Bu) <sub>6</sub> Si <sub>7</sub> O <sub>12</sub> }] ( <b>7</b> ) .....	153
A.2. UV-Vis spectrum of [Ti(NMe <sub>2</sub> ){HMe <sub>2</sub> Si(CH <sub>2</sub> ) <sub>3</sub> ( <i>i</i> -Bu) <sub>6</sub> Si <sub>7</sub> O <sub>12</sub> }] ( <b>8</b> ) .....	153
A.3. UV- Vis spectrum of ( <b>P1-8</b> ) .....	154
A.4. UV- Vis spectrum of ( <b>c-P1-8</b> ) .....	154
A.5. Typical GC chromatograph for epoxidation of 1-octene (73 g) using TBHP (31 mmol) and homogeneous catalysts ( <b>7-10</b> , 0.2mmol Ti) after 10 minutes (50 % conversion). .....	155
A.6. Typical GC chromatograph for epoxidation of 1-octene (20 g) using TBHP (0.55 mmol) and <b>P1-8</b> (0.06 mmol Ti) as catalyst after 1 hours (50 % conversion) .....	156
A.7. Typical GC chromatograph for epoxidation of 1-octene (20 g) using TBHP (0.55 mmol) and <b>c-P1-8</b> (0.02 mmol Ti)as catalyst after 16 hours (50 % conversion) .....	157
A.8. Typical GC chromatograph for epoxidation of 1-octene (73 g) using TBHP (31 mmol) and homogeneous catalysts ( <b>7-10</b> , 0.2mmol Ti) after 30 minutes (100 % conversion) .....	158
A.9. Typical GC chromatograph for epoxidation of 1-octene (20 g) using TBHP (0.55 mmol) and <b>P1-8</b> (0.06 mmol Ti) as catalyst after 2 hours (100 % conversion) .....	159

A. 10. Typical GC chromatograph for epoxidation of 1-octene (20 g) using TBHP (0.55 mmol) and <b>c-P1-8</b> (0.02 mmol Ti) as catalyst after 24 hours (100 % conversion) .....	160
A. 11. Typical GC chromatograph for epoxidation of cyclohexene (60 mmol) using TBHP (3 mmol) toluene as solvent, and chlorobenzene as internal standard and homogeneous catalysts ( <b>9-10</b> , 0.02 mmol Ti) after 10 minutes (98 % conversion) .....	161
A. 12. Typical GC chromatograph for epoxidation of cyclohexene (60 mmol) using TBHP (3 mmol) toluene as solvent, and chlorobenzene as internal standard and heterogeneous catalysts ( <b>P1-8 or c-P1-8</b> , 0.02 mmol Ti) after 12 hours (99 % conversion) .....	162
A. 13. Typical GC chromatograph for epoxidation of cyclohexene (3 mmol) using TBHP (3 mmol) toluene as solvent, and chlorobenzene as internal standard and heterogeneous catalysts ( <b>9-10</b> , 0.02 mmol Ti) after 40 minutes (70 % conversion) .....	163
A.14. Typical GC chromatograph for epoxidation of cyclohexene (3 mmol) using TBHP (3 mmol) toluene as solvent, and chlorobenzene as internal standard and heterogeneous catalysts ( <b>P1-8</b> , 0.02 mmol Ti) after 4 hours (70 % conversion) .....	164
A.15. Typical GC chromatograph for epoxidation of 1-methylcyclohexene (60 mmol) using TBHP (3 mmol) toluene as solvent, and chlorobenzene as internal standard and homogeneous catalysts ( <b>9-10</b> , 0.02 mmol Ti) after 10 minutes (92 % conversion) .....	165
A.16. Typical GC chromatograph for epoxidation of 1-methylcyclohexene (60 mmol) using TBHP (3 mmol) toluene as solvent, and chlorobenzene as internal standard and heterogeneous catalysts ( <b>P1-8 or c-P1-8</b> , 0.02 mmol Ti) after 4 hours (98 % conversion) .....	166

A.17. Typical GC chromatograph for epoxidation of 1-methylcyclohexene (3 mmol) using TBHP (3 mmol) toluene as solvent, and chlorobenzene as internal standard and homogeneous catalysts ( <b>10</b> , 0.02 mmol Ti) after 14 hours (85 % conversion) .....	167
A.18. Typical GC chromatograph for epoxidation of 1-methylcyclohexene (3 mmol) using TBHP (3 mmol) toluene as solvent, and chlorobenzene as internal standard and heterogeneous catalysts ( <b>P1-8</b> , 0.02 mmol Ti) after 20 hours (60 % conversion) .....	168
A.19. Typical GC chromatograph for epoxidation of limonene (60 mmol) using TBHP (3 mmol) toluene as solvent, and chlorobenzene as internal standard and homogeneous catalysts ( <b>9-10</b> , 0.02 mmol Ti) after 10 minutes (98 % conversion) .....	169
A.20. Typical GC chromatograph for epoxidation of limonene (60 mmol) using TBHP (3 mmol) toluene as solvent, and chlorobenzene as internal standard and heterogeneous catalysts ( <b>P1-8 or c-P1-8</b> , 0.02 mmol Ti) after 6.5 hours (70 % conversion) .....	170
A.21. Typical GC chromatograph for epoxidation of limonene (3 mmol) using TBHP (3 mmol) toluene as solvent, and chlorobenzene as internal standard and homogeneous catalysts ( <b>10</b> , 0.02 mmol Ti) after 10 minutes (71 % conversion) .....	171
A.22. Typical GC chromatograph for epoxidation of limonene (3 mmol) using TBHP (3 mmol) toluene as solvent, and chlorobenzene as internal standard and heterogeneous catalysts ( <b>P1-8</b> , 0.02 mmol Ti) after 30 hours (50 % conversion) .....	172
A. 23. Typical GC chromatograph for epoxidation of $\alpha$ -pinene (60 mmol) using TBHP (3 mmol) toluene as solvent, and chlorobenzene as internal standard and homogeneous catalysts ( <b>9-10</b> , 0.02 mmol Ti) after 10 minutes (90 % conversion) .....	173

A. 24. Typical GC chromatograph for epoxidation of $\alpha$ -pinene (60 mmol) using TBHP (3 mmol) toluene as solvent, and chlorobenzene as internal standard and homogeneous catalysts ( <b>P1-8</b> or <b>c-P1-8</b> , 0.02 mmol Ti) after 4 hours (76 % conversion) .....	174
A. 25. Typical GC chromatograph for epoxidation of $\alpha$ -pinene (3 mmol) using TBHP (3 mmol) toluene as solvent, and chlorobenzene as internal standard and homogeneous catalysts ( <b>10</b> , 0.02 mmol Ti) after 5 hours (72 % conversion) .....	175
A. 26. Typical GC chromatograph for epoxidation of 1-octene (60 mmol) using TBHP (3 mmol) toluene as internal standard and heterogeneous catalysts ( <b>P1-8</b> or <b>c-P1-8</b> , 0.02 mmol Ti) after 12 hours (70 % conversion) at 60 °C . .....	176
A.27. Typical GC chromatograph for epoxidation of cyclohexene (45 mmol) using H <sub>2</sub> O <sub>2</sub> (2 mmol) toluene as internal standard, ACN as solvent and heterogeneous catalyst ( <b>c-P1-8</b> , 0.02 mmol Ti) at 12 hours (100 % conversion H <sub>2</sub> O <sub>2</sub> ) at 60 °C .....	177
A.28. Typical GC chromatograph for epoxidation of cyclohexene (45 mmol) using H <sub>2</sub> O <sub>2</sub> (2 mmol) toluene as internal standard, IPA as solvent and heterogeneous catalyst ( <b>c-P1-8</b> , 0.02 mmol Ti) at 12 hours (100 % conversion H <sub>2</sub> O <sub>2</sub> ) at 60 °C .....	178
A.29. Typical GC chromatograph for epoxidation of cyclohexene (>45 mmol) using H <sub>2</sub> O <sub>2</sub> (2 mmol) toluene as internal standard, and heterogeneous catalyst ( <b>c-P1-8</b> , 0.02 mmol Ti) at 5 hours (60 % conversion H <sub>2</sub> O <sub>2</sub> ) at 60 °C.....	179
A.30. Typical GC chromatograph for epoxidation of cyclohexene (>45 mmol) using H <sub>2</sub> O <sub>2</sub> (2 mmol) toluene as internal standard, and heterogeneous catalyst ( <b>c-P1-8</b> , 0.02 mmol Ti) at 12 hours (100 % conversion H <sub>2</sub> O <sub>2</sub> ) at 60 °C.....	180



- A.31. Typical GC chromatograph for epoxidation of cyclohexene (>45 mmol) using H<sub>2</sub>O<sub>2</sub> (2 mmol) toluene as internal standard, DCE as solvent and heterogeneous catalyst (**c-P1-8**, 0.02 mmol Ti) at 6 hours (60 % conversion H<sub>2</sub>O<sub>2</sub>) at 60 °C ..... 181
- A.32. Typical GC chromatograph for epoxidation of cyclohexene (>45 mmol) using H<sub>2</sub>O<sub>2</sub> (2 mmol) toluene as internal standard, DCE as solvent and heterogeneous catalyst (**c-P1-8**, 0.02 mmol Ti) at 12 hours (100 % conversion H<sub>2</sub>O<sub>2</sub>) at 60 °C ..... 182

## LIST OF SCHEMES

Scheme	Page
Chapter 1	
1.1. Interaction of EO with DNA.....	5
1.2. Synthesis of ethylene oxide over Ag catalyst.....	6
1.3. Synthesis of epoxides from peracids .....	7
1.4. Synthesis of epoxides by the chlorohydrin process .....	7
1.5. Halcon process for the synthesis of epoxides.....	8
1.6. Catalytic Mechanism for epoxidation reactions employing Ti and V metal centers.....	10
1.7. Catalytic Mechanism for epoxidation reactions employing Mo and W metal centers.....	10
1.8. Synthesis of epichlorohydrin.....	12
1.9. Sharpless asymmetric epoxidation of olefins.....	13
1.10. Catalytic Mechanism of epoxidation reaction with Ti .....	18
Chapter 2	
2.1. Synthetic route to <b>2</b> , <b>3</b> , and <b>4</b> .....	39
2.2. Excision of one framework silicon. ....	40
2.3. Synthetic route for the formation of active catalysts <b>P1-8</b> and <b>c-P1-8</b> . ....	48

### Chapter 3

3.1. Synthetic route for <b>9</b> and <b>10</b> . .....	65
3.2. Synthetic route for <b>P1-8</b> and <b>c-P1-8</b> . .....	66

### Chapter 4

4.1. Epoxidation of cyclohexene employing H <sub>2</sub> O <sub>2</sub> as the oxidant .....	101
4.2. Synthetic route for <b>P1-8</b> and <b>c-P1-8</b> . .....	103
4.3. Mechanism for epoxidation reactions catalyzed by tripodal titanium. ....	111
4.4. Formation of 2-cyclohexene-1-ol and 1,2-cyclohexanediol. ....	112

### Chapter 5

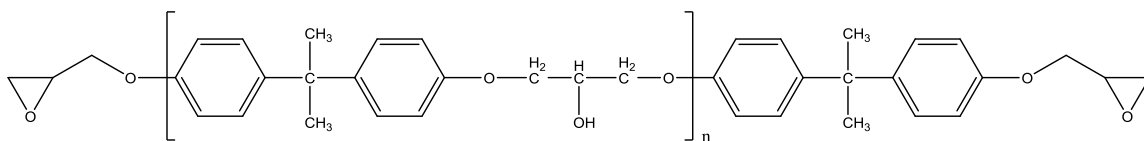
5.1. Different Routes to synthesize PO.....	115
5.2. Formation of H <sub>2</sub> O <sub>2</sub> on-site for Dow Chemical synthesis of PO .....	118
5.3. Reaction mechanism of PO formation with Au/TiO <sub>2</sub> catalysts .....	120
5.4. Using N <sub>2</sub> O as oxidant instead of H <sub>2</sub> . .....	125
5.5. Proposed route to Ti catalyst tethered to gold nanoparticle.....	127
5.6. Synthesis of tripodal Ti POSS .....	137

## Chapter 1: Introduction

### 1.1 Importance

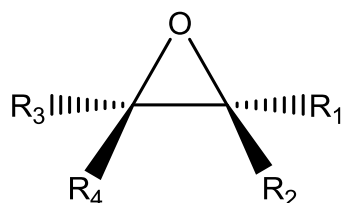
Epoxy resins, such as bisphenol A epoxy resin (Figure 1.1),<sup>2,3</sup> are used for numerous applications and billions of pounds are produced annually. In fact, 5-6 billion pounds of bisphenol A, starting reagent for bisphenol A epoxy resin, was produced in 2008.<sup>2</sup> An epoxy resin consists of an epoxide that can be cured or crosslinked, with a hardener such as an amine or alcohol containing compound. The majority of epoxy resins are employed in the protective coating industry due to numerous advantages: strength, flexibility, minimal amount of shrinkage upon curing, superior adhesion to various types of surfaces, and excellent resistance to chemicals and corrosion. Epoxy resins are also favored due to their ability to cure over a wide range of temperatures, allowing for use in electrical insulation and temperature sensitive materials.<sup>2-4</sup>

**Figure 1.1**—Bisphenol A epoxy resin

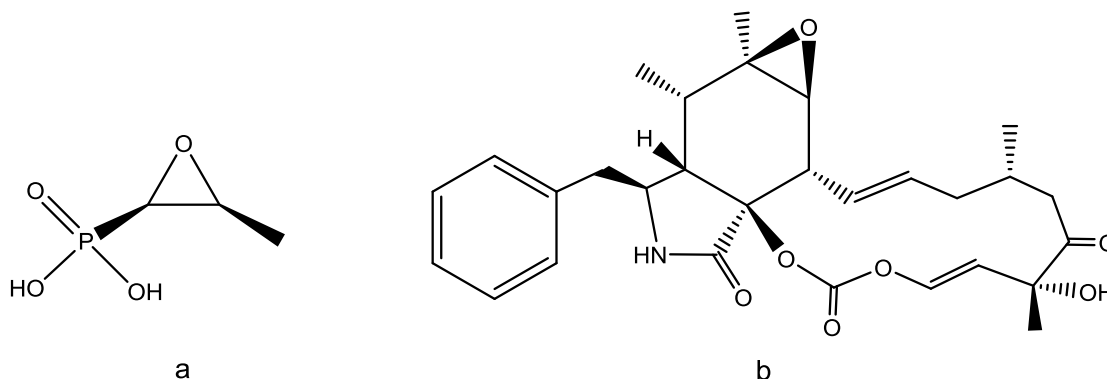


epoxides such as 1,2-epoxyoctane and 1,2-epoxyhexane can be employed as stabilizers for alkyl halides while cyclic olefins, such as cyclohexene oxide, can be used in the synthesis of pesticides or polymers. Epoxide compounds are also used in the pharmaceutical industry as antitumor, anticancer, anticonvulsant, antiepileptic and antibiotic medicines. For example, fosfomycin ((1R,2S)-(-)-(1,2)-epoxypropyl phosphonic acid, Figure 1.3 a) has wide-spectrum antibiotic activity and is synthesized via the epoxidation of *cis*-1-propenylphosphonic acid (CPPA) using a chiral W or Mo catalyst.<sup>7</sup> Cytochalasin E (Figure 1.3 b) is another epoxide containing medicine shown to inhibit angiogenesis and tumor growth by disrupting the actin stress fibers due to the high reactivity of epoxides.<sup>9</sup>

**Figure 1.2**—Epoxide structure

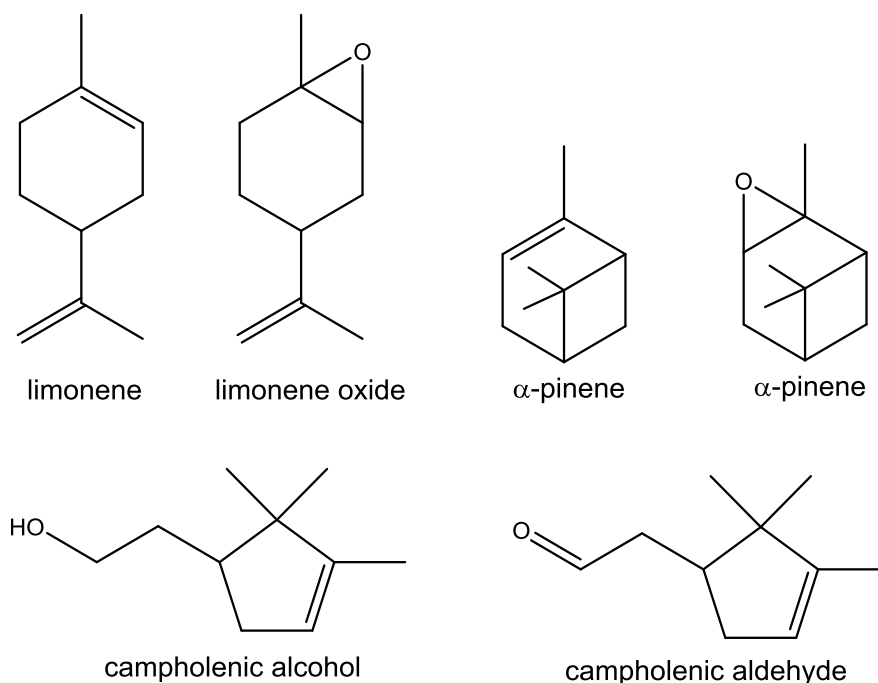


**Figure 1.3**— (a) Fosfomycin and (b) cytochalasin E



The fragrance and flavoring industry also employs numerous epoxides such as  $\beta$ -lonone epoxide that has a sweet berry fragrance and *trans*-carvone-5,6-oxide which has a herbal, mint fragrance; additional examples can be found in Table 1.1.<sup>10,11</sup>  $\alpha$ -Pinene oxide has a sweet, berry-like fragrance (Figure 1.4) and is produced commercially for the fragrance industry as an intermediate to  $\alpha$ -campholenic alcohol and campholenic aldehyde is used as a sandalwood scent.<sup>7,12</sup> Limonene (Figure 1.4), derived from citrus oils, is also used in the fragrance industry and can be oxidized to limonene oxide, which is used in perfumes.

**Figure 1.4**—Examples of compounds used in fragrance industry



**Table 1.1**—Epoxides used in the fragrance and flavoring industry<sup>10</sup>

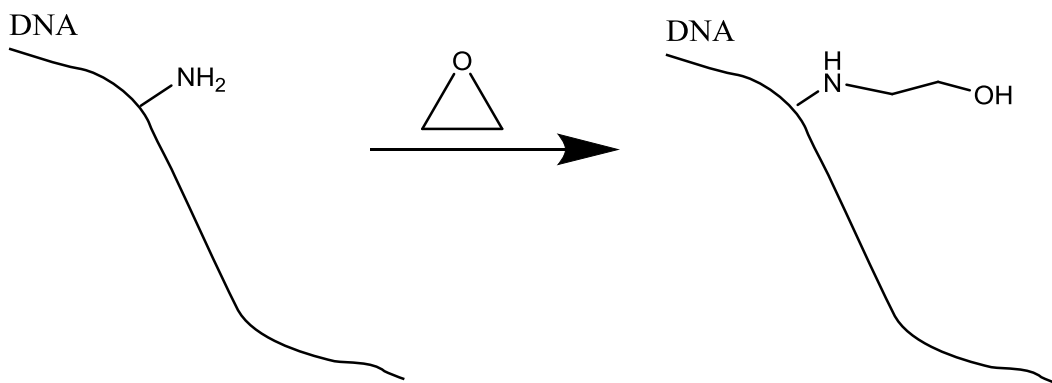
Flavoring Agent	Structure	Fragrance
4,5-Epoxy-(E)-2-decenal		Pungent metallic
$\beta$ -Ionone epoxide		Sweet, Berry
<i>trans</i> -Carvone-5,6-oxide		Herbal, mint
Epoxyoxophorone		Camphoreous type odor
Piperitenone oxide		Woody
$\beta$ -Caryophyllene oxide		Strawberry
Ethyl methyl- <i>para</i> -tolylglycidate		Sweet, floral, fruity, cherry

Due to the high demand for epoxides in different applications, efficient ways to synthesize epoxides needs to be developed that display high yield and selectivity. Additionally, the method should display high atom efficiency to keep production costs to a minimum.

## 1.2 Synthetic Methods

Ethylene oxide, EO, is a colorless, flammable gas used primarily to produce ethylene glycol and surfactants, making EO the most consumed epoxide material. Ethylene glycol is commonly used in the production of polyester fibers for the textile industry as well as resins and the formation of antifreeze.<sup>5,13</sup> In addition to the use of EO as an important intermediate, it is commonly used to sterilize temperature sensitive medical equipment such as plastics and electronic components. The sterilization occurs when the epoxide interacts with the amine functional group of DNA, thereby changing the DNA structure causing the microorganisms to be killed at room temperature (Scheme 1.1).<sup>5</sup> Industrial synthesis of ethylene oxide (EO) is one of the most efficient ways to form an epoxide.

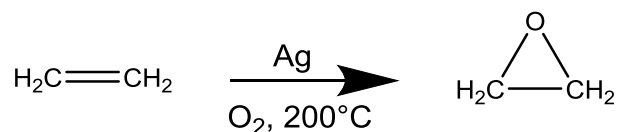
**Scheme 1.1**—Interaction of EO with DNA





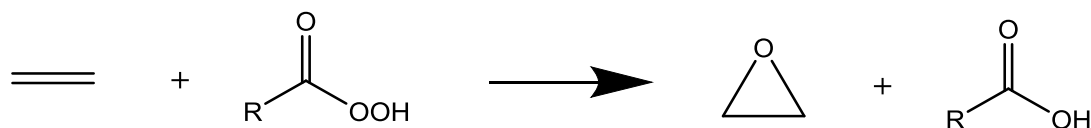
Synthesis of EO occurs over a silver (Ag) catalyst supported on low surface area  $\alpha$ - $\text{Al}_2\text{O}_3$  support using molecular oxygen as the oxidant (Scheme 1.2).<sup>14</sup> The direct epoxidation of ethylene displays high selectivity to epoxide (>85%) and high atom efficiency when promoters are added, making it very cost effective. Although this catalyst is very active for EO production, when propene was employed, the formation of propylene oxide was 16 times slower than the production of EO. Moreover, carbon dioxide formation was observed, resulting in low selectivities. Both low selectivities and low rate of reaction are due to the allylic hydrogens present in propylene, which are easily oxidized by the Ag catalyst.<sup>7,13</sup> Due to the inability of the Ag catalyst to effectively catalyze the epoxidation of olefins larger than ethylene, new alkene epoxidation methods need to be developed.

**Scheme 1.2**—Synthesis of ethylene oxide over Ag catalyst



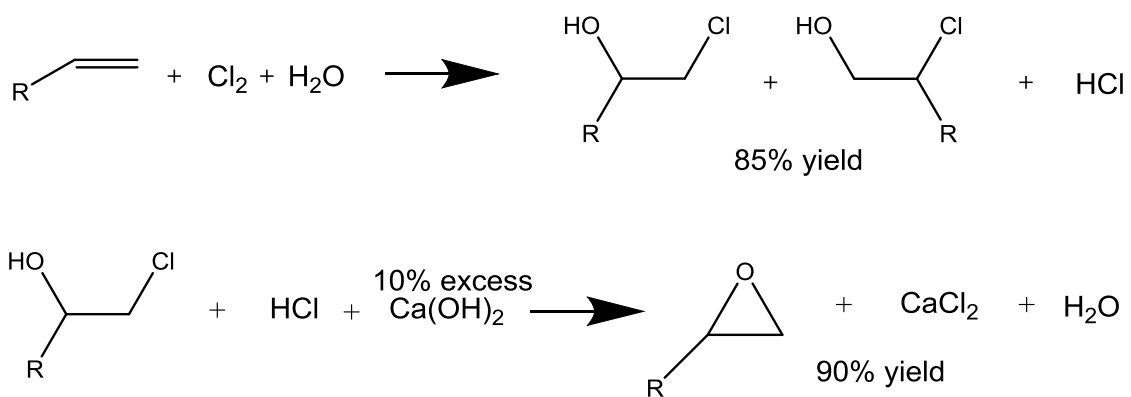
For the epoxidation of olefins larger than ethylene, organic peracids, such as *meta*-chloroperoxybenzoic acid (mCPBA), peroxyacetic acid, and perbenzoic acid, have been used as the oxidant (oxygen source) in the synthesis of epoxides however carboxylic acids are generated as by-products (Scheme 1.3).<sup>3-5</sup> Acids are known to easily ring-open an epoxide thus a buffer must be added to keep the solution neutral, preventing product degradation. Due to the unwanted by-product, along with the necessity to add a buffer, these reactions display very low atom efficiency, making this reaction high costing. In addition, there are numerous safety concerns with regards to storage, transport and handling of peracids.

### Scheme 1.3—Synthesis of epoxides from peracids



Alternatively, the chlorohydrin process (Scheme 1.4) was a primary industrial route for the synthesis of epoxides (as late as 2008) although this process is now viewed as unfavorable from an environmental standpoint because it employs chlorine which is toxic and more expensive than other materials such as peracids and alkylhydroperoxides.<sup>3</sup> In addition, the disposal of highly toxic by-products such as chlorinated organics, chlorinated water, and calcium chloride (CaCl<sub>2</sub>) present an ecological problem that needs to be addressed. Although this process has become less favored, it still accounts for a large percentage of the overall production of epoxides.<sup>14</sup>

### Scheme 1.4—Synthesis of epoxides by the chlorohydrin process<sup>14</sup>



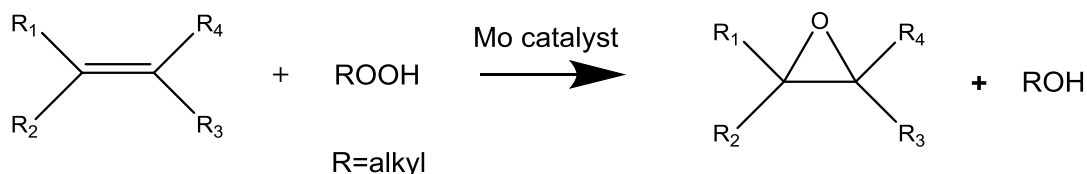
The numerous limitations and drawback of both peracids and chlorohydrin process led to the development of metal-catalyzed epoxidation reactions,

employing hydrogen peroxide (H<sub>2</sub>O<sub>2</sub>) or alkyl hydroperoxides (ROOH) as the sacrificial oxidant.

### 1.3 Catalytic Pathways

The Halcon process,<sup>3,15</sup> the first commercial catalytic process developed for alkene epoxidation, uses a homogeneous molybdenum (Mo) catalyst and an alkyl hydroperoxide (ROOH) as the oxidant (Scheme 1.5). After the success of the Halcon process, numerous other metals were explored such as rhenium,<sup>7,16-21</sup> tungsten,<sup>7,16,17,19,22-26</sup> vanadium,<sup>16,18,19,21,27-30</sup> ruthenium,<sup>7,16-19,21</sup> and titanium (Table 1.2).<sup>1,7,16-18,21,31-62</sup> Numerous studies have shown that a Lewis acid mechanism prevailed where two very similar pathways dominate. The first pathway involves formation of an alkylhydroperoxide species on the metal center followed by the nucleophilic attack of the olefin on the hydroperoxide to form the epoxide; this pathway is common for Ti and V (Scheme 1.6).<sup>19,50</sup> The second pathway, common for Mo and W, is when an alkylhydroperoxide (**C** in Scheme 1.7) coordinates an olefin to the metal (**D** in Scheme 1.7). The olefin then attacks the hydroperoxide oxygen generating the epoxide along with a metal carbonyl complex (Scheme 1.7).<sup>19,22,63</sup> From these mechanisms, we can deduce that metals with high Lewis acidity will display high catalytic activity. Highly Lewis acidic metals are beneficial for the epoxidation of olefins because the metal center withdraws electron density away from the peroxy-oxygen. Due to the lower electron density, the peroxy-oxygen is more susceptible to nucleophilic attack of the olefin to generate the epoxide. Although different metals can vary in the degree of Lewis acidity, the ligands play a major role by either donating or withdrawing electron density from the metal center. Hence electron withdrawing ligands allow for the best Lewis acids.

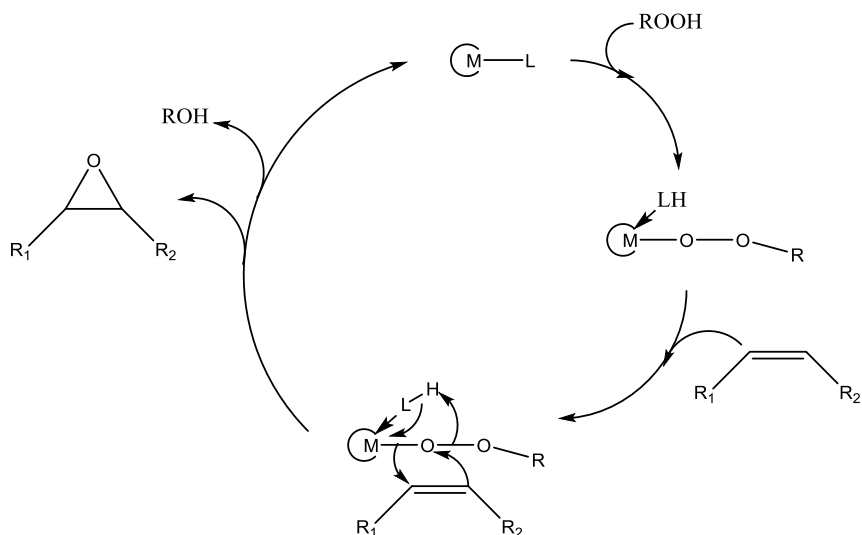
**Scheme 1.5**—Halcon process for the synthesis of epoxides



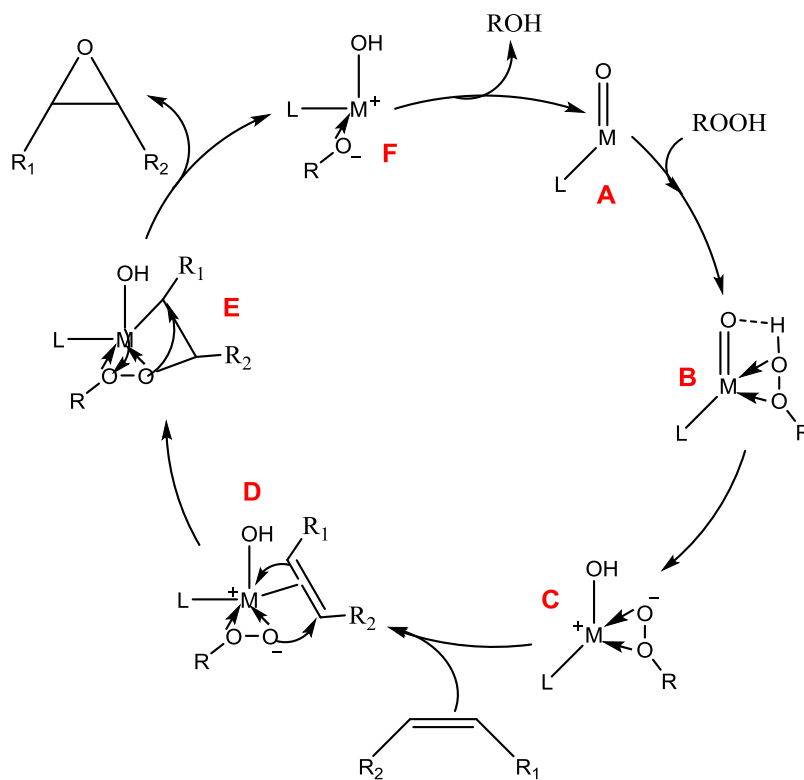
**Table 1.2**—Examples of various metal catalysts

<b>Catalyst</b>	<b>Reactive olefins</b>	<b>Drawbacks</b>	<b>Oxidant</b>	<b>Reference</b>
<b>TS-1</b>	Terminal small (less than 4 carbon) olefins, allyl alcohol	Inefficient for cyclic, bulky, or branched olefins	H <sub>2</sub> O <sub>2</sub>	7,46,49,57,64-68
<b>TiO<sub>2</sub>-SiO<sub>2</sub> aerogel</b>	Cyclic or tertiary olefins	Inefficient for terminal olefins	H <sub>2</sub> O <sub>2</sub> or hydroperoxides	7,37,69,70
<b>Sharpless (Ti<sup>IV</sup> tartrate)</b>	Trisubstituted and <i>trans</i> -1,2-disubstituted allyl alcohols	Must have allylic alcohol, Inefficient for <i>cis</i> -1,2-disubstituted allyl alcohols	TBHP	7,19,21
<b>Fe<sup>III</sup>(phen)</b>	Terminal, cyclic, aromatic	Inefficient for electron deficient olefins, Oxidant	Peracid	7
<b>Mn<sup>III</sup>(salen)</b>	Aromatic	Inefficient for terminal olefins	<i>m</i> -CPBA	7,19,71-73
<b>Mo(CO)<sub>6</sub></b>	Cyclic, Terminal	Homogeneous	TBHP	7,18,22,63
<b>V<sup>V</sup>(OPr<sup>t</sup>)(bis-hydroxamic)</b>	Trisubstituted and <i>trans</i> -1,2-disubstituted allyl alcohols	Inefficient for <i>cis</i> -1,2-disubstituted allyl alcohols	TBHP	7,21,29,30,61
<b>CH<sub>3</sub>ReO<sub>3</sub></b>	Terminal, Cyclic	Low activity	H <sub>2</sub> O <sub>2</sub>	7,16-18
<b>Ru<sup>II</sup>Cl<sub>2</sub>(PPh<sub>3</sub>)<sub>3</sub></b>	Cyclic	Inefficient for terminal olefins, low yields	TBHP	7,18,19,74

**Scheme 1.6**—Catalytic mechanism for epoxidation reactions employing Ti and V metal centers<sup>19,50</sup>



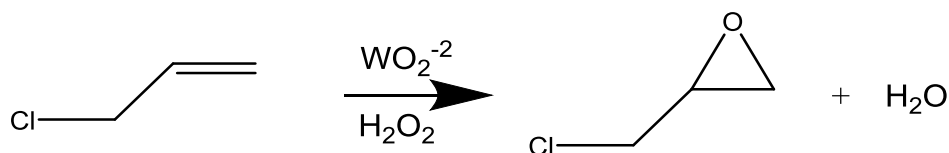
**Scheme 1.7**—Catalytic mechanism for epoxidation reactions employing Mo and W metal centers<sup>19,22,63</sup>



Due to the Halcon process using a molybdenum (VI) catalyst, numerous Mo complexes<sup>7,18,19,22,74-79</sup> have been studied as epoxidation catalysts using alkylhydroperoxides as the oxidant such as  $\text{Mo}(\text{CO})_6$ <sup>7,27,63</sup> and  $\text{MoO}_2(\text{acac})_2$ <sup>18,22</sup> which display high selectivity. Mo (VI) catalysts have been shown to be very effective catalysts for the epoxidation of several olefins including small olefins, such as ethylene, as well as larger olefins such as 1-octene. Mo catalysts are efficient epoxidation catalysts employing alkylhydroperoxides as the oxidant; although using  $\text{H}_2\text{O}_2$  as the oxidant would lead to higher atom efficiency because the co-product generated is water as compared to alkylhydroperoxides which generate an alcohol as co-product. Due to the deactivation of Mo catalysts in the presence of water, numerous attempts have been made to protect the Mo catalysts by immobilization onto an inert support in order to employ  $\text{H}_2\text{O}_2$  as the oxidant.<sup>22,23,74</sup> However, the immobilized catalysts displayed low selectivities and low turnover frequency leading to a need for improvements.

Similar to Mo(VI) catalysts, tungsten(VI) catalysts have been developed for the epoxidation of olefins however hydrogen peroxide ( $\text{H}_2\text{O}_2$ ) is employed as the oxidant instead of alkyl hydroperoxides, leading to high atom efficiency.<sup>16,19,22,23,74</sup> Industrially, a mixture of  $\text{WO}_2\cdot 2\text{H}_2\text{O}/\text{H}_2\text{O}_2$  is used to produce epichlorohydrin which is used for the production of epoxy resins, glycerol, etc. (Scheme 1.8).<sup>3,7</sup> Although using  $\text{H}_2\text{O}_2$  as the oxidant decreases the amount of by-products generated, water is known to retard the reaction rate and also cause decomposition of the epoxide to glycols therefore water must be removed from the reaction medium. Biphasic systems are often used with chlorinated or aromatic solvents and display high selectivity (>90%) for simple aliphatic alkenes.<sup>7,16,17,21,74</sup> Since the choice of olefin is limited, a more versatile catalyst needs to be developed which maintains high catalytic activity.

### Scheme 1.8—Synthesis of epichlorohydrin

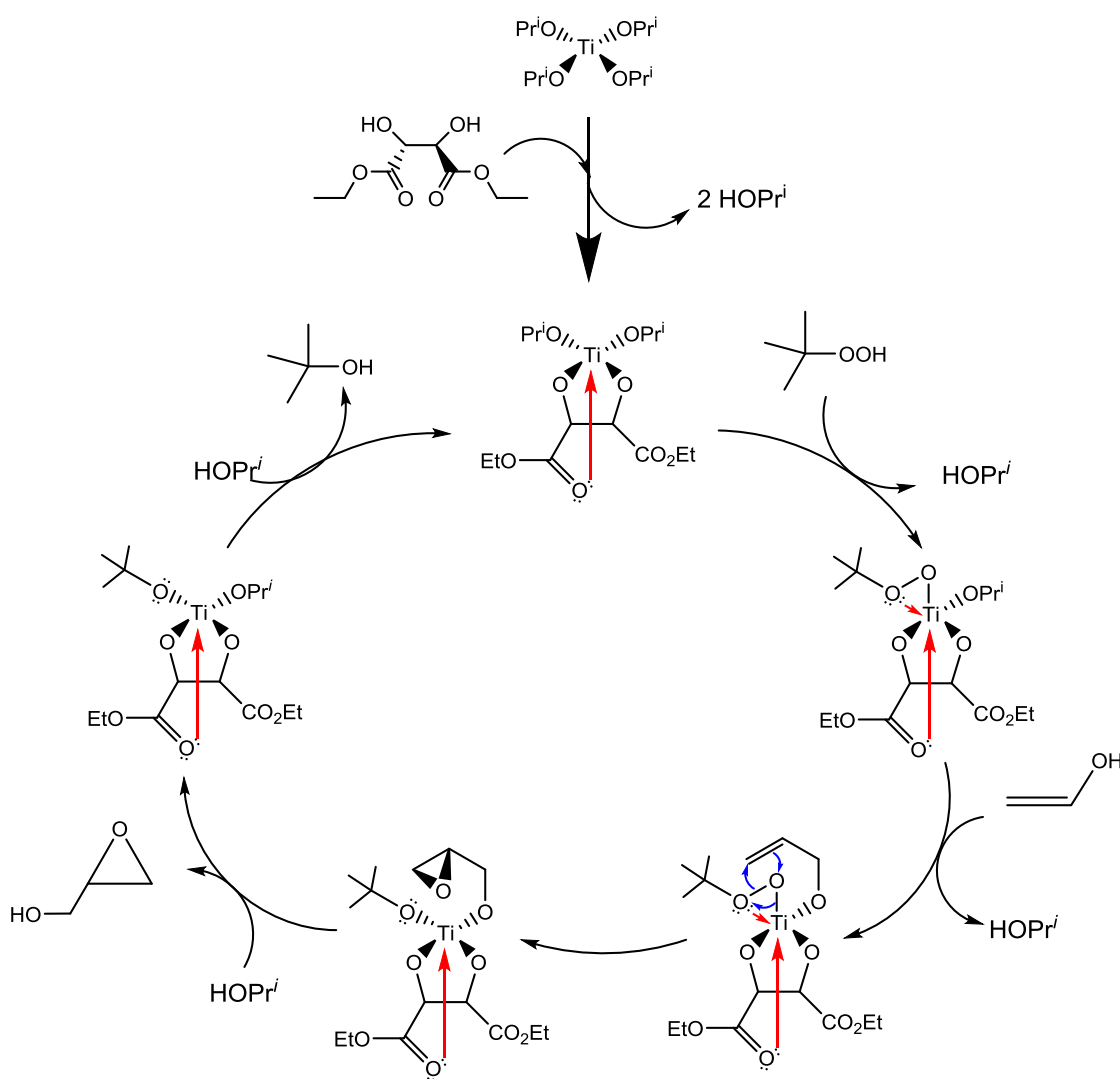


Due to higher Lewis acidity than Mo and W catalysts, vanadium (V) catalysts have been extensively studied<sup>7,18,19,28-30</sup> however they have been found to be less active compared to Mo catalysts except for the epoxidation of allylic alcohols where V catalysts are far superior compared to Mo catalysts.<sup>16,18,19,21,27</sup> The high catalytic activity of V catalysts for the epoxidation of allylic alcohols is presumably due to the higher Lewis acidity and oxophilicity of V compared to Mo catalysts. The high oxophilicity could allow the allylic alcohol to bind to the V center causing easier nucleophilic attack of the peroxy-oxygen by the olefin. Numerous other metals such as rhenium, ruthenium, zirconium, and iron complexes have been explored as epoxidation catalysts.<sup>7,16,18,19,22,74</sup> Oxorhenium (V) complexes<sup>20</sup> displayed catalytic activity for the epoxidation of cyclooctene albeit these catalysts are drastically slower compared to Mo, W, or Ti catalysts. Zr catalysts<sup>19,80</sup> have been shown to be less active compared to Ti catalysts however when  $\text{ZrO}_2$  was immobilized onto  $\text{SiO}_2$ , the epoxidation of 1-octene with TBHP as the oxidant was very selective albeit the support had to specifically be Aerosil- $\text{SiO}_2$ .<sup>80</sup> Iron (Fe) complexes<sup>25,81,82</sup> have also been tested with various different olefins however the yields are low (80%) compared to other metal catalysts such as Mo, W, or Ti.

Overall, the catalytically most active metals for the epoxidation of olefins are Mo, W, and V. However, when stereospecific olefins are employed, a racemic mixture was generated. Sharpless and coworkers were the first to develop an efficient asymmetric epoxidation catalyst consisting of  $\text{Ti}(\text{OPr}^i)_4$  in conjunction with a chiral tartrate diester; using TBHP as the oxidant (Scheme 1.9).<sup>7,48</sup> It was shown that the catalyst displayed high moisture sensitivity since the addition of


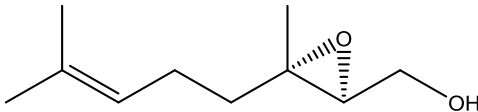
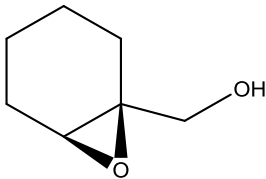
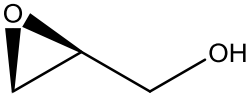
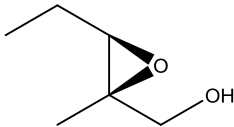
molecular sieves decreased the amount of catalyst required. Numerous olefins have been tested with Sharpless catalyst and are summarized in Table 1.3.<sup>7,19,48</sup> The main drawback is that there needed to be a directing group such as an allylic alcohol in order for the catalyst to be effective.

**Scheme 1.9**—Sharpless asymmetric epoxidation of olefins<sup>7,19,21,48</sup>



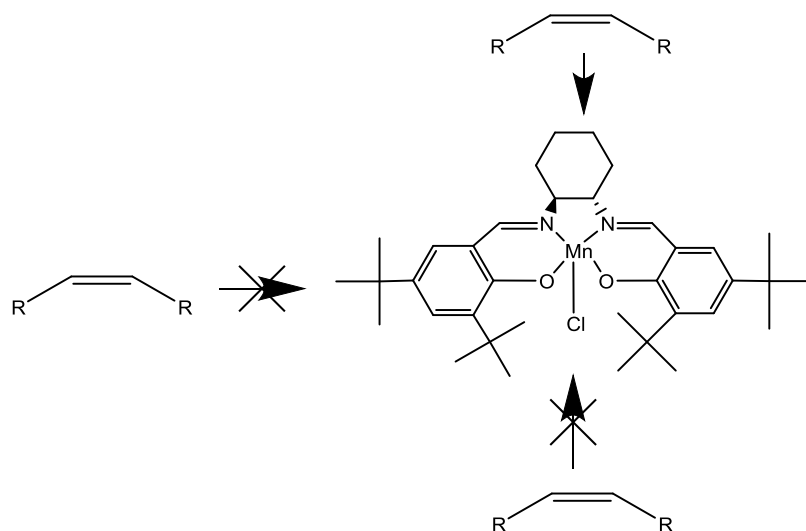


**Table 1.3**—Examples of olefins used in Sharpless asymmetric epoxidation<sup>19,48</sup>

Starting Material	Product	ee	Yield
(E)-2-Decen-1-ol		96 %	85 %
Geraniol		91 %	95 %
Cyclohexenylmethanol		77%	77 %
Allyl alcohol		90%	65 %
2-methyl-2-penten-1-ol		95 %	45 %

Akin to Sharpless' catalyst, Jacobsen's catalyst,<sup>7</sup> (Figure 1.5) a Mn (III) containing asymmetric salen-based catalyst is used in the synthesis of chiral epoxides with high enantiomeric purity.<sup>7</sup> Due to the steric environment around the metal center, the olefin does not need a directing group like the Sharpless catalyst. The stereochemistry around the metal center allows only one direction a *cis*-alkene can approach the metal center. However, the steric limitations also present a problem when terminal or *trans*-alkenes are used instead. Another drawback is the homogeneous nature of the catalyst, leading to a difficult to recycle catalyst.

**Figure 1.5—Jacobsen's catalyst<sup>7</sup>**

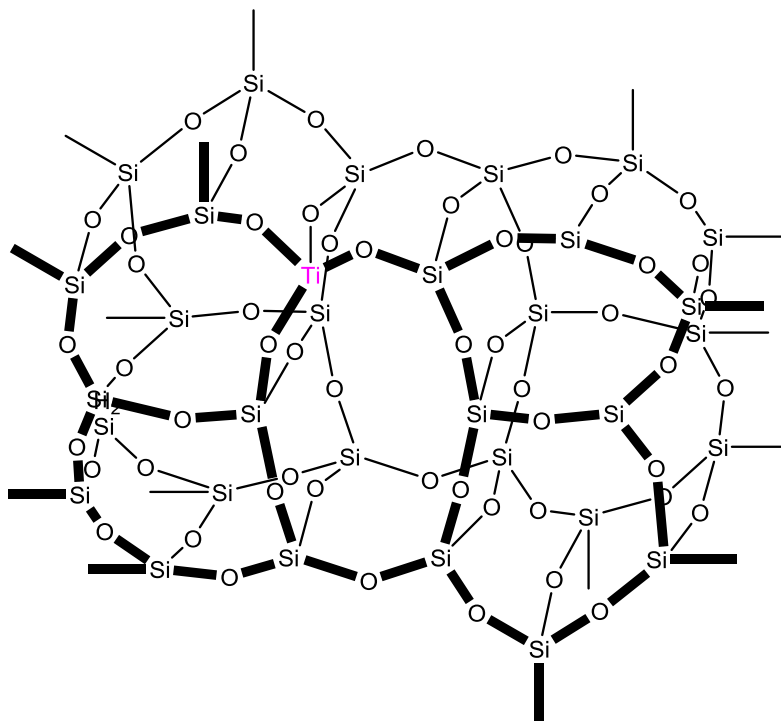


Due to the high catalytic activity of Jacobsen's catalyst, other manganese complexes were developed which mimicked catalysts found in nature.<sup>16,18,19,22,74</sup> Immobilized Mn (II)-hydrazide complex<sup>83</sup> displayed high selectivity for simple cyclic complexes using H<sub>2</sub>O<sub>2</sub> as the oxidant, albeit larger olefins such as stilbene were less efficient. Additionally, excess H<sub>2</sub>O<sub>2</sub> was required due to the decomposition of H<sub>2</sub>O<sub>2</sub> promoted by the catalyst. (Guanidine)manganese complexes<sup>73</sup> have also been used for the epoxidation of 1-octene however peracetic acid was used as the oxidant which generated a carboxylic acid as the by-product. Although there is some promise to Mn catalysts, numerous improvements need to be made in order for them to be industrially applicable.

Due to the excellent catalytic activity of titanium containing Sharpless' catalyst, industrial titanium catalysts were developed. Specifically the Shell catalyst (titania-on-silica, Figure 1.6)<sup>84</sup> employs alkyl hydroperoxides as the oxidant and TS-1 (titanium silicate-1)<sup>38,46,65,66,85</sup> uses H<sub>2</sub>O<sub>2</sub> as the oxidant. Both the Shell catalyst and TS-1 are heterogeneous and are very efficient for the epoxidation of small olefins such as cyclohexene. However, they are less effective using more demanding olefins, such as bulky olefins or allylic alcohols

due to the structural limitations of the catalysts. While numerous other supports,<sup>33,38,47,59,64,69,86-89</sup> such as MCM-41,<sup>47,51,56,90</sup> SBA-15,<sup>52,62,91</sup> and zeolites,<sup>41,92,93</sup> have been used in order to alleviate the steric limitations of TS-1, the resulting catalysts are less efficient for alkene epoxidation with H<sub>2</sub>O<sub>2</sub> than TS-1. The lower activity is due to the larger pores present in the catalysts, allowing water to deactivate the active site.<sup>69</sup>

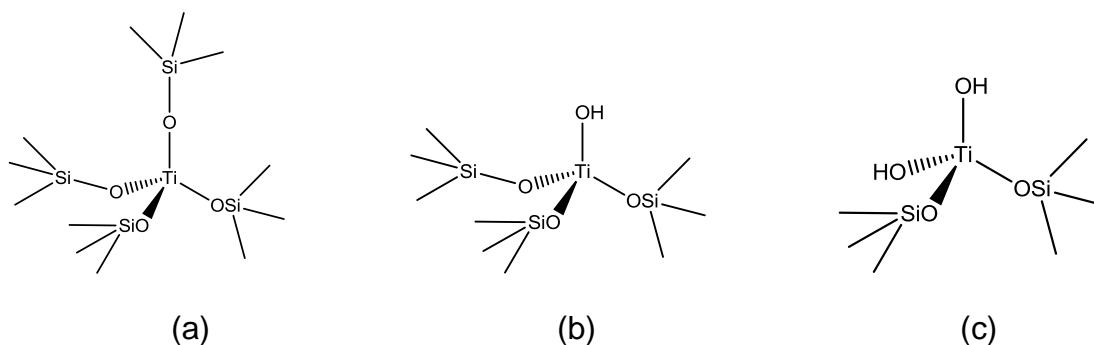
**Figure 1.6**—Generalized, condensed structure of titania silica supports<sup>45,46</sup>



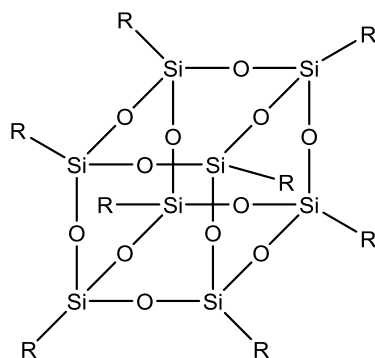
Both the Shell catalyst (titania-on-silica) and TS-1 contain multiple titanium (Ti) structural frameworks such as bipodal, tripodal, and tetrapodal sites (Figure 1.7). Polyhedral oligomeric silsesquioxanes (POSS, Figure 1.8)<sup>36,94-100</sup> complexes were developed as well-defined, homogeneous, model compounds to investigate which Ti structural framework (in the Shell catalyst and TS-1) displayed the highest catalytic activity.<sup>31,39,40,43,45,50,53,101</sup> Looking at the

mechanism for olefin epoxidation using Ti catalysts (Scheme 1.10), the first step is the formation of a Ti-OOR (R=H or alkyl) species followed by nucleophilic attack of the olefin in order to generate the epoxide. This means that a high Lewis acidic metal center will withdraw electron density from the oxygen making it easier for the olefin to attack. Tetrapodal Ti silsesquioxane exhibits the highest Lewis acidity,<sup>39,40</sup> compared to tripodal and bipodal, due to the electron withdrawing nature of the silsesquioxane ligand which is similar to that of a CF<sub>3</sub> group.<sup>41,102</sup> Even though a high Lewis acidic Ti center is preferred, the Ti center must also be accessible to the reactants. Thus, using 1-octene as the olefin and *tert*-butyl hydroperoxide (TBHP) as the oxidant (Table 1.4), tripodal Ti silsesquioxane complexes displayed high selectivities, yield, and turnover frequencies (TOF)<sup>37,39,40,42</sup> due to a balance between sterics and electronics. All structural frameworks of Ti displayed some catalytic activity for the epoxidation of 1-octene (Table 1.4), however, tripodal Ti displayed superior activity compared to bipodal titanium silsesquioxane, tetrapodal titanium silsesquioxane, Shell catalyst, and Mo based catalysts (Table 1.4).

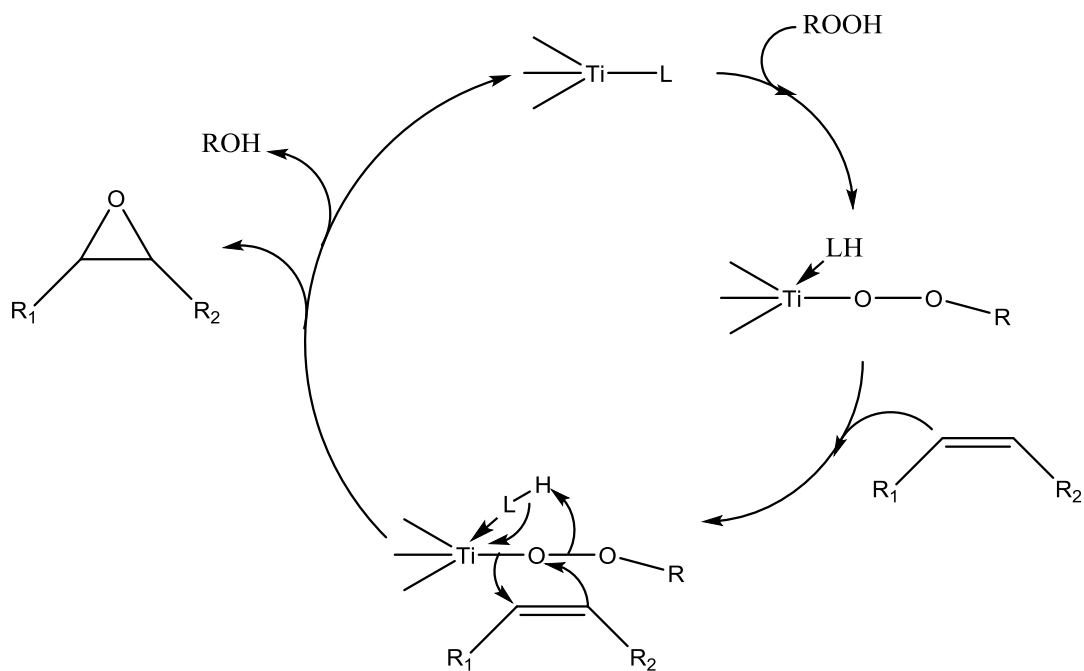
**Figure 1.7**— Possible titanium site structures in heterogeneous titanosilicates: (a) tetrapodal, (b) tripodal, and (c) bipodal<sup>40</sup>



**Figure 1.8**—Structure of polyhedral oligomeric silsesquioxanes (POSS)



**Scheme 1.10**—Catalytic mechanism of epoxidation reaction with  $\text{Ti}^{40,43,45,50}$



**Table 1.4**—Ti containing catalysts for the epoxidation of 1-octene<sup>40</sup>

Catalyst	$k_2 \times 10^2$ ( $\text{dm}^3 \text{mol}^{-1} \text{s}^{-1}$ )	Selectivity to epoxide (%)
$\text{MoO}_2(\text{acac})_2$	31	92
$\text{Mo}(\text{CO})_6$	6.1	94
$\text{TiO}_2/\text{SiO}_2$ (Shell Catalyst)	18.3	97
$\text{Ti}(\text{OPr})_2\{(\text{C}-\text{C}_6\text{H}_{11})_7\text{Si}_7\text{O}_{11}(\text{OSiMe}_3)\}$	9.3	75
$\text{Ti}\{(\text{C}-\text{C}_6\text{H}_{11})_7\text{Si}_7\text{O}_{11}(\text{OSiMe}_3)\}_2$	4.7	83
$\text{Ti}(\text{NMe}_2)\{(\text{C}_6\text{H}_{11})_7\text{Si}_7\text{O}_{12}\}$	139	99
$\text{Ti}(\text{NMe}_2)\{i\text{C}_4\text{H}_9\}_7\text{Si}_7\text{O}_{12}\}$	80	97

Conditions(1-octene): T= 353 K, Ti=0.2 mmol, TBHP=30mmol, 1-octene (75g) as solvent.

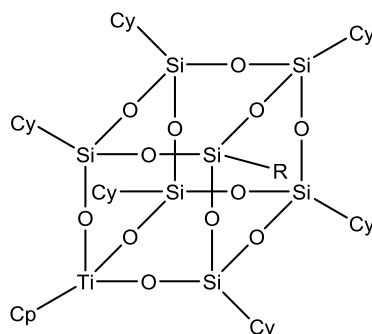
Given that tripodal titanium catalysts have been shown to be excellent catalysts for terminal olefins (1-octene) and simple cyclic olefins (cyclohexene or cyclooctene), the versatility of these complexes needs be investigated in order to fully determine their potential as efficient alkene epoxidation catalysts. Additionally, due to high catalytic activity, tripodal titanium silsesquioxane complexes are ideal candidates for immobilization in order to generate a robust, heterogeneous catalyst.

Immobilization of tripodal titanium onto a hydrophobic support would generate catalysts that had advantages of both homogeneous and heterogeneous materials. The active site would be uniform, easily accessible, and spatially isolated while the catalyst would be reusable and potentially more resistant to hydrolysis, making it more robust. Additionally, TBHP can be substituted with  $\text{H}_2\text{O}_2$  as the oxidant, leading to higher atom efficiency.  $\text{H}_2\text{O}_2$  cannot be employed as the oxidant using homogeneous tripodal Ti silsesquioxane catalysts since water deactivates the catalysts via hydrolysis of

the Ti to form  $\text{TiO}_2$ , a thermodynamically favorable reaction. Previously, heterogenization of titanium silsesquioxane complexes has been accomplished by attachment to a polymer or silica support,<sup>1,41,52,55,58,59,62,91,103,104</sup> or alternatively, by encapsulation in polydimethylsiloxane (PDMS) membrane.<sup>32</sup>

Although less active than tripodal Ti, tetrapodal titanium silsesquioxanes were successfully tethered onto mesoporous silica supports such as SBA-15<sup>62,91,104</sup> and dimethyl-silyl functionalized silica.<sup>58,59</sup> However, both types of immobilized catalysts displayed low conversions due in part to the less catalytically active tetrapodal titanium. Epoxidation of cyclooctene with TBHP catalyzed by  $\text{CpTi}[(\text{c-C}_5\text{H}_9)_7\text{Si}_7\text{O}_{12}]$  impregnated onto a silica support was investigated (Figure 1.9),<sup>54</sup> however only 39% yield of epoxide was observed after 4 hours leading to a turnover frequency (TOF) of  $20 \text{ hr}^{-1}$ . Under the same reaction conditions, homogeneous tetrapodal Ti ( $\text{Ti}[(\text{c-C}_5\text{H}_9)_8\text{Si}_8\text{O}_{13}]_2$ ) displayed 29% yield after 1.5 hours leading to a TOF of 39. When more demanding olefins were used such as limonene, the TOF was reduced to  $11\text{-}14 \text{ hr}^{-1}$  suggesting that improvements need to be made in order to develop a more efficient catalyst.<sup>54</sup> Additionally, when tetrapodal titanium POSS was tethered onto SBA-15 via a covalent linkage,<sup>104</sup> the Ti loading could not be altered and achieved a maximal loading of 0.3 wt% due to the physical limitations of the anchoring. Nonetheless, the catalyst displayed high selectivities (>85%) for the conversion of limonene although, only 30% of the olefin had been converted after 24 hours. The successful attachment of tetrapodal titanium POSS onto the silica support was confirmed by conducting a leaching study where no titanium was observed in the reaction medium although it is believed the POSS moiety was mainly on the surface of SBA-15.<sup>104</sup>

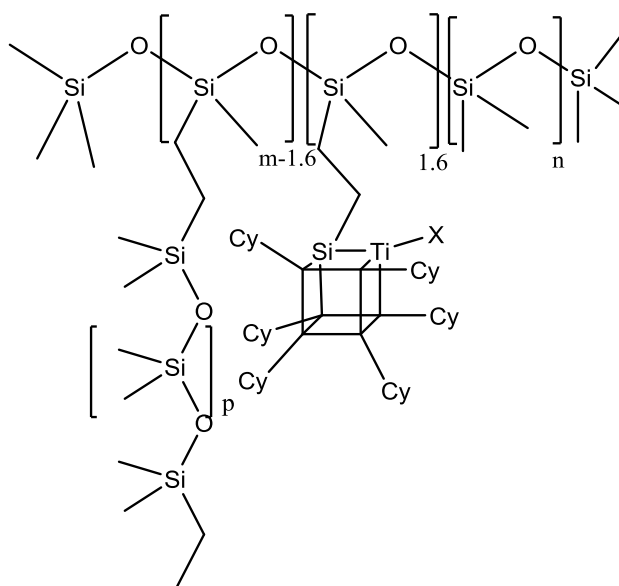
**Figure 1.9**— $\text{CpTi}[(\text{c-C}_5\text{H}_9)_7\text{Si}_7\text{O}_{12}]^{54}$



Heterogenization of tripodal titanium silsesquioxane was accomplished by grafting tripodal Ti onto a methylhydrosiloxane-dimethylsiloxane co-polymer followed by crosslinking with a vinyl-terminated siloxane polymer to form an insoluble organosilicon material (netted polysiloxysilane) that enclosed the Ti in a hydrophobic cavity (Figure 1.10).<sup>55</sup> This method allowed for the size of the cavity, used to encapsulate titanium, to be tuned for optimum accessibility by varying the starting materials. Epoxidation of cyclooctene with  $\text{H}_2\text{O}_2$  catalyzed by grafted tripodal Ti gave 80% yield of the epoxide and after hot filtration, the catalyst could be reused suggesting that this catalyst is indeed heterogeneous. When larger olefins were used, such as cyclododecane and 1-octene, the yield decreased to 45% and 62%, respectively. For the epoxidation of 1-octene, the catalyst displayed a TOF of  $20 \text{ hr}^{-1}$  where TS-1, under similar reaction conditions, has a TOF of  $80 \text{ hr}^{-1}$ .<sup>55</sup> Major drawbacks of this series of catalysts include lower activity compared to TS-1, difficulty in controlling the 3-D structure of the polymer which protects the Ti center, as well as numerous synthetic steps to generate active catalysts.



**Figure 1.10**—Tripodal Ti POSS tethered onto a linear polymer<sup>55</sup>



Lastly, tripodal titanium silsesquioxane has been successfully encapsulated within polydimethylsiloxane (PDMS) membrane and displayed high selectivity when the epoxidation of cyclohexene and 1-octene was explored.<sup>32</sup> PDMS is a hydrophobic elastomer providing a non-polar environment around the titanium center, preventing catalyst deactivation. Jacobsen's catalyst was encapsulated in PDMS and displayed high catalytic activity suggesting that PDMS was an ideal inert, hydrophobic support.<sup>105</sup> Although the epoxidation of 1-octene and cyclohexene catalyzed by immobilized tripodal titanium using  $H_2O_2$  as the oxidant showed excellent activity, the choice of solvent was limited to acetonitrile and methanol since only solvents that would not appreciably swell the PDMS membrane could be employed. If the membrane swelled, the pores would become larger and the catalysts would leach into solution due to the catalyst being held within the membrane simply by van der Waals interactions.<sup>32</sup> A new catalyst needs to be developed that displays higher versatility in solvents compared to tripodal Ti physically trapped in PDMS while maintaining high selectivity and catalytic activity.

## 1.4 Objective and Dissertation Outline

Tripodal titanium catalysts have been shown to be excellent catalysts for alkene epoxidation however the versatility of these catalysts has yet to be determined. Chapter 2 and 3 demonstrates that tripodal titanium effectively catalyzes the conversion of terminal, cyclic, and demanding olefins (limonene and  $\alpha$ -pinene) employing TBHP as the oxidant with high selectivity and excellent turnover frequency (TOF) making these catalysts excellent candidates for heterogenization.

Heterogenization of tripodal titanium would allow for the generation of catalysts which ideally display similar catalytic activity compared to the homogeneous analogs, and allow for versatility in solvents and oxidants that can be used. In addition, the catalysts would be reusable and be easily repaired when a loss in activity is observed. Chapter 2 discusses the successful immobilization of tripodal titanium onto a hydrophobic hyperbranched polymer. Hyperbranched polymers have recently attracted a lot of attention due to numerous advantageous properties; robust, inert, thermally stable, and easy to synthesize.<sup>106,107</sup> Immobilized tripodal Ti yielded very selective catalysts for the epoxidation of 1-octene with TBHP as the oxidant therefore, the versatility of these catalysts was explored in chapter 3, ranging from cyclic compounds to more demanding olefins such as limonene and  $\alpha$ -pinene. Remarkably, immobilized tripodal Ti catalysts remained very selective for cyclic olefins as well as limonene, showing similar selectivities compare to homogeneous analogs. Deviation from the selectivity displayed by the homogeneous analog was observed for  $\alpha$ -pinene however the heterogeneous tripodal Ti catalysts developed displayed higher selectivities compared to other Ti based heterogeneous analogs.

Immobilization allows for a more robust catalyst which can be recycled therefore chapter 2 and 3 discuss the recyclability of immobilized tripodal Ti catalysts using 1-octene and limonene as substrates. Even though the catalysts lost some activity after five recycles, the catalysts was easily repaired and

displayed identical catalytic activity compared to the pristine catalysts. Chapter 3 also divulges that the immobilized tripodal Ti catalysts are not diffusion controlled. This was accomplished by determining the apparent activation energy for heterogeneous complexes and comparing the values to the values for homogeneous analogs. Additionally, the stirring rate was altered where the initial rate constant remained unchanged suggesting that indeed, the rate of reaction is not diffusion limited.

Versatility of the oxidant was then explored in Chapter 4 when preliminary studies were conducted for the epoxidation of cyclohexene with  $\text{H}_2\text{O}_2$  catalyzed by tripodal Ti immobilized onto hyperbranched polysiloxysilane polymer. Using  $\text{H}_2\text{O}_2$  as the oxidant would allow for higher atom efficiency and the by-product would be water which is non-toxic thus limiting the environmental impacts associated with epoxidation reactions. As discussed previously, homogeneous tripodal Ti catalysts cannot withstand water due to hydrolysis. However, by immobilizing tripodal Ti onto a hydrophobic hyperbranched polymer, the amount of water reaching the Ti center would be limited generating active catalysts for the epoxidation of cyclohexene. Preliminary results demonstrated that water is very detrimental to the Ti catalysts and only biphasic solvent systems displayed good selectivities. Additional precautions were explored in order to limit the amount of water present in the reaction medium such as the addition of anhydrous  $\text{Na}_2\text{SO}_4$  (sodium sulfate) and using a phase transfer agent. Optimization of the reaction conditions yielded catalysts that were active for the epoxidation of cyclohexene with  $\text{H}_2\text{O}_2$  and displayed good selectivities.

As discussed previously, ethylene oxide (EO) is produced via epoxidation of ethylene using a Ag catalyst however when propene was employed, the catalyst was inefficient due to the presence of easily oxidized allylic hydrogens. Numerous attempts have been made to optimize the Ag catalyst for the direct epoxidation of propene however they are still ineffective. Recently, gold dispersed onto titanium containing silica supports have shown to be active catalysts for the direct epoxidation of propene. Immobilization of tripodal titanium

silsesquioxanes onto gold nanoparticles was explored in chapter 5 where the gold nanoparticles would generate  $H_2O_2$  *in situ* followed by the formation of the Ti-OOH species in order to successfully synthesize propylene oxide (PO).

Finally, chapter 6 will give concluding remarks as well as elucidate future directions which can be explored in order to optimize the catalysts developed within this dissertation.

## Chapter 2: Selective Epoxidation of 1-Octene with *tert*-Butyl Hydroperoxide Catalyzed by Tripodal Titanium Silsesquioxane Complexes Grafted to Hyperbranched Polysiloxysilane Matrices.

Note—This chapter was reprinted from

Peak, S.M.; Crocker, M.; Ladipo, F.T. Selective Epoxidation of 1-Octene with *tert*-Butyl Hydroperoxide Catalyzed by Tripodal Titanium Silsesquioxane Complexes Grafted to Hyperbranched Polysiloxysilane Matrices. *Catalysis Science & Technology* **2015**, Submitted

### 2.1. Introduction

Alkene epoxidation is not only important in the manufacture of bulk chemicals, but is also a widely used transformation in the fine chemicals industry.<sup>108-110</sup> While a number of homogeneous and heterogeneous alkene epoxidation catalysts that utilize alkyl hydroperoxides (ROOH) as the oxidant have been developed,<sup>111-114</sup> there is a continuing need for the development of catalysts which display both high activity and product selectivity, as well as high atom efficiency with respect to utilization of the oxidant. In this context, studies of titanium silsesquioxane complexes as well-defined homogeneous models for heterogeneous titanium-based alkene epoxidation catalysts have revealed that they are among the most active and most selective catalysts for the epoxidation of unactivated alkenes with alkyl hydroperoxides.<sup>40,50,84</sup> These studies have further shown that tripodal titanium silsesquioxane complexes are intrinsically more active and selective than related heterogeneous catalysts, such as titanium silicalite-1 (TS-1),<sup>38,115,116</sup> titania-on-silica,<sup>84,117</sup> and titania-silica mixed oxides,<sup>69</sup> which invariably contain non-uniform titanium sites that show different degrees of activity in catalyzing alkene epoxidation and/or peroxide decomposition.<sup>84,118-120</sup> The outstanding catalytic properties of tripodal titanium silsesquioxane complexes have largely been attributed to both the electron-withdrawing and steric properties of tripodal silsesquioxane ligand, which give rise to an optimal balance between high Lewis acidity and steric accessibility of the titanium center.<sup>40</sup> Given the

excellent promise of tripodal titanium silsesquioxane complexes as homogeneous catalysts, their use as precursors for the preparation of well-defined heterogeneous alkene epoxidation catalysts is highly attractive. In this regard, impregnation of the pores of MCM-41 with a tripodal titanium silsesquioxane complex followed by silylation of the outer surface of the MCM-41 with a bulky silane (to prevent leaching of the silsesquioxane complex) has been reported to furnish a material that was active for catalytic epoxidation of alkenes with *t*-butyl hydroperoxide (TBHP).<sup>121</sup> Furthermore, although control of their three-dimensional structure appears difficult, hydrophobic titanium polysiloxane materials that exhibited catalytic activity in alkene epoxidation with aqueous hydrogen peroxide (H<sub>2</sub>O<sub>2</sub>) have been prepared from tripodal titanium vinyl-silsesquioxane complexes, by in-situ copolymerization on a mesoporous SBA-15-supported polystyrene polymer,<sup>62</sup> or by grafting onto a siloxane copolymer (via Pt-catalyzed hydrosilylation) and crosslinking of the resulting polymer with a vinyl-terminated siloxane polymer.<sup>55</sup> Recently, we described the preparation of heterogeneous alkene epoxidation catalysts by encapsulation of tripodal Ti silsesquioxane complexes in polydimethylsiloxane (PDMS) membrane, thereby ensuring a hydrophobic environment around the titanium complex.<sup>32</sup> The catalysts displayed high activity, as well as excellent epoxide selectivity and H<sub>2</sub>O<sub>2</sub> efficiency, for cyclohexene- and 1-octene epoxidation with aqueous H<sub>2</sub>O<sub>2</sub>. Furthermore, the catalysts were highly recyclable.

Herein, we describe the preparation of Ti silsesquioxane catalyst materials via immobilization of tripodal Ti silsesquioxane complexes by covalent linkage to hyperbranched polysiloxysilane matrices, as well as results of preliminary studies of the efficiency of the materials for catalytic alkene epoxidation with *t*-butyl hydroperoxide (TBHP). In contrast to encapsulation of tripodal Ti silsesquioxane complexes in PDMS membrane, which relies on physical entrapment of the catalyst and thereby limits epoxidation reactions to solvents (acetonitrile and methanol) that promote catalyst retention in the membrane by not appreciably swelling PDMS,<sup>32</sup> covalent linkage of tripodal Ti silsesquioxane complexes to a hydrophobic hyperbranched polysiloxysilane matrix offers the opportunity for

greater flexibility in solvent choice while retaining the well-defined molecular features required for detailed analysis of catalytic events. In this context, it is noteworthy that hyperbranched polysiloxysilanes<sup>106,107,122-125</sup> are very attractive for commercial applications since they are easily prepared via a variety of one-step synthetic routes, which can reduce costs and environmental impacts. Equally important, characteristic properties of hyperbranched polysiloxysilanes include hydrophobicity, a wide interval of thermal and thermo-oxidative stability, and resistance against different chemical factors and environments.<sup>106,107,122-125</sup>

## 2.2 Experimental Methods

### 2.2.1 Materials and methods

All experiments were performed under an atmosphere of nitrogen either using standard Schlenk techniques or in a Vacuum Atmospheres glovebox. Solvents were dried and distilled by standard methods before use.<sup>126</sup> All solvents were stored in glovebox over 4Å molecular sieves that had been dried in a vacuum oven at 250 °C for at least 24 hours before use. All glassware were dried in an oven at 110 °C for 24 hours before use. Unless otherwise stated, all reagents were purchased from Aldrich Chemical Company and used without further purification. TBHP (5.5 M in nonane) and 1-octene were stored over 4Å molecular sieves in the glovebox along with Ti(NMe<sub>2</sub>)<sub>4</sub>. Allylisobutyl POSS (CH<sub>2</sub>=CHCH<sub>2</sub>(*i*-Bu)<sub>7</sub>Si<sub>8</sub>O<sub>12</sub> (**1**)), trisilanol isobutyl POSS, octaisobutyl POSS and trisilanol cyclohexyl POSS were purchased from Hybrid Plastics Inc. and dried overnight under vacuum at 50 °C prior to use. Platinum divinyl tetramethyl disiloxane (2.4% in xylene, Karstedt's catalyst), chlorodimethylsilane, vinyl dimethylchlorosilane, triethylsilane, and trichlorosilane were purchased from Gelest Inc. and used without further purification. Celite and activated charcoal were dried in a vacuum oven at 150 °C for 24 hours before use. The compounds [Ti(NMe<sub>2</sub>)<sub>2</sub>[(*i*-C<sub>4</sub>H<sub>9</sub>)<sub>7</sub>Si<sub>7</sub>O<sub>12</sub>]] (**9**)<sup>32</sup> and [Ti(NMe<sub>2</sub>)<sub>2</sub>[(*c*-C<sub>6</sub>H<sub>11</sub>)<sub>7</sub>Si<sub>7</sub>O<sub>12</sub>]] (**10**)<sup>40</sup> were prepared by literature methods. Vinyl-terminated hyperbranched polysiloxysilane **P1** (Scheme 3) was synthesized via Pt-catalyzed polymerization of HSi(OSiMe<sub>2</sub>CH=CH<sub>2</sub>)<sub>3</sub>,<sup>106</sup> and isolated as a viscous oil with molecular weight

( $M_n$ ) and polydispersity index (PDI) of 9318 g mol<sup>-1</sup> and 1.93, respectively. NMR (<sup>1</sup>H, <sup>13</sup>C, & <sup>29</sup>Si) and IR data of **P1** are consistent with literature data (see supplementary information).

<sup>1</sup>H, <sup>13</sup>C, and <sup>29</sup>Si NMR spectra were recorded on a Varian INOVA 400 MHz spectrometer employing VnmrJ software. All chemical shifts are reported in units of  $\delta$  (downfield of tetramethylsilane) and <sup>1</sup>H & <sup>13</sup>C chemical shifts were referenced to residual solvent peaks. <sup>29</sup>Si NMR spectra were recorded using inverse-gated proton decoupling in order to increase resolution and minimize nuclear Overhauser enhancement effects. To ensure accurate integrated intensities, [Cr(acac)<sub>3</sub>] (0.05 M) was added to <sup>13</sup>C and <sup>29</sup>Si NMR samples as a shiftless relaxation agent and a delay of at least 5 s was used between observation pulses for <sup>13</sup>C measurements and 10 s for <sup>29</sup>Si measurements.

GLC analyses were performed on an Agilent HP 6890 GC instrument equipped with a flame ionization detector (FID). A 1.0  $\mu$ L injection was employed and helium was used as the carrier gas. The FID was set to 300 °C and the inlet was isothermally maintained at 140 °C in split mode (split ratio 50:1; split flow 221 ml/min). An Agilent J&W HP-1 column (25 m  $\times$  320  $\mu$ m  $\times$  0.52  $\mu$ m) rated to 350 °C was employed, maintaining a constant pressure of 14.5 psi. The oven parameters were programmed to start at 35 °C; followed by a ramp of 45 °C/min to 200 °C and held for 2 minutes. The total run time was 8.67 minutes. Quantification was performed through the use of toluene as an internal standard. Chromatographic programming was performed using Agilent Chemstation software. Conversion and selectivity were calculated as follows:

$$\text{Conversion} = \frac{\text{moles of TBHP consumed}}{\text{initial moles of TBHP}} \times 100 \quad \text{Selectivity} = \frac{\text{moles of epoxyoctane formed}}{\text{moles of TBHP consumed}} \times 100$$

IR spectra were recorded on a Thermo Scientific Nicolet iS10 FT-IR Spectrometer. UV-vis spectra were collected on a Thermo Scientific Evolution 201 spectrophotometer using pentane solutions sealed in 1 cm cuvettes under N<sub>2</sub>. Gel permeation chromatography (GPC) analyses were carried out on an



Agilent Technologies PL-GPC 50 Integrated GPC equipped with a UV detector and a refractive index detector, as well as a Polymer Laboratories PL-AS RT GPC autosampler. The GPC was equipped with two PL gel Mini-MIX C columns (5 micron, 4.6 mm ID). The GPC columns were eluted with tetrahydrofuran at 30 °C at 0.3 mL/min and were calibrated using monodisperse polystyrene standards. Elemental analyses were performed by either Robertson Microlit laboratories or Galbraith laboratories, and typically included the use of a combustion aid. Proton-induced X-ray emission (PIXE) analyses were performed by Elemental Analysis Inc.

## 2.2.2. Catalyst Preparation

### 2.2.2.1. Synthesis of $\text{Et}_3\text{Si}(\text{CH}_2)_3(i\text{-C}_4\text{H}_9)_7\text{Si}_8\text{O}_{12}$ (**2**)

In a glovebox, fifteen drops of Karstedt's catalyst (tetramethyldivinyl disiloxane-platinum in xylenes) was added to a slurry of allylisobutyl POSS  $\text{CH}_2=\text{CHCH}_2(i\text{-C}_4\text{H}_9)_7\text{Si}_8\text{O}_{12}$  (**1**, 10.0 g, 11.7 mmol) and  $\text{Et}_3\text{SiH}$  (25 mL) in a thick-walled glass reactor equipped with a stir-bar. The reaction vessel was sealed with a Teflon screw-cap, placed in an oil bath maintained at 60 °C and allowed to stir overnight (~16 h). The reaction mixture quickly became homogeneous upon heating, yielding a dark brown solution. At completion, excess  $\text{Et}_3\text{SiH}$  was removed under reduced pressure to give an off-white solid, which was dissolved in diethyl ether (40 mL). The ether solution was transferred into a flask containing activated charcoal and stirred for 3 h. The ether suspension was filtered through Celite to remove activated charcoal and the filtrate was evaporated under reduced pressure to give  $\text{Et}_3\text{Si}(\text{CH}_2)_3(i\text{-C}_4\text{H}_9)_7\text{Si}_8\text{O}_{12}$  (**2**) as a white solid. Yield: 9.90 g, 90%.  $^1\text{H}$  NMR ( $\text{CDCl}_3$ ):  $\delta$  0.47 (q,  $^3J_{\text{H-H}} = 7.6$  Hz, 6 H,  $\text{Si}(\text{CH}_2\text{CH}_3)_3$ ), 0.58 (d,  $^3J_{\text{H-H}} = 8.0$  Hz, 14 H,  $\text{CH}_2\text{CH}(\text{CH}_3)_2$ ), 0.59 (t, partially overlapped, 2 H,  $\text{CH}_2\text{CH}_2\text{CH}_2\text{SiEt}_3$ ), 0.65 (t, 2 H,  $\text{CH}_2\text{CH}_2\text{CH}_2\text{SiEt}_3$ ), 0.89 (t,  $^3J_{\text{H-H}} = 7.6$  Hz, 9 H,  $\text{Si}(\text{CH}_2\text{CH}_3)_3$ ), 0.93 (d,  $^3J_{\text{H-H}} = 6.4$  Hz, 42 H,  $\text{CH}_2\text{CH}(\text{CH}_3)_2$ ), 1.41 (m, 2 H,  $\text{CH}_2\text{CH}_2\text{CH}_2\text{SiEt}_3$ ), 1.83 (sept,  $^3J_{\text{H-H}} = 6.8$  Hz, 7 H,  $\text{CH}_2\text{CH}(\text{CH}_3)_2$ ).  $^{13}\text{C}\{^1\text{H}\}$  NMR ( $\text{CDCl}_3$ ):  $\delta$  3.3 ( $\text{Si}(\text{CH}_2\text{CH}_3)_3$ ), 7.4 ( $\text{Si}(\text{CH}_2\text{CH}_3)_3$ ), 16.8 ( $\text{CH}_2\text{CH}_2\text{CH}_2\text{SiEt}_3$ ), 17.4 ( $\text{CH}_2\text{CH}_2\text{CH}_2\text{SiEt}_3$ ), 22.5 (br s,  $\text{CH}_2\text{CH}(\text{CH}_3)_2$ ), 23.8 (br s,  $\text{CH}_2\text{CH}(\text{CH}_3)_2$  and  $\text{CH}_2\text{CH}_2\text{CH}_2\text{SiEt}_3$ ), 25.7 (br s,  $\text{CH}_2\text{CH}(\text{CH}_3)_2$ ).  $^{29}\text{Si}$  NMR

(CDCl<sub>3</sub>):  $\delta$  6.2 (SiEt<sub>3</sub>), -67.6, -67.8, -67.9 (overlapping singlets, 1:3:3:1, SiCH<sub>2</sub>CHMe<sub>2</sub> and Si(CH<sub>2</sub>)<sub>3</sub>SiEt<sub>3</sub>).

#### 2.2.2.2. Synthesis of ClMe<sub>2</sub>Si(CH<sub>2</sub>)<sub>3</sub>(i-C<sub>4</sub>H<sub>9</sub>)<sub>7</sub>Si<sub>8</sub>O<sub>12</sub> (**3**)

In a glovebox, fifteen drops of Karstedt's catalyst (tetramethyldivinyl disiloxane-platinum in xylenes) was added to a slurry of allylisobutyl POSS CH<sub>2</sub>=CHCH<sub>2</sub>(i-C<sub>4</sub>H<sub>9</sub>)<sub>7</sub>Si<sub>8</sub>O<sub>12</sub> (**1**, 10.0 g, 11.7 mmol) and HSiMe<sub>2</sub>Cl (25 mL) in a thick-walled glass reactor equipped with a stir-bar. The reaction vessel was sealed with a Teflon screw-cap, placed in an oil bath maintained at 60 °C and stirred overnight (~16 h). The reaction mixture quickly became homogeneous upon heating, yielding a brown solution. At completion, excess HSiMe<sub>2</sub>Cl was removed under reduced pressure to give an off-white solid, which was dissolved in diethyl ether (40 mL). The ether solution was transferred into a flask containing activated charcoal and stirred for 3 h. The ether suspension was filtered through Celite to remove activated charcoal and the filtrate was evaporated under reduced pressure to give ClMe<sub>2</sub>Si(CH<sub>2</sub>)<sub>3</sub>(i-C<sub>4</sub>H<sub>9</sub>)<sub>7</sub>Si<sub>8</sub>O<sub>12</sub> (**3**) as a white solid. Yield: 9.79 g, 88%. <sup>1</sup>H NMR (CDCl<sub>3</sub>):  $\delta$  0.37 (s, 6 H, Si(CH<sub>3</sub>)<sub>2</sub>Cl), 0.58 (d, <sup>3</sup>J<sub>H-H</sub> = 7.0 Hz, 14 H, CH<sub>2</sub>CH(CH<sub>3</sub>)<sub>2</sub>), 0.68 (t, <sup>3</sup>J<sub>H-H</sub> = 8.0 Hz, 2 H, CH<sub>2</sub>CH<sub>2</sub>CH<sub>2</sub>SiMe<sub>2</sub>Cl), 0.88 (t, <sup>3</sup>J<sub>H-H</sub> = 8.0 Hz, 2 H, CH<sub>2</sub>CH<sub>2</sub>CH<sub>2</sub>SiMe<sub>2</sub>Cl), 0.94 (d, <sup>3</sup>J<sub>H-H</sub> = 6.4 Hz, 42 H, CH<sub>2</sub>CH(CH<sub>3</sub>)<sub>2</sub>), 1.53 (m, 2 H, CH<sub>2</sub>CH<sub>2</sub>CH<sub>2</sub>SiMe<sub>2</sub>Cl), 1.84 (sept, <sup>3</sup>J<sub>H-H</sub> = 6.8 Hz, 7 H, CH<sub>2</sub>CH(CH<sub>3</sub>)<sub>2</sub>). <sup>13</sup>C{<sup>1</sup>H} NMR (CDCl<sub>3</sub>):  $\delta$  1.6 (Si(CH<sub>3</sub>)<sub>2</sub>Cl), 15.9 (CH<sub>2</sub>CH<sub>2</sub>CH<sub>2</sub>SiMe<sub>2</sub>Cl), 16.6 (CH<sub>2</sub>CH<sub>2</sub>CH<sub>2</sub>SiMe<sub>2</sub>Cl), 22.5 (CH<sub>2</sub>CH(CH<sub>3</sub>)<sub>2</sub>), 23.8 (CH<sub>2</sub>CH(CH<sub>3</sub>)<sub>2</sub> and CH<sub>2</sub>CH<sub>2</sub>CH<sub>2</sub>SiMe<sub>2</sub>Cl), 25.7 (CH<sub>2</sub>CH(CH<sub>3</sub>)<sub>2</sub>). <sup>29</sup>Si NMR (CDCl<sub>3</sub>):  $\delta$  31.1 (SiMe<sub>2</sub>Cl), -67.7 to -68.0 (overlapping singlets, 1:3:3:1, SiCH<sub>2</sub>CHMe<sub>2</sub> and Si(CH<sub>2</sub>)<sub>3</sub>SiMe<sub>2</sub>Cl).

#### 2.2.2.3. Synthesis of HMe<sub>2</sub>Si(CH<sub>2</sub>)<sub>3</sub>(i-C<sub>4</sub>H<sub>9</sub>)<sub>7</sub>Si<sub>8</sub>O<sub>12</sub> (**4**)

LiAlH<sub>4</sub> in diethyl ether (2.50 mL, 2.50 mmol) was added slowly via syringe into a diethyl ether (100 mL) solution of **2** (2.40 g, 2.50 mmol) in a 250 mL Schlenk flask equipped with a stir bar. The reaction mixture was stirred overnight (~16 h) at room temperature and then filtered through Celite. The filtrate was cautiously added to a mixture of aqueous HCl (1 M, 100 mL) and ice. The

organic layer was separated, washed thrice with brine (3 × 30 mL), and dried over anhydrous Na<sub>2</sub>SO<sub>4</sub> for 16 h. After removal of Na<sub>2</sub>SO<sub>4</sub> by filtration, the filtrate was concentrated to dryness under reduced pressure to give HMe<sub>2</sub>Si(CH<sub>2</sub>)<sub>3</sub>(*i*-C<sub>4</sub>H<sub>9</sub>)<sub>7</sub>Si<sub>8</sub>O<sub>12</sub> (**4**) as a white solid. Yield: 1.76 g, 79.6 %. <sup>1</sup>H NMR (CDCl<sub>3</sub>): δ 0.065 (d, <sup>3</sup>J<sub>H-H</sub> = 4.0 Hz, 6 H, Si(CH<sub>3</sub>)<sub>2</sub>H), 0.61 (d, <sup>3</sup>J<sub>H-H</sub> = 6.0 Hz, 14 H, SiCH<sub>2</sub>CH(CH<sub>3</sub>)<sub>2</sub>), 0.64-0.74 (m, 4 H, CH<sub>2</sub>CH<sub>2</sub>CH<sub>2</sub>SiMe<sub>2</sub>H), 0.97 (d, <sup>3</sup>J<sub>H-H</sub> = 6.4 Hz, 42 H, CH<sub>2</sub>CH(CH<sub>3</sub>)<sub>2</sub>), 1.50 (m, 2 H, CH<sub>2</sub>CH<sub>2</sub>CH<sub>2</sub>SiMe<sub>2</sub>H), 1.88 (sept, <sup>3</sup>J<sub>H-H</sub> = 6.4 Hz, 7 H, CH<sub>2</sub>CH(CH<sub>3</sub>)<sub>2</sub>), 3.85 (m, 1 H, SiMe<sub>2</sub>H). <sup>13</sup>C{<sup>1</sup>H} NMR (CDCl<sub>3</sub>): δ -4.6 (Si(CH<sub>3</sub>)<sub>2</sub>H), 16.0 (CH<sub>2</sub>CH<sub>2</sub>CH<sub>2</sub>SiMe<sub>2</sub>H), 17.8 (CH<sub>2</sub>CH<sub>2</sub>CH<sub>2</sub>SiMe<sub>2</sub>H), 22.5 (CH<sub>2</sub>CH(CH<sub>3</sub>)<sub>2</sub>), 23.9 (CH<sub>2</sub>CH(CH<sub>3</sub>)<sub>2</sub> and CH<sub>2</sub>CH<sub>2</sub>CH<sub>2</sub>SiMe<sub>2</sub>H), 25.7 (CH<sub>2</sub>CH(CH<sub>3</sub>)<sub>2</sub>). <sup>29</sup>Si NMR (CDCl<sub>3</sub>): δ -13.9 (SiMe<sub>2</sub>H), -67.7 to -68.3 (overlapping s, 1:3:3:1, SiCH<sub>2</sub>CHMe<sub>2</sub> and Si(CH<sub>2</sub>)<sub>3</sub>SiMe<sub>2</sub>H). ATR-IR (ν, cm<sup>-1</sup>): 2110 (Si-H).

#### 2.2.2.4. Synthesis of Et<sub>3</sub>Si(CH<sub>2</sub>)<sub>3</sub>(*i*-C<sub>4</sub>H<sub>9</sub>)<sub>6</sub>Si<sub>7</sub>O<sub>9</sub>(OH)<sub>3</sub> (**5**)

A solution of Et<sub>3</sub>Si(CH<sub>2</sub>)<sub>3</sub>(*i*-C<sub>4</sub>H<sub>9</sub>)<sub>7</sub>Si<sub>8</sub>O<sub>12</sub> (**2**, 0.40 g, 0.41 mmol) and 35% w/w aqueous Et<sub>4</sub>NOH (0.190 g, 0.45 mmol) in THF (15 mL) was heated at reflux with stirring for 8 h. The solution was then neutralized with dilute aqueous HCl (1 M). Evaporation of volatiles afforded white solids, which were dissolved in diethyl ether (25 mL). The solution was dried over anhydrous Na<sub>2</sub>SO<sub>4</sub> overnight. After removal of Na<sub>2</sub>SO<sub>4</sub> by filtration, the filtrate was concentrated to dryness under reduced pressure. The resulting colorless gel was recrystallized from toluene-acetonitrile (1:5 ratio) to furnish, after drying under vacuum, a mixture of Et<sub>3</sub>Si(CH<sub>2</sub>)<sub>3</sub>(*i*-C<sub>4</sub>H<sub>9</sub>)<sub>6</sub>Si<sub>7</sub>O<sub>9</sub>(OH)<sub>3</sub> (**5**) regiomers as a colorless gel. Yield: 0.17 g, 48%. <sup>1</sup>H NMR (CDCl<sub>3</sub>): δ 0.48 (q, <sup>3</sup>J<sub>H-H</sub> = 7.6 Hz, 6 H, Si(CH<sub>2</sub>CH<sub>3</sub>)<sub>3</sub>), 0.50-0.78 (m, 14 H, CH<sub>2</sub>CH(CH<sub>3</sub>)<sub>2</sub> and CH<sub>2</sub>CH<sub>2</sub>CH<sub>2</sub>SiEt<sub>3</sub>), 0.80-1.00 (m, 47 H, CH<sub>2</sub>CH(CH<sub>3</sub>)<sub>2</sub>, CH<sub>2</sub>CH<sub>2</sub>CH<sub>2</sub>SiEt<sub>3</sub> and Si(CH<sub>2</sub>CH<sub>3</sub>)<sub>3</sub>), 1.40 (m, 2 H, CH<sub>2</sub>CH<sub>2</sub>CH<sub>2</sub>SiEt<sub>3</sub>), 1.87 (m, 6 H, CH<sub>2</sub>CH(CH<sub>3</sub>)<sub>2</sub>), 6.50 (br s, 3 H, Si-OH). <sup>13</sup>C{<sup>1</sup>H} NMR (CDCl<sub>3</sub>): δ 3.6 (Si(CH<sub>2</sub>CH<sub>3</sub>)), 7.7 (Si(CH<sub>2</sub>CH<sub>3</sub>)), 17.2 (CH<sub>2</sub>CH<sub>2</sub>CH<sub>2</sub>SiEt<sub>3</sub>), 17.7 (CH<sub>2</sub>CH<sub>2</sub>CH<sub>2</sub>SiEt<sub>3</sub>), 22.8, 22.9 (overlapping singlets, CH<sub>2</sub>CH(CH<sub>3</sub>)<sub>2</sub>), 24.2, 24.3 (overlapping singlets, CH<sub>2</sub>CH(CH<sub>3</sub>)<sub>2</sub> and CH<sub>2</sub>CH<sub>2</sub>CH<sub>2</sub>SiEt<sub>3</sub>), 26.0, 26.1 (overlapping singlets, CH<sub>2</sub>CH(CH<sub>3</sub>)<sub>2</sub>). <sup>29</sup>Si NMR (CDCl<sub>3</sub>): δ 6.2 (SiEt<sub>3</sub>), -58.7 (Si-

OH) -67.9, -68.3, -68.6 (SiCH<sub>2</sub>CHMe<sub>2</sub> and Si(CH<sub>2</sub>)<sub>3</sub>SiEt<sub>3</sub>); Si-OH: Si(alkyl) = ~3:4.  
ATR-IR (ν, cm<sup>-1</sup>): 3150 (O-H)

#### 2.2.2.5. Synthesis of HMe<sub>2</sub>Si(CH<sub>2</sub>)<sub>3</sub>(*i*-C<sub>4</sub>H<sub>9</sub>)<sub>6</sub>Si<sub>7</sub>O<sub>9</sub>(OH)<sub>3</sub> (**6**)

A solution of HMe<sub>2</sub>Si(CH<sub>2</sub>)<sub>3</sub>(*i*-C<sub>4</sub>H<sub>9</sub>)<sub>7</sub>Si<sub>8</sub>O<sub>12</sub> (**4**, 0.40 g, 0.44 mmol) and 35% w/w aqueous Et<sub>4</sub>NOH (0.205 g, 0.48 mmol) in THF (15 mL) was heated at reflux with stirring for 8 h. The solution was then neutralized with dilute aqueous HCl (1 M) and worked up as described for synthesis of **5**. The regiomer mixture of HMe<sub>2</sub>Si(CH<sub>2</sub>)<sub>3</sub>(*i*-C<sub>4</sub>H<sub>9</sub>)<sub>6</sub>Si<sub>7</sub>O<sub>9</sub>(OH)<sub>3</sub> (**6**) was obtained as a colorless gel. Yield: 0.14 g, 45%. <sup>1</sup>H NMR: δ 0.06-0.21 (m, 6 H, Si(CH<sub>3</sub>)<sub>2</sub>H), 0.55-0.66 (m, 14 H, CH<sub>2</sub>CH(CH<sub>3</sub>)<sub>2</sub> and CH<sub>2</sub>CH<sub>2</sub>CH<sub>2</sub>SiMe<sub>2</sub>H), 0.70-1.15 (m, 40 H, CH<sub>2</sub>CH<sub>2</sub>CH<sub>2</sub>SiMe<sub>2</sub>H and CH<sub>2</sub>CH(CH<sub>3</sub>)<sub>2</sub>), 1.85 (m, 6 H, SiCH<sub>2</sub>CH(CH<sub>3</sub>)<sub>2</sub>), 3.75 (1 H, Si-H, overlap with THF), and 5.70 (br s, 3 H, Si-OH). <sup>13</sup>C {<sup>1</sup>H} NMR (CDCl<sub>3</sub>): δ -4.6 (Si(CH<sub>3</sub>)<sub>2</sub>H), 16.8 (CH<sub>2</sub>CH<sub>2</sub>CH<sub>2</sub>SiMe<sub>2</sub>H), 17.8 (CH<sub>2</sub>CH<sub>2</sub>CH<sub>2</sub>SiMe<sub>2</sub>H), 22.5 (CH<sub>2</sub>CH(CH<sub>3</sub>)<sub>2</sub>), 23.0 (CH<sub>2</sub>CH<sub>2</sub>CH<sub>2</sub>SiMe<sub>2</sub>H), 23.9 (CH<sub>2</sub>CH(CH<sub>3</sub>)<sub>2</sub>), 25.7 (CH<sub>2</sub>CH(CH<sub>3</sub>)<sub>2</sub>). <sup>29</sup>Si NMR (CDCl<sub>3</sub>): δ 58.9 (Si-OH), -67.5 (br s, Si-CH<sub>2</sub>CHMe<sub>2</sub>), -68.00 to -70 (br s, Si-CH<sub>2</sub>CHMe<sub>2</sub>); Si-OH:Si(alkyl) = 3:4. ATR-IR (ν, cm<sup>-1</sup>): 3395 (Si-OH), 2114 (Si-H). Anal. Calcd. for C<sub>29</sub>H<sub>70</sub>O<sub>12</sub>Si<sub>8</sub>: C, 41.69; H, 8.44. Found: C, 41.27; H, 8.33.

#### 2.2.2.6. Synthesis of [Ti(NMe<sub>2</sub>)<sub>2</sub>{Et<sub>3</sub>Si(CH<sub>2</sub>)<sub>3</sub>(*i*-C<sub>4</sub>H<sub>9</sub>)<sub>6</sub>Si<sub>7</sub>O<sub>12</sub>}] (**7**)

In the glovebox, Ti(NMe<sub>2</sub>)<sub>4</sub> (47.4 mg, 0.211 mmol) was added via syringe to a stirred solution of the regiomer mixture of Et<sub>3</sub>Si(CH<sub>2</sub>)<sub>3</sub>(*i*-C<sub>4</sub>H<sub>9</sub>)<sub>6</sub>Si<sub>7</sub>O<sub>9</sub>(OH)<sub>3</sub> (**5**, 180 mg, 0.200 mmol) in diethyl ether (15 mL). Stirring was continued at room temperature for 30 min, after which the yellow solution was concentrated to dryness under reduced pressure. The residue was dissolved in toluene (1 mL) and acetonitrile (15 mL) was added to precipitate a yellow solid, which was isolated by filtration and washed three times with acetonitrile (5 mL) and then dried under vacuum to give a regiomer mixture of [Ti(NMe<sub>2</sub>)<sub>2</sub>{Et<sub>3</sub>Si(CH<sub>2</sub>)<sub>3</sub>(*i*-C<sub>4</sub>H<sub>9</sub>)<sub>6</sub>Si<sub>7</sub>O<sub>12</sub>}] (**7**) as a highly moisture-sensitive yellow gel. Yield: 171 mg, 89%. <sup>1</sup>H NMR (CDCl<sub>3</sub>): δ 0.16 (br m, 6 H, Si(CH<sub>2</sub>CH<sub>3</sub>)<sub>3</sub>), 0.50-0.80 (br m, 16 H, CH<sub>2</sub>CH(CH<sub>3</sub>)<sub>2</sub>, CH<sub>2</sub>CH<sub>2</sub>CH<sub>2</sub>SiEt<sub>3</sub> and CH<sub>2</sub>CH<sub>2</sub>CH<sub>2</sub>SiEt<sub>3</sub>), 0.80-1.10 (br m, 45 H,

CH<sub>2</sub>CH(CH<sub>3</sub>)<sub>2</sub> and Si(CH<sub>2</sub>CH<sub>3</sub>)<sub>3</sub>, 1.15-1.50 (br m, 2 H, CH<sub>2</sub>CH<sub>2</sub>CH<sub>2</sub>SiEt<sub>3</sub>), 1.90 (br m, CH<sub>2</sub>CH(CH<sub>3</sub>)<sub>2</sub>), 2.50 (br m, NMe<sub>2</sub>H), 3.00-3.30 (br m, Ti-NMe<sub>2</sub> and Ti-NMe<sub>2</sub>H) 3.50-3.80 (br s, NMe<sub>2</sub>H and Ti-NMe<sub>2</sub>H). <sup>13</sup>C{<sup>1</sup>H} NMR (CDCl<sub>3</sub>): δ 3.6 (Si(CH<sub>2</sub>CH<sub>3</sub>)<sub>3</sub>), 7.7 (Si(CH<sub>2</sub>CH<sub>3</sub>)<sub>3</sub>), 22.8, (br s, CH<sub>2</sub>CH(CH<sub>3</sub>)<sub>2</sub>), 23.4 (br m), 24.2 (br s, CH<sub>2</sub>CH(CH<sub>3</sub>)<sub>2</sub>), 26.0, 26.1 (br s, CH<sub>2</sub>CH(CH<sub>3</sub>)<sub>2</sub>), 39.6 (br s, NMe<sub>2</sub>H). Both slow hydrolysis and exchange between Ti(NMe<sub>2</sub>) and NMe<sub>2</sub>H made observing the Ti(NMe<sub>2</sub>) resonance by <sup>13</sup>C NMR difficult (see Results & Discussion Section). <sup>29</sup>Si NMR (CDCl<sub>3</sub>): δ 6.2 (br s, SiEt<sub>3</sub>), -66.0 to -71.0 (br m (overlapping singlets), Si-CH<sub>2</sub>CHMe<sub>2</sub> and Si-(CH<sub>2</sub>)<sub>3</sub>SiEt<sub>3</sub>); SiEt<sub>3</sub>:Si(POSS) = 1:7. Uv-vis: λ<sub>max</sub> = 203 nm

#### 2.2.2.7. Synthesis of [Ti(NMe<sub>2</sub>)<sub>2</sub>{HMe<sub>2</sub>Si(CH<sub>2</sub>)<sub>3</sub>(i-C<sub>4</sub>H<sub>9</sub>)<sub>6</sub>Si<sub>7</sub>O<sub>12</sub>}] (**8**)

In the glovebox, Ti(NMe<sub>2</sub>)<sub>4</sub> (47.4 mg, 0.211 mmol) was added via syringe to a stirred solution of the regiomic mixture of HMe<sub>2</sub>Si(CH<sub>2</sub>)<sub>3</sub>(i-C<sub>4</sub>H<sub>9</sub>)<sub>6</sub>Si<sub>7</sub>O<sub>9</sub>(OH)<sub>3</sub> (**6**, 167 mg, 0.200 mmol) in diethyl ether (15 mL). Stirring was continued at room temperature for 30 min. After work-up as described for synthesis of **7**, a regiomic mixture of [Ti(NMe<sub>2</sub>)<sub>2</sub>{HMe<sub>2</sub>Si(CH<sub>2</sub>)<sub>3</sub>(i-C<sub>4</sub>H<sub>9</sub>)<sub>6</sub>Si<sub>7</sub>O<sub>12</sub>}] (**8**) was isolated as a highly moisture-sensitive yellow gel. Yield: 0.170 g, 93%. <sup>1</sup>H NMR (CDCl<sub>3</sub>): δ 0.15 (br m, 6 H, Si(CH<sub>3</sub>)<sub>2</sub>H), 0.50-0.70 (br m, 14 H, CH<sub>2</sub>CH(CH<sub>3</sub>)<sub>2</sub> and CH<sub>2</sub>CH<sub>2</sub>CH<sub>2</sub>SiMe<sub>2</sub>H), 0.90-1.10 (br m, 38 H, CH<sub>2</sub>CH<sub>2</sub>CH<sub>2</sub>SiMe<sub>2</sub>H and CH<sub>2</sub>CH(CH<sub>3</sub>)<sub>2</sub>), 1.20-1.30 (br m, 2 H, CH<sub>2</sub>CH<sub>2</sub>CH<sub>2</sub>SiMe<sub>2</sub>H), 1.84 (br m, 6 H, CH<sub>2</sub>CH(CH<sub>3</sub>)<sub>2</sub>), 2.42 (HNMe<sub>2</sub>), 2.47, 2.64 (TiNMe<sub>2</sub>H), 3.07, 3.14, 3.20, 3.26 (6 H, TiNMe<sub>2</sub>), 3.50-3.80 (br m, 1 H, SiH, NMe<sub>2</sub>H). <sup>13</sup>C{<sup>1</sup>H} NMR (CDCl<sub>3</sub>): δ -4.4 (SiMe<sub>2</sub>H), 16.9, 17.0 (CH<sub>2</sub>CH<sub>2</sub>CH<sub>2</sub>SiMe<sub>2</sub>H), 17.8, 17.9 (CH<sub>2</sub>CH<sub>2</sub>CH<sub>2</sub>SiMe<sub>2</sub>H), 22.6 (CH<sub>2</sub>CH(CH<sub>3</sub>)<sub>2</sub>), 23.1 (CH<sub>2</sub>CH<sub>2</sub>CH<sub>2</sub>SiMe<sub>2</sub>H), 23.9, 24.0 (CH<sub>2</sub>CH(CH<sub>3</sub>)<sub>2</sub>), 25.8, 25.9 CH<sub>2</sub>CH(CH<sub>3</sub>)<sub>2</sub>), 38.9 (HNMe<sub>2</sub>), 43.4, (TiNMe<sub>2</sub>). <sup>29</sup>Si NMR (CDCl<sub>3</sub>): δ -66.0 to -69.8 (br m (overlapping singlets), Si-CH<sub>2</sub>CHMe<sub>2</sub> and Si-(CH<sub>2</sub>)<sub>3</sub>SiMe<sub>2</sub>H). ATR-IR (ν, cm<sup>-1</sup>): 2113 (Si-H). Uv-vis: λ<sub>max</sub> = 212 nm. Anal. Calcd. for C<sub>31</sub>H<sub>73</sub>NO<sub>12</sub>Si<sub>8</sub>Ti: C, 40.27; H, 7.96; N, 1.51. Found C, 40.09 H, 7.76; N, 1.23.

#### 2.2.2.8. Synthesis of **P1-6** (Grafting **6** onto **P1**)

A round-bottom three-neck flask (50 mL) equipped with a magnetic stir bar, condenser with N<sub>2</sub> inlet, and thermometer was charged with vinyl-terminated hyperbranched polysiloxysilane **P1** (4.00 g, 0.429 mmol, ~23.8 mmol CH=CH<sub>2</sub> groups), HMe<sub>2</sub>Si(CH<sub>2</sub>)<sub>3</sub>(*i*-C<sub>4</sub>H<sub>9</sub>)<sub>6</sub>Si<sub>7</sub>O<sub>9</sub>(OH)<sub>3</sub> (**6**, 1.00 g, 1.20 mmol), toluene (40 mL), and Karstedt's catalyst (0.2 mL). The reaction mixture was heated at 60 °C overnight (~16 h) at which point complete disappearance of the Si-H groups was confirmed by <sup>1</sup>H NMR spectroscopy. The reaction mixture was cooled to room temperature and volatiles were removed under reduced pressure to afford **P1-6** (~20% by weight of **6**) as a viscous colorless material. Yield: 4.30 g, 86%. <sup>1</sup>H NMR (CDCl<sub>3</sub>): δ 0.05-0.20 (m, Si(CH<sub>3</sub>)<sub>2</sub>H and polymer Si(CH<sub>3</sub>)<sub>2</sub>), 0.30-0.65 (m, SiCH<sub>2</sub>CH(CH<sub>3</sub>)<sub>2</sub>, CH<sub>2</sub>CH<sub>2</sub>CH<sub>2</sub>SiMe<sub>2</sub>H, polymer SiCH<sub>2</sub>), 0.90-1.10 (m, SiCH<sub>2</sub>CH(CH<sub>3</sub>)<sub>2</sub>, CH<sub>2</sub>CH<sub>2</sub>CH<sub>2</sub>SiMe<sub>2</sub>H), 1.85 (m, SiCH<sub>2</sub>CH(CH<sub>3</sub>)<sub>2</sub>), 5.70 (m, polymer *H<sup>vinyl</sup>*), 5.93 (m, polymer *H<sup>vinyl</sup>*), 6.11 (m, polymer *H<sup>vinyl</sup>*). <sup>13</sup>C{<sup>1</sup>H} NMR (CDCl<sub>3</sub>): δ -0.7, 0.23, 5.7, 8.3, 9.6, 22.8, 23.0 (CH<sub>2</sub>CH(CH<sub>3</sub>)<sub>2</sub>), 23.9 (CH<sub>2</sub>CH(CH<sub>3</sub>)<sub>2</sub>), 25.7 (CH<sub>2</sub>CH(CH<sub>3</sub>)<sub>2</sub>), 131.6 (*vinyl*), 139.2 (*vinyl*). <sup>29</sup>Si NMR (CDCl<sub>3</sub>): δ 8.3 (m, *polysiloxysilane*), -3.2 to -4.7 (*polysiloxysilane*), -58.2 (POSS *Si-OH*), -64.5, to -66.0 (m, *polysiloxysilane*), -67.6, -67.9, -68.3 (*Si-CH<sub>2</sub>CHMe<sub>2</sub>* and *Si-(CH<sub>2</sub>)<sub>3</sub>SiMe<sub>2</sub>H*). ATR-IR (ν, cm<sup>-1</sup>): 3300 (O-H), 1596 (CH=CH<sub>2</sub>).

#### 2.2.2.9. Synthesis of **c-P1-6**

A round-bottom three-neck flask (50 mL) equipped with a magnetic stir bar, condenser with N<sub>2</sub> inlet, and thermometer was charged with vinyl-terminated hyperbranched polysiloxysilane **P1** (4.00 g, 0.429 mmol, ~23.8 mmol CH=CH<sub>2</sub> groups), HMe<sub>2</sub>Si(CH<sub>2</sub>)<sub>3</sub>(*i*-C<sub>4</sub>H<sub>9</sub>)<sub>6</sub>Si<sub>7</sub>O<sub>9</sub>(OH)<sub>3</sub> (**6**, 1.00 g, 1.20 mmol), toluene (40 mL), and Karstedt's catalyst (0.2 mL). The reaction mixture was heated at 60 °C overnight (~16 h) at which point complete disappearance of the Si-H groups was confirmed by <sup>1</sup>H NMR spectroscopy. The reaction mixture was cooled to room temperature and then charged with 1,1,3,3,5,5-hexamethyltrisiloxane (4.75 g, 22.8 mmol) and Karstedt's catalyst (0.2 mL). After stirring the solution at 60 °C overnight (~16 h), it was cooled to room temperature and volatiles were removed

under reduced pressure, affording the crosslinked hyperbranched polymer **c-P1-6** (5.10 g, ~52% yield, ~10.3% by weight of **6**) as a colorless elastomeric solid. Poor solubility of **c-P1-6** prevented its characterization by solution NMR spectroscopy. However, its ATR-IR spectrum was absent of vinyl absorptions (see supplementary information).

#### 2.2.2.10. Synthesis of titanium silsesquioxane material **P1-8**

In a glovebox,  $\text{Ti}(\text{NMe}_2)_4$  (0.300 g, 1.34 mmol) was added by syringe to a stirred toluene solution (15 mL) of **P1-6** (4.30 g, 1.03 mmol of **6**). The resulting deep yellow solution was allowed to stir for 1 h and then concentrated to dryness under reduced pressure. The residue was washed with acetonitrile until the washings were no longer colored and then dried under vacuum to give **P1-8** as a viscous orange gel. Yield: 4.31 g, 98%.  $^1\text{H}$  NMR ( $\text{CDCl}_3$ ):  $\delta$  0.05-0.20 (m,  $\text{Si}(\text{CH}_3)_2\text{H}$  and polymer  $\text{Si}(\text{CH}_3)_2$ ), 0.30-0.65 (m,  $\text{SiCH}_2\text{CH}(\text{CH}_3)_2$ ,  $\text{CH}_2\text{CH}_2\text{CH}_2\text{SiMe}_2\text{H}$ , polymer  $\text{SiCH}_2$ ), 0.90-1.10 (m,  $\text{SiCH}_2\text{CH}(\text{CH}_3)_2$ ,  $\text{CH}_2\text{CH}_2\text{CH}_2\text{SiMe}_2\text{H}$ ), 1.85 (m,  $\text{SiCH}_2\text{CH}(\text{CH}_3)_2$ ), 3.06, 3.25 ( $\text{TiNMe}_2$ ) 5.70 (m, polymer  $H^{\text{vinyl}}$ ), 5.93 (m, polymer  $H^{\text{vinyl}}$ ), 6.11 (m, polymer  $H^{\text{vinyl}}$ ).  $^{13}\text{C}\{^1\text{H}\}$  NMR ( $\text{CDCl}_3$ ):  $\delta$  -0.7, 0.22, 0.27, 5.7, 8.3, 8.6, 9.6, 22.8, 23.0 ( $\text{CH}_2\text{CH}(\text{CH}_3)_2$ ), 23.9 ( $\text{CH}_2\text{CH}(\text{CH}_3)_2$ ), 25.7 ( $\text{CH}_2\text{CH}(\text{CH}_3)_2$ ), 43.2 ( $\text{TiNMe}_2$ ) 131.6 (*vinyl*), 139.2 (*vinyl*).  $^{29}\text{Si}$  NMR ( $\text{CDCl}_3$ ):  $\delta$  8.3 (m, *polysiloxysilane*), -3.2 to -4.7 (*polysiloxysilane*), -64.5, to -66.0 (m, *polysiloxysilane*), -66.2, to -69.0 ( $\text{Si-CH}_2\text{CHMe}_2$  and  $\text{Si-}(\text{CH}_2)_3\text{SiMe}_2\text{H}$ ). ATR-IR ( $\nu$ ,  $\text{cm}^{-1}$ ): 1596 ( $\text{CH}=\text{CH}_2$ ). Uv-vis:  $\lambda_{\text{max}} = 203$  nm. Anal. Calcd. for **P1-8**: Ti, 1.07. Found: Ti, 1.13 (5% relative error).

#### 2.2.2.11. Synthesis of titanium silsesquioxane material **c-P1-8**

In a glovebox,  $\text{Ti}(\text{NMe}_2)_4$  (0.300 g, 1.34 mmol) was added by syringe to a stirred toluene solution (15 mL) of **c-P1-6** (5.10 g, 0.063 mmol of **6**). The resulting deep yellow solution was let stir for 1 h then concentrated to dryness under reduced pressure. The residue was washed with acetonitrile until the washings were no longer colored and then dried under vacuum to give **c-P1-8** as an orange solid. Yield: 5.09 g, 99%. Poor solubility of **c-P1-8** prevented its

characterization by solution NMR spectroscopy. ATR-IR ( $\nu$ ,  $\text{cm}^{-1}$ ): 2240 (Si-H). Uv-vis:  $\lambda_{\text{max}} = 199 \text{ nm}$ . Anal. Calcd. for **c-P1-8**: Ti, 0.59. Found: Ti, 0.45 (5% relative error).

### 2.2.3. Procedure for catalytic alkene epoxidation

#### 2.2.3.1. Epoxidation of 1-octene with *t*-butyl hydroperoxide (TBHP) catalyzed by titanium silsesquioxanes **7-10**

Epoxidation tests were performed in a magnetically stirred 250 mL three-necked flask, equipped with a condenser, thermometer probe and septum for withdrawing samples. All runs were performed under an atmosphere of dry nitrogen. Typically, 1-octene (73 g, 0.65 mol), TBHP (5.7 mL, 0.031 mol), toluene (3 g, 0.03 mol as internal standard), and a stirrer bar were placed in the flask. The reaction mixture was warmed to 80 °C and maintained at the temperature for 1h. A quantity of catalyst (equivalent to 0.2 mmol of Ti) in 1-octene (10 mL, 0.063 mol) was then added *via* syringe. Immediately a sample was taken for GC analysis, further samples for analysis being taken at regular intervals. Rate constant for TBHP consumption  $k_1$ , where ( $k_1 = k_2[\text{Ti}] = k_3[\text{Ti}][\text{Olefin}]$ ) is determined from pseudo-first order rate plot ( $-\ln[\text{TBHP}]$  versus  $t$ ).

#### 2.2.3.2. Epoxidation of 1-Octene with *t*-butyl hydroperoxide (TBHP) catalyzed by titanium silsesquioxane materials **P1-8** and **c-P1-8**

Epoxidation tests were performed in a magnetically stirred 50 mL three-necked flask, equipped with a condenser, thermometer probe, and septum for withdrawing samples. Typically, 1-octene (20.0 g, 0.18 mol), TBHP (100  $\mu\text{L}$ , 0.55 mmol), toluene (2 g, 0.022 mol as internal standard), a quantity of titanium silsesquioxane material (**P1-8** or **c-P1-8**) and a stirrer bar were placed in the flask. The reaction mixture was heated to 80° C. A sample was immediately taken for GC analysis and additional samples for analysis were taken at regular intervals.



#### 2.2.3.3. **c-P1-8**-catalyzed epoxidation of 1-octene with *t*-butyl hydroperoxide (TBHP) in the presence of added *t*-butanol

The experimental procedure is the same as described for 1-octene epoxidation with TBHP at 80 °C using **c-P1-8** as catalyst, however, *t*-butanol (50  $\mu$ L) was added to the reaction mixture before it was warmed to 80 °C.

#### 2.2.4. Catalyst recycling studies

The experimental procedure is the same as described for 1-octene epoxidation with TBHP at 80 °C using **P1-8** or **c-P1-8** as catalyst. After the reaction had proceeded for a specified amount of time (Table 2.3), the reaction mixture was cooled to room temperature and then concentrated to dryness under reduced pressure. The catalyst material was washed with copious amounts of acetonitrile to remove residual organics, and dried under vacuum overnight (~16 h). The catalyst was then reused for 1-octene epoxidation as previously described.

#### 2.2.5. Catalyst Repair

A sample of **c-P1-8** catalyst that had been recycled five times for 1-octene epoxidation was swelled by stirring in toluene (5 mL) for 3h.  $\text{Ti}(\text{NMe}_2)_4$  (47.4 mg, 0.211 mmol) was then added by syringe and the mixture was allowed to stir for 2 h, after which the mixture was concentrated to dryness under reduced pressure. The residue was washed with copious amounts of acetonitrile (until the washings were colorless) and then dried under vacuum. The repaired material was used for 1-octene epoxidation under our typical conditions (*vide supra*).

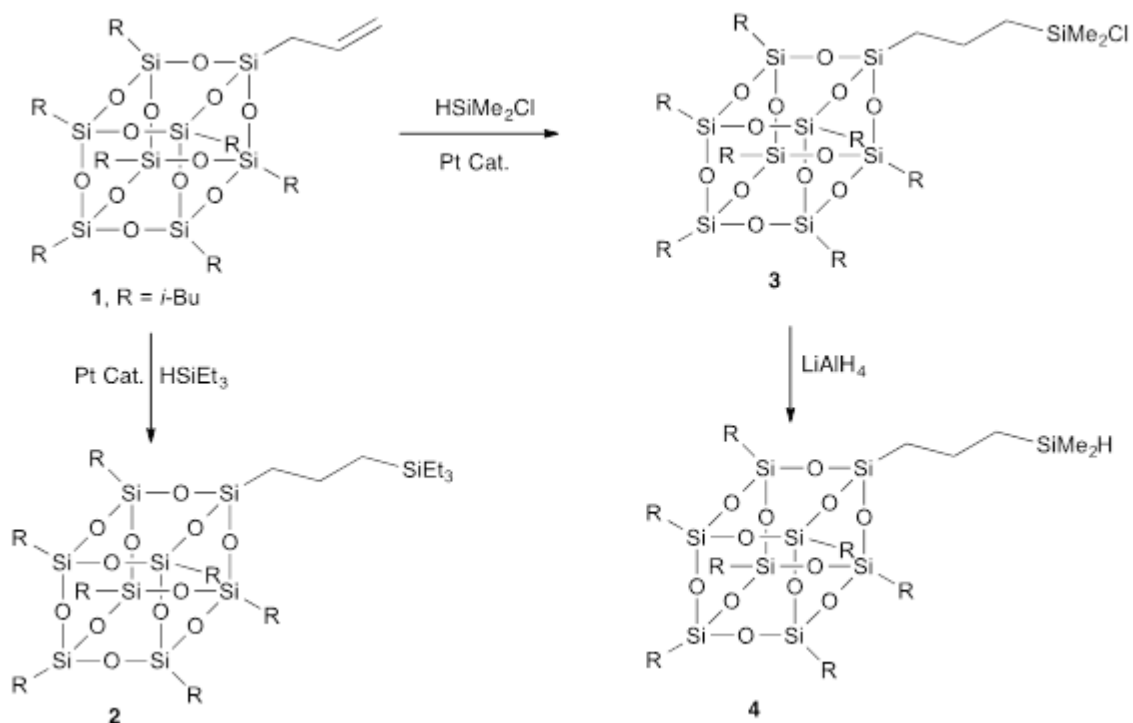
## 2.3. Results and Discussion

### 2.3.1. Preparation and characterization of trisilanolisobutyl-POSS ligands

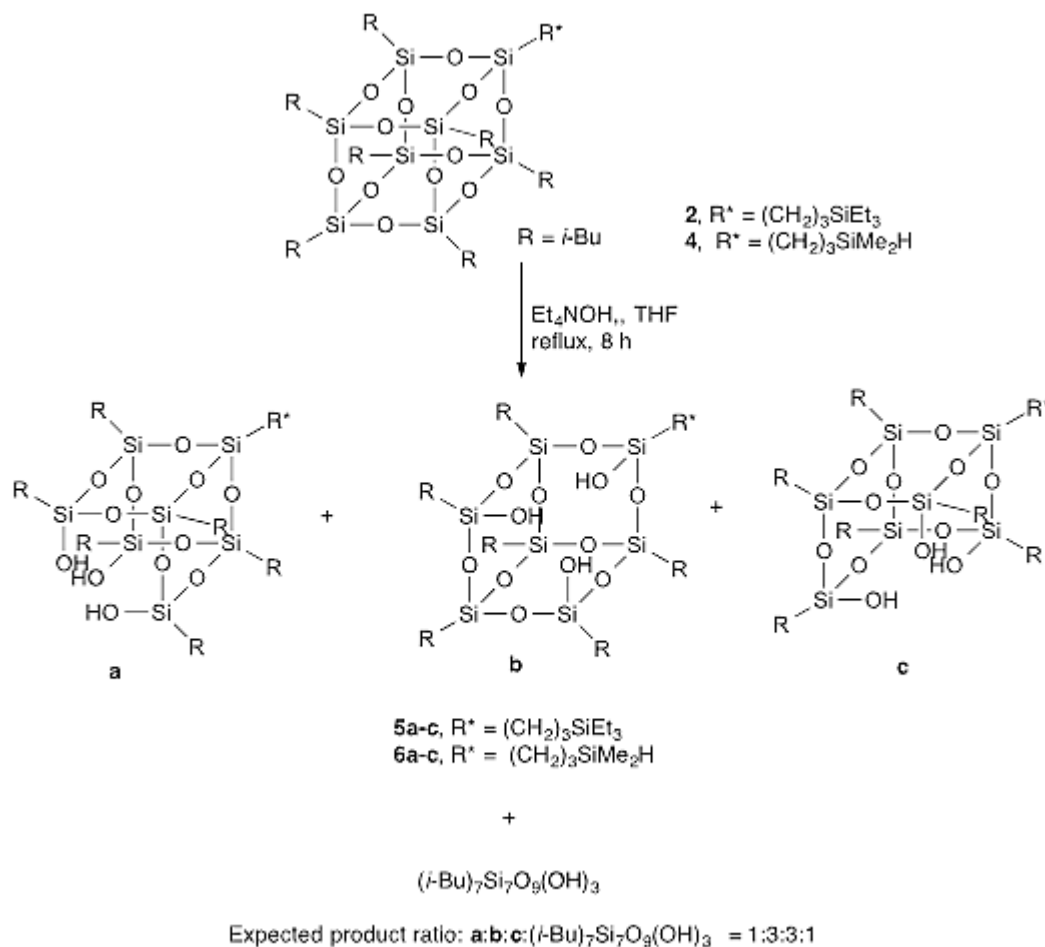
Trisilanolisobutyl-POSS (incompletely condensed silsesquioxane) ligands that bear a (silyl)propyl group,  $\text{Et}_3\text{Si}(\text{CH}_2)_3(i\text{-Bu})_6\text{Si}_7\text{O}_9(\text{OH})_3$  (**5**) and  $\text{HMe}_2\text{Si}(\text{CH}_2)_3(i\text{-Bu})_6\text{Si}_7\text{O}_9(\text{OH})_3$  (**6**), were synthesized starting from commercially available  $\text{CH}_2=\text{CHCH}_2(i\text{-Bu})_7\text{Si}_8\text{O}_{12}$  (**1**) via routes depicted in Schemes 2.1 and

2.2. Pt-catalyzed hydrosilylation of  $\text{CH}_2=\text{CHCH}_2(i\text{-Bu})_7\text{Si}_8\text{O}_{12}$  (**1**) with  $\text{HSiEt}_3$  and  $\text{HSiMe}_2\text{Cl}$  at  $60^\circ\text{C}$  overnight furnished after work-up excellent yields of  $\text{Et}_3\text{Si}(\text{CH}_2)_3(i\text{-Bu})_7\text{Si}_8\text{O}_{12}$  (**2**) and  $\text{ClMe}_2\text{Si}(\text{CH}_2)_3(i\text{-Bu})_7\text{Si}_8\text{O}_{12}$  (**3**), respectively (Scheme 2.1). Reduction of **3** with  $\text{LiAlH}_4$  in diethyl ether at room temperature gave  $\text{HMe}_2\text{Si}(\text{CH}_2)_3(i\text{-Bu})_7\text{Si}_8\text{O}_{12}$  (**4**) in good yield after work-up (Scheme 2.1).

**Scheme 2.1**—Synthetic route to **2**, **3**, and **4**



**Scheme 2.2**—Excision of one framework silicon



The formulation and structure of **2-4** were mainly established by solution  $^1\text{H}$ ,  $^{13}\text{C}$ , &  $^{29}\text{Si}$  NMR data. Both the  $^1\text{H}$  &  $^{13}\text{C}$  NMR spectra for **2** and **3** confirmed the complete absence of the allyl resonances characteristic of **1**. Moreover, **2** showed a  $^1\text{H}$  NMR methylene resonance at  $\delta$  0.47 and a  $^{13}\text{C}$  NMR methylene resonance at  $\delta$  3.3 for the  $\text{Si}(\text{CH}_2\text{CH}_3)_3$  substituent. Similarly, **3** showed a  $^1\text{H}$  NMR methyl resonance at  $\delta$  0.37 and a  $^{13}\text{C}$  NMR methyl resonance at  $\delta$  1.6 for the  $\text{SiMe}_2\text{Cl}$  substituent while **4** displayed a  $^1\text{H}$  NMR methyl resonance at  $\delta$  0.065 and a  $^{13}\text{C}$  NMR methyl resonance at  $\delta$  -4.6 for the  $\text{SiMe}_2\text{H}$  substituent. Also, a silyl hydride resonance at  $\delta$  3.85 was observed in the  $^1\text{H}$  NMR spectrum of **4** for the  $\text{SiMe}_2\text{H}$  group; the presence of  $\text{SiMe}_2\text{H}$  was also confirmed by IR spectroscopy, which showed a Si-H stretch at  $2110\text{ cm}^{-1}$ . Consistent with the  $\text{C}_{3v}$

symmetry expected for **2-4**, their  $^{29}\text{Si}$  NMR spectra showed overlapping resonances between  $\delta$  -67 and -68 that are characteristic of the silsesquioxane cage Si atoms<sup>32,40</sup> (four closely positioned resonances in ~1:3:3:1 ratio are expected, see Experimental Section). In addition, **2-4** each displayed a  $^{29}\text{Si}$  NMR resonance for a pendant  $\text{SiEt}_3$ ,  $\text{SiMe}_2\text{Cl}$ , or  $\text{SiMe}_2\text{H}$  substituent at  $\delta$  6.2, 31.1, and -13.9, respectively.

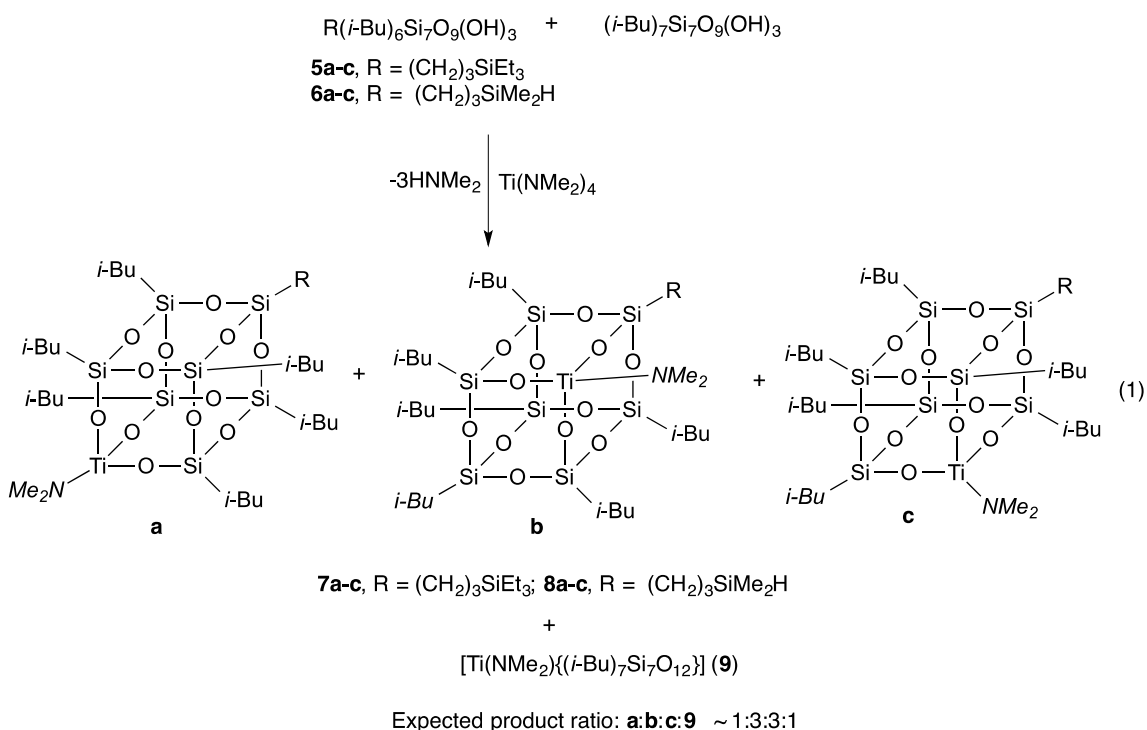
The preparation of (silyl)propyl-trisilanolisobutyl-POSS compounds **5** and **6** (Scheme 2.2) was accomplished via modification of the method reported by Feher and colleagues for selective formation of incompletely condensed silsesquioxanes, that is, base-catalyzed excision of a framework Si atom from fully condensed ( $\text{R}_8\text{Si}_8\text{O}_{12}$ ) silsesquioxanes.<sup>99</sup> By design, the unique  $\text{Et}_3\text{Si}(\text{CH}_2)_3$  or  $\text{HMe}_2\text{Si}(\text{CH}_2)_3$  substituent of **2** and **4** was chosen to have comparable electronic and steric properties to the isobutyl substituents so that extraction of a (silyl)propyl-substituted silsesquioxane Si atom should occur with similar efficiency as extraction of isobutyl-substituted silsesquioxane Si atom. In this regard, Feher and colleagues previously showed that Si centers possessing less bulky H or OH groups were much more readily extracted from the silsesquioxane framework than Si centers possessing more bulky, electron-rich groups. For instance, both  $(\text{c-C}_6\text{H}_{11})_7(\text{H})\text{Si}_8\text{O}_{12}$  and  $(\text{c-C}_6\text{H}_{11})_7(\text{OH})\text{Si}_8\text{O}_{12}$  reacted in similar fashion with aqueous  $\text{Et}_4\text{NOH}$  (1.1 equiv) in THF at reflux for 1 h to give  $(\text{c-C}_6\text{H}_{11})_7\text{Si}_7\text{O}_9(\text{OH})_3$  in >50% yield.<sup>99</sup> Based on the 7:1 isobutyl:(silyl)propyl substituent ratio and our hypothesis that extraction of (silyl)propyl- and isobutyl-substituted silsesquioxane Si atoms would occur with similar efficiency, reaction of **2** (or **4**) with  $\text{Et}_4\text{NOH}$  would be expected to furnish **5** (or **6**) and  $(i\text{-Bu})_7\text{Si}_7\text{O}_9(\text{OH})_3$  in 7:1 ratio, with **5** (or **6**) consisting of three regiomers **a-c** (Scheme 2) in 1:3:3 ratio. We found that the reaction of  $\text{HMe}_2\text{Si}(\text{CH}_2)_3(i\text{-Bu})_7\text{Si}_8\text{O}_{12}$  (**4**) with aqueous  $\text{Et}_4\text{NOH}$  (1.1 equiv) in THF at reflux for 4 h proceeded to only about 50% completion;  $^{29}\text{Si}$  NMR spectroscopic study of the product mixture revealed resonances for silanol Si atoms and silsesquioxane Si atoms in 1.5:6.5 integral ratio rather than the expected 3:4 ratio (*vide infra*). In contrast, the reaction of  $(i\text{-Bu})_8\text{Si}_8\text{O}_{12}$  with aqueous  $\text{Et}_4\text{NOH}$  under identical

conditions proceeded to completion in 4 h to give  $(i\text{-Bu})_7\text{Si}_7\text{O}_9(\text{OH})_3$  in ~40% isolated yield, consistent with literature report.<sup>99</sup> Thus, we studied the reaction of **4** with aqueous  $\text{Et}_4\text{NOH}$  (1.1 equiv) in THF at reflux over time and found that an increase in the reaction time to 8 hours led to complete consumption of **4** and isolation of a regiomer mixture of  $\text{HMe}_2\text{Si}(\text{CH}_2)_3(i\text{-Bu})_6\text{Si}_7\text{O}_9(\text{OH})_3$  (**6**) as a colorless gel in 45% yield after work-up (Scheme 2.2). Analogous reaction of  $\text{Et}_3\text{Si}(\text{CH}_2)_3(i\text{-Bu})_7\text{Si}_8\text{O}_{12}$  (**2**) with aqueous  $\text{Et}_4\text{NOH}$  for 8 h proceeded to provide a regiomer mixture of  $\text{Et}_3\text{Si}(\text{CH}_2)_3(i\text{-Bu})_6\text{Si}_7\text{O}_9(\text{OH})_3$  (**5**) as a colorless gel in 48% yield after work-up.

$^1\text{H}$ ,  $^{13}\text{C}$ , &  $^{29}\text{Si}$  NMR and IR data were mainly used to characterize regiomer mixtures **5** and **6**. The formulation of **6** was also confirmed by microanalysis. However as for many polyhedral silsesquioxane compounds, obtaining consistent elemental analyses for **5** proved very challenging, even with use of a combustion aid such as  $\text{WO}_3$  to suppress the formation of silicon carbide. The  $^{29}\text{Si}$  NMR spectra of **5** and **6** were particularly informative, the resonance observed for the silanol Si atoms at  $\delta$  -58.7 for **5** and  $\delta$  -58.9 for **6**, being consistent with the chemical shift ( $\delta$  -58.5) previously reported for the silanol Si atoms of  $(i\text{-Bu})_7\text{Si}_7\text{O}_9(\text{OH})_3$ .<sup>99</sup> The silanol signal also displayed the expected 3:4 integral ratio with overlapping resonances for silsesquioxane Si atoms found between  $\delta$  -67.5 and -69.9 for both **5** and **6**. Furthermore, the resonance for the silanol Si atoms displayed the expected 3:1 integral ratio versus the resonance for the pendant  $\text{Et}_3\text{Si}(\text{CH}_2)_3$  substituent of **5** (at  $\delta$  6.2). Regrettably, the Si resonance for the  $\text{HMe}_2\text{Si}(\text{CH}_2)_3$  substituent of **6** was not observed, preventing analogous integral ratio evaluation. However, both the  $^1\text{H}$  and  $^{13}\text{C}$  NMR spectra of **6** showed resonances at  $\delta$  0.06-0.21 and -4.6 for methyl groups of the  $\text{HMe}_2\text{Si}(\text{CH}_2)_3$  substituent. In the  $^1\text{H}$  NMR spectra, a broad resonance at  $\delta$  6.35 for **5** and  $\delta$  5.70 for **6** was observed for the silanol protons. Further confirming the presence of silanol groups was the observation of a broad O-H stretch at  $3150\text{ cm}^{-1}$  for **5** and  $3395\text{ cm}^{-1}$  for **6**, while a Si-H stretch at  $2114\text{ cm}^{-1}$  was observed for **6**.

### 2.3.2. Preparation and characterization of tripodal titanium silsesquioxane complexes

Regiomer mixtures of tripodal titanium silsesquioxane complexes [Ti(NMe<sub>2</sub>)<sub>2</sub>{Et<sub>3</sub>Si(CH<sub>2</sub>)<sub>3</sub>(*i*-Bu)<sub>6</sub>Si<sub>7</sub>O<sub>12</sub>}] (**7**) and [Ti(NMe<sub>2</sub>)<sub>2</sub>{HMe<sub>2</sub>Si(CH<sub>2</sub>)<sub>3</sub>(*i*-Bu)<sub>6</sub>Si<sub>7</sub>O<sub>12</sub>}] (**8**) were prepared in excellent yield via protonolysis of Ti(NMe<sub>2</sub>)<sub>4</sub> with one equivalent of Et<sub>3</sub>Si(CH<sub>2</sub>)<sub>3</sub>(*i*-Bu)<sub>6</sub>Si<sub>7</sub>O<sub>9</sub>(OH)<sub>3</sub> (**5**) and HMe<sub>2</sub>Si(CH<sub>2</sub>)<sub>3</sub>(*i*-Bu)<sub>6</sub>Si<sub>7</sub>O<sub>9</sub>(OH)<sub>3</sub> (**6**), respectively (equation 1). Reasoning that the differences in regiochemistry may lead to different reactivity of the titanium



centers, we also prepared symmetrically substituted Ti silsesquioxane complexes [Ti(NMe<sub>2</sub>)<sub>2</sub>{(*i*-C<sub>4</sub>H<sub>9</sub>)<sub>7</sub>Si<sub>7</sub>O<sub>12</sub>}] (**9**)<sup>32</sup> and [Ti(NMe<sub>2</sub>)<sub>2</sub>{(*c*-C<sub>6</sub>H<sub>11</sub>)<sub>7</sub>Si<sub>7</sub>O<sub>12</sub>}] (**10**)<sup>40</sup> by the literature methods and evaluated the potential of **7-10** as homogeneous catalysts for 1-octene epoxidation with TBHP under identical conditions (*vide infra*).

Whereas **9** and **10** are air- and moisture-sensitive yellow crystalline solids, Ti silsesquioxane regiomer mixtures **7** and **8** were isolated as air- and highly moisture-sensitive yellow gels. Both **7** and **8** display good solubility in a range of aliphatic and aromatic hydrocarbon solvents, such as pentane, hexane, THF,

diethyl ether, chloroform, dichloromethane, benzene and toluene, but show poor solubility in acetonitrile and acetone.

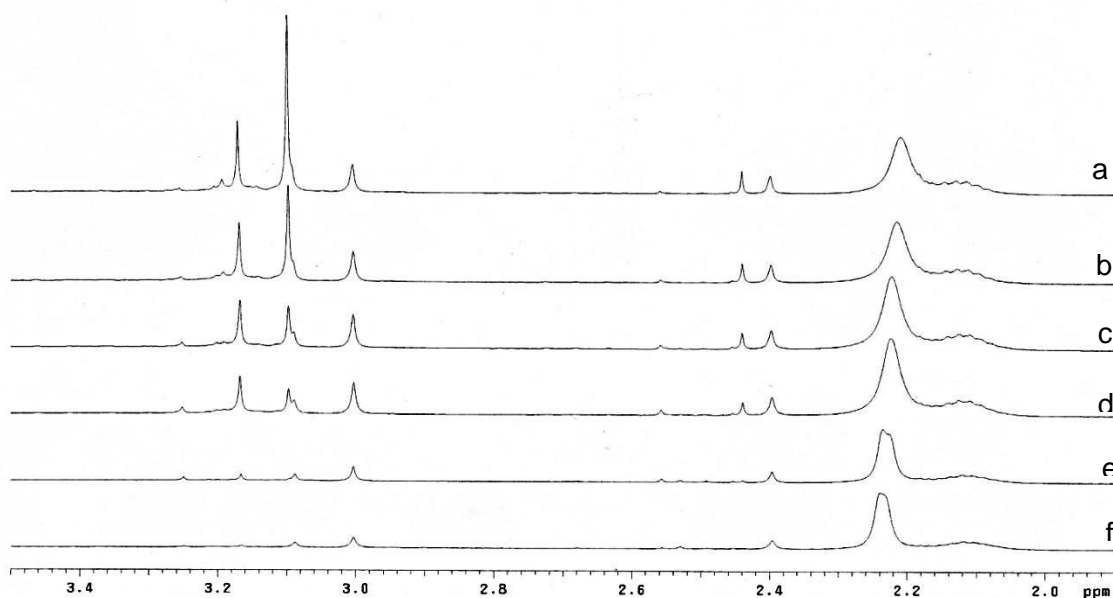
The formulation and structure of **7** and **8** were established by a combination of microanalysis, solution ( $^1\text{H}$ ,  $^{13}\text{C}$ , &  $^{29}\text{Si}$ ) NMR, IR, and UV-vis data. Consistent with the predominant regiomers of Ti silsesquioxanes **7** and **8** being  $C_1$ -symmetric (i.e. regiomers **b** and **c**, equation 1), their  $^{29}\text{Si}$  NMR spectra showed broad overlapping resonances in the range expected for framework silsesquioxane Si atoms (between  $\delta$  -66 and -70). Furthermore, consistent with previous observations for Ti silsesquioxane complexes,<sup>127,128</sup> the resonance for the Si atoms bearing OH groups (at  $\delta$  -58.7 for **5** and  $\delta$  -58.9 for **6**) shifts upfield (by ca. 7 ppm) upon co-ordination of the oxygen with titanium. The Si atom of the  $\text{Et}_3\text{Si}(\text{CH}_2)_3$  group of **7** was observed as a singlet resonance at  $\delta$  6.2. For **8**,  $^1\text{H}$  and  $^{13}\text{C}$  NMR resonances for methyl groups of the  $\text{HMe}_2\text{Si}(\text{CH}_2)_3$  substituent were observed at  $\delta$  0.15 and -4.4, respectively. While the Si-H resonance overlapped with N-H resonance of the  $\text{HNMe}_2$  by-product in the  $^1\text{H}$  NMR spectrum (*vide infra*), the IR spectrum of **8** confirmed a Si-H stretch at  $2113\text{ cm}^{-1}$  and complete absence of an O-H stretch.

$^1\text{H}$  NMR spectra of **7** and **8** revealed that the yellow gels contained some residual  $\text{HNMe}_2$  (the protonolysis reaction by-product, equation 1) and that binding of  $\text{HNMe}_2$  to the Ti center and slow exchange between  $\text{HNMe}_2$  and  $\text{Ti-NMe}_2$  occurred to broaden the  $\text{Ti-NMe}_2$  resonances observed between  $\delta$  3.02 and 3.25, the expected range for the  $\text{Ti-NMe}_2$  resonance of  $\text{Me}_2\text{N-Ti-silsesquioxane}$  complexes.<sup>40</sup> All attempts to remove the residual  $\text{HNMe}_2$  by either drying the gels under vacuum with gentle heating or by washing the gels with copious amounts of acetonitrile were unsuccessful; hydrolysis of  $\text{Ti-NMe}_2$  by adventitious water in acetonitrile was a major problem, due to high moisture-sensitivity of the compounds. In contrast, symmetrically substituted Ti silsesquioxanes  $[\text{Ti}(\text{NMe}_2)\{(\textit{i}\text{-C}_4\text{H}_9)_7\text{Si}_7\text{O}_{12}\}]$  (**9**) and  $[\text{Ti}(\text{NMe}_2)\{(\textit{c}\text{-C}_6\text{H}_{11})_7\text{Si}_7\text{O}_{12}\}]$  (**10**) were obtained as crystalline solids (*vide supra*) and free of  $\text{HNMe}_2$ . That **7** and **8** weakly bind  $\text{HNMe}_2$  and slowly exchange the  $\text{Ti-NMe}_2$  group is supported

by results of a titration experiment wherein one equivalent of  $\text{HMe}_2\text{Si}(\text{CH}_2)_3(i\text{-Bu})_6\text{Si}_7\text{O}_9(\text{OH})_3$  (**6**) was added in small fractions to a  $\text{CDCl}_3$  solution of  $\text{Ti}(\text{NMe}_2)_4$  at room temperature and followed by  $^1\text{H}$  NMR. As shown in Figure 2.1, when sub-equimolar amounts of **6** were added to a  $\text{CDCl}_3$  solution of  $\text{Ti}(\text{NMe}_2)_4$ , the  $^1\text{H}$  NMR spectra (a-d) contained a broad resonance at  $\delta$  2.2 for free  $\text{HNMe}_2$  and  $\delta$  3.1 for unreacted  $\text{Ti}(\text{NMe}_2)_4$ , along with two broad resonances at  $\sim \delta$  2.44 and 2.40 for Ti-bound  $\text{HNMe}_2$  as well as Ti- $\text{NMe}_2$  resonances between  $\delta$  3.00 and 3.25. As addition of an equimolar amount of **6** was approached and  $\text{Ti}(\text{NMe}_2)_4$  was effectively consumed to produce a regiomeric mixture of **8**, the Ti- $\text{NMe}_2$  resonances for **8** (between  $\delta$  3.00 and 3.25) broadened significantly and resonances for Ti-bound  $\text{HNMe}_2$  groups coalesced to a single broad peak, consistent with slow exchange between free- and Ti-bound  $\text{HNMe}_2$  as well as the Ti- $\text{NMe}_2$  group. In further support of this suggestion, we found that similar broadening of the Ti- $\text{NMe}_2$  resonance was observed by  $^1\text{H}$  NMR when a sub-equimolar amount of  $\text{HNMe}_2$  was introduced into  $\text{CDCl}_3$  solutions of  $[\text{Ti}(\text{NMe}_2)\{(i\text{-C}_4\text{H}_9)_7\text{Si}_7\text{O}_{12}\}]$  (**9**) and  $[\text{Ti}(\text{NMe}_2)\{(c\text{-C}_6\text{H}_{11})_7\text{Si}_7\text{O}_{12}\}]$  (**10**). UV-vis data for regiomeric **7** and **8** are also consistent with predominance of a tetrahedral Ti site in the complexes. Specifically, the UV-vis spectra of **7** and **8** contained an intense absorption at 203 and 212 nm, respectively (see appendix); these absorptions are close to the range (212–228 nm) previously reported for Ti silsesquioxane complexes and are assigned to a ligand to metal charge transfer transition involving four-coordinated titanium bearing oxygen ligands.<sup>40</sup> The UV-vis spectrum displayed a broad shoulder peak extending to about 280 nm, due presumably to formation of six-coordinated Ti by coordination of two  $\text{HNMe}_2$  molecules. In this context, we note that bands above 250 nm are generally indicative of octahedral Ti sites.<sup>129</sup>



**Figure 2.1**— $^1\text{H}$  NMR spectra corresponding to titrations of  $\text{Ti}(\text{NMe}_2)_4$  with sub-equimolar amounts of **6**. ( $\text{Ti}(\text{NMe}_2)_4$ :**6** ratios: *a* = 2.2:1; *b* = 2:1; *c* = 1.8:1; *d* = 1.6:1; *e* = 1.4:1; *f* = 1.2:1)



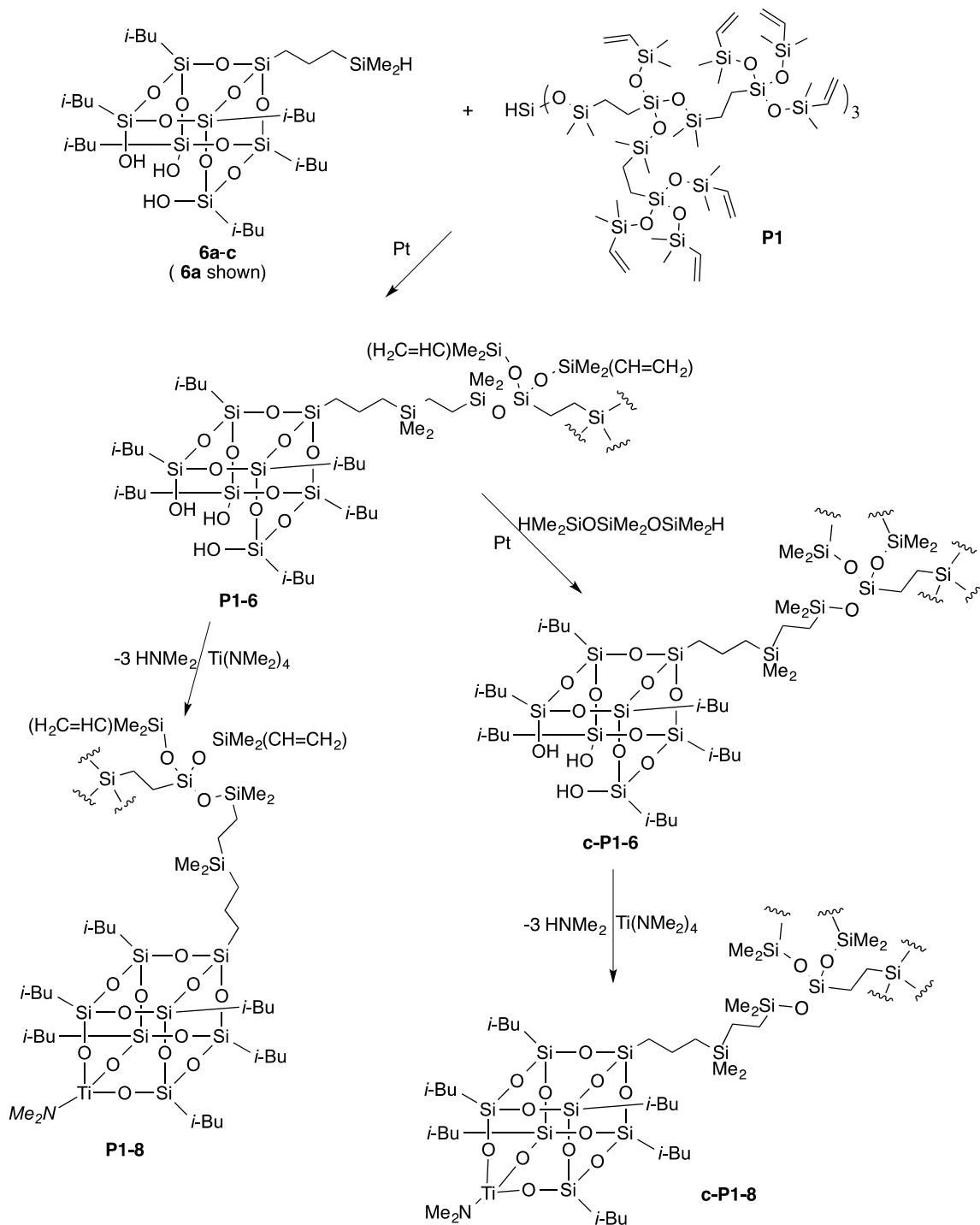
### 2.3.3. Covalent grafting of tripodal titanium silsesquioxane complexes to hyperbranched polysiloxysilane matrices

The immobilization of tripodal Ti silsesquioxane materials was accomplished by covalently grafting trisilanolisobutyl-POSS ligand to hyperbranched polysiloxysilane matrices and then reacting the resulting materials with  $\text{Ti}(\text{NMe}_2)_4$  (Scheme 2.3). Vinyl-terminated hyperbranched polysiloxysilane **P1** (Scheme 2.3) was synthesized by modification of the literature method, via Pt-catalyzed polymerization of  $\text{HSi}(\text{OSiMe}_2\text{CH}=\text{CH}_2)_3$ ,<sup>106</sup> and isolated as a viscous oil with molecular weight ( $M_n$ ) and polydispersity index (PDI) of  $9318 \text{ g mol}^{-1}$  and 1.93, respectively. Pt-catalyzed hydrosilylation of **P1** with  $\text{HMe}_2\text{Si}(\text{CH}_2)_3(i\text{-Bu})_6\text{Si}_7\text{O}_9(\text{OH})_3$  (**6**, ~5 mol% relative to moles of **P1** vinyl groups) in toluene produced **P1-6** (Scheme 2.3) as a colorless viscous gel after work-up. Consistent with covalent attachment of trisilanolisobutyl-POSS ligand to **P1**, both the  $^1\text{H}$  and  $^{13}\text{C}$  NMR spectra of **P1-6** contained methyl resonances characteristic of the silsesquioxane-bound isobutyl group at  $\delta \sim 0.96$  and between  $\delta$  20-25,

respectively. The  $^{13}\text{C}$  NMR spectrum further showed peaks between  $\delta$  -0.7 to 9.7 for Si-Me and methylene carbons of the polysiloxysilane backbone, as well as resonances at  $\delta$  131.6 and 139.2 for vinyl carbons. The  $^{29}\text{Si}$  NMR data were especially informative, showing resonances for silanol Si atoms at  $\delta$  -58.2 and silsesquioxane Si atoms at  $\delta$  -67.0 to -68.3, along with resonances characteristic of **P1** Si atoms at  $\delta$  8.3 ( $\text{OSiMe}_2\text{CH}_2$ ), -3.2 to -4.6 ( $\text{OSiMe}_2\text{CH}=\text{CH}_2$ ), and -64.6 to -65.0 ( $\text{CH}_2\text{Si}(\text{OSiMe}_2\text{CH}=\text{CH}_2)_3$ ).<sup>106</sup> Also, the IR spectrum of **P1-6** contained a very broad silanol O-H stretch at  $\sim 3300\text{ cm}^{-1}$ .

**Scheme 2.3**—Synthetic route for the formation of active catalysts **P1-8** and **c-P1-**

**8**



The corresponding crosslinked derivative **c-P1-6** (Scheme 2.3), free of vinyl groups as established by absence of a vinyl stretch in its IR spectrum, was prepared via Pt-catalyzed hydrosilylation of **P1-6** with 1,1,3,3,5,5-hexamethyltrisiloxane ( $\text{HMe}_2\text{SiOSiMe}_2\text{OSiMe}_2\text{H}$ , ~2 equivalents of Si-H groups relative to number of moles of polymer vinyl groups). **c-P1-6** was obtained as a colorless solid material. Whereas **P1-6** was soluble in ether, THF, pentane, hexane, 1-octene and chloroform, **c-P1-6** was only sparingly soluble in pentane, toluene, 1-octene, and THF but completely insoluble in chloroform and methylene chloride; both materials were completely insoluble in methanol, acetone, and acetonitrile. Thus, the titanium catalysts derived from these materials should be readily recovered by precipitation at the end of epoxidation reactions (*vide infra*).

Tripodal Ti silsesquioxane materials **P1-8** and **c-P1-8** were prepared by reacting an excess of  $\text{Ti}(\text{NMe}_2)_4$  with the corresponding trisilanol POSS material **P1-6** or **c-P1-6** in toluene for 1 h (Scheme 2.3). After removing toluene under reduced pressure, the materials were washed with acetonitrile to remove residual  $\text{HNMe}_2$  and  $\text{Ti}(\text{NMe}_2)_4$  and dried under vacuum. **P1-8** was isolated as a viscous orange gel while **c-P1-8** was obtained as an orange solid. While **P1-8** was soluble in chloroform, poor solubility of **c-P1-8** in common organic solvents (such as chloroform, methylene chloride, toluene and THF) rendered its characterization by solution NMR techniques difficult. Nonetheless, the formation of tripodal Ti silsesquioxane materials was confirmed by a combination of IR, UV-vis, and elemental analysis data. The absence of a silanol O-H stretch in the IR spectra of **P1-8** and **c-P1-8** revealed that the silanol groups of the corresponding **P1-6** and **c-P1-6** precursors were completely consumed. Furthermore, the  $^1\text{H}$  NMR spectrum of **P1-8** did not contain a resonance for Si-OH and showed resonances for Ti-NMe<sub>2</sub> in the expected chemical shift range at  $\delta$  3.06-3.25, along with a small HNMe<sub>2</sub> resonance between  $\delta$  2.4 and 2.5. Equally important, the  $^{29}\text{Si}$  NMR spectrum for **P1-8** was absent a resonance for silanol Si atoms (typically observed at  $\sim \delta$  -58). Consistent with previous observations for Ti silsesquioxane complexes (*vide supra*), the resonance for silanol Si atoms of **P1-**

**6** (at  $\delta$  -58.2) shifted upfield (by ca. 7 ppm) upon co-ordination of the oxygen with titanium, to between  $\delta$  -66.2 to -69.0.

The UV–vis data for **P1-8** and **c-P1-8** are consistent with the retention of a tetrahedral Ti site in the materials. Specifically, the UV–vis spectra of **P1-8** and **c-P1-8** contained an intense absorption at 203 and 199 nm, respectively (see appendix); these absorptions are in the same range (*vide supra*) observed for [Ti(NMe<sub>2</sub>){Et<sub>3</sub>Si(CH<sub>2</sub>)<sub>3</sub>(*i*-Bu)<sub>6</sub>Si<sub>7</sub>O<sub>12</sub>}] (**7**) and [Ti(NMe<sub>2</sub>){HMe<sub>2</sub>Si(CH<sub>2</sub>)<sub>3</sub>(*i*-Bu)<sub>6</sub>Si<sub>7</sub>O<sub>12</sub>}] (**8**) and are likewise assigned to a ligand to metal charge transfer transition involving four-coordinated titanium bearing oxygen ligands.<sup>40</sup> Similar to the spectra for regiomeric mixtures **7** and **8**, UV–vis spectra for **P1-8** and **c-P1-8** displayed a broad shoulder peak extending to about 280 nm, which is likely due to octahedral Ti sites, formed by coordination of two HNMe<sub>2</sub> molecules (*vide supra*). Proton-induced X-ray emission (PIXE) analysis of the Ti silsesquioxane materials found that **P1-8** contained 1.13 weight percent (wt%) of Ti which is in good agreement with the calculated value (1.07 wt%). Similarly, **c-P1-8** contained 0.45 wt% Ti which is close to the calculated value (0.59 wt%). Presumably, some of the trisilanol-POSS ligands present in **c-P1-6** are less accessible than those present in **P1-6**.

#### 2.3.4. Alkene Epoxidation activity

##### 2.3.4.1. Alkene Epoxidation activity of tripodal titanium silsesquioxane complexes

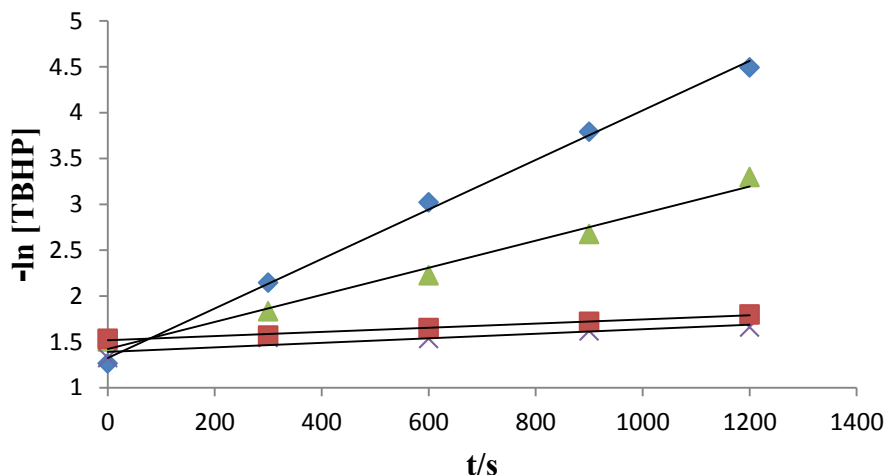
In order to gauge the effect different regiochemistry about the Ti center on reactivity of Ti silsesquioxane materials, we investigated the epoxidation of 1-octene with TBHP at 80 °C under pseudo-first-order conditions (1-octene:TBHP of 20:1) using regiomeric mixtures of tripodal titanium silsesquioxane complexes [Ti(NMe<sub>2</sub>){Et<sub>3</sub>Si(CH<sub>2</sub>)<sub>3</sub>(*i*-Bu)<sub>6</sub>Si<sub>7</sub>O<sub>12</sub>}] (**7**) and [Ti(NMe<sub>2</sub>){HMe<sub>2</sub>Si(CH<sub>2</sub>)<sub>3</sub>(*i*-Bu)<sub>6</sub>Si<sub>7</sub>O<sub>12</sub>}] (**8**), as well as symmetrically substituted Ti silsesquioxane complexes [Ti(NMe<sub>2</sub>){(*i*-C<sub>4</sub>H<sub>9</sub>)<sub>7</sub>Si<sub>7</sub>O<sub>12</sub>}] (**9**) and Ti(NMe<sub>2</sub>){(*c*-C<sub>6</sub>H<sub>11</sub>)<sub>7</sub>Si<sub>7</sub>O<sub>12</sub>}] (**10**), as catalysts (see Experimental Section). As the reaction rate plots in Figure 2.2 clearly show, pseudo-first-order kinetics are observed corresponding to equation 2. The second-order rate

$$d[\text{epoxide}]/dt = k_1[\text{TBHP}] \quad (2)$$

(where  $k_1 = k_2[\text{Ti}] = k_3[\text{Ti}][\text{olefin}]$ )

constants determined for TBHP conversion ( $k_2 = k_1/[\text{Ti}]$ ) for complexes **7-10** are shown in Table 1. The measured values of  $k_2$  for regiomer mixtures of tripodal titanium silsesquioxanes **7** and **8** are markedly lower than those obtained for symmetrically substituted Ti silsesquioxane complexes **9** and **10**. As discussed in Section 3.2, **7** and **8** predominantly contained  $C_1$ -symmetric Ti silsesquioxane regiomers (equation 1) while **9** and **10** are  $C_{3v}$ -symmetric. Furthermore, while **9** and **10** were isolated as base-free crystalline complexes, **7** and **8** were obtained as yellow gels containing weakly bound  $\text{HNMe}_2$  molecules that are slowly exchanged with  $\text{Ti-NMe}_2$ . Presumably, both slow displacement of  $\text{HNMe}_2$  from the Ti center by TBHP (to ultimately form catalytically active  $\text{Ti-OOBu}^t$  species)<sup>40</sup> and differences in activities of the Ti centers in the different  $C_1$ -symmetric regiomers contribute to the reduced activity of **7** and **8** relative to **9** and **10**. Nonetheless, although **8** displayed somewhat lower activity than **7**, both **7** and **8** show comparable or superior activity in the epoxidation of 1-octene with TBHP relative to homogeneous Mo catalysts, such as  $\text{MoO}(\text{acac})_2$ ,<sup>130</sup> as well as heterogeneous Ti-containing catalysts such as the Shell catalyst<sup>131</sup> (Table 2.1). Moreover, we expect that substitution of the amide ligand present in regiomer mixtures of Ti silsesquioxanes **7** and **8** with a less basic  $\text{OPr}^i$ ,  $\text{OPh}$ , or  $\text{OSiMe}_3$  ligand would result in greater  $k_2$  values, due to formation of a weaker base than  $\text{HNMe}_2$  upon protonolysis with TBHP, *i.e.*  $\text{HOPr}^i$ ,  $\text{HOPh}$ , or  $\text{HOSiMe}_3$ ; these studies are currently underway in our laboratories. In this context, the activities of  $[\text{Ti}(\text{L})\{(\text{C-C}_6\text{H}_{11})_7\text{Si}_7\text{O}_{12}\}]$  ( $\text{L} = \text{NMe}_2$ ,  $\text{OPr}^i$ , or  $\text{OPh}$ ) in the epoxidation of 1-octene with TBHP have been shown to increase in the order:  $\text{L} = \text{NMe}_2 < \text{OPr}^i < \text{OPh}$ .<sup>40</sup> Incidentally, the lower activity of **9** versus **10** is best attributed to the greater steric bulk of isobutyl- versus cyclohexyl substituents. In this regard, it has been demonstrated that less bulky silsesquioxane substituents allow better access to the Ti center and thereby give rise to greater reactivity of Ti silsesquioxane complexes.<sup>40</sup>

**Figure 2.2**—Pseudo-first order rate plots for the epoxidation of 1-octene with TBHP catalyzed by titanium silsesquioxane complexes:  $\blacktriangle$  **9**,  $\diamond$  **10**,  $\blacksquare$  **7** and  $\times$  **8**.

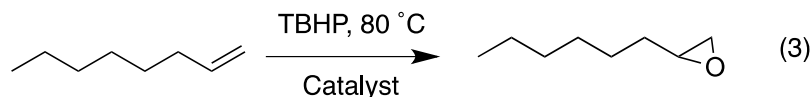


**Table 2.1**—Epoxidation of 1-octene with TBHP catalyzed by titanium silsesquioxane complexes and related materials

Catalyst	Selectivity to epoxide (%) <sup>a</sup>	$10^2 k_2/\text{dm}^3 \text{mol}^{-1} \text{s}^{-1}$	Ref.
<b>7</b>	$92 \pm 2.0$	$24 \pm 3.5$	
<b>8</b>	$70 \pm 1.5$	$15 \pm 2.4$	
<b>9</b>	$86 \pm 4.5$	$86 \pm 8.8$	
<b>10</b>	$95 \pm 4.0$	$139 \pm 3.0$	
MoO(acac) <sub>2</sub>	92	31	110
TiO <sub>2</sub> /SiO <sub>2</sub> (Shell Catalyst)	97	18	114

Conditions: T = 80 °C, Ti = 0.2 mmol, TBHP = 30 mmol, 1-octene (75g) as solvent. <sup>a</sup>Selectivity = (mol 1,2-epoxyoctane formed/mol TBHP consumed) × 100; selectivities were determined at 90% TBHP consumption. Values quoted represent the average from at least three trials +/- the standard deviation.

For all of the Ti silsesquioxane complexes tested in this study, 1,2-epoxyoctane was the only product (equation 3) formed under the reaction conditions employed, selectivity referring to



the yield of epoxide based on TBHP consumed. Interestingly, while the regiomer mixture of  $[\text{Ti}(\text{NMe}_2)\{\text{Et}_3\text{Si}(\text{CH}_2)_3(i\text{-Bu})_6\text{Si}_7\text{O}_{12}\}]$  (**7**) showed high selectivity to epoxide (> 90%), comparable to **9** and **10** (Table 2.1), the regiomer mixture of  $[\text{Ti}(\text{NMe}_2)\{\text{HMe}_2\text{Si}(\text{CH}_2)_3(i\text{-Bu})_6\text{Si}_7\text{O}_{12}\}]$  (**8**) showed only moderate (70%) selectivity to epoxide. In this context, we anticipated that oxidation of the Si-H moiety of **8** could occur under the reaction conditions employed,<sup>132</sup> and hence prepared **7** which bears a  $\text{SiEt}_3$  moiety that is resistant to oxidation. However, while the much lower activity of **8** compared to  $[\text{Ti}(\text{NMe}_2)\{(i\text{-C}_4\text{H}_9)_7\text{Si}_7\text{O}_{12}\}]$  (**9**) (Table 2.1) does not appear to be due to oxidation of the Si-H moiety, the drastic drop in selectivity to epoxide observed for **8** (versus **7**, **9** and **10**) is presumably a consequence of TBHP consumption due to oxidation of the silane moiety.

#### 2.3.4.2. Alkene Epoxidation activity of tripodal titanium silsesquioxane materials

The efficiency of Ti silsesquioxane materials **P1-8** and **c-P1-8** as epoxidation catalysts was investigated given that regiomer mixtures of Ti silsesquioxanes **7** and **8** displayed competitive activities and very high selectivities in catalytic epoxidation of 1-octene with TBHP (*vide supra*). The epoxidation of 1-octene (neat) with TBHP was studied at 80 °C and the reaction progress was followed by taking samples for GC analysis at regular intervals. Whereas **P1-8** dissolved completely in solution under the reaction conditions, crosslinked Ti silsesquioxane material **c-P1-8** was only sparingly soluble in the reaction mixture. When **P1-8** (0.05 mmol Ti, 9.1 mol% Ti relative to TBHP) was used as the catalyst, the epoxidation of 1-octene with TBHP (0.55 mmol) proceeded in 2 h to high conversion (> 99%) with excellent TBHP efficiency to selectively produce 1-



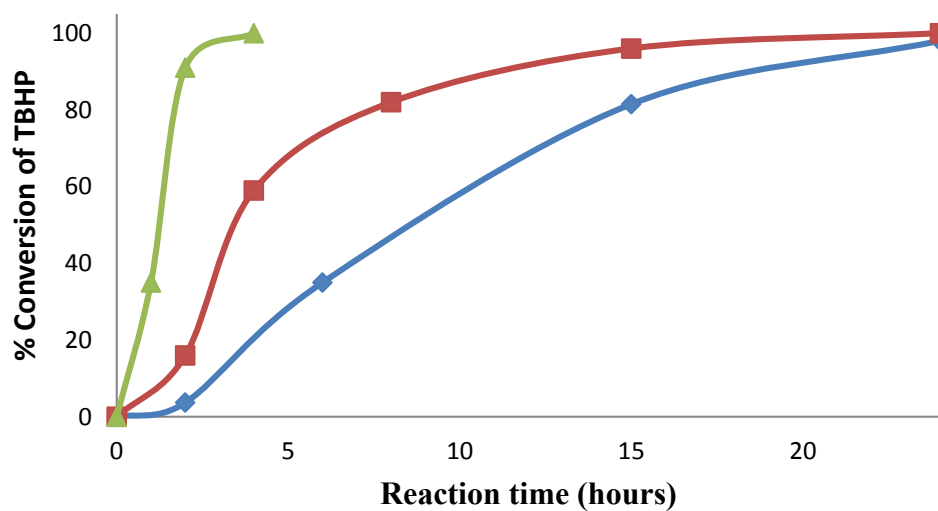
epoxyoctane (Table 2.2). With **c-P1-8** (0.02 mmol Ti, 3.6 mol% Ti relative to TBHP) as the catalyst, the reaction of 1-octene with TBHP (0.55 mmol) similarly proceeded with high TBHP efficiency to selectively form 1-epoxyoctane (Table 2.2) but required 24 h to achieve >90% TBHP conversion. Interestingly, while **P1-8**-catalyzed 1-octene epoxidation with TBHP proceeded with high 1-epoxyoctane selectivity over the reaction course and steady TBHP consumption was observed until late stages of the reaction (Figure 2.3), **c-P1-8**-catalyzed epoxidation of 1-octene with TBHP proceeded with sluggish TBHP consumption early in the reaction (~10% TBHP consumption was observed in 4 h) and seemingly gave mixed selectivities for 1-epoxyoctane until ~60% of TBHP had been consumed, even though no other product was observed. We reasoned that in addition to the lower Ti content in aforementioned **c-P1-8**-catalyzed reactions, poor solubility and slow swelling of **c-P1-8** contributed to the drastic difference observed in epoxidation efficiency of **P1-8** and **c-P1-8** catalysts. Thus, a reaction wherein **c-P1-8** was allowed to swell in 1-octene at 80 °C for 4 h prior to the addition of TBHP was carried out. Under these reaction conditions, the initial rate of TBHP consumption (and resulting 1-epoxyoctane formation) improved dramatically (Figure 2.3) albeit it still took 24 h to achieve >90% TBHP conversion. This result suggests that swelling of the Ti silsesquioxane material **c-P1-8** allows for greater partitioning of TBHP into the material and leads to faster 1-octene epoxidation. However, the reaction rate slows down with decreasing concentration of TBHP (especially late in the reaction when most of the TBHP has been consumed).

**Table 2.2**—Epoxidation of 1-octene with TBHP catalyzed by titanium silsesquioxane materials **P1-8** and **c-P1-8**.

Catalyst	Time (h)	Selectivity to epoxide (%) <sup>a</sup>	TBHP Conversion (%)
<b>P1-8</b> <sup>a</sup>	2	97.8 ± 0.3	99.8 ± 0.5
<b>c-P1-8</b> <sup>b</sup>	24	93.9 ± 3.0	95.7 ± 4.7

Conditions: T = 80 °C, TBHP = 0.55 mmol, 1-octene (20 g), 0.05 mmol Ti for **P1-8** and 0.02 mmol Ti for **c-P1-8**. <sup>a</sup>Selectivity = (mol 1,2-epoxyoctane formed/mol TBHP consumed) × 100; determined at TBHP conversion shown. Values quoted represent the average from at least three trials +/- the standard deviation.

**Figure 2.3**—TBHP conversion as a function of time for the epoxidation of 1-octene catalyzed by ▲ **P1-8**, □ **c-P1-8** (preswelled for 4 h), and ◇ **c-P1-8** (reaction conditions: T = 80 °C, TBHP = 0.55 mmol, 1-octene (20 g), 0.05 mmol Ti for **P1-8** and 0.02 mmol Ti for **c-P1-8**).



#### 2.3.4.3. Titanium leaching and catalyst recycling studies

To further establish that the Ti centers in Ti silsesquioxane materials **P1-8** and **c-P1-8** were the catalytically active sites and that the materials are robust alkene epoxidation catalysts, we conducted catalyst recycling studies. As shown in Table 2.3, the selectivity to epoxide was excellent and highly reproducible for the five recycles studied for Ti silsesquioxane materials **P1-8** and **c-P1-8** (see Experimental Section). However, the percentage of *t*-butyl hydroperoxide (TBHP) converted dropped drastically after two recycles (three epoxidation cycles) due to the fact that the reaction is autoretarded by the *t*-butanol co-product, which was retained in the materials in increasing concentration after each use; that alkene epoxidation is autoretarded by alcohol co-product has previously been observed for a variety of homogeneous and heterogeneous titanium and vanadium catalysts.<sup>133</sup> Additional evidence for autoretardation of 1-octene epoxidation by *t*-butanol by-product was obtained by adding a small amount of *t*-butanol (50  $\mu$ L) to a solution of 1-octene and TBHP containing pristine **P1-8** as catalyst (Table 2.3, entry 8). As expected, the reaction proceeded at a slower rate when *t*-butanol was added at the outset (77% TBHP conversion after 2h) than when it was not (essentially complete TBHP conversion after 2h, Table 2.2). Nonetheless, it is noteworthy that the selectivity for 1-epoxyoctane remained very high even for the reactions slowed by increased *t*-butanol concentrations, suggesting minimal (if any) catalyst degradation over the reaction course. Consistent with the preceding suggestion, as well as minimal leaching of titanium, PIXE analysis of recycled **c-P1-8** catalyst (isolated by precipitation from the reaction with CH<sub>3</sub>CN after five recycles) revealed that the Ti content was 0.38% in comparison with 0.45% found for pristine **c-P1-8**. Also remarkable, these Ti silsesquioxane catalysts are readily reparable. For example, after six epoxidation cycles using **c-P1-8** as catalyst, the material was isolated, treated with Ti(NMe<sub>2</sub>)<sub>4</sub> (yellow) in toluene, and then washed with acetonitrile until the washings were colorless and dried under vacuum. When the resulting material (repaired catalyst) was used as catalyst for the epoxidation of 1-octene under our typical epoxidation conditions, the selectivity to 1-

epoxyoctane and the TBHP conversion (Table 2.3, entry 14) were essentially identical to those of pristine **c-P1-8** (Table 2.2).

**Table 2.3**—Catalyst recyclability, retardation, and reparability studies<sup>a</sup>

Entry	Epox. Recycle #	Catalyst	Time (h)	Selectivity to Epoxide (%) <sup>b</sup>	TBHP Conversion (%)
1	1	<b>P1-8</b>	2	93	90
2	2	<b>P1-8</b>	2	96	76
3	3	<b>P1-8</b>	2	95	60
4	4	<b>P1-8</b>	2	100	45
5	4	<b>P1-8</b>	10	91	100
6	5	<b>P1-8</b>	2	99	45
7	5	<b>P1-8</b>	10	89	60
8	-	<b>P1-8</b> (50 $\mu$ L <i>t</i> -BuOH added)	2	92	77
9	1	<b>c-P1-8</b>	24	91	70
10	2	<b>c-P1-8</b>	24	93	56
11	3	<b>c-P1-8</b>	24	96	48
12	4	<b>c-P1-8</b>	24	88	51
13	5	<b>c-P1-8</b>	24	85	30
14	-	<b>c-P1-8</b> (repaired) <sup>c</sup>	24	93	100%

<sup>a</sup> Conditions: T = 80 °C, TBHP = 0.55 mmol, 1-octene (20 g), 0.05 mmol Ti for **P1-8** and 0.02 mmol Ti for **c-P1-8**. <sup>b</sup> Selectivity = (mol 1,2-epoxyoctane formed/mol TBHP consumed)  $\times$  100; determined at TBHP conversion shown. <sup>c</sup> See Experimental Section for details of catalyst repair.

## 2.4 Conclusions

Titanium silsesquioxane materials **P1-8** and **c-P1-8**, containing a mixture of tripodal titanium silsesquioxane regiomers covalently grafted to hyperbranched polysiloxysilane matrices, were investigated for the catalytic epoxidation of 1-octene with *t*-butyl hydroperoxide (TBHP). Using either **P1-8** or **c-P1-8** as catalyst, the epoxidation of 1-octene with TBHP proceeded with excellent selectivity to 1-epoxyoctane, consistent with previously reported catalytic properties of tripodal titanium silsesquioxane complexes.<sup>40</sup> While **P1-8** and **c-P1-8** display lower activity in the epoxidation of 1-octene with TBHP than the related symmetrically-substituted homogeneous catalyst [Ti(NMe<sub>2</sub>)<sub>2</sub>{(*i*-C<sub>4</sub>H<sub>9</sub>)<sub>7</sub>Si<sub>7</sub>O<sub>12</sub>}] (**9**), the activity of **P1-8**, which dissolved completely under our epoxidation conditions, was competitive with activities of homogeneous Mo catalysts, such as MoO(acac)<sub>2</sub>,<sup>130</sup> as well as heterogeneous Ti-containing catalysts such as the Shell catalyst<sup>131</sup> in 1-octene epoxidation with TBHP. The reduced activity of **c-P1-8** versus **P1-8** appears, in part, to be due to its slow swelling behavior under the reaction conditions; poor swelling hinders partitioning of TBHP into the material and results in slower 1-octene epoxidation. Both titanium silsesquioxane materials **P1-8** and **c-P1-8** are highly recyclable 1-octene epoxidation catalysts; high selectivity to epoxide was maintained through the six epoxidation cycles studied. However, autoretardation of 1-octene epoxidation by the *t*-butanol co-product retained in the materials led to a slow decrease in catalyst activity after each recycle. Finally, the catalysts are readily repairable, with the repaired material displaying identical activity and selectivity as the pristine catalyst.

## Chapter 3: Epoxidation of unactivated alkenes with TBHP catalyzed by tripodal titanium silsesquioxanes immobilized on a hyperbranched poly(siloxysilane) polymer

### 3.1 Introduction

Tripodal titanium silsesquioxanes have proven to be excellent catalysts for the epoxidation of unactivated alkenes with hydroperoxides<sup>40</sup> and display greater catalytic activity compared to related heterogeneous titanium catalysts such as titania-on-silica (Shell catalyst),<sup>84</sup> titanium silicate-1 (TS-1)<sup>38</sup> and titania-silica mixed oxides<sup>69</sup> which contain non-uniform active sites. The high catalytic activity of tripodal titanium is due to a balance between high Lewis acidity of the titanium center and the accessibility of the active center to the olefin.<sup>40,50,84</sup> Numerous studies have been conducted exploring the catalytic activity of tripodal titanium silsesquioxanes<sup>39,45,50,58,95</sup> using 1-octene, cyclohexene or cyclooctene however their versatility had yet to be explored. The results presented in Chapter 2 demonstrated that tripodal titanium silsesquioxanes can be immobilized onto a hyperbranched poly(siloxysilane) polymer, generating well-defined heterogeneous catalysts. Epoxidation of 1-octene employing *tert*-butyl hydroperoxide (TBHP) as the oxidant demonstrated that the materials produced are very selective, recyclable, and repairable catalysts.

Herein we report the successful epoxidation of cyclohexene, 1-methyl cyclohexene, limonene, and  $\alpha$ -pinene using homogeneous tripodal titanium POSS complexes. Additionally, we establish that when tripodal titanium silsesquioxanes are immobilized onto hyperbranched matrices, the resulting catalysts display similar activity compared to their homogeneous analogs for more demanding olefins. Finally, we demonstrate that the rate of reaction for immobilized tripodal titanium catalysts is not diffusion limited by determining the apparent activation energy and determining the initial rate of reaction under different stirring rates.

## 3.2 Experimental

All experiments were performed under an atmosphere of nitrogen either using standard Schlenk techniques or in a Vacuum Atmospheres glovebox. Solvents were dried and distilled by standard methods before use.<sup>126</sup> All solvents were stored in glovebox over 4Å molecular sieves that had been dried in a vacuum oven at 250 °C for at least 24 hours before use. All glassware were dried in an oven at 110 °C for 24 hours before use. Unless otherwise stated, all reagents were purchased from Aldrich Chemical Company and used without further purification. TBHP (5.5 M in nonane) was purchased from Aldrich Chemical Company which was stored over 4Å molecular sieves in the refrigerator. 1-octene were stored over 4Å molecular sieves in the glovebox along with Ti(NMe<sub>2</sub>)<sub>4</sub>. Allylisobutyl POSS (CH<sub>2</sub>=CHCH<sub>2</sub>(*i*-Bu)<sub>7</sub>Si<sub>8</sub>O<sub>12</sub> (**1**)), trisilanol isobutyl POSS, and trisilanol cyclohexyl POSS were purchased from Hybrid Plastics Inc. and dried overnight under vacuum at 60 °C prior to use. Karstedt's catalyst (2.4% Platinum divinyl tetramethyl disiloxane in xylene), chlorodimethylsilane, vinyl dimethylchlorosilane, and trichlorosilane were purchased from Gelest Inc. and used without further purification. Celite and activated charcoal were dried in a vacuum oven at 150 °C for 24 hours before use. The compounds ClMe<sub>2</sub>Si(CH<sub>2</sub>)<sub>3</sub>(*i*-Bu)<sub>7</sub>Si<sub>8</sub>O<sub>12</sub> (**3**), HMe<sub>2</sub>Si(CH<sub>2</sub>)<sub>3</sub>(*i*-Bu)<sub>7</sub>Si<sub>8</sub>O<sub>12</sub> (**4**), HMe<sub>2</sub>Si(CH<sub>2</sub>)<sub>3</sub>(*i*-C<sub>4</sub>H<sub>9</sub>)<sub>6</sub>Si<sub>7</sub>O<sub>9</sub>(OH)<sub>3</sub> (**6**, regiomeric mixture), [Ti(NMe<sub>2</sub>)}{(*i*-C<sub>4</sub>H<sub>9</sub>)<sub>7</sub>Si<sub>7</sub>O<sub>12</sub>} (**9**),<sup>32</sup> [Ti(NMe<sub>2</sub>)}{(*c*-C<sub>6</sub>H<sub>11</sub>)<sub>7</sub>Si<sub>7</sub>O<sub>12</sub>} (**10**),<sup>40</sup> **P1-6**, and **P1-8** were prepared by literature methods and shown in chapter 2. Vinyl-terminated hyperbranched polysiloxysilane **P1** (Scheme 3) was synthesized via Pt-catalyzed polymerization of HSi(OSiMe<sub>2</sub>CH=CH<sub>2</sub>)<sub>3</sub>,<sup>106</sup> and isolated as a viscous oil with molecular weight (*M<sub>n</sub>*) and polydispersity index (PDI) of 9318 g mol<sup>-1</sup> and 1.93, respectively. NMR (<sup>1</sup>H, <sup>13</sup>C, & <sup>29</sup>Si) and IR data of **P1** are consistent with literature data.

<sup>1</sup>H, <sup>13</sup>C, and <sup>29</sup>Si NMR spectra were recorded on a Varian INOVA 400 MHz spectrometer employing VnmrJ software. All chemical shifts are reported in units of δ (downfield of tetramethylsilane) and <sup>1</sup>H & <sup>13</sup>C chemical shifts were

referenced to residual solvent peaks.  $^{29}\text{Si}$  NMR spectra were recorded using inverse-gated proton decoupling in order to increase resolution and minimize nuclear Overhauser enhancement effects. To ensure accurate integrated intensities,  $[\text{Cr}(\text{acac})_3]$  (0.05 M) was added to  $^{13}\text{C}$  and  $^{29}\text{Si}$  NMR samples as a shiftless relaxation agent and a delay of at least 1.1 s was used between observation pulses for  $^{13}\text{C}$  and  $^{29}\text{Si}$  measurements.

GLC analyses were performed on an Agilent HP 6890 GC instrument equipped with a flame ionization detector (FID). A 1.0  $\mu\text{L}$  injection was employed and helium was used as the carrier gas. The FID was set to 300  $^\circ\text{C}$  and the inlet was isothermally maintained at 140  $^\circ\text{C}$  in split mode (split ratio 50:1; split flow 221 ml/min). An Agilent J&W HP-1 column (25 m  $\times$  320  $\mu\text{m}$   $\times$  0.52  $\mu\text{m}$ ) rated to 350  $^\circ\text{C}$  was employed, maintaining a constant pressure of 14.5 psi. The oven parameters were programmed to start at 35  $^\circ\text{C}$ ; followed by a ramp of 45  $^\circ\text{C}/\text{min}$  to 200  $^\circ\text{C}$  and held for 2 minutes. The total run time was 8.67 minutes. Quantification was performed through the use of toluene as an internal standard. Chromatographic programming was performed using Agilent Chemstation software. Conversion and selectivity were calculated as follows:

$$\text{Conversion (C}_{\text{TBHP}}) = \frac{\text{moles TBHP consumed}}{\text{initial moles of TBHP}} \times 100$$

$$\text{Selectivity (S}_{\text{TBHP}}) = \frac{\text{moles of epoxide formed}}{\text{moles of TBHP consumed}} \times 100$$

$$\text{Conversion (C}_{\text{olefin}}) = \frac{\text{moles of olefin consumed}}{\text{initial moles of olefin}} \times 100$$

$$\text{Selectivity (S}_{\text{olefin}}) = \frac{\text{moles of epoxide formed}}{\text{moles of olefin consumed}} \times 100$$

$$\text{TON (turnover number)} = \frac{\text{moles of epoxide formed}}{\text{moles of Ti}}$$

$$\text{TOF (Turnover frequency)} = \frac{\text{TON}}{\text{time (hr)}}$$



IR spectra were recorded on a Thermo Scientific Nicolet iS10 FT-IR Spectrometer. UV-vis spectra were collected on a Thermo Scientific Evolution 201 spectrophotometer using pentane solutions sealed in 1 cm cuvettes under N<sub>2</sub>. Gel permeation chromatography (GPC) analyses were carried out on an Agilent Technologies PL-GPC 50 Integrated GPC equipped with a UV detector and a refractive index detector, as well as a Polymer Laboratories PL-AS RT GPC autosampler. The GPC was equipped with two PL gel Mini-MIX C columns (5 micron, 4.6 mm ID). The GPC columns were eluted with tetrahydrofuran at 30 °C at 0.3 mL/min and were calibrated using monodisperse polystyrene standards. Elemental analyses were performed by either Robertson Microlit laboratories or Galbraith laboratories, and typically included the use of a combustion aid. Proton-induced X-ray emission (PIXE) analyses were performed by Elemental Analysis Inc.

### 3.2.1 Synthesis of *c-P1-6*

A round-bottom three-neck flask (50 mL) equipped with a magnetic stir bar, condenser with N<sub>2</sub> inlet, and thermometer was charged with vinyl-terminated hyperbranched polysiloxysilane **P1** (4.06 g, 0.429 mmol, ~24 mmol CH=CH<sub>2</sub> groups), *HMe<sub>2</sub>Si(CH<sub>2</sub>)<sub>3</sub>(i-C<sub>4</sub>H<sub>9</sub>)<sub>6</sub>Si<sub>7</sub>O<sub>9</sub>(OH)<sub>3</sub>* (**6**, 2.01 g, 2.41 mmol), toluene (40 mL), and Karstedt's catalyst (0.2 mL). The reaction mixture was heated at 60 °C overnight (~16 h) at which point complete disappearance of the Si-H groups was confirmed by <sup>1</sup>H NMR spectroscopy. The reaction mixture was cooled to room temperature and then charged with 1,1,3,3,5,5-hexamethyltrisiloxane (3.75 g, 18 mmol) and Karstedt's catalyst (0.2 mL). After stirring the solution at 60 °C overnight (~16 h), it was cooled to room temperature and volatiles were removed under reduced pressure, affording the crosslinked hyperbranched polymer **c-P1-6** (7.4 g, ~75% yield, ~20.4% by weight of **6**) as a colorless elastomeric solid. Poor solubility of **c-P1-6** prevented its characterization by solution NMR spectroscopy. However, its ATR-IR spectrum was absent of vinyl absorptions.

### 3.2.2 Synthesis of titanium silsesquioxane material P1-8

In a glovebox,  $\text{Ti}(\text{NMe}_2)_4$  (0.300 g, 1.34 mmol) was added by syringe to a stirred toluene solution (15 mL) of **P1-6** (4.60 g, 1.24 mmol of **6**). The resulting deep yellow solution was allowed to stir for 1 h then concentrated to dryness under reduced pressure. The residue was washed with acetonitrile until the washings were no longer colored and then dried under vacuum to give **P1-8** as a viscous orange gel. Yield: 4.61 g, 94%. Uv-vis:  $\lambda_{\text{max}} = 203 \text{ nm}$ . Anal. Calcd. for **P1-8**: Ti, 1.28. Found: Ti, 1.11 (5% relative error).

### 3.2.3 Synthesis of titanium silsesquioxane material c-P1-8

In a glovebox,  $\text{Ti}(\text{NMe}_2)_4$  (0.44 g, 1.96 mmol) was added by syringe to a stirred toluene solution (15 mL) of **c-P1-6** (7.4 g, 1.8 mmol of **6**). The resulting deep yellow solution was let stir for 1 h then concentrated to dryness under reduced pressure. The residue was washed with acetonitrile until the washings were no longer colored and then dried under vacuum to give **c-P1-8** as an orange solid. Yield: 7.4 g, 96%. Poor solubility of **c-P1-8** prevented its characterization by solution NMR spectroscopy. Anal. Calcd. for **c-P1-8**: Ti= 1.16 Found: Ti= 0.935 (5% relative error).

### 3.2.4 Epoxidation trials

#### 3.2.4.1 Trials for various olefins

Epoxidation trials were performed in a magnetically stirred 50 mL three-necked flask equipped with condenser, thermometer probe, and septum for withdrawing samples. Typically, titanium polymer catalysts (0.02 mmol of Ti), TBHP (3 mmol), chlorobenzene (1 g, 8 mmol as internal standard), toluene as solvent (20 mL) and quantity of olefin (1:1 ratio = 3 mmol; 20:1 ratio = 60 mmol) was added to a 3-neck flask which was heated at 80 °C. A sample was immediately taken for GC analysis and additional samples for analysis were taken at regular intervals.

#### 3.2.4.2 Analysis for determination of apparent activation energy

Typically, a solution of 1-octene (20 g, 0.18 mol), TBHP (100  $\mu$ L, 0.55 mmol), toluene (2 g, 0.02 mol as internal standard), and titanium polymer catalyst (0.02 mmol) were added to a 3-neck flask with thermometer, condenser with nitrogen inlet, and a magnetic stir bar were heated at different temperatures. A sample was taken immediately for GC analysis and additional samples were taken at regular intervals until at least 30% conversion with a total of at least four points for rate constant determination.

Apparent activation energy was calculated by plotting  $1/T$  vs.  $\ln(k_2)$  where the slope of the resulting straight line corresponds to  $E_a/R$  where  $R$  is the gas constant (8.314 J/mol $\cdot$ K),  $k_2$ =rate constant for reaction, and  $T$ =temperature (K).

#### 3.2.4.3 Recyclability of **NCP-9** and **CP-9**

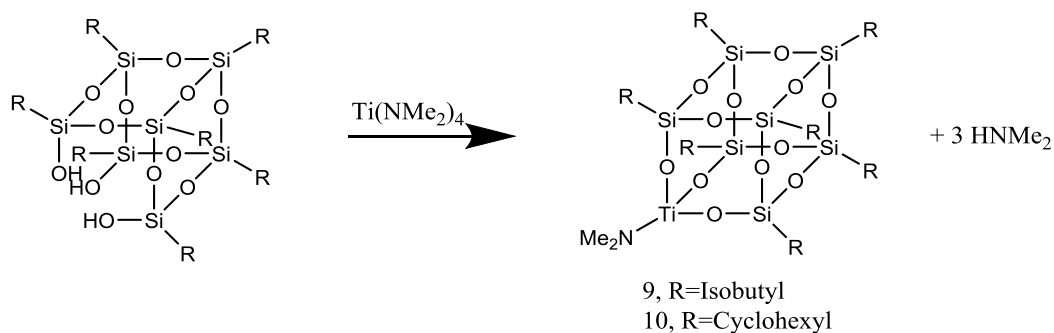
The experimental procedure is the same as described for olefin epoxidation (20:1 ratio) with TBHP at 80° C using **P1-8** or **c-P1-8** as catalysts. After the reaction had proceeded for a specific amount of time (Table 3.16), the reaction mixture was cooled to room temperature and concentrated to dryness under reduced pressure. The catalyst material was washed with acetonitrile to remove residual organic followed by drying under vacuum overnight. The catalyst was then reused for limonene epoxidation as previously described.

### 3.3 Results/Discussion

#### 3.3.1 Preparation of catalysts

Homogeneous tripodal Ti analogs, specifically  $[\text{Ti}(\text{NMe}_2)\{\text{(i-C}_4\text{H}_9)_7\text{Si}_7\text{O}_{12}\}]$  (**9**) and  $\text{Ti}(\text{NMe}_2)\{\text{(c-C}_6\text{H}_{11})_7\text{Si}_7\text{O}_{12}\}$  (**10**) were prepared in excellent yields via protonolysis (Scheme 3.1) of the trisilanol precursor with  $\text{Ti}(\text{NMe}_2)_4$  as shown in chapter 2. The complexes are air- and moisture-sensitive orange-yellow crystalline solids soluble in common organic solvents.

**Scheme 3.1**—Synthetic route for **9** and **10**



In chapter 2, we showed that **P1-8** and **c-P1-8** (Scheme 3.2) are active catalysts for the epoxidation of 1-octene employing *tert*-butyl hydroperoxide (TBHP). **P1-8** and **c-P1-8** were synthesized by grafting a regiomer mixture of (silyl)propyl-trisilanol isobutyl POSS (**6**) ligand onto vinyl terminated hyperbranched poly(siloxysilane) via hydrosilylation reaction. **6** was synthesized via Pt-catalyzed hydrosilylation of  $\text{CH}_2=\text{CHCH}_2(i\text{-Bu})_7\text{Si}_8\text{O}_{12}$  (**1**) with  $\text{HSiMe}_2\text{Cl}$  to give  $\text{ClMe}_2\text{Si}(\text{CH}_2)_3(i\text{-Bu})_7\text{Si}_8\text{O}_{12}$  (**3**) in excellent yield. Reduction of **3** with  $\text{LiAlH}_4$  afforded  $\text{HMe}_2\text{Si}(\text{CH}_2)_3(i\text{-Bu})_7\text{Si}_8\text{O}_{12}$  (**4**) where one framework silicon was removed via a modified procedure adapted from Feher and colleagues<sup>98,99</sup> to produce  $\text{HMe}_2\text{Si}(\text{CH}_2)_3(i\text{-C}_4\text{H}_9)_6\text{Si}_7\text{O}_9(\text{OH})_3$  (**6**), consisting of three regiomers.



**P1-8** was prepared by grafting (silyl)propyl-trisilanolisobutyl-POSS ligand (**6**, ~5 mol% relative to moles of **P1** vinyl groups) onto hyperbranched poly(siloxysilane) matrices containing vinyl terminated groups, via Pt-catalyzed hydrosilylation to yield **P1-6** as a colorless viscous gel. Finally, **P1-6** was reacted with  $\text{Ti}(\text{NMe}_2)_4$  (1.1 equiv) to yield **P1-8** as an orange viscous gel which was soluble in common organic solvents (toluene, methylene chloride, THF, chloroform, and 1-octene). The formulation and structure of **P1-8** was confirmed by solution NMR, IR, UV-vis, and elemental analysis. Proton-induced X-ray emission (PIXE) analysis found 1.11 weight percent (wt%) of Ti in **P1-8**.

Alternatively, **c-P1-8** was prepared by attaching (silyl)propyl-trisilanolisobutyl-POSS ligand (**6**, ~10 mol% relative to moles of **P1** vinyl groups) onto the hyperbranched poly(siloxysilane) matrix containing vinyl terminated groups followed by crosslinking with 1,1,3,3,5,5-hexamethyltrisiloxane. The catalyst was insoluble in common organic solvents making solution characterization impossible however IR and PIXE (0.94 wt% Ti) were conducted to confirm the successful formation of **c-P1-8**.

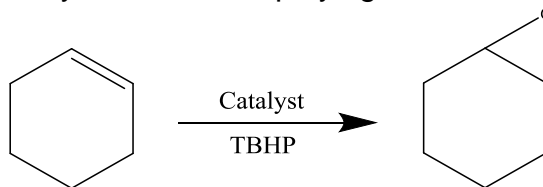
### *3.3.2 Alkene Epoxidation activity*

#### *3.3.2.1 Homogeneous tripodal titanium catalysts using a 20:1 olefin/TBHP ratio*

Previous work has revealed the excellent activity of tripodal titanium silsesquioxanes catalysts for the epoxidation of 1-octene using TBHP as the oxidant; however these catalysts had yet to be explored using more demanding olefins such as limonene or  $\alpha$ -pinene. A series of unactivated alkenes was studied beginning with cyclohexene which is known to be more reactive than terminal olefins such as 1-octene. 1-methylcyclohexene was then explored in order to determine if the addition of steric bulk around the olefin would inhibit the catalytic activity. Limonene and  $\alpha$ -pinene were also explored as these pose unique challenges. For example, limonene contains an internal and terminal olefin while  $\alpha$ -pinene is very prone to rearrangements. Epoxidation of limonene and  $\alpha$ -pinene are also attractive because their oxidation products are used in the fragrance industry.

Homogeneous analogs [Ti(NMe<sub>2</sub>)<sub>2</sub>]{(*i*-C<sub>4</sub>H<sub>9</sub>)<sub>7</sub>Si<sub>7</sub>O<sub>12</sub>}] (**9**) and [Ti(NMe<sub>2</sub>)<sub>2</sub>]{(*c*-C<sub>6</sub>H<sub>11</sub>)<sub>7</sub>Si<sub>7</sub>O<sub>12</sub>}] (**10**) (0.67 mol% Ti relative to TBHP), displayed excellent catalytic activity for the epoxidation of cyclohexene employing TBHP as the oxidant at 80 °C under pseudo-first-order conditions (olefin:TBHP of 20:1) where the reaction progress was followed by taking samples for GC analysis at regular intervals (Table 3.1). A 20:1 olefin:TBHP ratio was explored because numerous industrial processes use a large excess of olefin to yield faster reaction rates and the unreacted olefin can be easily recycled. Remarkably, it was observed that both **9** and **10** (Table 3.1, entry 1 and 2) were extremely selective and provided complete, instantaneous conversion of TBHP. This resulted in a high turnover frequency (TOF) of 1771 hr<sup>-1</sup> which is better than heterogeneous titanium analog catalysts such as Ti-MCM-41 (5 hr<sup>-1</sup>),<sup>134</sup> Ti-aerogel catalysts (35 hr<sup>-1</sup>),<sup>70,134</sup> and TS-1 (13.5 hr<sup>-1</sup>),<sup>47</sup> as well as the homogeneous catalyst Ti(OSiMe<sub>3</sub>)<sub>4</sub> (1470 hr<sup>-1</sup>).<sup>135</sup> Additionally, the TOF calculated for **9** and **10** are conservative values given that the TOF was calculated at high olefin conversion and reactions generally slow down near completion.

**Table 3.1**—Catalytic activity of tripodal titanium catalysts (**9** and **10**) for epoxidation of cyclohexene employing a 20:1 olefin:TBHP ratio



Entry	Catalyst	Time (min)	S <sub>TBHP</sub> <sup>*</sup> (%)	C <sub>TBHP</sub> (%)	TON <sup>#</sup>	TOF <sup>#</sup> (hr <sup>-1</sup> )
1	<b>9</b>	< 5	99	100	147	≥1771
2	<b>10</b>	< 5	>99	98	147	≥1771

Conditions: T = 80 °C, Ti = 0.02 mmol, TBHP = 3 mmol, Toluene as solvent (20 mL), Chlorobenzene (1 g) as internal standard, and olefin (20:1 ratio = 60 mmol). Selectivity and conversion values represent the average from at least three trials +/- the standard deviation

\*Selectivity for cyclohexene oxide and calculated at time reported

$$* S_{\text{TBHP}} = \frac{\text{moles of epoxide formed}}{\text{moles of TBHP consumed}} \times 100$$

$$C_{\text{TBHP}} = \frac{\text{moles of TBHP consumed}}{\text{initial moles of TBHP}} \times 100$$

$$\text{TON calculated by } \frac{\text{moles of epoxide formed}}{\text{moles of Ti}}$$

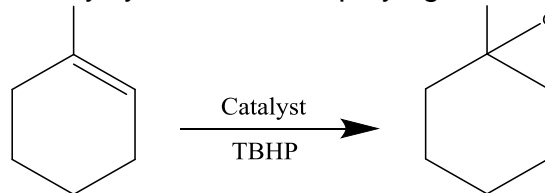
$$\text{TOF calculated by } \frac{\text{TON}}{\text{time (hr)}}$$

<sup>#</sup>TON and TOF calculated at the conversion shown in the table (C<sub>TBHP</sub>)

The epoxidation of 1-methylcyclohexene with added steric bulk around the olefin was explored. It was hypothesized the rate of reaction may drop slightly due to the steric hindrance of the olefin reacting at the active site. However, **10** displayed similar activity for the epoxidation of 1-methylcyclohexene (100% conversion, 95% selectivity, 1717 hr<sup>-1</sup> TOF, Table 3.2) compared to cyclohexene. Alternatively, **9** ([Ti(NMe<sub>2</sub>)<sub>2</sub>]{(*i*-C<sub>4</sub>H<sub>9</sub>)<sub>7</sub>Si<sub>7</sub>O<sub>12</sub>}) required slightly longer reaction time compared to **10** (80% of TBHP at 5 minutes). However within 10 minutes, all the TBHP had been consumed while maintaining high selectivity and high TOF (1373 hr<sup>-1</sup>). Previously, we have shown that for the epoxidation of 1-octene, **9** intrinsically has a slower rate compared to **10** ([Ti(NMe<sub>2</sub>)<sub>2</sub>]{(*c*-C<sub>6</sub>H<sub>11</sub>)<sub>7</sub>Si<sub>7</sub>O<sub>12</sub>}) , therefore this result was not surprising.



**Table 3.2**—Catalytic activity of tripodal titanium catalysts (**9** and **10**) for epoxidation of 1-methylcyclohexene employing a 20:1 olefin:TBHP ratio



Entry	Catalyst	Time (min)	S <sub>TBHP</sub> <sup>*</sup> (%)	C <sub>TBHP</sub> (%)	TON <sup>#</sup>	TOF <sup>#</sup> (hr <sup>-1</sup> )
1	<b>9</b>	5	>95	80 ±2	114	1373
2	<b>9</b>	10	>95	100		
3	<b>10</b>	5	>95	100	143	1717

Conditions: T = 80 °C, Ti = 0.02 mmol, TBHP = 3 mmol, Toluene as solvent (20 mL), Chlorobenzene (1 g) as internal standard, and olefin (20:1 ratio = 60 mmol) Selectivity and conversion values represent the average from at least three trials +/- the standard deviation

\*Selectivity for 1-methylcyclohexene oxide and calculated at time reported

$$* S_{TBHP} = \frac{\text{moles of epoxide}}{\text{moles of epoxide} + \text{moles of other products formed}} \times 100$$

$$C_{TBHP} = \frac{\text{moles of TBHP consumed}}{\text{initial moles of TBHP}} \times 100$$

$$\text{TON calculated by } \frac{\text{moles of epoxide formed}}{\text{moles of Ti}} \quad \text{TOF calculated by } \frac{\text{TON}}{\text{time (hr)}}$$

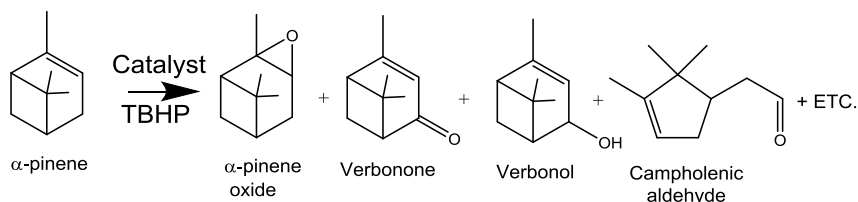
<sup>#</sup>TON and TOF calculated at the conversion shown in the table (C<sub>TBHP</sub>)

Limonene offered a unique challenge due to the potential for competitive reaction between the internal and terminal olefins. Previously, it has been shown that the internal olefin is favored for epoxidation using Ti catalysts such as Ti-SBA<sup>136</sup> and homogeneous tetrapodal titanium.<sup>54</sup> Therefore, we expected to observe mainly the epoxidation of internal olefin. Remarkably, both **9** and **10** completely converted the internal olefin of limonene to give limonene oxide in 10 minutes (Table 3.3). Both **9** and **10** exhibited excellent catalytic activity although there was a slight decrease in the turnover frequency (TOF) for limonene epoxidation compared to 1-methylcyclohexene epoxidation. When the epoxidation of limonene was catalyzed by homogenous tetrapodal titanium (Ti[(c-





**Table 3.4**—Catalytic activity of tripodal titanium catalysts (**9** and **10**) for epoxidation of  $\alpha$ -pinene employing a 20:1 olefin:TBHP ratio



Entry	Catalyst	Time (min)	S <sub>TBHP</sub> <sup>*</sup> (%)	C <sub>TBHP</sub> (%)	TON <sup>#</sup>	TOF <sup>#</sup> (hr <sup>-1</sup> )
1	<b>9</b>	10	95 ± 3	87 ± 4	124	743
2	<b>9</b>	30	92 ± 1	100		
3	<b>10</b>	10	96 ± 2	89 ± 2	124	743
4	<b>10</b>	30	91 ± 4	100		

Conditions: T = 80 °C, Ti = 0.02 mmol, TBHP = 3 mmol, Toluene as solvent (20 mL), Chlorobenzene (1 g) as internal standard, and olefin (20:1 ratio = 60 mmol) Selectivity and conversion values represent the average from at least three trials +/- the standard deviation

\*Selectivity for  $\alpha$ -pinene oxide and calculated at time reported

$$* S_{\text{TBHP}} = \frac{\text{moles of epoxide formed}}{\text{moles of TBHP consumed}} \times 100$$

$$C_{\text{TBHP}} = \frac{\text{moles of TBHP consumed}}{\text{initial moles of TBHP}} \times 100$$

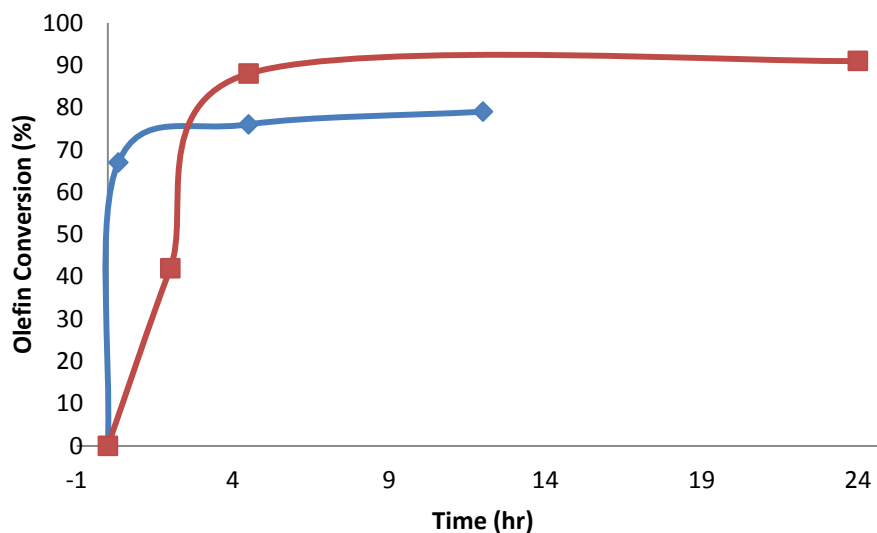
$$\text{TON calculated by } \frac{\text{moles of epoxide formed}}{\text{moles of Ti}} \quad \text{TOF calculated by } \frac{\text{TON}}{\text{time (hr)}}$$

<sup>#</sup>TON and TOF calculated at the conversion shown in the table (C<sub>TBHP</sub>)

### 3.3.2.2 Homogeneous tripodal titanium catalysts using a 1:1 olefin/TBHP ratio

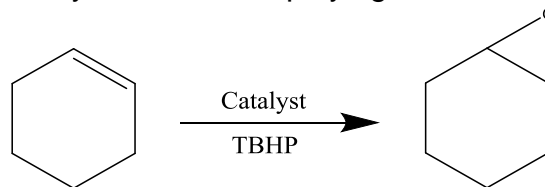
Due to the excellent epoxidation activity of [Ti(NMe<sub>2</sub>)<sub>2</sub>]{(i-C<sub>4</sub>H<sub>9</sub>)<sub>7</sub>Si<sub>7</sub>O<sub>12</sub>} (**9**) and [Ti(NMe<sub>2</sub>)<sub>2</sub>]{(c-C<sub>6</sub>H<sub>11</sub>)<sub>7</sub>Si<sub>7</sub>O<sub>12</sub>} (**10**) employing a 20:1 olefin/TBHP ratio, a 1:1 olefin:TBHP ratio was explored to determine if the catalysts remained extremely selective. Employing a 1:1 olefin:TBHP ratio resulted in lower concentration of reactants near completion of the reaction, all reactions therefore required longer reaction times, resulting in lower turnover frequencies (TOF). After about 50% consumption of the different olefins explored (Figure 3.2), the reactions leveled off and slowed down drastically.

**Figure 3.2**—Reaction profile for the epoxidation of 1-methylcyclohexene (■) and limonene (◇) employing **10** as the catalyst



Remarkably, for the epoxidation of cyclohexene (Table 3.5), both **9** and **10** displayed excellent selectivity (95%) and TBHP efficiency (95%), suggesting that significant decomposition of TBHP did not occur over the longer time (4.5 hrs) required for complete conversion of TBHP. Furthermore, as shown in Table 3.5, both **9** and **10** catalyze cyclohexene epoxidation very quickly, converting 69% and 76% cyclohexene respectively in 40 minutes. However the reaction then slows down, due presumably to reduced concentration of the reactants. Additionally, the turnover frequencies (TOF) for **9** and **10**, calculated at 69% and 76% olefin conversion respectively are high and generally surpass those reported for titanium catalysts such as (Ti-MCM-41 ( $5 \text{ hr}^{-1}$ ),<sup>134</sup> Ti-aerogel catalysts ( $35 \text{ hr}^{-1}$ ),<sup>70,134</sup> and TS-1 ( $13.5 \text{ hr}^{-1}$ ) all calculated at less than 25% cyclohexene conversion).<sup>47</sup> Additionally, the TOF calculated for **9** and **10** are conservative values given that the TOF was calculated at high olefin conversion and reactions generally slow down near completion.

**Table 3.5**—Catalytic activity of tripodal titanium catalysts (**9** and **10**) for epoxidation of cyclohexene employing a 1:1 olefin:TBHP ratio



Entry	Catalyst	Time (hr)	S <sub>olefin</sub> <sup>*</sup> (%)	C <sub>olefin</sub> (%)	S <sub>TBHP</sub> (%)	TON <sup>#</sup>	TOF <sup>#</sup> (hr <sup>-1</sup> )
1	<b>9</b>	40 min	93 ± 4	69 ± 5	90 ± 2	96	144
2	<b>9</b>	4.5	96 ± 3	96	95 ± 5		
3	<b>10</b>	40 min	94 ± 3	76 ± 5	100	107	161
4	<b>10</b>	4.5	96 ± 3	95 ± 2	96 ± 4		

Conditions: T = 80 °C, Ti = 0.02 mmol, TBHP = mmol, Toluene as solvent (20 mL), Chlorobenzene (1 g) as internal standard, and olefin (1:1 ratio = 3 mmol)  
 Selectivity, Conversion, and TBHP efficiency values represent the average from at least three trials +/- the standard deviation

\*Selectivity for cyclohexene oxide and calculated at time reported

$$\text{*Selectivity (S}_{\text{olefin}}) = \frac{\text{moles of epoxide formed}}{\text{moles of olefin consumed}} \times 100$$

$$\text{Conversion (C}_{\text{olefin}}) = \frac{\text{moles of olefin consumed}}{\text{initial moles of olefin}} \times 100$$

$$\text{Selectivity based on TBHP (S}_{\text{TBHP}}) = \frac{\text{moles of epoxide formed}}{\text{moles of TBHP consumed}} \times 100$$

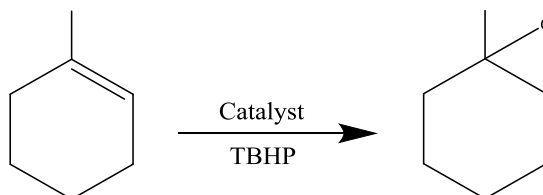
$$\text{TON calculated by } \frac{\text{moles of epoxide formed}}{\text{moles of Ti}} \quad \text{TOF calculated by } \frac{\text{TON}}{\text{time (hr)}}$$

#TON and TOF calculated at the conversion shown in the table (C<sub>TBHP</sub>)

Increased steric bulk of the alkene influences in the activity of the catalysts. Nonetheless, **10** ([Ti(NMe<sub>2</sub>)<sub>2</sub>]{(C-C<sub>6</sub>H<sub>11</sub>)<sub>7</sub>Si<sub>7</sub>O<sub>12</sub>}) still displayed high selectivity to epoxide (>95%, Table 3.6). At 4.5 hours, we observed 100% conversion of cyclohexene (Table 3.5) while only 88% of 1-methylcyclohexene was converted (Table 3.6). The catalyst drastically slows down after 4.5 hour; only 90% of 1-methylcyclohexene was consumed after 24 hours. While extending the reaction time to 48 hours resulted in only an additional 2% conversion. Although **10** demonstrated lower activity at a 1:1 ratio (olefin:TBHP) compared to the 20:1 ratio, it is significant that the selectivity remain very high throughout the reaction. This suggests that these tripodal titanium

silsesquioxane complexes are efficient catalysts although the TOF for 1-methylcyclohexene ( $71 \text{ hr}^{-1}$ ) decreased slightly compared to cyclohexene ( $161 \text{ hr}^{-1}$ ).

**Table 3.6**—Catalytic activity of tripodal titanium catalyst (**10**) for epoxidation of 1-methylcyclohexene employing a 1:1 olefin:TBHP ratio



Entry	Catalyst	Time (hr)	S <sub>olefin</sub> <sup>*</sup> (%)	C <sub>olefin</sub> (%)	S <sub>TBHP</sub> (%)	TON <sup>#</sup>	TOF <sup>#</sup> (hr <sup>-1</sup> )
1	<b>10</b>	40 min	> 95	33 ± 3	> 95	47	71
2	<b>10</b>	4.5	> 95	88 ± 1	> 95		
3	<b>10</b>	24	> 95	91 ± 1	> 95		

Conditions: T = 80 °C, Ti = 0.02 mmol, TBHP = mmol, Toluene as solvent (20 mL), Chlorobenzene (1 g) as internal standard, and olefin (1:1 ratio = 3 mmol)  
Selectivity, Conversion, and TBHP efficiency values represent the average from at least three trials +/- the standard deviation

\*Selectivity for 1-methylcyclohexene oxide and calculated at time reported

$$* \text{ Selectivity (S}_{\text{olefin}}) = \frac{\text{moles of epoxide}}{\text{moles of epoxide} + \text{moles of other products formed}} \times 100$$

$$\text{Conversion (C}_{\text{olefin}}) = \frac{\text{moles of olefin consumed}}{\text{initial moles of olefin}} \times 100$$

$$\text{Selectivity based on TBHP (S}_{\text{TBHP}}) = \frac{\text{moles of epoxide formed}}{\text{moles of TBHP consumed}} \times 100$$

$$\text{TON calculated by } \frac{\text{moles of epoxide formed}}{\text{moles of Ti}} \quad \text{TOF calculated by } \frac{\text{TON}}{\text{time (hr)}}$$

<sup>#</sup>TON and TOF calculated at the conversion shown in the table (C<sub>TBHP</sub>)

It was anticipated with the epoxidation of limonene that epoxidation of the terminal olefin would become competitive at 1:1 olefin:TBHP ratio. As expected, the bis-epoxide (Table 3.7) was observed as a by-product. Using **10** as catalyst (Table 3.7) resulted in 67% limonene conversion along with 87% selectivity for the internal epoxide and 81% conversion of TBHP (59% TBHP efficiency) after

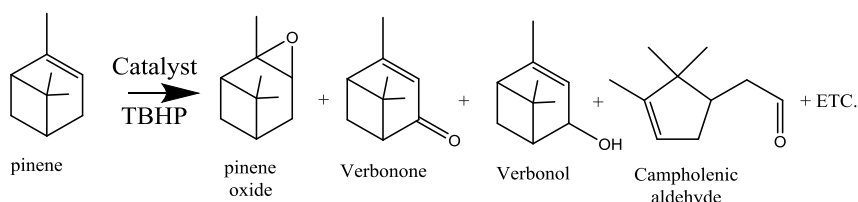
40 minutes. However after 12 hours, the reaction had only proceeded to 79% conversion of the olefin although all the TBHP was consumed. It was observed that Ti largely prefers the internal olefin since the only products formed were limonene oxide (internal epoxide) as well as the bis-epoxide (presumably 13% selectivity for the formation of the bis-epoxide). Bis-epoxide was the main co-product because less internal olefins were present in the reaction mixture near completion leaving a large amount of terminal olefins present. Due to a large amount of terminal olefins present in the reaction mixture, the bis-epoxide was formed, however no external epoxide was observed. This confirms that the Ti largely prefers the internal olefin since the epoxidation of the terminal olefin only occurs after the internal olefin was first oxidized. The TOF (calculated at 40 minutes) for the epoxidation of limonene ( $131 \text{ hr}^{-1}$ ) increases compared to 1-methylcyclohexene ( $71 \text{ hr}^{-1}$ ) suggesting that limonene is more reactive initially although the reaction also slows down faster than the epoxidation of 1-methylcyclohexene. These results suggest that tripodal titanium silsesquioxane complexes are extremely active for the epoxidation of limonene irrespective of the olefin:TBHP ratio. **10** also shows greater catalytic activity compared to other titanium containing catalysts such as homogenous tetrapodal titanium ( $\text{Ti}[(\text{c-C}_5\text{H}_9)_7\text{Si}_7\text{O}_{11}(\text{OSiMe}_2\text{CHCH}_2)]_2$ ) (TOF of  $12 \text{ hr}^{-1}$  calculated at 30% limonene conversion)<sup>54</sup> and heterogeneous analogs Ti-MCM-41 and Ti/SiO<sub>2</sub> ( $20 \text{ hr}^{-1}$  and  $19 \text{ hr}^{-1}$  respectively, calculated at 1 hour (37% limonene conversion)).<sup>137</sup>





produce campholenic aldehyde, leading to low selectivities (<50%) for  $\alpha$ -pinene oxide.<sup>104</sup>

**Table 3.8**—Catalytic activity of tripodal titanium catalyst (**10**) for epoxidation of  $\alpha$ -pinene employing a 1:1 olefin:TBHP ratio



Entry	Catalyst	Time	S <sub>olefin</sub> <sup>*</sup> (%)	C <sub>olefin</sub> (%)	S <sub>TBHP</sub> (%)	TON <sup>#</sup>	TOF <sup>#</sup> (hr <sup>-1</sup> )
1	<b>10</b>	40 min	78 ± 9	25 ± 5	75	29	44
2	<b>10</b>	5 hr	58 ± 6	71 ± 5	52		

Conditions: T = 80 °C, Ti = 0.02 mmol, TBHP = mmol, Toluene as solvent (20 mL), Chlorobenzene (1 g) as internal standard, and olefin (1:1 ratio = 3 mmol)  
 Selectivity, Conversion, and TBHP efficiency values represent the average from at least three trials +/- the standard deviation

\*Selectivity for  $\alpha$ -pinene oxide and calculated at time reported

$$\text{*Selectivity (S}_{\text{olefin}}) = \frac{\text{moles of epoxide formed}}{\text{moles of olefin consumed}} \times 100$$

$$\text{Conversion (C}_{\text{olefin}}) = \frac{\text{moles of olefin consumed}}{\text{initial moles of olefin}} \times 100$$

$$\text{Selectivity based on TBHP (S}_{\text{TBHP}}) = \frac{\text{moles of epoxide formed}}{\text{moles of TBHP consumed}} \times 100$$

$$\text{TON calculated by } \frac{\text{moles of epoxide formed}}{\text{moles of Ti}} \quad \text{TOF calculated by } \frac{\text{TON}}{\text{time (hr)}}$$

#TON and TOF calculated at the conversion shown in the table (C<sub>TBHP</sub>)

Although [Ti(NMe<sub>2</sub>)<sub>2</sub>]{(C-C<sub>6</sub>H<sub>11</sub>)<sub>7</sub>Si<sub>7</sub>O<sub>12</sub>} (**10**) required longer reaction times for a 1:1 olefin:TBHP ratio, the catalysts remain extremely selective for the epoxidation of cyclohexene, 1-methylcyclohexene, and limonene. From the TOF, we observed that sterics do play a role in the 1:1 olefin:TBHP epoxidation reactions where the order of initial reactivity is cyclohexene>limonene>1-methylcyclohexene> $\alpha$ -pinene. Overall, the selectivities and TOF were high,

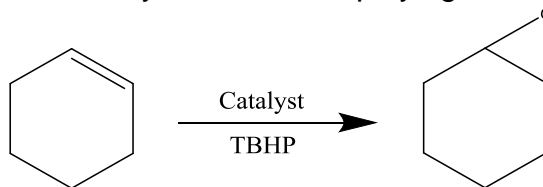
making these catalyst excellent candidates for the immobilization onto inert supports.

### 3.3.2.3 Immobilized tripodal titanium catalysts using a 20:1 olefin/TBHP ratio

Due to the excellent activity of homogeneous tripodal titanium complexes (**9** and **10**), two immobilized catalysts were explored, **P1-8**, a viscous, soluble material and **c-P1-8** which was only slightly soluble in the reaction mixture. Epoxidation trials of **P1-8** and **c-P1-8** (0.67 mol% Ti relative to TBHP), were explored using TBHP as the oxidant, toluene as a solvent, and chlorobenzene as the internal standard at 80 °C where the reaction progress was followed by taking samples for GC analysis at regular intervals. .

When epoxidation of cyclohexene was explored, both **P1-8** and **c-P1-8** invariably required longer reaction times compared to the homogenous derivatives **9** and **10**. TBHP was completely consumed in 20 minutes using **P1-8** as catalyst (Table 3.9) while **c-P1-8** required 12 hours for complete consumption of TBHP (Table 3.9). The longer reaction time of **c-P1-8** compared to **P1-8** is due to the necessity to swell **c-P1-8**, as shown previously in chapter 2. The TOF for **P1-8** and **c-P1-8** (Table 3.9), 300 hr<sup>-1</sup> and 41 hr<sup>-1</sup> respectively was lower than those of homogeneous analogs. However, **P1-8** and **c-P1-8** exhibited higher TOF than TS-1 (13.5 hr<sup>-1</sup>, calculated at >25% cyclohexene conversion)<sup>47</sup> and Ti-MCM-41 (5 hr<sup>-1</sup>, calculated at >25% cyclohexene conversion).<sup>134</sup> Additionally, the TOF calculated for **P1-8** and **c-P1-8** are conservative values given that the TOF was calculated at high olefin conversion and reactions generally slow down near completion. Even though the epoxidation of cyclohexene catalyzed by **P1-8** or **c-P1-8** required longer reaction time to achieve complete conversion compared to the analogous homogeneous catalysts, both **P1-8** and **c-P1-8** displayed excellent selectivity and were comparable to the homogeneous analogs.

**Table 3.9**—Catalytic activity of immobilized tripodal titanium catalysts (**P1-8** and **c-P1-8**) for epoxidation of cyclohexene employing a 20:1 olefin:TBHP ratio



Entry	Catalyst	Time	S <sub>TBHP</sub> <sup>*</sup> (%)	C <sub>TBHP</sub> (%)	TON <sup>#</sup>	TOF <sup>#</sup> (hr <sup>-1</sup> )
1	<b>P1-8</b>	30 min	>99	100	150	300
2	<b>c-P1-8</b>	2.5 hr	> 99	72 ± 6	103	41
3	<b>c-P1-8</b>	12 hr	>99	94 ± 5		

Conditions: T = 80 °C, Ti = 0.02 mmol, TBHP = 3 mmol, Toluene as solvent (20 mL), Chlorobenzene (1 g) as internal standard, and olefin (20:1 ratio = 60mmol)  
Selectivity and conversion values represent the average from at least three trials +/- the standard deviation

\*Selectivity for cyclohexene oxide and calculated at time reported

$$* S_{\text{TBHP}} = \frac{\text{moles of epoxide formed}}{\text{moles of TBHP consumed}} \times 100$$

$$C_{\text{TBHP}} = \frac{\text{moles of TBHP consumed}}{\text{initial moles of TBHP}} \times 100$$

$$\text{TON calculated by } \frac{\text{moles of epoxide formed}}{\text{moles of Ti}}$$

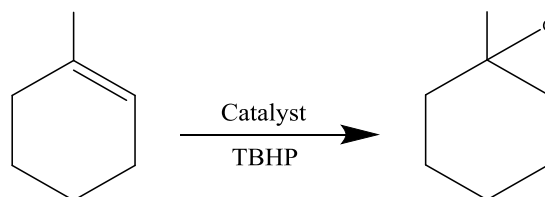
$$\text{TOF calculated by } \frac{\text{TON}}{\text{time (hr)}}$$

#TON and TOF calculated at the conversion shown in the table (C<sub>TBHP</sub>)

The catalytic activity of **P1-8** or **c-P1-8** in the epoxidation of 1-methylcyclohexene was investigated. Both catalysts displayed excellent selectivity (>95%) although, **P1-8** required a dramatic increase in reaction time for the complete consumption of TBHP (4 hours for 1-methylcyclohexene vs. 30 minutes for cyclohexene, Table 3.10). For **P1-8**, the longer reaction time required for the epoxidation of 1-methylcyclohexene is possibly due in part to the additional steric bulk around the olefin, resulting in the nucleophilic attack of the Ti-OOH species more difficult. In contrast to **P1-8**, **c-P1-8** completely converted TBHP in 12 hours, analogous to what was found for the epoxidation of cyclohexene. It appears that additional steric bulk of 1-methylcyclohexene does not inhibit the overall catalytic activity of **c-P1-8**. A comparison of the TOF of

cyclohexene (41 hr<sup>-1</sup>) and 1-methylcyclohexene (39 hr<sup>-1</sup>) further shows that the increased steric bulk of 1-methylcyclohexene did not play a major role on the catalytic activity of **c-P1-8**. However there is a large difference in TOF for the epoxidation of cyclohexene (300 hr<sup>-1</sup>) and 1-methylcyclohexene (152 hr<sup>-1</sup>) catalyzed by **P1-8** presumably due to the additional steric bulk around the olefin.

**Table 3.10**—Catalytic activity of immobilized tripodal titanium catalysts (**P1-8** and **c-P1-8**) for epoxidation of 1-methylcyclohexene employing a 20:1 olefin:TBHP ratio



Entry	Catalyst	Time (hr)	S <sub>TBHP</sub> <sup>*</sup> (%)	C <sub>TBHP</sub> (%)	TON <sup>#</sup>	TOF <sup>#</sup> (hr <sup>-1</sup> )
1	<b>P1-8</b>	30 min	> 95	53 ± 4	76	152
2	<b>P1-8</b>	4	>95	98 ± 2		
3	<b>c-P1-8</b>	2.5	> 95	68 ± 8	97	39
4	<b>c-P1-8</b>	12	>95	95 ± 5		

Conditions: T = 80 °C, Ti = 0.02 mmol, TBHP = 3 mmol, Toluene as solvent (20 mL), Chlorobenzene (1 g) as internal standard, and olefin (20:1 ratio = 60mmol)  
Selectivity and conversion values represent the average from at least three trials +/- the standard deviation

\*Selectivity for 1-methylcyclohexene oxide and calculated at time reported

$$* S_{\text{TBHP}} = \frac{\text{moles of epoxide}}{\text{moles of epoxide} + \text{moles of other products formed}} \times 100$$

$$C_{\text{TBHP}} = \frac{\text{moles of TBHP consumed}}{\text{initial moles of TBHP}} \times 100$$

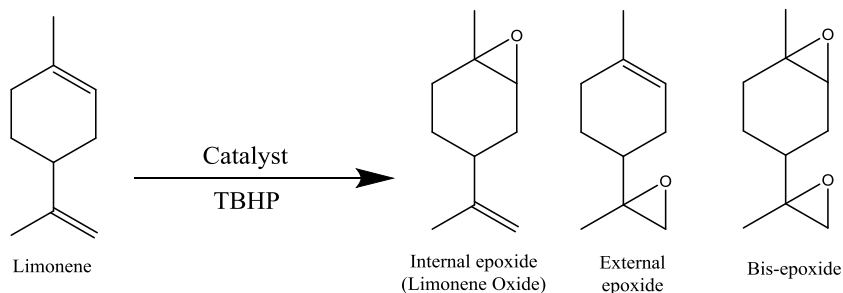
$$\text{TON calculated by } \frac{\text{moles of epoxide formed}}{\text{moles of Ti}}$$

$$\text{TOF calculated by } \frac{\text{TON}}{\text{time (hr)}}$$

#TON and TOF calculated at the conversion shown in the table (C<sub>TBHP</sub>)

As previously stated, limonene provided a unique challenge by containing both internal and terminal olefins. Remarkably, both **P1-8** and **c-P1-8** exclusively formed the internal epoxide with no external epoxide observed. This was also observed for the epoxidation of limonene catalyzed by homogeneous catalysts **9** and **10** suggesting that when there is an excess of olefin present, the titanium center largely favors the internal olefin over the terminal olefin. **P1-8** displayed complete consumption of TBHP in 4.5 hours, in good agreement with the results obtained for 1-methylcyclohexene (Table 3.11). The TOF for the epoxidation of limonene catalyzed by **P1-8** ( $157 \text{ hr}^{-1}$ ) was also comparable to the epoxidation of 1-methylcyclohexene ( $152 \text{ hr}^{-1}$ ). **c-P1-8** displayed a TOF ( $30 \text{ hr}^{-1}$ ) for the epoxidation of limonene which was slightly lower compared to 1-methylcyclohexene ( $39 \text{ hr}^{-1}$ ). Additionally, with **c-P1-8** 77% of TBHP was converted at 12 hours using limonene as the olefin whereas with 1-methylcyclohexene, nearly all of the TBHP was consumed. It is interesting to note that even at 24 hours, the conversion of TBHP was 87% for **c-P1-8**, suggesting that the reaction drastically slowed down after about 60% conversion (after 2.5 hours, Figure 3.3). Limonene and limonene oxide are larger molecules compared to 1-methylcyclohexene therefore different partitioning of the reactant and/or product through the polymer matrix could have caused the reaction to slow down. Additionally, Ti is oxophilic leading to the possibility that after the epoxidation of limonene, limonene oxide could coordinate with the Ti center leading to a high concentration of product within the polymer matrix. We observe that as the alkene gets larger (cyclohexene < 1-methylcyclohexene < limonene), the epoxidation reaction required longer times for high conversion to be achieved. Nonetheless, **P1-8** and **c-P1-8** display excellent catalytic activity, show high selectivity and display high TOF when compared to heterogeneous titanium catalysts such as Ti-MCM-41 and Ti/SiO<sub>2</sub> ( $20 \text{ h}^{-1}$  and  $19 \text{ h}^{-1}$  respectively calculated at 37% limonene conversion).<sup>137</sup>

**Table 3.11**—Catalytic activity of immobilized tripodal titanium catalysts (**P1-8** and **c-P1-8**) for epoxidation of limonene employing a 20:1 olefin:TBHP ratio



Entry	Catalyst	Time (hr)	S <sub>TBHP</sub> <sup>*</sup> (%)	C <sub>TBHP</sub> (%)	TON <sup>#</sup>	TOF <sup>#</sup> (h <sup>-1</sup> )
1	<b>P1-8</b>	30 min	95 ± 3	55 ± 6	78	157
2	<b>P1-8</b>	4	97 ± 3	98 ± 1		
3	<b>c-P1-8</b>	2.5	87 ± 4	58 ± 5	75	30
4	<b>c-P1-8</b>	12	98 ± 1	77 ± 2		

Conditions: T = 80 °C, Ti = 0.02 mmol, TBHP = 3 mmol, Toluene as solvent (20 mL), Chlorobenzene (1 g) as internal standard, and olefin (20:1 ratio = 60mmol)  
 Selectivity and conversion values represent the average from at least three trials +/- the standard deviation

\*Selectivity for limonene oxide and calculated at time reported

$$* S_{TBHP} = \frac{\text{moles of epoxide formed}}{\text{moles of TBHP consumed}} \times 100$$

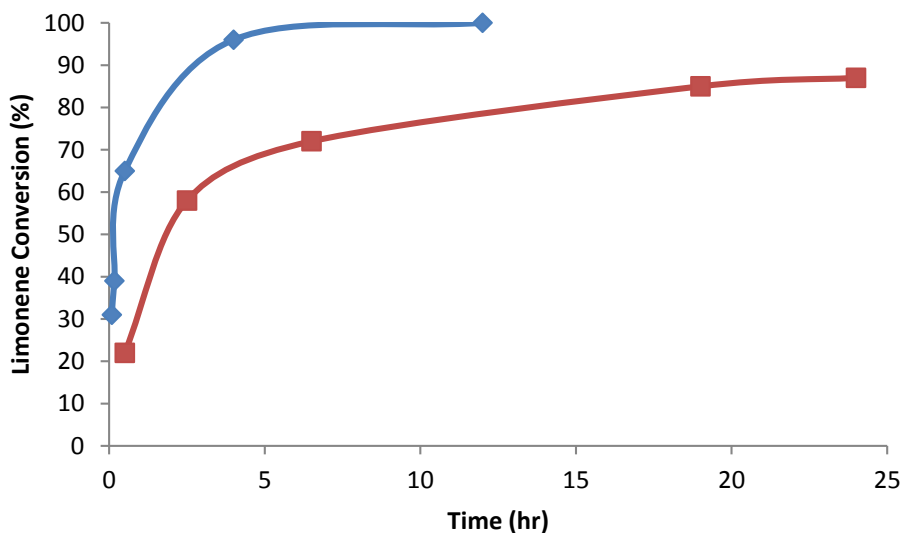
$$C_{TBHP} = \frac{\text{moles of TBHP consumed}}{\text{initial moles of TBHP}} \times 100$$

$$\text{TON calculated by } \frac{\text{moles of epoxide formed}}{\text{moles of Ti}}$$

$$\text{TOF calculated by } \frac{\text{TON}}{\text{time (hr)}}$$

<sup>#</sup>TON and TOF calculated at the conversion shown in the table (C<sub>TBHP</sub>)

**Figure 3.3**—Reaction Profile for the epoxidation of limonene employing **P1-8** (◇) or **c-P1-8** (■) as catalyst

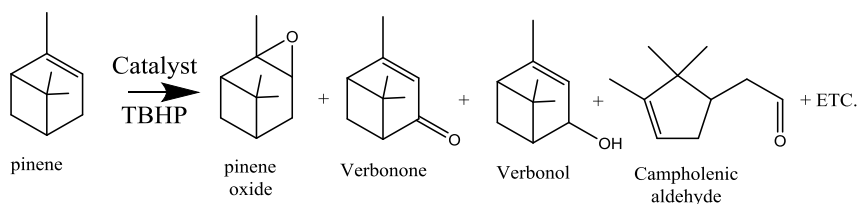


As mentioned previously,  $\alpha$ -pinene provides another unique challenge, being prone to rearrangements as well as oxidation at the allylic position. When **P1-8** and **c-P1-8** were used as catalysts,  $\alpha$ -pinene oxide was formed with 74% and 52% selectivity respectively; TOF were  $99 \text{ hr}^{-1}$  and  $16 \text{ hr}^{-1}$  respectively (Table 3.12). While the observed selectivities are lower than those achieved with homogeneous catalysts **9** and **10**, the lower selectivity could not be attributed solely to longer reaction time. In fact, an experiment was performed where  $\alpha$ -pinene oxide and **P1-8** were placed solution at  $80 \text{ }^\circ\text{C}$  and analyzed for decomposition products. Under these conditions, minimal amount of  $\alpha$ -pinene oxide was lost, suggesting that  $\alpha$ -pinene oxide is reasonably stable under our reaction conditions. In the GC-FID and GC-MS spectra, various by-products were observed such as verbenol, verbenone, and campholenic aldehyde which are common by-products. Notwithstanding, **P1-8** and **c-P1-8** are comparable or more active than catalyst derived from tetrapodal Ti POSS immobilized on SBA-15 or  $\text{SiO}_2$ ,<sup>104</sup> which displayed <20% conversion at 24 hours and selectivities for  $\alpha$ -pinene oxide of <60% where the main by-product was campholenic aldehyde. Ti-POM ( $[\text{Ti}_2(\text{OH})_2\text{As}_2\text{W}_{19}\text{O}_{67}(\text{H}_2\text{O})]^{8-}$ , POM=polyoxometalates) catalyst<sup>87</sup> have



also been explored using H<sub>2</sub>O<sub>2</sub> as the oxidant however minimal amount of  $\alpha$ -pinene oxide was observed and instead campholenic aldehyde was the major product formed. Immobilized tripodal titanium catalysts (**P1-8** and **c-P1-8**) displayed lower selectivities compared to the homogeneous analogs ([Ti(NMe<sub>2</sub>)<sub>2</sub>[(*i*-C<sub>4</sub>H<sub>9</sub>)<sub>7</sub>Si<sub>7</sub>O<sub>12</sub>]] (**9**) and [Ti(NMe<sub>2</sub>)<sub>2</sub>[(*c*-C<sub>6</sub>H<sub>11</sub>)<sub>7</sub>Si<sub>7</sub>O<sub>12</sub>]] (**10**)) therefore we need to alter the heterogeneous catalysts, possibly by using a lower molecular weight polymer, in order to achieve optimal  $\alpha$ -pinene conversions and selectivities.

**Table 3.12**—Catalytic activity of immobilized tripodal titanium catalysts (**P1-8** and **c-P1-8**) for epoxidation of  $\alpha$ -pinene employing a 20:1 olefin:TBHP ratio



Entry	Catalyst	Time (min)	S <sub>TBHP</sub> <sup>*</sup> (%)	C <sub>TBHP</sub> (%)	TON <sup>#</sup>	TOF <sup>#</sup> (hr <sup>-1</sup> )
1	<b>P1-8</b>	30 min	>99	33 ± 3	50	99
2	<b>P1-8</b>	4	74 ± 7	72 ± 3		
3	<b>c-P1-8</b>	2.5	66 ± 1	41 ± 4	41	16
4	<b>c-P1-8</b>	12	52 ± 2	63 ± 2		

Conditions: T = 80 °C, Ti = 0.02 mmol, TBHP = 3 mmol, Toluene as solvent (20 mL), Chlorobenzene (1 g) as internal standard, and olefin (20:1 ratio = 60mmol) Selectivity and conversion values represent the average from at least three trials +/- the standard deviation

\*Selectivity for  $\alpha$ -pinene oxide and calculated at time reported

$$* S_{\text{TBHP}} = \frac{\text{moles of epoxide formed}}{\text{moles of TBHP consumed}} \times 100$$

$$C_{\text{TBHP}} = \frac{\text{moles of TBHP consumed}}{\text{initial moles of TBHP}} \times 100$$

$$\text{TON calculated by } \frac{\text{moles of epoxide formed}}{\text{moles of Ti}}$$

$$\text{TOF calculated by } \frac{\text{TON}}{\text{time (hr)}}$$

#TON and TOF calculated at the conversion shown in the table (C<sub>TBHP</sub>)

For cyclohexene, 1-methylcyclohexene, as well as limonene, immobilized tripodal titanium catalysts (**P1-8** and **c-P1-8**) displayed remarkable catalytic activity showing similar selectivities compared to the homogeneous complexes, **9** and **10**. Additionally, the TOF displayed were higher compared to heterogeneous titanium catalysts such as Ti-MCM-41 and TS-1. This further confirms that **P1-8** and **c-P1-8** are excellent catalysts even though a longer reaction time is needed compared to the homogeneous analogs.

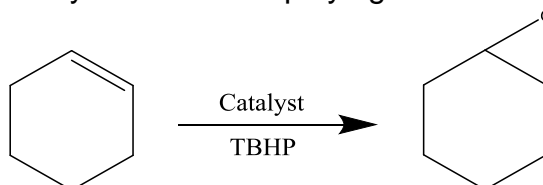
#### *3.3.2.4 Immobilized tripodal titanium catalysts using a 1:1 olefin/TBHP ratio*

Due to the excellent catalytic activity observed employing a 20:1 olefin/TBHP ratio, we explored epoxidation reactions with a 1:1 olefin/TBHP ratio catalyzed by immobilized tripodal titanium silsesquioxane catalyst **P1-8**. Homogeneous complexes, **9** and **10** displayed similar selectivities irrespective of the olefin:TBHP ratio therefore we wanted to determine how heterogenization of tripodal titanium silsesquioxanes would affect the selectivity. Employing a 1:1 olefin:TBHP ratio resulted in lower concentration of reactants near completion of the reaction; therefore, all reactions required longer reaction times and thus displayed lower turnover frequencies (TOFs). The reactions leveled off and slowed down drastically after about 50% consumption of the different olefins explored.

Employing **P1-8**, the epoxidation of cyclohexene (Table 3.13) proceeded quickly to 59% conversion after 4.5 hours (TOF=17 h<sup>-1</sup>) then, the catalyst activity leveled off with minimal additional conversion observed after 20 hours (75% conversion of olefin). Even though the reaction does require more time, it is promising that the selectivity for cyclohexene oxide remains high and no other products are formed. It has been observed that cyclohexene is absorbed into the polymer matrix leading to an apparent selectivity which is lower than the true value. This also accounts for an exaggeration of the olefin conversion. Due to the absorption of cyclohexene into the polymer matrix, the selectivity based on TBHP consumption is more reliable especially since we have shown that

cyclohexene oxide and TBHP are not retained in the polymer matrix to any appreciable extent.

**Table 3.13**—Catalytic activity of immobilized tripodal titanium catalyst (**P1-8**) for epoxidation of cyclohexene employing a 1:1 olefin:TBHP ratio



Entry	Catalyst	Time (hr)	S <sub>olefin</sub> *	C <sub>olefin</sub> (%)	S <sub>TBHP</sub> (%)	TON <sup>#</sup>	TOF <sup>#</sup> (hr <sup>-1</sup> )
1	<b>P1-8</b>	4.5	87 ± 4	59 ± 6	91 ± 9	77	17
2	<b>P1-8</b>	20	73 ± 7	77 ± 1	78 ± 8		

Conditions: T = 80 °C, Ti = 0.02 mmol, TBHP = 3 mmol, Toluene as solvent (20 mL), Chlorobenzene (1 g) as internal standard, and olefin (1:1 ratio = 3mmol)  
Selectivity, Conversion, and TBHP efficiency values represent the average from at least three trials +/- the standard deviation

\*Selectivity for cyclohexene oxide and calculated at time reported

$$*Selectivity (S_{olefin}) = \frac{\text{moles of epoxide formed}}{\text{moles of olefin consumed}} \times 100$$

$$Conversion (C_{olefin}) = \frac{\text{moles of olefin consumed}}{\text{initial moles of olefin}} \times 100$$

$$Selectivity based on TBHP (S_{TBHP}) = \frac{\text{moles of epoxide formed}}{\text{moles of TBHP consumed}} \times 100$$

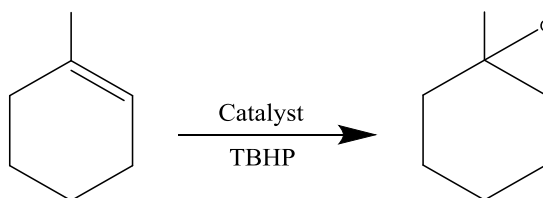
$$TON \text{ calculated by } \frac{\text{moles of epoxide formed}}{\text{moles of Ti}} \quad TOF \text{ calculated by } \frac{TON}{\text{time (hr)}}$$

<sup>#</sup>TON and TOF calculated at the conversion shown in the table (C<sub>TBHP</sub>)

When the epoxidation of 1-methylcyclohexene (Table 3.14) was explored with **P1-8**, increase steric bulk of the alkene begins to play a larger role in the rate of epoxidation however the selectivity remains high throughout the reaction. As shown in Table 3.14, it is seen that **P1-8** only has converted 33% of TBHP (1:1 ratio) at 4.5 hours while the 20:1 ratio (Table 3.10) shows 59% conversion of TBHP. At 24 hours we observed 57% conversion of 1-methylcyclohexene compared to 73% conversion for the epoxidation of cyclohexene (Table 3.13). The TOF of cyclohexene (17 h<sup>-1</sup>) versus 1-methylcyclohexene (10 h<sup>-1</sup>) further

demonstrates that increased steric bulk of 1-methylcyclohexene begins to play a role in the epoxidation reaction. Even though the reaction time needed to be extended for the epoxidation of 1-methylcyclohexene, the selectivity remains high (> 95%) suggesting that the immobilized catalyst (**P1-8**) are comparable to the homogeneous analog, **10** ([Ti(NMe<sub>2</sub>)<sub>2</sub>{(C-C<sub>6</sub>H<sub>11</sub>)<sub>7</sub>Si<sub>7</sub>O<sub>12</sub>}]<sub>2</sub>).

**Table 3.14**—Catalytic activity of immobilized tripodal titanium catalyst (**P1-8**) for epoxidation of 1-methylcyclohexene employing a 1:1 olefin:TBHP ratio



Entry	Catalyst	Time (h)	S <sub>olefin</sub> <sup>*</sup> (%)	C <sub>olefin</sub> (%)	S <sub>TBHP</sub> (%)	TON <sup>#</sup>	TOF <sup>#</sup> (h <sup>-1</sup> )
1	<b>P1-8</b>	4.5	> 95	33 ± 5	> 95	47	10
2	<b>P1-8</b>	20	> 95	57 ± 1	> 95		

Conditions: T = 80 °C, Ti = 0.02 mmol, TBHP = 3 mmol, Toluene as solvent (20 mL), Chlorobenzene (1 g) as internal standard, and olefin (1:1 ratio = 3mmol) Selectivity, Conversion, and TBHP efficiency values represent the average from at least three trials +/- the standard deviation

\*Selectivity for 1-methylcyclohexene oxide and calculated at time reported

$$* S_{\text{olefin}} = \frac{\text{moles of epoxide}}{\text{moles of epoxide} + \text{moles of other products formed}} \times 100$$

$$\text{Conversion (C}_{\text{olefin}}) = \frac{\text{moles of olefin consumed}}{\text{initial moles of olefin}} \times 100$$

$$\text{Selectivity based on TBHP (S}_{\text{TBHP}}) = \frac{\text{moles of epoxide formed}}{\text{moles of TBHP consumed}} \times 100$$

$$\text{TON calculated by } \frac{\text{moles of epoxide formed}}{\text{moles of Ti}} \quad \text{TOF calculated by } \frac{\text{TON}}{\text{time (hr)}}$$

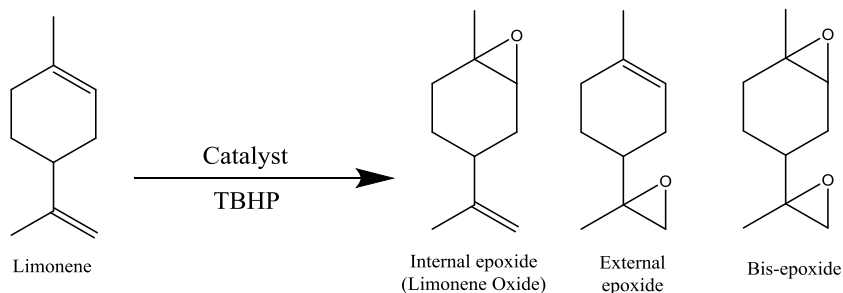
<sup>#</sup>TON and TOF calculated at the conversion shown in the table (C<sub>TBHP</sub>)

From the results of the epoxidation of limonene with the homogeneous analog (**10**) we expected that the bis-epoxide would be a by-product when **P1-8** was employed as catalysts with a 1:1 olefin/TBHP ratio. Under these conditions, 23% of limonene was consumed with 78% selectivity to limonene oxide (internal

olefin) after 4.5 hours (Table 3.15). Thus, **P1-8** displayed a lower TOF ( $6 \text{ hr}^{-1}$ ) for limonene epoxidation compared to both cyclohexene and 1-methylcyclohexene epoxidations. As the reaction time was extended, the conversion of olefin only increased slightly with time. However, the selectivity decreased slightly. In fact, at 48 hours, only 44% of limonene had been converted while 81% of TBHP had been consumed (77% TBHP efficiency). The selectivity for the internal epoxide decreased to 63% and a large amount of the bis-epoxide was formed.

Presumably, the large quantity of the bis-epoxide formed is due to the product being retained in the polymer matrix, as was discussed for the 20:1 trials. That is, the product remained in close proximity to the Ti center causing a second oxidation to occur. Similar to **10**, it is interesting to note that epoxidation of the terminal olefin was not observed and the only two products were the 1,2-epoxide along with the bis-epoxide.

**Table 3.15**—Catalytic activity of immobilized tripodal titanium catalyst (**P1-8**) for epoxidation of limonene employing a 1:1 olefin:TBHP ratio



Entry	Catalyst	Time	S <sub>olefin</sub> <sup>*</sup> (%)	C <sub>olefin</sub> (%)	S <sub>TBHP</sub> (%)	TON <sup>#</sup>	TOF <sup>#</sup> (hr <sup>-1</sup> )
1	<b>P1-8</b>	40 min	78 ± 10	23 ± 1	77 ± 1	27	6
2	<b>P1-8</b>	30 hr	63 ± 2	44 ± 4	48 ± 2		

Conditions: T = 80 °C, Ti = 0.02 mmol, TBHP = 3 mmol, Toluene as solvent (20 mL), Chlorobenzene (1 g) as internal standard, and olefin (1:1 ratio = 3mmol)  
 Selectivity, Conversion, and TBHP efficiency values represent the average from at least three trials +/- the standard deviation

\*Selectivity for limonene oxide and calculated at time reported

$$\text{*Selectivity (S}_{\text{olefin}}) = \frac{\text{moles of epoxide formed}}{\text{moles of olefin consumed}} \times 100$$

$$\text{Conversion (C}_{\text{olefin}}) = \frac{\text{moles of olefin consumed}}{\text{initial moles of olefin}} \times 100$$

$$\text{Selectivity based on TBHP (S}_{\text{TBHP}}) = \frac{\text{moles of epoxide formed}}{\text{moles of TBHP consumed}} \times 100$$

$$\text{TON calculated by } \frac{\text{moles of epoxide formed}}{\text{moles of Ti}} \quad \text{TOF calculated by } \frac{\text{TON}}{\text{time (hr)}}$$

<sup>#</sup>TON and TOF calculated at the conversion shown in the table (C<sub>TBHP</sub>)

Due to the modest activity of **P1-8** in the epoxidation of α-pinene using a 20:1 olefin:TBHP ratio, a 1:1 olefin:TBHP ratio was not explored. However, it is remarkable that when employing a 1:1 ratio for cyclohexene, 1-methylcyclohexene, and limonene (up to 4.5 hours) we observed excellent selectivities, comparable to the selectivities of homogeneous catalyst **10**, demonstrating the excellent catalytic activity of immobilized tripodal titanium complexes. Indeed, when **P1-8** was used as an epoxidation catalyst, the turnover frequencies (TOFs) were comparable or better than those reported for heterogeneous titanium containing catalysts such as Ti-MCM-41, Ti/SiO<sub>2</sub>, TS-1, and Ti-SBA-15.<sup>47,134,137</sup> Use of high olefin:TBHP ratio is common industrially

hence the excellent results obtained for **P1-8** and **c-P1-8** at 20:1 olefin:TBHP ratio are highly exciting.

### 3.3.3 Recyclability of P1-8 and c-P1-8 with limonene

**P1-8** and **c-P1-8** demonstrated consistently good selectivity when the catalysts were reused up to five cycles with limonene as the olefin (Table 3.16). After a typical limonene epoxidation reaction, the catalysts were recovered by removing the volatiles followed by washing with copious amount of acetonitrile. After drying under vacuum, the catalysts were reused under typical epoxidation reaction conditions. Akin to the recyclability studies described in chapter 2 for 1-octene, the conversion of TBHP dropped after three cycles due to the presence of *t*-butanol (co-product from the epoxidation reactions) which autoretards the reaction. Additionally, the selectivity decreased slightly over time however the second recycle trial show a markedly lower selectivity compared to the other trials. Presumably catalysts degradation occurs partially due to Ti loss leading to a decrease in olefin conversion for each cycle. Based on the  $C_{TBHP}$ , most of the Ti lost occurs between the 1<sup>st</sup> and 2<sup>nd</sup> cycle. The third cycle demonstrates an increase in selectivity along with a decrease in conversion suggesting that the Ti was lost from washing the catalyst.

**Table 3.16**—Recyclability of **NCP-9** and **CP-9** with limonene

Entry	Catalyst	Time (hr)	Cycle	S <sub>TBHP</sub> *	C <sub>TBHP</sub>
1	<b>P1-8</b>	12	1	80	100
2	<b>P1-8</b>	12	2	73	96
3	<b>P1-8</b>	12	3	81	75
4	<b>P1-8</b>	24	3	81	95
5	<b>P1-8</b>	12	4	76	53
6	<b>P1-8</b>	12	5	91	65
7	<b>c-P1-8</b>	12	1	98	50
8	<b>c-P1-8</b>	12	2	53	72
9	<b>c-P1-8</b>	12	3	78	57
10	<b>c-P1-8</b>	24	3	78	72
11	<b>c-P1-8</b>	12	4	90	49
12	<b>c-P1-8</b>	12	5	72	43

Conditions: T= 80 °C, Ti=0.02 mmol, TBHP=3 mmol, Toluene as solvent (20 mL), Chlorobenzene (1 g) as internal standard, and olefin (20:1 ratio = 60 mmol)

\*Selectivity for limonene oxide and calculated at time reported

$$* S_{TBHP} = \frac{\text{moles of epoxide formed}}{\text{moles of olefin consumed}} \times 100$$

$$\text{Conversion (C}_{TBHP}\text{)} = \frac{\text{moles of TBHP consumed}}{\text{initial moles of TBHP}} \times 100$$

After five recycles, the titanium content was analyzed by ICP and showed 0.47% Ti loss for **P1-8** (pristine = 1.11%) and 0.47% Ti loss for **c-P1-8** (pristine=0.94%). Although the conversion rate drops over time and there is observed loss in titanium content, the selectivity remains high and it has been previously shown in chapter 2 that these catalysts can be repaired by simply adding Ti(NMe<sub>2</sub>)<sub>4</sub> to the spent catalyst to regain the original catalytic activity.



### 3.3.4 Epoxidation of 1-octene

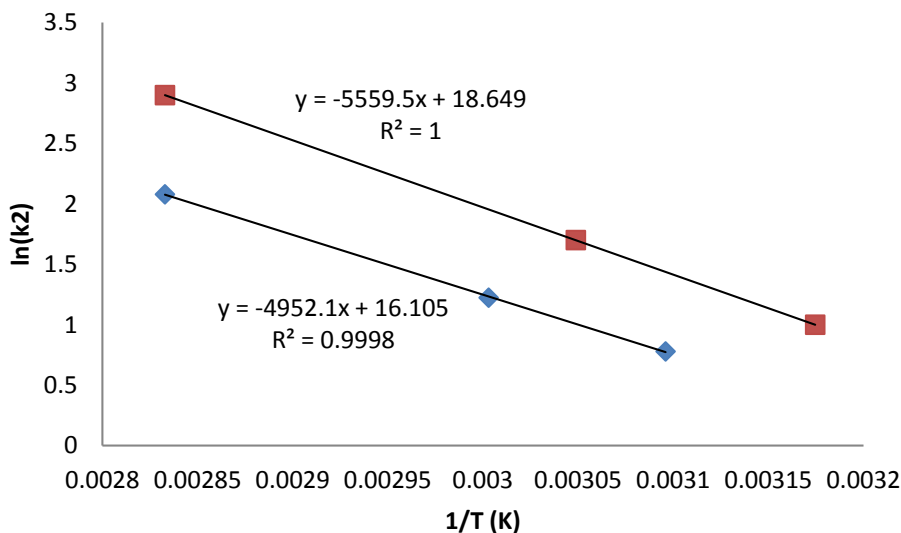
In chapter 2, **P1-8** and **c-P1-8** were shown to be active using 9.1 mol% or 3.6 mol% titanium relative to TBHP, respectively. The exploration of a lower Ti concentration (0.67 mol% titanium relative to TBHP) was investigated in order to determine if the catalysts continued to be selective even with higher turnover number (TON).

**P1-8** and **c-P1-8** displayed excellent selectivity (>88%) comparable to that previously reported (>94%). The main difference was that the reaction time needed to be extended for **P1-8** (5 hours vs 2 hours) however **c-P1-8** achieved similar results (>90% conversion) at 24 hours. Employing a lower mol% of titanium increases the turnover number (TON) or amount of cycles each titanium center must complete meaning that both **P1-8** and **c-P1-8** are excellent catalysts for the epoxidation of 1-octene. Additionally, we were able to compare **P1-8** and **c-P1-8** which had similar amounts of Ti content, (1.11 wt% Ti for **P1-8** vs 0.95 wt% for **c-P1-8**). In chapter 2, **P1-8** and **c-P1-8** contained 1.13 wt% and 0.45 wt% respectively therefore direct comparison was difficult. These results suggest that **c-P1-8** still required longer reaction time (24 hrs for >90% conversion) compared to **P1-8** ( 5hours) however the difference in reaction time is not as large compared to that previously reported.

The apparent activation energy was determined and proved that the reaction was not diffusion limited. By analyzing the initial rates of the epoxidation of 1-octene (neat) with TBHP as the oxidant at different temperatures (40 to 80 °C), a plot of  $\ln k$  vs.  $1/T$  resulted in a straight line for both **P1-8** and **c-P1-8** (Figure 3.4) where the slope of the line equals  $E_a/R$  where  $E_a$  is the apparent activation energy and  $R$  is the gas constant. From this data, we determined that the apparent activation energy for **P1-8** and **c-P1-8** were 46 and 42 kJ/mol respectively which is in good agreement with that previously reported for homogeneous catalyst **10** (42.4 kJ/mol).<sup>40</sup> Due to the similar activation energies, we can infer that the epoxidation reactions employing **P1-8** and **c-P1-8** are not diffusion-controlled. Further evidence that the reactions are not diffusion limited

comes from comparing the initial rates of reaction with different stirring speeds. For both **P1-8** and **c-P1-8** the initial rate remained unchanged irrespective of the stirring speed (100-870 rpm).

**Figure 3.4**—Determination of apparent activation energy ■=**P1-8** and ◇=**c-P1-8**



### 3.4 Conclusion:

Previously, we demonstrated that tripodal Ti silsesquioxanes tethered to a hyperbranched poly(siloxysilane) matrix function as a selective, efficient, recyclable, repairable heterogeneous catalyst for the epoxidation of 1-octene. Herein, we demonstrated that tripodal titanium silsesquioxanes and immobilized tripodal Ti silsesquioxane materials are versatile epoxidation catalysts by using various olefins ranging from simple cyclic olefins such as cyclohexene and 1-methylcyclohexene to more demanding olefins such as limonene and  $\alpha$ -pinene. Homogeneous tripodal Ti POSS, [Ti(NMe<sub>2</sub>)<sub>2</sub>]{(*i*-C<sub>4</sub>H<sub>9</sub>)<sub>7</sub>Si<sub>7</sub>O<sub>12</sub>} (**9**) and [Ti(NMe<sub>2</sub>)<sub>2</sub>]{(*c*-C<sub>6</sub>H<sub>11</sub>)<sub>7</sub>Si<sub>7</sub>O<sub>12</sub>} (**10**), displayed excellent selectivity and turnover frequency (TOF) for the epoxidation of cyclohexene, 1-methylcyclohexene, limonene and  $\alpha$ -pinene irrespective of the olefin:TBHP ratio; however, with lower

olefin:TBHP ratio, longer reaction time was needed. Additionally, the TBHP efficiency for the homogeneous catalysts was extremely high although there was a slight drop when a 1:1 olefin:TBHP ratio was employed with limonene (Table 3.7). This was due to the formation of the bis-epoxide as a by-product.

Immobilized tripodal titanium silsesquioxane catalysts, **P1-8** and **c-P1-8**, also displayed excellent selectivity, TOF, and TBHP efficiency for the epoxidation of cyclohexene, 1-methylcyclohexene, limonene and  $\alpha$ -pinene employing a 20:1 olefin:TBHP ratio. The epoxidation of  $\alpha$ -pinene displayed slightly lower selectivities compared cyclohexene, 1-methylcyclohexene, and limonene. However, both **P1-8** and **c-P1-8** display greater catalytic activity compared to similar Ti catalysts where a large amount of campholenic aldehyde<sup>87,104</sup> was produced. When a 1:1 olefin:TBHP ratio was explored, **P1-8** displayed excellent selectivity for cyclohexene, 1-methylcyclohexene and limonene even though longer reaction time was needed. The reaction never achieved 100% conversion when a 1:1 olefin:TBHP ratio was employed suggesting that the reaction rate slowed drastically as the reactant concentration decreased.

Aside from being effective epoxidation catalysts, we demonstrated that the rate of reaction for both **P1-8** and **c-P1-8** is not diffusion limited. This was achieved by determining the apparent activation energy, as well as comparing the initial rate of reaction under different stirring speeds. Finally, we showed that both **P1-8** and **c-P1-8** can be recycled with minimal loss in activity over time in the epoxidation of limonene. Even when a loss in activity is observed, chapter 2 demonstrated that both **P1-8** and **c-P1-8** can be repaired simply by reacting the spent catalysts with  $\text{Ti}(\text{NMe}_2)_4$  which restored the activity of the catalysts akin to the pristine catalysts (See Chapter 2).

## Chapter 4: Preliminary studies of immobilized tripodal titanium silsesquioxanes onto a hyperbranched poly(siloxysilane) polymer for the epoxidation of cyclohexene using H<sub>2</sub>O<sub>2</sub> as an oxidant

### 4.1 Introduction:

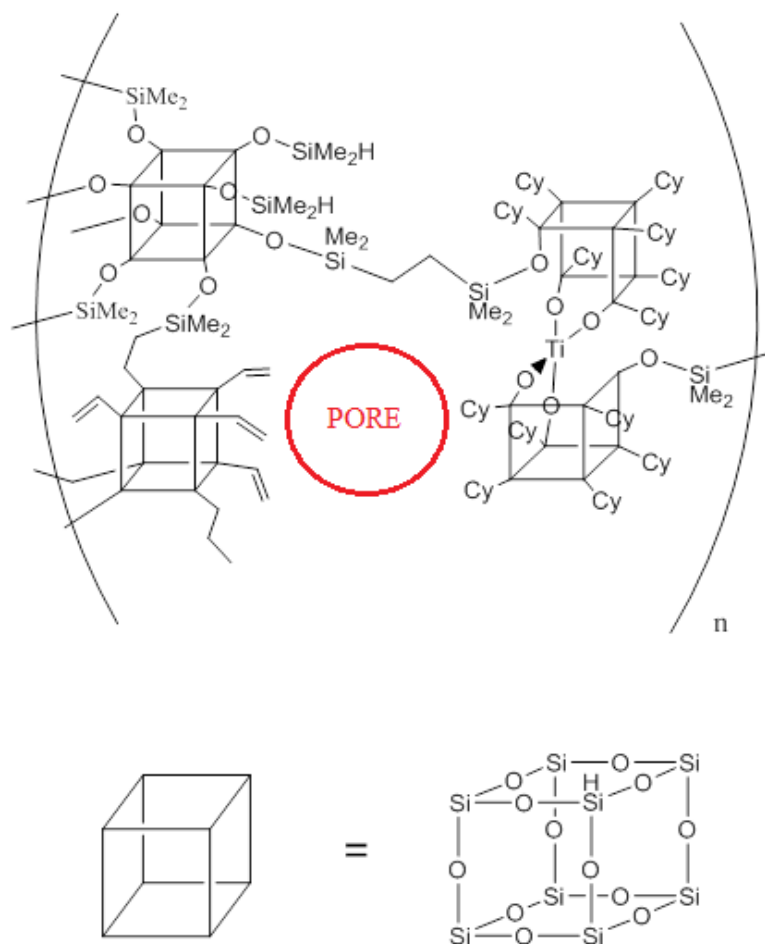
Titanium silicate-1 (TS-1) has been shown to have excellent catalytic activity for olefin epoxidation using hydrogen peroxide (H<sub>2</sub>O<sub>2</sub>) as the oxidant.<sup>37,46,49,50,65,66,74,90,135,138</sup> Additionally, TS-1 is used in industry by DOW Chemicals and selectively (>95%) produces propylene oxide.<sup>17</sup> TS-1 is very efficient (>90% selectivity) for the epoxidation of small olefins such as cyclohexene; however, due to the structural limitations of the catalysts, epoxidation of more demanding olefins, such as bulky olefins or allylic alcohols, are ineffective. While numerous supports such as MCM-41,<sup>47,51,56,90</sup> SBA-15,<sup>52,62,91</sup> and zeolites<sup>41,92,93</sup> have been explored in order to alleviate the steric limitations of TS-1,<sup>33,38,47,59,64,69,86-89</sup> the resulting catalysts are less efficient for alkene epoxidation with H<sub>2</sub>O<sub>2</sub> than TS-1. The lower activity is due to the larger pores present in the catalysts allowing water to deactivate the titanium active site.<sup>69</sup>

Chapters 2 and 3 discussed the development of titanium silsesquioxane complexes as homogeneous models for heterogeneous materials, specifically the Shell (titania-on-silica) and TS-1 catalysts. With *tert*-butyl hydroperoxide (TBHP) as the oxidant, tripodal titanium silsesquioxanes displayed the highest catalytic activity compared to bi- and tetrapodal titanium silsesquioxanes. Additionally, it was shown in chapter 3 that tripodal titanium silsesquioxane complexes are among the most active catalysts for the epoxidation of different olefins ranging from cyclic (cyclohexene and 1-methylcyclohexene), to terminal (1-octene), to demanding olefins used in the fine chemical industry (limonene and  $\alpha$ -pinene). Although tripodal titanium silsesquioxane catalysts are extremely active epoxidation catalysts, they suffer from being homogeneous in nature making them susceptible to degradation, as well as being difficult to reuse.

Additionally,  $\text{H}_2\text{O}_2$  cannot be employed as the oxidant since water deactivates the catalysts via hydrolysis of the Ti to form  $\text{TiO}_2$ , a thermodynamically favorable reaction. Immobilization of tripodal titanium would generate catalysts that had advantages of both homogeneous and heterogeneous materials. The active site would be uniform, easily accessible, and spatially isolated while the catalysts would be reusable and more resistant to hydrolysis, making them more robust.

Multiple reports of the heterogenization of titanium silsesquioxanes have been reported, for example via attachment to a polymer or silica support,<sup>1,41,52,55,58,59,62,91,103,104</sup> or alternatively, by encapsulation in polydimethylsiloxane (PDMS) membrane.<sup>32</sup> Wada *et al.* reported the synthesis of silsesquioxane gels housing tetrapodal titanium (Figure 4.1) which were active catalysts for the epoxidation of cyclooctene to 1-epoxyoctane using  $\text{H}_2\text{O}_2$  as the oxidant (70% yield). However, the gels required up to 60 days to prepare, suggesting that a new synthetic method needs to be developed that is less time consuming. Moreover, both yield and selectivity could be improved.

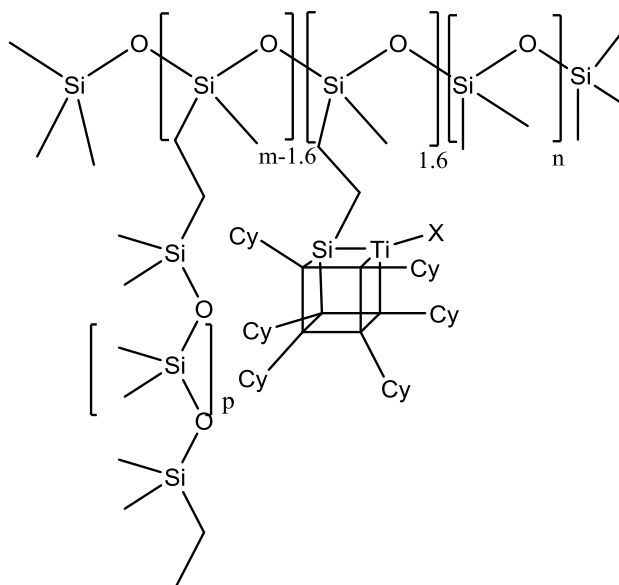
**Figure 4.1**—Silsesquioxane gels developed<sup>1</sup>



Tripodal titanium silsesquioxane has been grafted onto a methylhydrosiloxane-dimethylsiloxane co-polymer and then crosslinked with a vinyl-terminated siloxane polymer to form insoluble organosilicon materials (netted polysiloxysilane) that encloses the Ti in a hydrophobic cavity (Figure 4.2).<sup>55</sup> This method allowed for the size of the cavity, used to encapsulate titanium, to be tuned for optimum accessibility by varying the starting materials. Epoxidation of cyclooctene with H<sub>2</sub>O<sub>2</sub> catalyzed by grafted tripodal Ti gave 80% yield of the epoxide and after hot filtration, the catalysts could be reused suggesting that this catalyst is indeed heterogeneous. When larger olefins were used such as cyclododecane and 1-octene, the yield decreased to 45% and

62%, respectively. For the epoxidation of 1-octene, the catalysts displayed a TOF of  $20 \text{ hr}^{-1}$  where TS-1, under similar reaction conditions, has a TOF of  $80 \text{ hr}^{-1}$  suggesting that improvements could be made to the reaction rate.<sup>55</sup> Major drawbacks of this catalyst series include the many synthetic steps and the fact that control of the 3-D structure of the polymer is difficult; precise control of the polymer structure is required to ensure the Ti center is protected.

**Figure 4.2**—Tripodal Ti POSS tethered onto a linear polymer

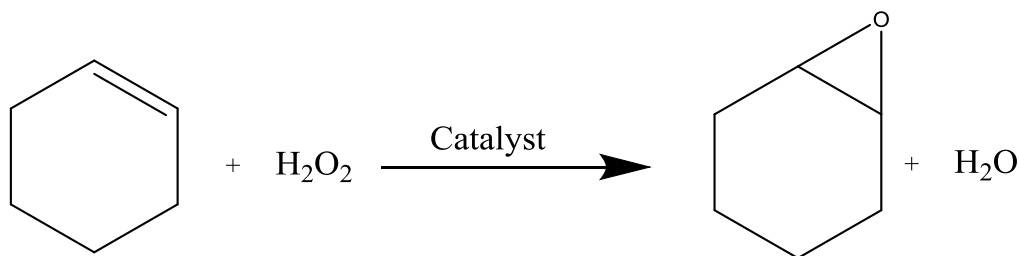


Previously, we have shown that tripodal titanium silsesquioxanes can be successfully trapped within a hydrophobic PDMS membrane to protect the titanium from degrading.<sup>32</sup> However, in order to prevent titanium from leaching into solution, the solvent choice was limited to solvents that did not appreciably swell the membrane. A covalent linkage between a hydrophobic inert support and tripodal titanium silsesquioxane complex would generate catalysts with numerous advantages including allowing greater versatility in the range of solvents that can be used in epoxidation reactions. Also the catalyst would be more robust compared to catalysts restrained via physical entrapment in PDMS.

The results described in chapter 2 show that tripodal titanium silsesquioxanes immobilized on hyperbranched poly(siloxysilane) matrices afford highly selective, robust, recyclable, and repairable catalysts that display similar catalytic activity to the homogeneous analogs for olefin epoxidation reactions with TBHP. The hydrophobicity of the hyperbranched matrix would limit the amount of water at the Ti active site thereby leading to less degradation of the Ti center via hydrolysis. This suggests that immobilized tripodal titanium on a non-polar hyperbranched poly(siloxysilane) matrix, may afford active catalysts for the epoxidation of olefins with  $\text{H}_2\text{O}_2$  as the oxidant.

Herein, we report preliminary studies of the epoxidation of cyclohexene catalyzed by immobilized tripodal titanium silsesquioxane with  $\text{H}_2\text{O}_2$  as the oxidant.  $\text{H}_2\text{O}_2$  generates  $\text{H}_2\text{O}$  as the co-product (Scheme 4.1) resulting in a higher atom efficiency than when TBHP is employed. Additionally, employing  $\text{H}_2\text{O}_2$  as the oxidant has less environmental impacts due to not producing benign co-products.

**Scheme 4.1**—Epoxidation of cyclohexene employing  $\text{H}_2\text{O}_2$  as the oxidant



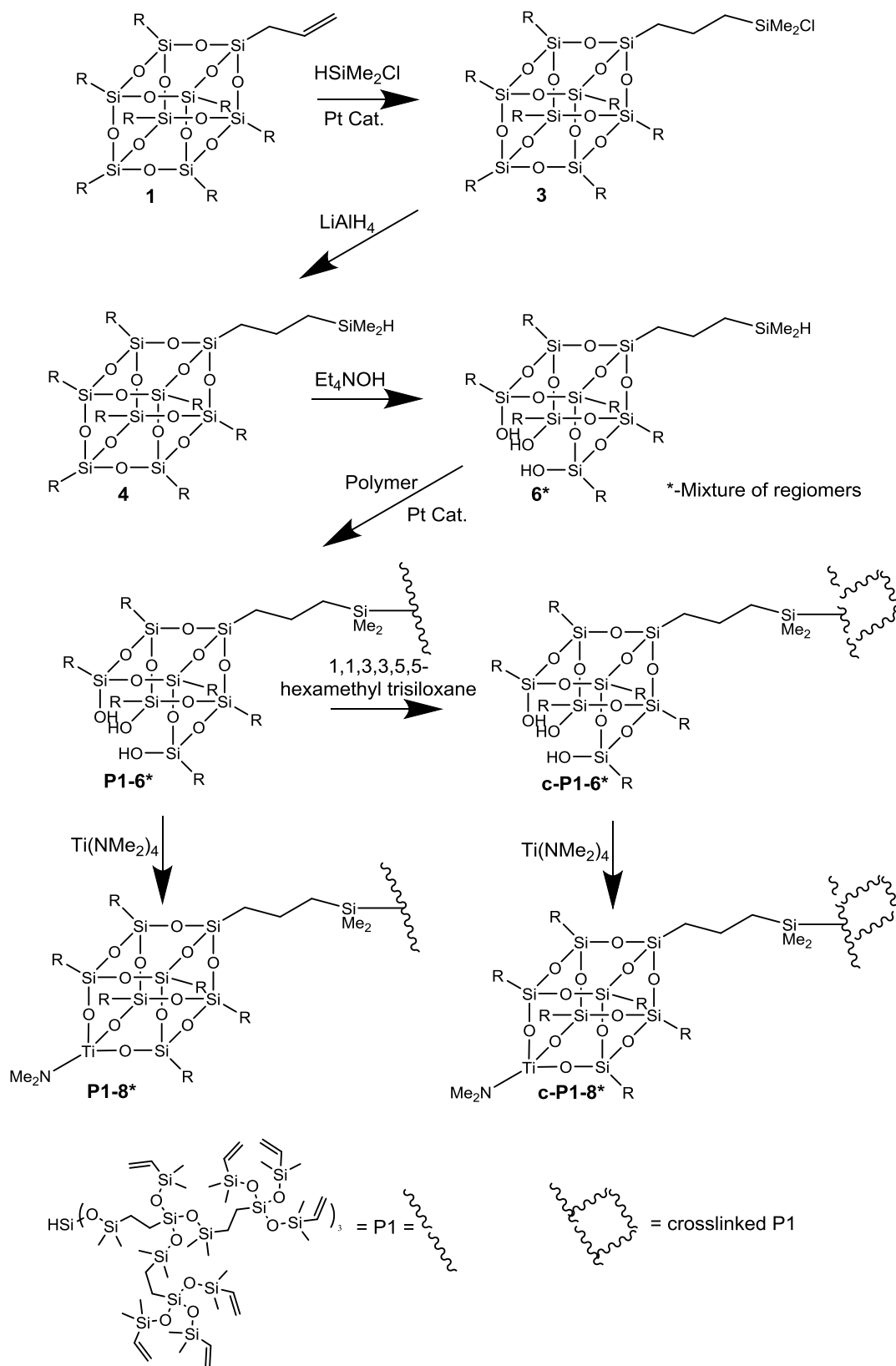


## 4.2 Results/Discussion:

### 4.2.1 Synthesis P1-8 and c-P1-8

Previously, we have shown the successful formation of **P1-8** and **c-P1-8**, (Scheme 4.2) which are active catalysts for the epoxidation of various olefins, such as cyclohexene, 1-methylcyclohexene, 1-octene, limonene, and  $\alpha$ -pinene, employing *tert*-butyl hydroperoxide (TBHP) as the oxidant. **P1-8** was synthesized by grafting regiomeric mixture of (silyl)propyl-trisilanol isobutyl POSS (**6**) ligand onto vinyl terminated hyperbranched poly(siloxysilane) via hydrosilation reaction. **6** was synthesized from  $\text{HMe}_2\text{Si}(\text{CH}_2)_3(i\text{-Bu})_7\text{Si}_8\text{O}_{12}$  (**4**) via a modified procedure adapted from Feher and colleagues<sup>98,99</sup> where one framework silicon was removed to yield a regiomeric mixture of **6**. The synthesis of  $\text{HMe}_2\text{Si}(\text{CH}_2)_3(i\text{-Bu})_7\text{Si}_8\text{O}_{12}$  (**4**) included Pt-catalyzed hydrosilylation of  $\text{CH}_2=\text{CHCH}_2(i\text{-Bu})_7\text{Si}_8\text{O}_{12}$  (**1**) with  $\text{HSiMe}_2\text{Cl}$  to give  $\text{ClMe}_2\text{Si}(\text{CH}_2)_3(i\text{-Bu})_7\text{Si}_8\text{O}_{12}$  (**3**) followed by reduction of **3** with  $\text{LiAlH}_4$ .

**Scheme 4.2—Synthetic route for P1-8 and c-P1-8**



**P1-6** was synthesized by grafting (silyl)propyl-trisilanolisobutyl-POSS ligand (**6**, ~5mol% relative to moles of **P1** vinyl groups) onto hyperbranched poly(siloxysilane) matrices via Pt-catalyzed hydrosilylation. **P1-6** was reacted with  $\text{Ti}(\text{NMe}_2)_4$  (1.1 equiv) to yield **P1-8** as an orange viscous gel which was soluble in common organic solvents (toluene, methylene chloride, THF, chloroform, and 1-octene). The formation of **P1-8** was confirmed by solution NMR, IR, UV-vis, and elemental analysis. Proton-induced X-ray emission (PIXE) analysis found 1.11 weight percent (wt%) of Ti in **P1-8**.

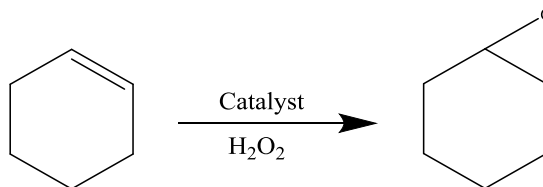
**c-P1-6** was prepared by attaching (silyl)propyl-trisilanolisobutyl-POSS ligand (**6**, ~10 mol% relative to moles of **P1** vinyl groups) onto the hyperbranched poly(siloxysilane) matrix containing vinyl terminated groups followed by crosslinking with 1,1,3,3,5,5-hexamethyltrisiloxane. The successful formation of **c-P1-6** was analyzed by IR which showed a silanol stretch at 3350 as well as the loss of vinyl stretch at 3030. **c-P1-6** was then reacted with  $\text{Ti}(\text{NMe}_2)_4$  (1.1 equiv) to yield **c-P1-8** as an orange non-crystalline solid. **c-P1-8** was insoluble in common organic solvents (toluene, methylene chloride, THF, chloroform, and 1-octene) making solution characterization difficult. However, IR was used to show the loss of silanol stretch, UV-vis confirmed the presence of tetrahedral Ti, and PIXE (0.94 wt% Ti) were used to confirm the successful formation of **c-P1-8**.

#### 4.2.2 Epoxidation of Cyclohexene

The epoxidation of cyclohexene was explored neat with **c-P1-8** (0.02 mmol of Ti), using toluene as internal standard (Table 4.1, entry 1). After 12 hours, complete consumption of  $\text{H}_2\text{O}_2$  was observed with 54% cyclohexene oxide selectivity ( $S_{\text{H}_2\text{O}_2}$ ) based on  $\text{H}_2\text{O}_2$ . In contrast, for cyclohexene oxide selectivity ( $S_{\text{olefin}}$ ) based on olefin consumption was only 37%. Due to the large excess of cyclohexene present in the neat reaction trials, minimal consumption of olefin occurred (<2%). Therefore, minor errors in olefin concentration measurements would be magnified, leading to inaccurate results. Thus the  $S_{\text{olefin}}$  values are reported for all neat epoxidation trials, however the  $S_{\text{H}_2\text{O}_2}$  has inherently less error associated. Additionally, the  $S_{\text{H}_2\text{O}_2}$  was calculated after all the  $\text{H}_2\text{O}_2$  had

been consumed. The low ( $S_{H_2O_2}$ ) selectivity can be attributed to the formation of 2-cyclohexene-1-ol as the main by-product along with a small amount of 1,2-cyclohexanediol. The formation of 2-cyclohexene-1-ol was not observed when tripodal titanium silsesquioxanes were trapped within PDMS membrane therefore different solvents were explored. The epoxidation of cyclohexene, catalyzed by **c-P1-8** was evaluated employing 1,2-dichloroethane (DCE), acetonitrile (ACN), and isopropyl alcohol (IPA) as solvents. With water miscible solvents (ACN and IPA), the selectivities were very poor when compared to water immiscible solvent systems such as DCE and neat cyclohexene. With ACN and IPA, water miscible solvents, water is in closer proximity to the Ti center than when water immiscible solvents, DCE and cyclohexene, are used which exclude the water from the organic phase.

**Table 4.1**—Catalytic activity of immobilized tripodal titanium (**c-P1-8**) for epoxidation of cyclohexene employing a 20:1 olefin:H<sub>2</sub>O<sub>2</sub> ratio



Entry	Catalyst	Solvent	S <sub>H<sub>2</sub>O<sub>2</sub></sub> (%) <sup>*</sup>	Conversion H <sub>2</sub> O <sub>2</sub> (%)	S <sub>olefin</sub> (%) <sup>*</sup>
1	<b>c-P1-8</b>	Neat	54	100	37
2	<b>c-P1-8</b>	DCE	21	70	60
3	<b>c-P1-8</b>	ACN	23	70	--
4	<b>c-P1-8</b>	IPA	20	80	--

Conditions: T= 60 °C, Time=12 hr, Ti=0.02 mmol (preswelled catalyst), H<sub>2</sub>O<sub>2</sub>=2 mmol, Toluene as internal standard (1 g), and olefin (> 45 mmol)

<sup>\*</sup>Selectivity for cyclohexene oxide and calculated at time reported

<sup>\*</sup> S<sub>H<sub>2</sub>O<sub>2</sub></sub> =  $\frac{\text{moles of epoxide formed}}{\text{moles of H}_2\text{O}_2 \text{ consumed}} \times 100$  Calculated when all H<sub>2</sub>O<sub>2</sub> had been consumed

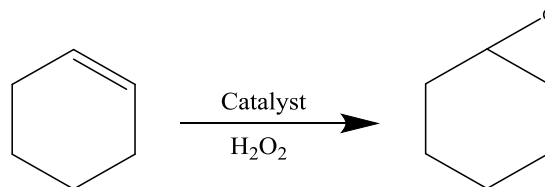
Conversion H<sub>2</sub>O<sub>2</sub> =  $\frac{\text{moles of H}_2\text{O}_2 \text{ consumed}}{\text{initial moles of H}_2\text{O}_2} \times 100$

S<sub>olefin</sub> =  $\frac{\text{moles of epoxide formed}}{\text{moles of olefin consumed}} \times 100$

In order to remove excess water from the reaction medium, epoxidation reactions catalyzed by **c-P1-8** were explored with anhydrous Na<sub>2</sub>SO<sub>4</sub> added to the reaction mixture. Epoxidation trials were conducted at 60 °C using toluene as internal standard, a 20:1 olefin:TBHP ratio, and preswelled **c-P1-8** to minimize the swelling effects on the catalytic activity. When the epoxidation of neat cyclohexene was conducted with the addition of equimolar (relative to H<sub>2</sub>O<sub>2</sub> (100 mol%)) amount of anhydrous Na<sub>2</sub>SO<sub>4</sub>, the epoxide selectivity based on H<sub>2</sub>O<sub>2</sub> (S<sub>H<sub>2</sub>O<sub>2</sub></sub>, calculated at complete consumption of H<sub>2</sub>O<sub>2</sub>) increased from 54% to 78% (Table 4.2 entry 1 and 2). However, the main co-product observed was still 2-cyclohexene-1-ol. When 150 mol% (relative to H<sub>2</sub>O<sub>2</sub>) was used (Table 4.2 entry

3), the selectivity based on  $\text{H}_2\text{O}_2$  decreased, suggesting there is an optimal amount of anhydrous  $\text{Na}_2\text{SO}_4$  that can be added. Alternatively, adding an equimolar or excess amount of  $\text{NaSO}_4$  did not alter the selectivity based on  $\text{H}_2\text{O}_2$  for the epoxidation of cyclohexene in 1,2-dichloroethane (DCE). In fact, the selectivity decreased slightly with the addition of 100 mol% anhydrous  $\text{Na}_2\text{SO}_4$ . When the epoxidation of cyclohexene was explored using DCE as the solvent and 150 mol% anhydrous  $\text{Na}_2\text{SO}_4$ , the selectivity skyrocketed to 85%, the highest selectivity observed for **c-P1-8**. Chapter 2 demonstrated that the swelling of **c-P1-8** played a pivotal role in the initial rate of reaction. Swelling of **c-P1-8** could be attributing to the difference in selectivities observed for neat epoxidation reactions verses when DCE is used as the solvent. The high selectivity observed for the epoxidation of cyclohexene in DCE could be due to a higher degree of swelling, resulting in a larger concentration of olefin near the Ti center compared to neat epoxidation trials.

**Table 4.2**—Catalytic activity of immobilized tripodal titanium (**c-P1-8**) for epoxidation of cyclohexene employing a 20:1 olefin:H<sub>2</sub>O<sub>2</sub> ratio with anhydrous Na<sub>2</sub>SO<sub>4</sub>



Entry	Catalyst	Solvent	mol% Na <sub>2</sub> SO <sub>4</sub>	S <sub>olefin</sub> (%) <sup>*</sup>	S <sub>H<sub>2</sub>O<sub>2</sub></sub> (%) <sup>*</sup>
1	<b>c-P1-8</b>	Neat	0	37	54
2	<b>c-P1-8</b>	Neat	100	40	78
3	<b>c-P1-8</b>	Neat	150	24	54
4	<b>c-P1-8</b>	DCE	0	60	21
5	<b>c-P1-8</b>	DCE	100	53	22
6	<b>c-P1-8</b>	DCE	150	85	27

Conditions: T= 60 °C, Time=12 hr, Ti=0.02 mmol (preswelled catalyst), H<sub>2</sub>O<sub>2</sub>=2 mmol, Toluene as internal standard (1 g), olefin (> 45 mmol), and 15 g solvent

\*Selectivity for cyclohexene oxide and calculated at time reported

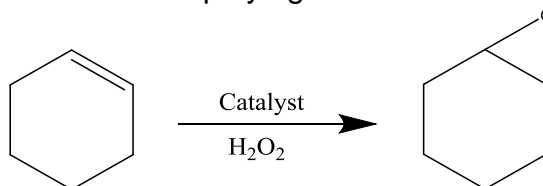
$$S_{\text{olefin}} = \frac{\text{moles of epoxide formed}}{\text{moles of olefin consumed}} \times 100$$

$$S_{\text{H}_2\text{O}_2} = \frac{\text{moles of epoxide formed}}{\text{moles of H}_2\text{O}_2 \text{ consumed}} \times 100 \quad \text{Calculated when all H}_2\text{O}_2 \text{ had been consumed}$$

Instead of using anhydrous Na<sub>2</sub>SO<sub>4</sub>, epoxidation reactions were explored using a phase transfer agent, typically an ammonium based salt. The epoxidation of cyclohexene (neat) was explored by adding tetraethylammonium bromide (TEAB) to the reaction mixture. TEAB helps transfer H<sub>2</sub>O<sub>2</sub> into the organic phase via ionic interactions as well as removing water from the organic phase resulting in less water in the bulk reaction medium. When 10 mol% (relative to H<sub>2</sub>O<sub>2</sub>) of TEAB was added, the selectivity decreased slightly however the H<sub>2</sub>O<sub>2</sub> efficiency increased (Table 4.3). Alternatively, when 20 mol% TEAB was added, the selectivity dramatically increased (66 %) while the H<sub>2</sub>O<sub>2</sub>

efficiency (53%) was lower compared to the 10 mol% trial (63%). When TEAB was added to epoxidation trials employing DCE as the solvent, both the selectivity and H<sub>2</sub>O<sub>2</sub> efficiency plummeted and a large amount of 2-cyclohexene-1-ol was observed.

**Table 4.3**—Catalytic activity of immobilized tripodal titanium (**c-P1-8**) for epoxidation of cyclohexene employing a 20:1 olefin:H<sub>2</sub>O<sub>2</sub> ratio with TEAB



Entry	Catalyst	Solvent	mol% TEAB	S <sub>olefin</sub> (%) <sup>*</sup>	S <sub>H<sub>2</sub>O<sub>2</sub></sub> (%) <sup>*</sup>
1	<b>c-P1-8</b>	Neat	0	37	54
2	<b>c-P1-8</b>	Neat	10	23	63
3	<b>c-P1-8</b>	Neat	20	66	53
4	<b>c-P1-8</b>	DCE	0	60	21
5	<b>c-P1-8</b>	DCE	10	17	8
6	<b>c-P1-8</b>	DCE	20	7	6

Conditions: T= 60 °C, Time=12 hr, Ti=0.02 mmol (preswelled catalyst), H<sub>2</sub>O<sub>2</sub>=2 mmol, Toluene as internal standard (1 g), olefin (> 45 mmol), and 15 g solvent

\*Selectivity for cyclohexene oxide and calculated at time reported

$$S_{\text{olefin}} = \frac{\text{moles of epoxide formed}}{\text{moles of olefin consumed}} \times 100$$

$$S_{\text{H}_2\text{O}_2} = \frac{\text{moles of epoxide formed}}{\text{moles of H}_2\text{O}_2 \text{ consumed}} \times 100 \quad \text{Calculated when all H}_2\text{O}_2 \text{ had been consumed}$$

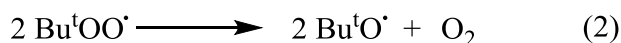
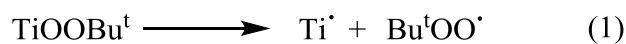
**c-P1-8** displayed comparable or better catalytic activity than other reported titanium catalysts such as Ti-SBA(65)-573,<sup>136</sup> Ti/SiO<sub>2</sub>,<sup>136</sup> Ti(OPr)<sup>i</sup>-MCM,<sup>44</sup> and Ti-POMs<sup>64</sup> (POM=polyoxometalates), which displayed minimal olefin conversion (<30%), low H<sub>2</sub>O<sub>2</sub> efficiency (~20%), and low selectivity for cyclohexene oxide (<30%). For example, when Ti(OPr)<sub>4</sub> was embedded into



MCM-41, the resulting catalysts under similar conditions (80 °C, 20:1 olefin:H<sub>2</sub>O<sub>2</sub> ratio, 0.4 mol% Ti) displayed 9% yield for cyclohexene oxide at 24 hours.<sup>44</sup> Although **c-P1-8** displayed comparable or better catalytic activity compared to other Ti catalysts for the epoxidation of cyclohexene using H<sub>2</sub>O<sub>2</sub> as the oxidant, **c-P1-8** did not display similar activity compared to epoxidation reactions employing TBHP as the oxidant. Epoxidation of cyclohexene catalyzed by **c-P1-8** using TBHP as the oxidant also displayed complete oxidant conversion at 12 hours albeit cyclohexene oxide was exclusively formed.

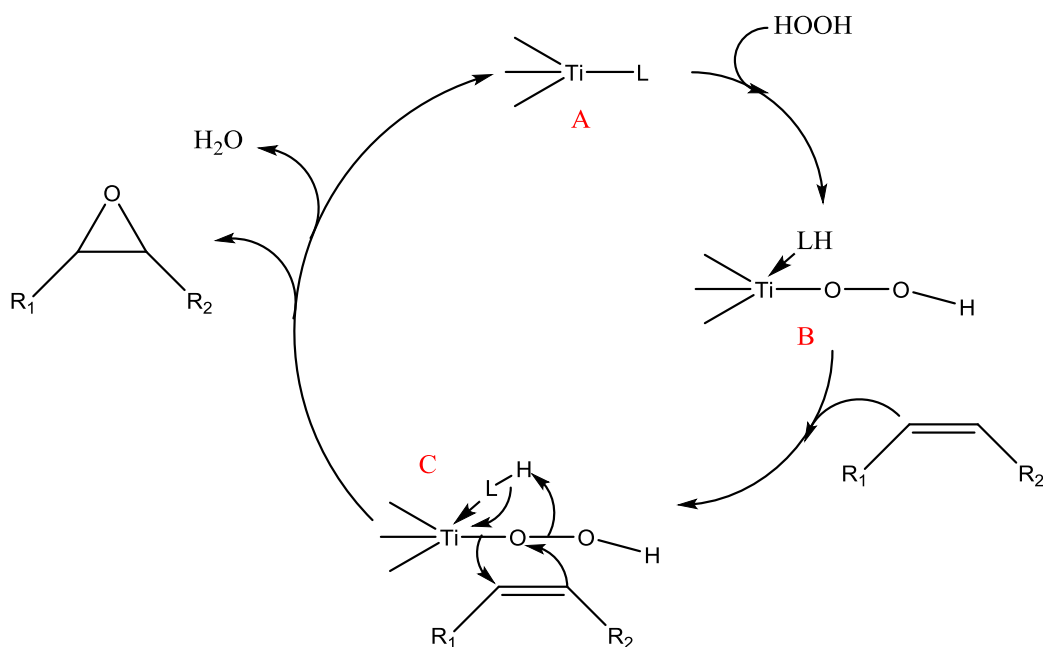
It was hypothesized that excess water was problematic causing cyclohexene oxide to be readily converted to the diol which then possibly dehydrates to form 2-cyclohexene-1-ol. A reaction was conducted where cyclohexene, cyclohexene oxide, and hydrogen peroxide were heated at 60 °C and showed that 1,2-cyclohexanediol is formed however no 2-cyclohexene-1-ol was observed. Thus, the presence of **c-P1-8** is needed in order for 2-cyclohexene-1-ol to be observed as a product.

Previously, it has been observed that when Ti-MCM-36,<sup>47</sup> Ti-MCM-41,<sup>44,47</sup> or Ti/SiO<sub>2</sub><sup>136</sup> is employed as catalyst for the epoxidation of cyclohexene, 2-cyclohexene-1-ol was the major product formed. In the generally accepted mechanism for epoxidation reactions employing titanium catalysts and H<sub>2</sub>O<sub>2</sub> as the oxidant, the olefin attacks a hydroperoxotitanium species (B in Scheme 4.3) to form an epoxide. In other studies reported, when excess TBHP was mixed with tripodal titanium silsesquioxane complexes, TBHP slowly converted into *t*-butanol (Bu<sup>t</sup>OH), Bu<sup>t</sup>OOBu<sup>t</sup>, and oxygen following equations 1-4.<sup>40</sup>

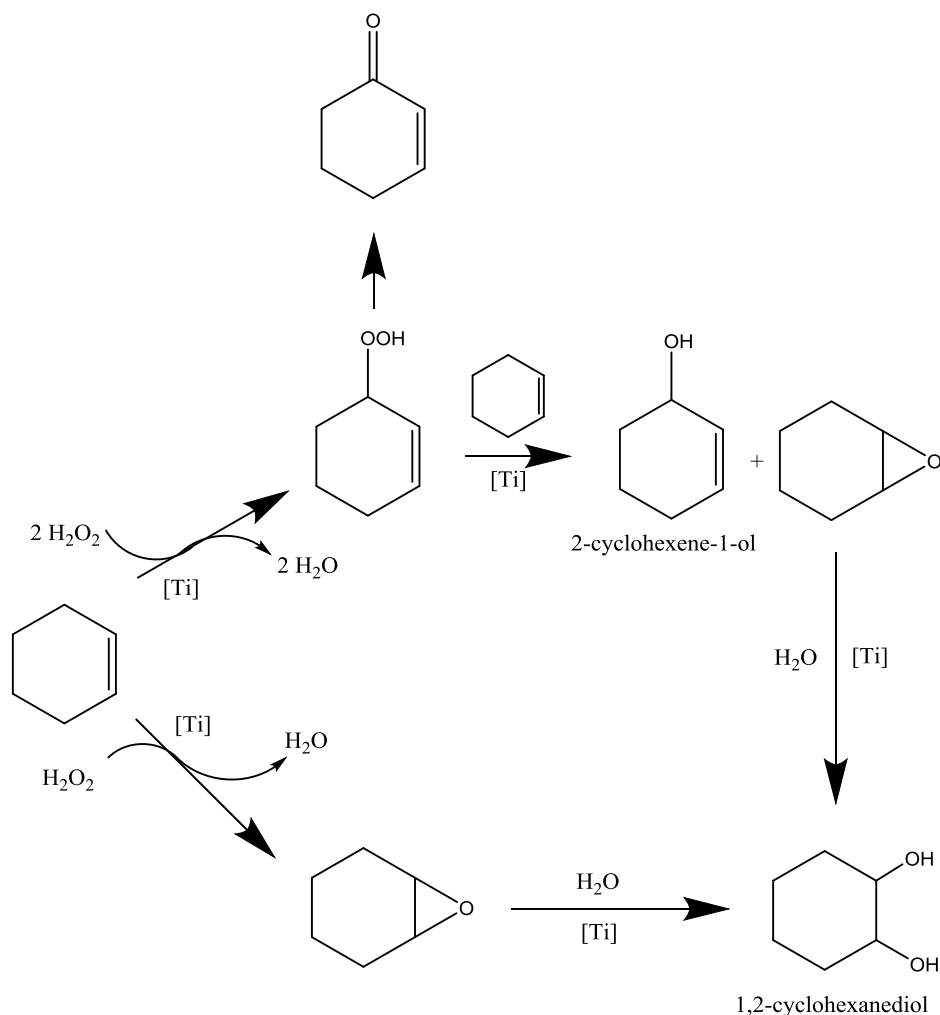


The hydroperoxide species formed was not stable at room temperature and decomposed via homolytic fission (equation 1). Analogous observations have been seen for molybdenum and iron catalysts also.<sup>19,40,44,139-141</sup> Our reactions employ H<sub>2</sub>O<sub>2</sub> as the oxidant instead of TBHP, however similar decomposition pathways can be inferred. For **c-P1-8**, the free radical (HOO•) abstracts a proton from the allylic position of cyclohexene to form the allylic hydroperoxide and water as shown in scheme 4.4. The allylic hydroperoxide species is then used as the oxidant for the epoxidation of cyclohexene where 2-cyclohexene-1-ol is formed as the co-product. Based on the low selectivities observed, presumably, the rate of olefin attack is slower than that of the decomposition of Ti-OOH to form the allylic hydroperoxide. Further support comes from the epoxidation of 1-octene catalyzed by **c-P1-8** and **P1-8** employing H<sub>2</sub>O<sub>2</sub> as the oxidant. Minimal conversion of 1-octene was observed albeit the oxidant was completely consumed. If there is not sufficient olefin concentration around the Ti center, the rate of Ti-OOH decomposition becomes the dominant reaction.

**Scheme 4.3**—Mechanism for epoxidation reactions catalyzed by tripodal titanium



**Scheme 4.4**—Formation of 2-cyclohexene-1-ol and 1,2-cyclohexanediol



### 4.3 Conclusion:

**c-P1-8** displayed superior activity employing  $\text{H}_2\text{O}_2$  as the oxidant compared to homogeneous tripodal titanium silsesquioxane complexes. Tripodal titanium silsesquioxanes were successfully tethered onto a hyperbranched polysiloxysilane matrix, allowing the Ti center to be protected from hydrolysis. This confirmed that covalently linking tripodal titanium onto a hydrophobic hyperbranched polymer generated catalytically active complexes for epoxidation reactions employing  $\text{H}_2\text{O}_2$  as the oxidant. Furthermore, compared to other titanium containing catalysts such as Ti-SBA(65)-573,<sup>136</sup> Ti/SiO<sub>2</sub>,<sup>136</sup> Ti(OPr<sup>i</sup>)-

MCM,<sup>44</sup> and Ti-POMs<sup>64</sup> (POM=polyoxometalates), **c-P1-8** displayed similar or better catalytic activity for the epoxidation of cyclohexene employing H<sub>2</sub>O<sub>2</sub> as the oxidant.

Low selectivities were due to the excess water present therefore a biphasic solvent system (neat and DCE) was employed. Additionally, anhydrous Na<sub>2</sub>SO<sub>4</sub> and a phase transfer agent were used to reduce excess water present at the Ti center. Using 1,2-dichloroethane (DCE) as the solvent, **c-P1-8** displayed the highest selectivity (85%) when 150 mol% (relative to H<sub>2</sub>O<sub>2</sub>) of anhydrous Na<sub>2</sub>SO<sub>4</sub> was added to the reaction mixture. For neat cyclohexene epoxidation reactions, the highest selectivity (66%) was when 20 mol% (relative to H<sub>2</sub>O<sub>2</sub>) of tetraethylammonium bromide (TEAB) was employed.

**c-P1-8** displayed comparable or better catalytic activity to other titanium catalysts. However, improvement to **c-P1-8** may result from altering of the molecular weight and/or degree of branching of the polymer to allow better access of the olefin to the Ti center, thereby lowering the rate of decomposition of the Ti-OOH species while maintaining the hydrophobic environment for the Ti center.

## Chapter 5: Immobilization of Tripodal Titanium Silsesquioxanes onto Gold-on-Silica for the Direct Epoxidation of Propylene

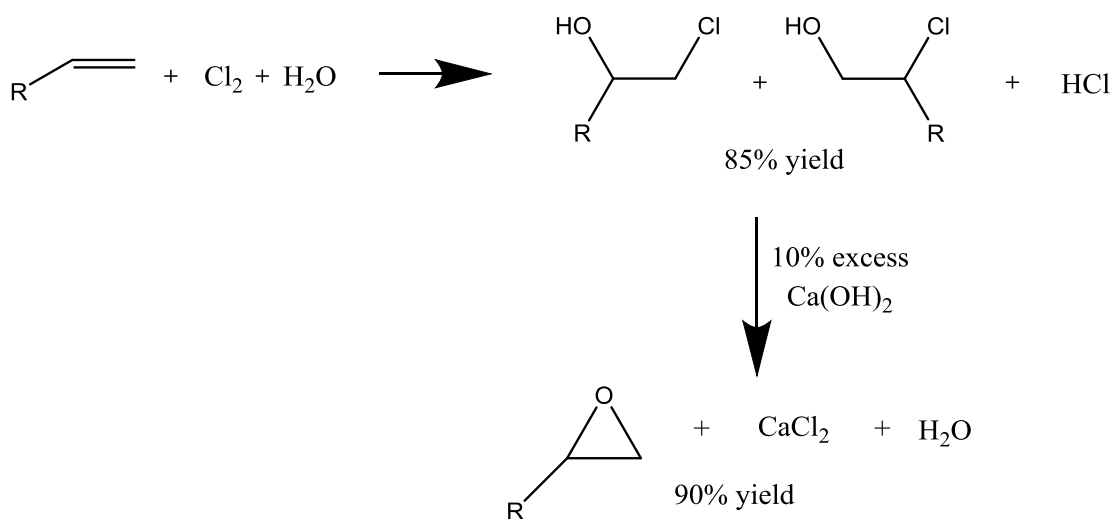
### 5.1 Introduction:

Propylene oxide (PO), first synthesized in 1861, is a compound which plays a very significant role in organic chemistry as an intermediate to various products including propylene glycol, ethers, alcohols, and polyurethanes. PO is on the top 50 bulk chemical list because PO serves as an excellent chemical intermediate, due to its ability to react with various compounds such as acids, bases, amines, carbon dioxide, and water.<sup>14</sup> In industry, propylene epoxidation reactions are typically operated via two different routes: chlorohydrin and hydroperoxide process, which are both multi-step reactions and require multiple reactors. In 2008, the main route to produce propylene oxide (PO) was the chlorohydrin (CHPO) route followed by hydroperoxide routes to generate styrene (SMPO) and *t*-butyl alcohol (PO/TBA) as co-products.<sup>84,142</sup>

The chlorohydrin process (Scheme 5.1), discussed in greater detail in chapter 1, begins with the production of propylene chlorohydrin by reacting propene with HOCl, formed from Cl<sub>2</sub> and H<sub>2</sub>O. Propylene chlorohydrin is then reacted with 10% excess calcium hydroxide (Ca(OH)<sub>2</sub>) to form propylene oxide, water, and calcium chloride (CaCl<sub>2</sub>). Major drawbacks of the chlorohydrin process include the use of chlorine (expensive, toxic, corrosive), generation of toxic chlorinated by-products, and the disposal of chlorinated water and CaCl<sub>2</sub>. Today, due to the environmental issues associated with the chlorohydrin route, the majority of PO produced is from hydroperoxide process which generates co-products such as *t*-butyl alcohol that needs to be disposed of or sold for various other applications. However, the chlorohydrin process still contributes to 43% of overall PO production.<sup>142</sup>

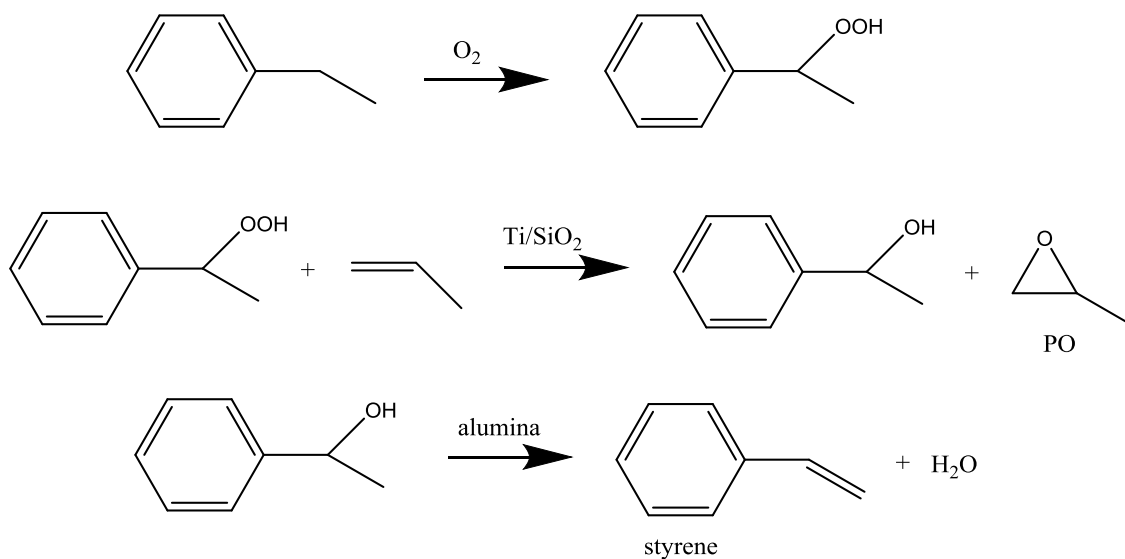
### Scheme 5.1—Different Routes to synthesize PO

#### Chlorohydrin Route



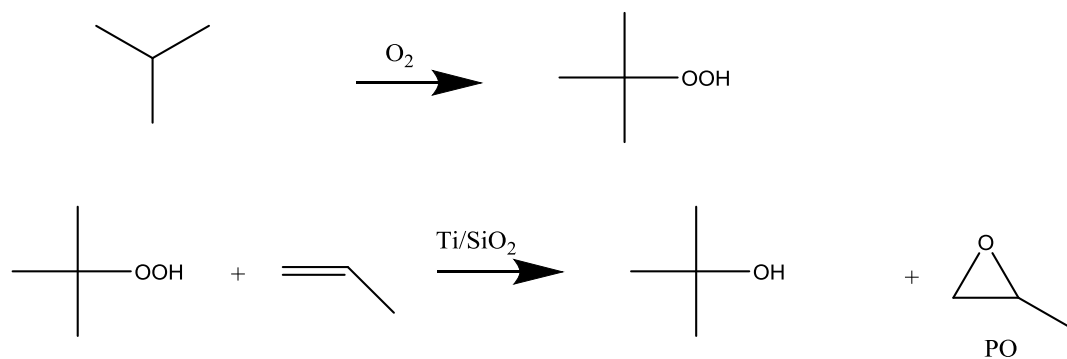
#### Hydroperoxide Routes

##### *Styrene (SMPO, Shell)<sup>84</sup>*

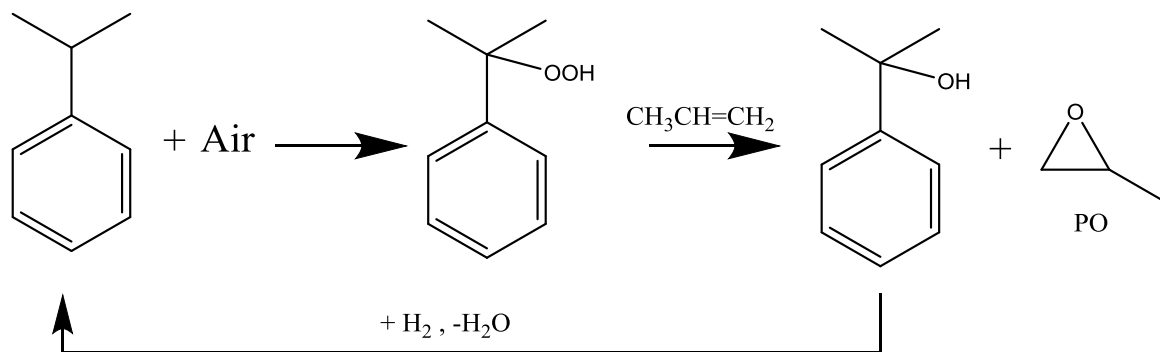


**Scheme 5.1—Continued....**

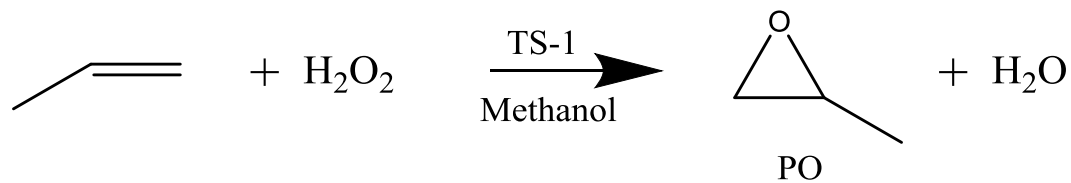
*t*-butyl alcohol (PO/TBA, Lyondell)



*Cumene recycling process (Sumitomo Chemical)*<sup>143</sup>



DOW route



Hydroperoxide routes are commonly used in industry employing alkylhydroperoxides as the oxidant: organic hydroperoxide by Lyondell and Shell (styrene and *t*-butyl alcohol) and cumene recycling by Sumitomo Chemical. Styrene monomer propylene oxide (SMPO) process has been operated by Shell since 1979 (Scheme 5.1). SMPO process involves air oxidation of ethyl benzene to form ethylbenzene hydroperoxide, the oxidant for the epoxidation of propene. Formation of propylene oxide (PO) is catalyzed over a titanium-on-silica catalyst which generates methyl phenyl carbinol as a co-product.<sup>84</sup> After separation of the products, methyl phenyl carbinol is then dehydrated over alumina to form styrene. Similar to the SMPO process, *t*-butanol can be formed via the epoxidation of propene with TBHP (PO/TBA, Scheme 5.1); this method is used by Lyondell Chemical Company. Air oxidation of isobutane is used to produce *t*-butyl hydroperoxide which is used to oxidize propylene to form propylene oxide over titanium-on-silica catalysts where the co-product is *t*-butanol. Both the SMPO process and PO/TBA generate a large amount of co-products, styrene and *t*-butanol, that need to be sold or disposed of if there is not a high demand for the co-products compared to PO.<sup>143</sup>

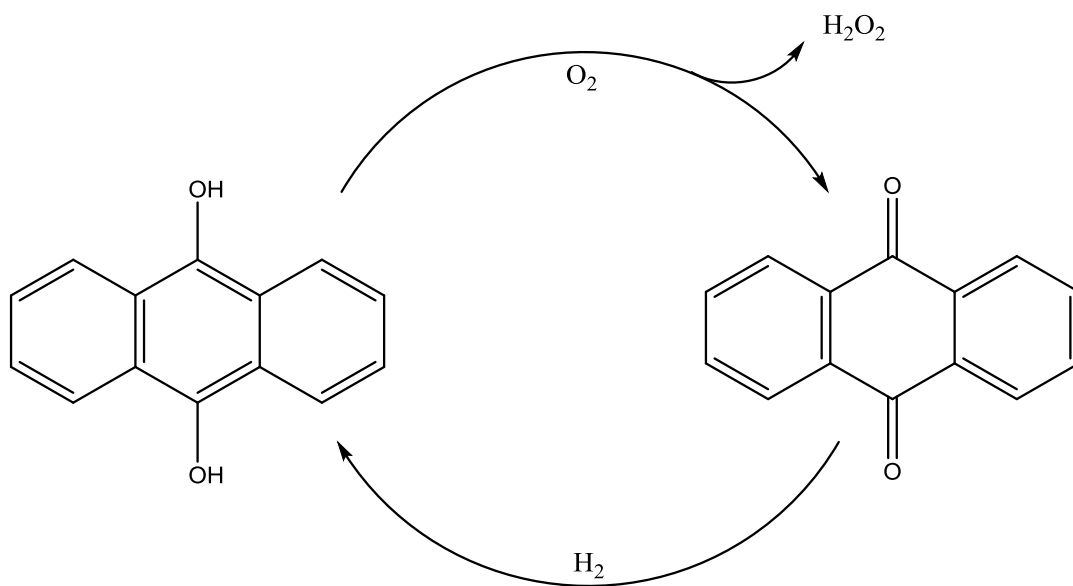
Sumitomo Chemical Company developed the cumene recycling process (Scheme 5.1) in 2003 where the co-product can be reused for the epoxidation of propene.<sup>143</sup> Cumene is oxidized under air to generate the oxidant, cumene hydroperoxide, used for the epoxidation of propene to produce PO and cumene alcohol. Cumene can then be regenerated by first dehydrating cumene alcohol to form  $\alpha$ -methyl styrene followed by hydrogenation to form cumene. Cumene recycling process selectively produces PO while only generating water as waste.

A relatively new minor route for the synthesis of PO is a hydroperoxide route, implemented by DOW Chemicals, using hydrogen peroxide ( $H_2O_2$ ) as the oxidant over titanium silicate-1 (TS-1) catalyst (Scheme 5.1). Although this route is environmentally friendly and considered green, due to the co-product being water, there are also drawbacks due to  $H_2O_2$  being difficult to store and transport.<sup>17</sup> Therefore,  $H_2O_2$  is generated on-site by oxidation of



anthrahydroquinone to form anthraquinone followed by hydrogenation to reform anthrahydroquinone (Scheme 5.2).<sup>143</sup> Due to the mass production and wide usage of epoxides, a new catalyst needs to be developed which minimizes the amount of waste generated and is economical for the use in industry.

**Scheme 5.2**—Formation of H<sub>2</sub>O<sub>2</sub> on-site for Dow Chemical synthesis of PO



In the production of ethylene oxide, gaseous ethene and molecular oxygen are used over a silver catalyst however this catalyst is not effective for higher alkenes such as propene due to the presence of allylic hydrogens which are easily oxidized (discussed in more detail in Chapter 1).<sup>13</sup> The rate of formation of PO on supported silver is about 16 times slower than ethylene oxide and the rate of carbon dioxide formation is 6 times higher leading to a low selectivity for the epoxide. Numerous reports have been published detailing efforts to optimize the silver catalyst for the formation of PO but all have so far been met with limited success.<sup>14,143-148</sup> Direct epoxidation of propene is attractive

because it eliminates production of hazardous waste, as well as use of expensive reactants such as  $\text{H}_2\text{O}_2$ .<sup>3</sup>

Recently, nanoparticles research has been gaining interest due to their interesting and unique properties. A nanoparticle can have a variety of different shapes but can be loosely defined as having one dimension in the nanometer range up to 100 nm. Nanoparticles have been utilized as early as the 9<sup>th</sup> century where they were used in the decoration of pots. However, there was no technique available to analyze these particles. With the improvements and development of high power microscopes, nanoparticles are being visualized and studied by electron microscopes, atomic force microscopy, x-ray photoelectron spectroscopy, and powder x-ray diffraction.<sup>149</sup>

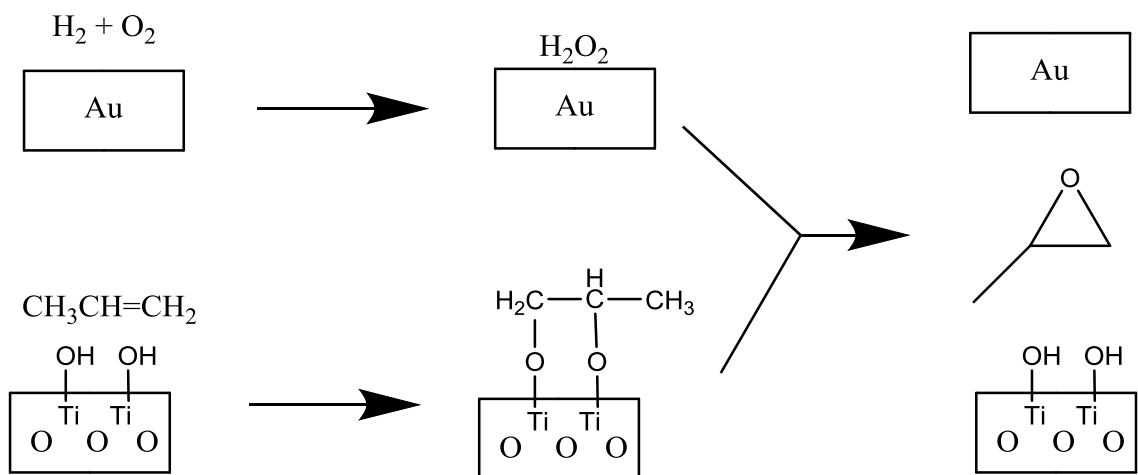
In particles larger than one micrometer ( $\mu\text{m}$ ), surface atoms are insignificant compared to the atoms in the bulk material. However, as the particles reach the nanometer (nm) scale, the percentage of surface atoms becomes significant where the higher surface area causes unique properties to be observed: melting point suppression, supermagnetism, higher absorption of solar radiation, etc. For example, zinc oxide nanoparticles are used in modern sunscreen lotions because these particles block UV waves. However, bulk zinc does not exhibit the same blocking power. Gold is known as an inert metal with a high melting point (1064 °C). In comparison, gold nanoparticles melt around 300 °C and react with various compounds.<sup>149,150</sup>

Gold dispersed on various metal oxide supports have shown to be catalytically active for hydrogenation, hydrogenolysis, and oxidation reactions.<sup>151,152</sup> In 1998, Haruta and colleagues showed that, in the presence of  $\text{O}_2$  and  $\text{H}_2$ , Au dispersed on  $\text{TiO}_2$  ( $\text{Au}/\text{TiO}_2$ ) was very selective (>90%) for the production of propylene oxide (PO) from propene albeit with low conversion (1%) and hydrogen efficiency (34%). Studies have been conducted demonstrating that Au nanoparticles catalyze the formation of  $\text{H}_2\text{O}_2$ .<sup>153-159</sup> Therefore, the mechanism for the epoxidation of propene includes Au nanoparticles creating  $\text{H}_2\text{O}_2$  *in situ* where the  $\text{H}_2\text{O}_2$  then reacts with the Ti centers in the support, which

catalyze the epoxidation of propene.<sup>153,158,160,161</sup> The active nanoparticles for epoxidation reactions have been identified to be in the 2-5 nm range while nanoparticles smaller than 2 nm are believed to cause hydrogenation of propene to propane.<sup>162</sup> Additionally, nanoparticles that are larger than 5 nm have shown to be inactive for the epoxidation of propene.<sup>138,162,163</sup> Since Haruta discovered Au/TiO<sub>2</sub> were active catalysts for the epoxidation of propene, numerous studies have been conducted focusing on three main objectives: understanding the mechanism of Au/TiO<sub>2</sub>, improvement of catalyst life, or achieving higher hydrogen efficiency.

The generally accepted mechanism for PO formation using Au/TiO<sub>2</sub> as catalyst involves the adsorption of H<sub>2</sub> and O<sub>2</sub> on the gold surface prior to forming H<sub>2</sub>O<sub>2</sub> which is believed to be the rate determining step (Scheme 5.3). H<sub>2</sub>O<sub>2</sub> then spills over onto the bidentate propoxy Ti species to form PO.<sup>164</sup> Strong binding of PO to the support surface is believed to be one of its degradation pathways. This mechanism can be broken down into three main components: (1) formation of H<sub>2</sub>O<sub>2</sub> catalyzed by the Au nanoparticles, (2) formation of the active bidentate Ti species, and (3) the conversion of propene to PO (Scheme 5.3).

**Scheme 5.3**—Reaction mechanism of PO formation with Au/TiO<sub>2</sub> catalysts<sup>164</sup>



For the Au nanoparticles to produce  $\text{H}_2\text{O}_2$ , the nanoparticles need to be in correct size range and in close proximity to the Ti support. The preparation method for Au nanoparticles on titanium-containing supports has been extensively studied.<sup>68,160,165,166</sup> When depositing particles onto a surface, there are a variety of techniques that can be used, such as impregnation or deposition-precipitation (DP). Impregnation involves dissolving gold precursor into an aqueous or organic medium. The solution is then added to the support followed by drying to remove volatiles and calcination to activate the catalysts.<sup>167</sup> The gold nanoparticles generated by impregnation are spherical and have limited contact with the surface, making these Au nanoparticles less effective at converting  $\text{H}_2$  and  $\text{O}_2$  to  $\text{H}_2\text{O}_2$  (Figure 5.1).<sup>168</sup> For deposition-precipitation preparation method, the pH is raised resulting in deposition of the metal as hydroxide. The pH is raised with neutralizing agents such as  $\text{CsOH}$ ,  $\text{NH}_4\text{OH}$ , and  $\text{Na}_2\text{CO}_3$ .<sup>148</sup> DP yielded a very narrow nanoparticle size distribution and the Au nanoparticles were hemispherical (Figure 5.1) and had a large contact area with the support.<sup>168</sup> Additionally, Au nanoparticles dispersed on titania by deposition-precipitation display the highest catalytic activity for the formation of  $\text{H}_2\text{O}_2$ , in turn leading to the highest catalytic activity for the epoxidation of propene.<sup>140,144,155,156,162,169,170</sup>

**Figure 5.1**—Au nanoparticles formed with impregnation (a) or DP (b)

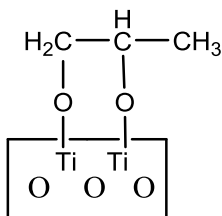


Although DP has been shown to be the optimum preparation method<sup>147</sup> for Au/TiO<sub>2</sub> there are also multiple neutralizing agents that can be utilized in the preparations of Au/TiO<sub>2</sub>. CsOH, NH<sub>4</sub>OH, and Na<sub>2</sub>CO<sub>3</sub> were used as neutralizing agents in order to determine if the neutralizing agent would play a role in the activity of the catalyst since harsh washings after the preparation of the catalyst affected the catalyst activity.<sup>148</sup> It was shown that Au/TiO<sub>2</sub> which was prepared with either Na<sub>2</sub>CO<sub>3</sub> or CsOH, had less acetone formation in the epoxidation trials as compared to NH<sub>4</sub>OH. Au nanoparticles that were prepared with Na<sub>2</sub>CO<sub>3</sub> showed the highest yield of PO for all the neutralizing agents tested. From XPS analysis of catalysts that had been treated with Na<sub>2</sub>CO<sub>3</sub> or CsOH, the presence of Na<sup>+</sup> or Cs<sup>+</sup> ions was observed on the catalyst surface after calcination. Alternatively, XPS analysis of catalysts treated with NH<sub>4</sub>OH, showed no alkali counter ions present on the surface after calcination. The higher catalytic activity of Au/TiO<sub>2</sub> synthesized by DP using Na<sub>2</sub>CO<sub>3</sub> or CsOH can be attributed to the presence of alkali ions on the catalyst surface. Alkali ions have been shown to increase the activity of Au/TiO<sub>2</sub> catalysts by blocking Lewis acidic sites on TiO<sub>2</sub>; acidic Ti sites lead to the degradation of PO.

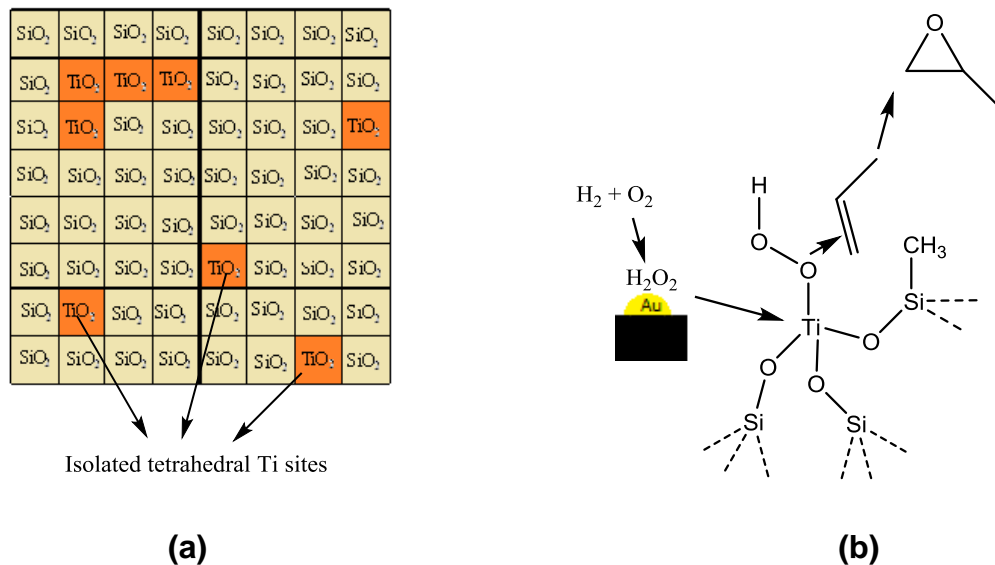
In addition to the size of the Au nanoparticles and the preparation method, the choice of support is also crucial to the conversion of propene and the selectivity of PO. Although Au/TiO<sub>2</sub> was the first catalyst shown to be active for the epoxidation of propene it suffers from quick catalyst degradation.<sup>171,172</sup> The main deactivation pathway is believed to be the formation of a bidentate propoxy species (Figure 5.2) formed on the surface of the support<sup>145,164</sup> which can then promote PO polymerization. Titanium dispersed onto silica supports displayed higher catalytic activity and longevity compared to Au/TiO<sub>2</sub> because the bidentate propoxy species does not bind to the surface as easily, causing less deactivation (Figure 5.3).<sup>172</sup> Silica supports such as TS-1,<sup>67,154,169,173-176</sup> SBA-15,<sup>165,177</sup> MCM-41,<sup>166</sup> and MCM-48<sup>152,178,179</sup> have been used for the epoxidation of propene using H<sub>2</sub> and O<sub>2</sub> where the Si/Ti ratio was altered to determine the most active catalysts.<sup>172</sup> Increased activity was observed for catalysts having a high Si/Ti ratio suggesting that isolated Ti<sup>+4</sup> are the most active for propene epoxidation

(Figure 5.3).<sup>172,180,181</sup> The generally accepted mechanism for PO formation using Au dispersed on titanosilicates as catalyst involves the adsorption of H<sub>2</sub> and O<sub>2</sub> on the gold surface prior to forming H<sub>2</sub>O<sub>2</sub> (Figure 5.3). H<sub>2</sub>O<sub>2</sub> then spills over onto the Ti species to form Ti-OOH which is believed to be one of the rate determining steps.<sup>172,180</sup> Once the Ti-OOH has formed, the propene attacks the hydroperoxide species forming PO. Additionally, it is believed that in titanium silicate supports, the Ti sites might be an anchor for the Au clusters thus ensuring close proximity of the isolated Ti and Au species.<sup>182</sup>

**Figure 5.2**—Bidentate peroxy species formed with Au/TiO<sub>2</sub><sup>164</sup>



**Figure 5.3**—Schematic representation of isolated Ti sites in heterogeneous materials (a)<sup>172</sup> and propene epoxidation with Au dispersed on titanosilicates (b)<sup>162</sup>

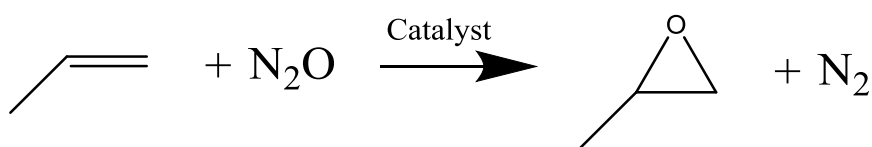


One way of optimizing catalyst efficiency is to add a promoter in the reactant gas mixture. Haruta and colleges have demonstrated that the addition of a small amount of trimethylamine, which is a strong Lewis base, improved the performance of Au on titanosilicates by blocking Lewis acidic sites on the support that absorb PO; preventing degradation by oligomerization.<sup>183</sup> Additionally, metal cations such as cobalt, calcium, and barium have shown to increase the catalytic activity for the epoxidation of propene by blocking acidic Ti sites that promote degradation.<sup>166,184,185</sup> Positive ions also lead to high catalytic activity by increasing the gold loading on the support. During the deposition-precipitation process, both the support and the gold being deposited are negatively charged, with the addition of positive ions onto the support, the gold anions are strongly attracted to the support leading to an increase in gold loading.<sup>185,186</sup> A third example of a promoter is the addition of water to the reactant gas mixture. One of the main deactivation pathways is the conversion of PO to a bidentate propoxy species (Figure 5.2). By adding water, methanol, or acetone into the reactant

mixture, they compete with PO to bind to the titania support blocking the sites which lead to catalyst deactivation.<sup>187,188</sup>

It is currently believed that in order for this process to be industrially relevant, the catalyst must facilitate about 10% propene conversion, 90% PO selectivity, and 50% hydrogen efficiency.<sup>155</sup> Presently, extremely low H<sub>2</sub> efficiency is a major problem with Au on titanium containing supports. The rate of H<sub>2</sub> consumption is 10 times higher than the formation of PO. One way to increase the H<sub>2</sub> efficiency is to co-feed CO into the reaction stream. Such an approach has been shown to lower the rate of propene hydrogenation although the reason for this inhibition is unclear.<sup>181</sup> Recently, propene epoxidation has been explored with N<sub>2</sub>O instead of H<sub>2</sub> and O<sub>2</sub>. This serves as an interesting alternative since N<sub>2</sub>O is a greenhouse gas which could be converted to N<sub>2</sub> (Scheme 5.4). Au-Cu/TiO<sub>2</sub> catalyst have been used which show up to 5% propene conversion along with 60% selectivity for PO. Although this method has yet to be optimized, it does give an interesting alternative to using explosive H<sub>2</sub>.<sup>189</sup>

**Scheme 5.4**—Using N<sub>2</sub>O as oxidant instead of H<sub>2</sub>



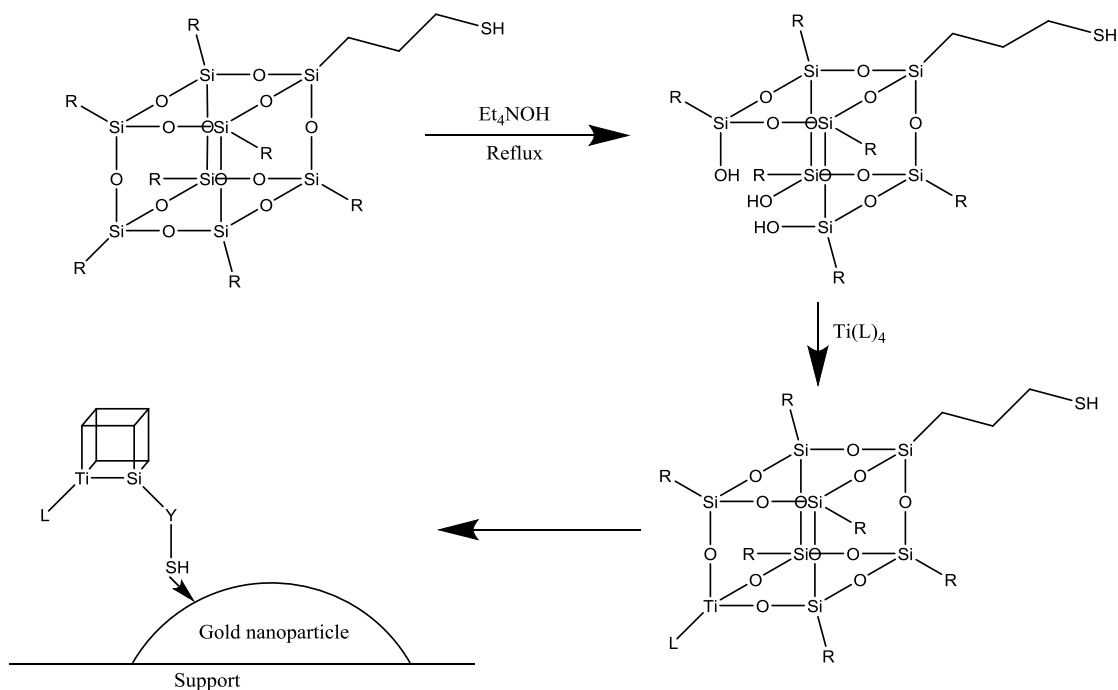
In heterogeneous catalysis, often times there are a variety of different active sites present. Previously it has been reported that tripodal titanium silsesquioxanes are the most active form of Ti for alkene epoxidation reactions.<sup>40</sup> From the literature reports, it has been shown that a probable mechanism of PO formation consists of three main components: (1) formation of H<sub>2</sub>O<sub>2</sub> by the Au



nanoparticles, (2) the formation of the Ti-OOH species, and (3) the conversion of propene to PO.

From literature studies, we reasoned that it should be possible to generate a catalyst that would keep tripodal Ti POSS in close proximity to the Au nanoparticles (NP), and thereby facilitate high selectivity for PO and good conversion of propene (Scheme 5.5). Tethering tripodal titanium onto Au nanoparticles generates isolated, uniform Ti centers in close proximity to the Au nanoparticles which have been shown to be the most active for the epoxidation of propene. Additionally, the main deactivation pathway, formation of a bidentate species, can be eliminated by using an inert support such as SiO<sub>2</sub> which does not bind PO as effectively. Tripodal titanium silsesquioxanes can be tethered onto Au nanoparticles by synthesizing tripodal Ti POSS containing a unique thiol tail since thiols are known to bind strongly with Au. Finally, we reasoned that using tripodal titanium silsesquioxanes would allow the catalyst to be tuned and altered by varying the length and structure of the tether to find the best distance required for epoxidation of propene to occur.

### Scheme 5.5—Proposed route to Ti catalyst tethered to gold nanoparticle



## 5.2 Experimental:

### 5.2.1 General Considerations

All experiments were performed under an atmosphere of nitrogen either using standard Schlenk techniques or in a Vacuum Atmospheres glovebox. Solvents were dried and distilled by standard methods before use.<sup>126</sup> All solvents were stored in glovebox over 4Å molecular sieves that had been dried in a vacuum oven at 250 °C for at least 24 hours before use. All glassware were dried in an oven at 110 °C for 24 hours before use. Unless otherwise stated, all reagents were purchased from Aldrich Chemical Company and used without further purification. Mercaptopropylsilyl POSS and trisilanol cyclohexyl POSS were purchased from Hybrid Plastics Inc. and dried overnight under vacuum at 60 °C prior to use.

$^1\text{H}$ ,  $^{13}\text{C}$ , and  $^{29}\text{Si}$  NMR spectra were recorded on a Varian INOVA 400 MHz spectrometer employing VnmrJ software. All chemical shifts are reported in

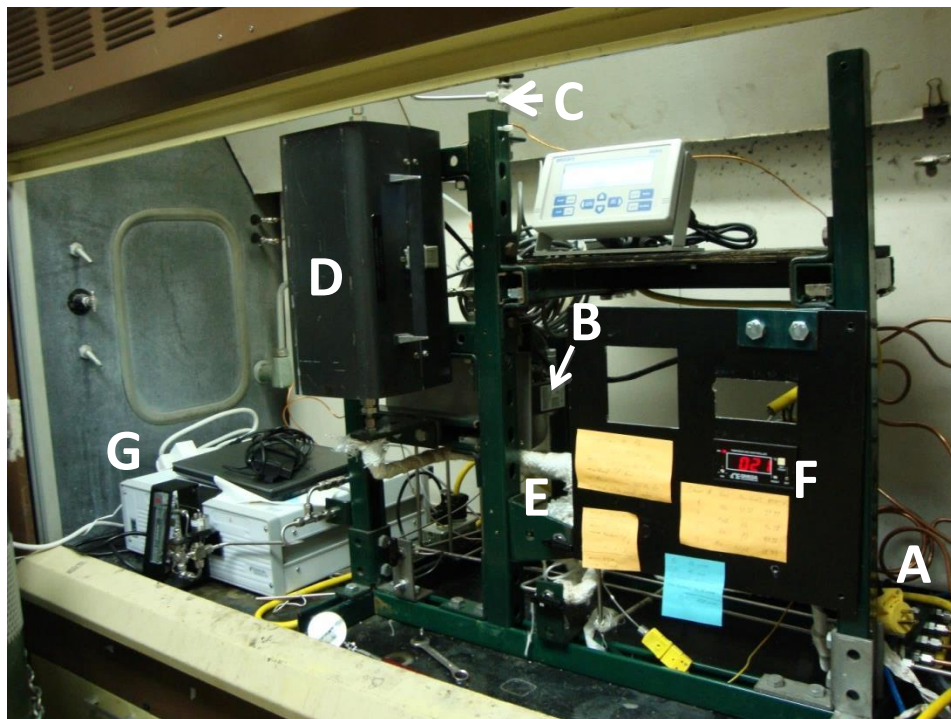
units of  $\delta$  (downfield of tetramethylsilane) and  $^1\text{H}$  &  $^{13}\text{C}$  chemical shifts were referenced to residual solvent peaks.  $^{29}\text{Si}$  NMR spectra were recorded using inverse-gated proton decoupling in order to increase resolution and minimize nuclear Overhauser enhancement effects. To ensure accurate integrated intensities,  $[\text{Cr}(\text{acac})_3]$  (0.05 M) was added to  $^{13}\text{C}$  and  $^{29}\text{Si}$  NMR samples as a shiftless relaxation agent and a delay of at least 1.1 s was used between observation pulses for  $^{13}\text{C}$  and  $^{29}\text{Si}$  measurements. IR spectra were recorded on a Thermo Scientific Nicolet iS10 FT-IR Spectrometer.

### 5.2.2 Reactor Setup

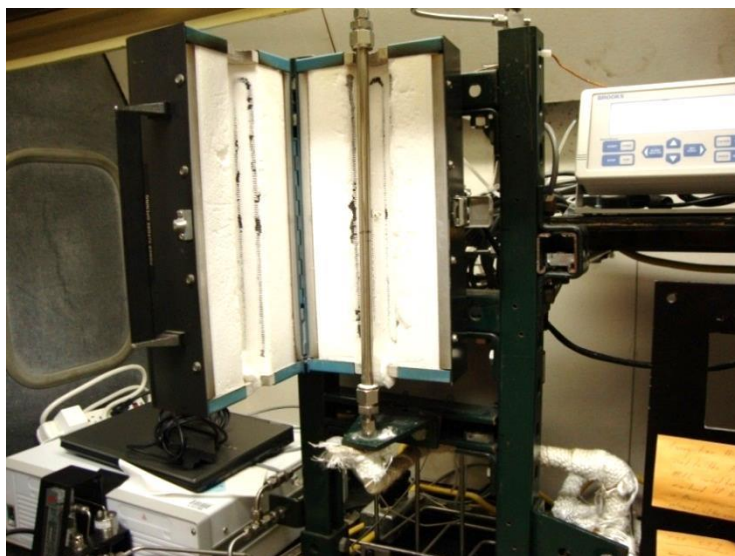
To begin, the gases (propene, hydrogen, oxygen (as air), and nitrogen to balance since mixtures of  $\text{H}_2$  and  $\text{O}_2$  are explosive) were connected to the reactor via four ports as seen in Figure 5.4 labeled A. These four different lines are then connected to mass flow controllers (B in Figure 5.4) which control the rate of each gas flow individually. After the four gases are passed through the mass flow controllers, they merge to form one steady stream. At the top of this gas line (C in Figure 5.4), there are two different paths: one allows gas to flow through the reaction column and the other bypasses the column completely in order to test total flows or composition of gases. The column (Figure 5.5), which holds the catalyst, is held within an oven (D in Figure 5.4), in order to control the reaction temperature. After the gases have passed through the reaction column, the products must be analyzed. In order to prevent condensation of any products formed, the tube traveling to the residual gas analyzer (RGA) is heat traced and can be set at various temperatures (E and F in Figure 5.4). Finally the gaseous products formed are analyzed by RGA (G in Figure 5.4) which has four different columns in tandem to separate and analyze numerous products. Once all the parts of the reactor were connected, gas was allowed to flow through and each and every junction was tested to ensure there were no leaks present in the system. This is also performed after the reaction column is removed to load or unload the catalyst, as well as any other time a part is removed.

**Figure 5.4**—Reactor setup

- A.** Ports for gases; **B.** Mass flow controllers; **C.** Bypass valve; **D.** Oven which hold reaction column; **E.** Heat trace; **F.** Heat trace control box; **G.** RGA



**Figure 5.5**—Column held within the oven



Once the setup of the reactor was complete, each gas was individually calibrated through its mass flow controller in order to ensure the correct amount of gas flow. After each gas was calibrated and equations generated to achieve correct setting on mass flow controllers, a total flow of 100 standard cubic centimeter per minute (sccm) was used to test these equations. The gas mixture desired was 10 % propene, 10 % hydrogen, 10 % oxygen, balanced with nitrogen. Based upon the equations generated, all the gases were turned on and mass flow controllers set accordingly. At the bypass location (C in Figure 5.3), the total flow was measured using a flow meter. Total sccm ranged from 99-103 over a total of 25 trials with an average of 100. After the total flow was confirmed, the bypass valve was connected directly to the RGA to analyze the gas mixture. The analysis confirmed a 10:10:10 percent ratio of propene, hydrogen and oxygen. This procedure was repeated when the total flow rate was changed.

The RGA also had to be calibrated for carbon dioxide, carbon monoxide, propene, acetaldehyde, acrolein, ethane, oxygen, and propylene oxide in order to ensure accurate measurements. After the reactor was set up, RGA calibrated,

and gas flows and concentrations confirmed, the reactor was ready to test various catalysts. Main products expected from the epoxidation reaction include propylene oxide, water, carbon dioxide, propene, acetaldehyde, and acrolein which were all accounted for in the calibration.

### 5.2.3 Synthesis

#### 5.2.3.1 Synthesis of $(\text{HS}(\text{CH}_2)_3(i\text{-C}_4\text{H}_9)_6\text{Si}_7\text{O}_9(\text{OH})_3$ (**12**)

A solution of  $\text{HS}(\text{CH}_2)_3(i\text{-C}_4\text{H}_9)_7\text{Si}_8\text{O}_{12}$  (**11**, 0.4 g, 0.45 mmol) and 35% w/w aqueous  $\text{Et}_4\text{NOH}$  (0.21 g, 0.49 mmol) in 15 mL of THF was heated to reflux with stirring for 4 hours. The solution was then neutralized with aqueous HCl (1 M). Evaporation of the volatiles afforded white solids which were dissolved in diethyl ether (30 mL). The solutions was dried over  $\text{Na}_2\text{SO}_4$  overnight. After removal of  $\text{Na}_2\text{SO}_4$  by filtration, the filtrate was concentrated to dryness under reduced pressure. The resulting white solid was then recrystallized by dissolving solid in toluene (1 mL) and acetonitrile added (5 mL) to yield, after drying, a regiomeric mixture of  $(\text{HS}(\text{CH}_2)_3(i\text{-C}_4\text{H}_9)_6\text{Si}_7\text{O}_9(\text{OH})_3$  (**12**) as a white solid. Yield: 0.21g, 58%

**$^1\text{H}$  NMR:**  $\delta$  0.63-0.66 (m, 12 H,  $\text{SiCH}_2\text{CH}(\text{CH}_3)_2$ ), 0.70-1.15 (m, 6 H,  $\text{Si}(\text{CH}_2)_3\text{SH}$ ), 0.98 (d, 36 H,  $\text{SiCH}_2\text{CH}(\text{CH}_3)_2$ ), 1.90 (m, 6 H,  $\text{SiCH}_2\text{CH}(\text{CH}_3)_2$ ), 4.1 (broad, 1H, S-H), and 6.56 (broad, 3H, Si-OH)

**$^{13}\text{C}$  NMR ( $\text{CDCl}_3$ ):**  $\delta$  22.8 ( $\text{SiCH}_2\text{CH}_2\text{CH}_2\text{SH}$ ), 23.1 ( $\text{SiCH}_2\text{CH}_2\text{CH}_2\text{SH}$ ), 23.9 ( $\text{CH}_2\text{CH}_2\text{CH}_2\text{SH}$ ), 24.1 ( $\text{SiCH}_2\text{CH}(\text{CH}_3)_2$ ), 24.8 ( $\text{SiCH}_2\text{CH}(\text{CH}_3)_2$ ), 26.1 ( $\text{SiCH}_2\text{CH}(\text{CH}_3)_2$ ).

**$^{29}\text{Si}$  NMR ( $\text{CDCl}_3$ ):**  $\delta$  -59.1 ( $\text{Si-OH}$ , 3 Si), -68.2 and -68.8 ( $\text{Si-CH}_2\text{CHMe}_2$ , 1Si and 3Si)

**IR (ATR,  $\nu$ ,  $\text{cm}^{-1}$ ):** 3200 (Si-OH), 2580 (S-H).

### 5.2.3.2 Synthesis of $\{Ti(NMe_2)(HS(CH_2)_3)(i-C_4H_9)_6Si_7O_{12}\}$ (**13**)

In the glovebox,  $Ti(NMe_2)_4$  (47 mg, 0.21 mmol) was added via syringe to a stirred solution of the regiomic mixture of **12** (0.16 g, 0.2 mmoles) in diethyl ether (15 mL) and let stir at room temperature for 30 minutes. The yellow solution was concentrated to dryness under reduced pressure. Residue was dissolved in toluene (1 mL) and acetonitrile (15 mL) was added to precipitate a yellow solid which was isolated via filtration and washed three times with acetonitrile followed by drying under vacuum to give a regiomic mixture of  $\{Ti(NMe_2)(HS(CH_2)_3)(i-C_4H_9)_6Si_7O_{12}\}$  (**13**) as yellow non-crystalline material. Yield: 0.14 g, 80%

**$^1H$  NMR (CDCl<sub>3</sub>):**  $\delta$  0.59 (12 H,  $CH_2CH(CH_3)_2$ ), 0.70-1.15 (m, 6 H,  $Si(CH_2)_3SH$ ), 0.96 (d, 36 H,  $CH_2CH(CH_3)_2$ ), 1.93 (6H,  $CH_2CH(CH_3)_2$ ), 3.0-3.2 (broad,  $Ti-N(CH_3)_2$ ) and 4.03 (S-H).

**$^{29}Si$  NMR (CDCl<sub>3</sub>):**  $\delta$  -68.9 (7 Si, multiplet, overlapping,  $Si-CH_2CHMe_2$ )

**IR (ATR,  $\nu$ , cm<sup>-1</sup>):** 2580 (S-H).

### 5.2.3.3 Synthesis of $\{Ti(OPr^i)(HS(CH_2)_3)(i-C_4H_9)_6Si_7O_{12}\}$ (**14**)

In the glovebox,  $Ti(OPr^i)_4$  (60 mg, 0.21 mmol) was added via syringe to a stirred solution of the regiomic mixture of **12** (0.16 g, 0.2 mmoles) in diethyl ether (15 mL) and let stir at room temperature for 30 minutes. The colorless solution was concentrated to dryness under reduced pressure. Work up was the same as reported for **13** to yield a regiomic mixture of  $\{Ti(NMe_2)(HS(CH_2)_3)(i-C_4H_9)_6Si_7O_{12}\}$  (**13**) as white non-crystalline material. Yield: 0.16 g, 88%

**$^1H$  NMR (CDCl<sub>3</sub>):**  $\delta$  0.58 (12 H,  $CH_2CH(CH_3)_2$ ), 0.70-1.15 (m, 6 H,  $Si(CH_2)_3SH$ ), 0.96 (d, 36 H,  $CH_2CH(CH_3)_2$ ), 1.27 ppm (6H,  $OCH(CH_3)_2$ ), 1.94 (6H,  $CH_2CH(CH_3)_2$ ), 3.0-3.2 (broad,  $Ti-N(CH_3)_2$ ), 4.03 (1H, S-H) and 4.49 ppm (1H,  $OCH(CH_3)_2$ )

**$^{29}Si$  NMR (CDCl<sub>3</sub>):**  $\delta$  -68.7 (7 Si, multiplet, overlapping,  $Si-CH_2CHMe_2$ )

**IR (ATR,  $\nu$ ,  $\text{cm}^{-1}$ ):** 2580 (S-H).

#### 5.2.3.4 Au/SiO<sub>2</sub>

Au/SiO<sub>2</sub> was prepared by deposition-precipitation method using gold (III) chloride as the gold precursor at room temperature. SiO<sub>2</sub> (10 g) was dispersed in DI water (100 mL) with vigorous stirring. 2.5% ammonium hydroxide was added to raise the pH of the solution to a value between 9.4 and 9.6. Over a 1 hour period, the gold (AuCl<sub>3</sub> (187 mg) dissolved in DI water (40 mL)) was added while the pH was maintained between 9.4 and 9.6. The mixture was allowed to stir for an additional hour after which it was filtered and washed with DI water (200 mL) thrice to yield a yellow solid material. The catalyst was dried at 60°C overnight followed with activation by calcination for 2 hours at 120°C followed by 4 hours at 400°C to yield purple powder. Au nanoparticles (NP) were analyzed by TEM where at least 100 NPs were measured for calculations.

#### 5.2.3.5 Tethering of {Ti(NMe<sub>2</sub>)(HS(CH<sub>2</sub>)<sub>3</sub>)(i-C<sub>4</sub>H<sub>9</sub>)<sub>6</sub>Si<sub>7</sub>O<sub>12</sub>) } (**13**) onto Au/SiO<sub>2</sub> (**13-Au/SiO<sub>2</sub>**)

In glovebox, {Ti(NMe<sub>2</sub>)(HS(CH<sub>2</sub>)<sub>3</sub>)(i-C<sub>4</sub>H<sub>9</sub>)<sub>6</sub>Si<sub>7</sub>O<sub>12</sub>) } (**13**, 5 or 10 wt%) was dissolved in diethyl ether (25 mL) followed by the addition of Au/SiO<sub>2</sub> (5g) which was allowed to stir for 30 minutes at room temperature. Upon completion, the mixture was concentrated to dryness under reduced pressure and washed thrice with copious amounts of acetonitrile to yield **13-Au/SiO<sub>2</sub>** as a purple solid.

#### 5.2.3.6 Tethering of {Ti(OPr<sup>i</sup>)(HS(CH<sub>2</sub>)<sub>3</sub>)(i-C<sub>4</sub>H<sub>9</sub>)<sub>6</sub>Si<sub>7</sub>O<sub>12</sub>) } (**14**) onto Au/SiO<sub>2</sub> (**14-Au/SiO<sub>2</sub>**)

In glovebox, {Ti(OPr<sup>i</sup>)(HS(CH<sub>2</sub>)<sub>3</sub>)(i-C<sub>4</sub>H<sub>9</sub>)<sub>6</sub>Si<sub>7</sub>O<sub>12</sub>) } (**14**, (5 or 10 wt%)) was dissolved in diethyl ether (25 mL) followed by the addition of Au/SiO<sub>2</sub> (5g) which was allowed to stir for 30 minutes at room temperature. Upon completion, the mixture was concentrated to dryness under reduced pressure and washed thrice with copious amounts of acetonitrile to yield **14-Au/SiO<sub>2</sub>** as a purple solid.



### 5.2.3.7 Impregnation of $[Ti(OPr^i)\{(c-C_6H_{11})_7Si_7O_{12}\}]$ (**10**) onto Au/SiO<sub>2</sub> (**15-Au**)

In glovebox,  $[Ti(OPr^i)\{(c-C_6H_{11})_7Si_7O_{12}\}]$  (**10**, (5 or 40 wt%)) was dissolved in diethyl ether (25 mL) followed by the addition of Au/SiO<sub>2</sub> (5g) which was allowed to stir for 30 minutes at room temperature. Upon completion, the mixture was concentrated to dryness under reduced pressure and washed thrice with copious amounts of acetonitrile to yield **15**→**Au/SiO<sub>2</sub>** as purple solid.

### 5.2.3 Epoxidation Trials

In order to test a catalyst, glass wool was lightly packed in the bottom of the column until the thermocouple came in contact with the glass wool. This was performed so that the thermocouple would reside in the catalysts bed yielding a more accurate temperature reading. 0.4 g of catalyst was added followed by glass wool lightly packed to keep catalyst in place. Oven was set to desired temperature and allowed to stabilize. The heat tape along output lines were set at 100 °C. After the oven and heat tape were stable, the gas mixture was allowed to flow through reaction column. RGA analysis was taken every 5 minutes and recorded.

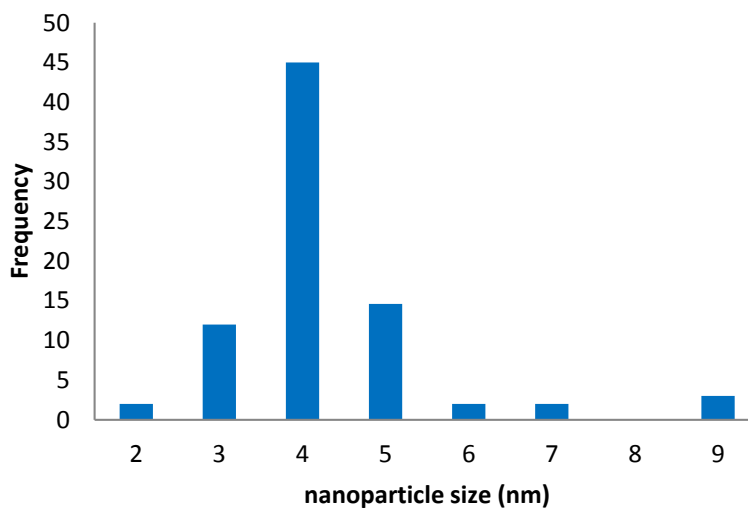
## 5.3 Results/Discussion:

### 5.3.1 Grafting of tripodal Ti POSS onto Au/SiO<sub>2</sub> supports

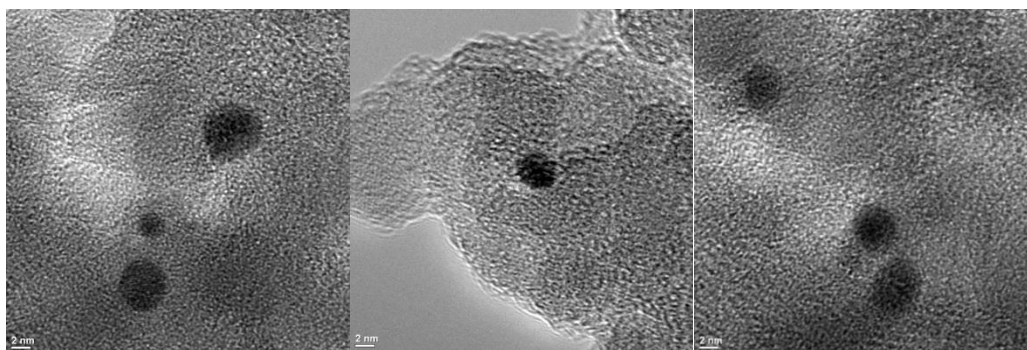
First, the Au nanoparticles were deposited onto SiO<sub>2</sub> via deposition-precipitation method described previously.<sup>164,170,187,190</sup> The support is dispersed in water and the pH is raised by adding 2.5% ammonium hydroxide (NH<sub>4</sub>OH) until the pH value was between 9.4 and 9.6. Then, gold (AuCl<sub>3</sub> in DI water) was slowly added while maintaining the pH between 9.4 and 9.6. The mixture was filtered, washed and activated by calcination, resulting in the successful formation of Au/SiO<sub>2</sub> which was characterized by TEM. A narrow size distribution (2-5 nm) was observed for Au nanoparticles dispersed on SiO<sub>2</sub> which were air-cooled after calcination (Figure 5.6). Additionally, TEM micrographs (Figure 5.7) showed that the gold nanoparticles were isolated and did not overlap with each other. In order to prevent water formation on the surface, another series of

Au/SiO<sub>2</sub> supports were synthesized as described previously except the material was cooled under N<sub>2</sub> after the calcination step (Figure 5.8 and 5.9). N<sub>2</sub>-cooled Au/SiO<sub>2</sub> showed isolated Au nanoparticles but had a slightly larger nanoparticle size distribution (2-6 nm) compared to air-cooled Au/SiO<sub>2</sub>. Nanoparticles in the 2-5 nm range have been reported to be the most active for the epoxidation of propene therefore both Au/SiO<sub>2</sub> supports should display catalytic activity for the formation of H<sub>2</sub>O<sub>2</sub> from H<sub>2</sub> and O<sub>2</sub>.

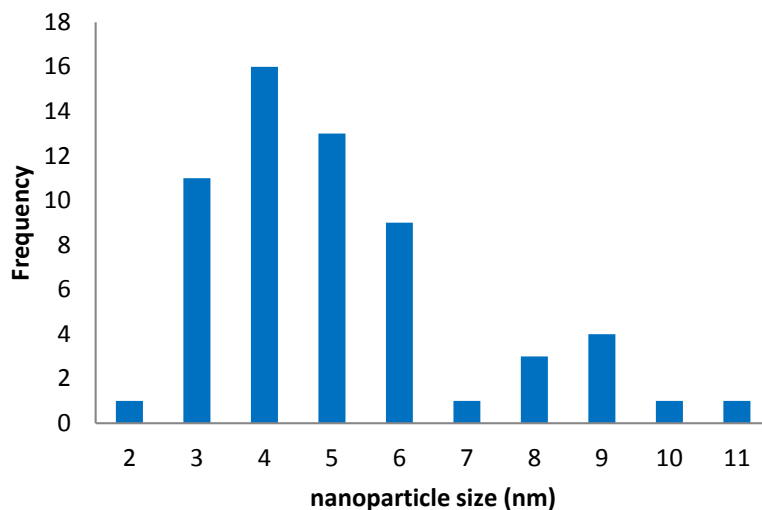
**Figure 5.6**—Size distribution of Au/SiO<sub>2</sub> nanoparticles air-cooled after calcination step



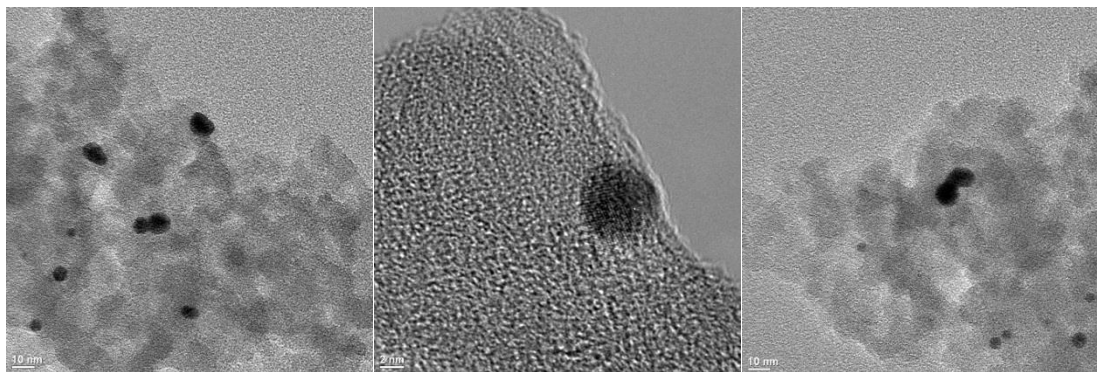
**Figure 5.7**—TEM micrographs of Au/SiO<sub>2</sub> nanoparticles air-cooled after calcination step



**Figure 5.8**—Size distribution of Au/SiO<sub>2</sub> nanoparticles N<sub>2</sub>-cooled after calcination step



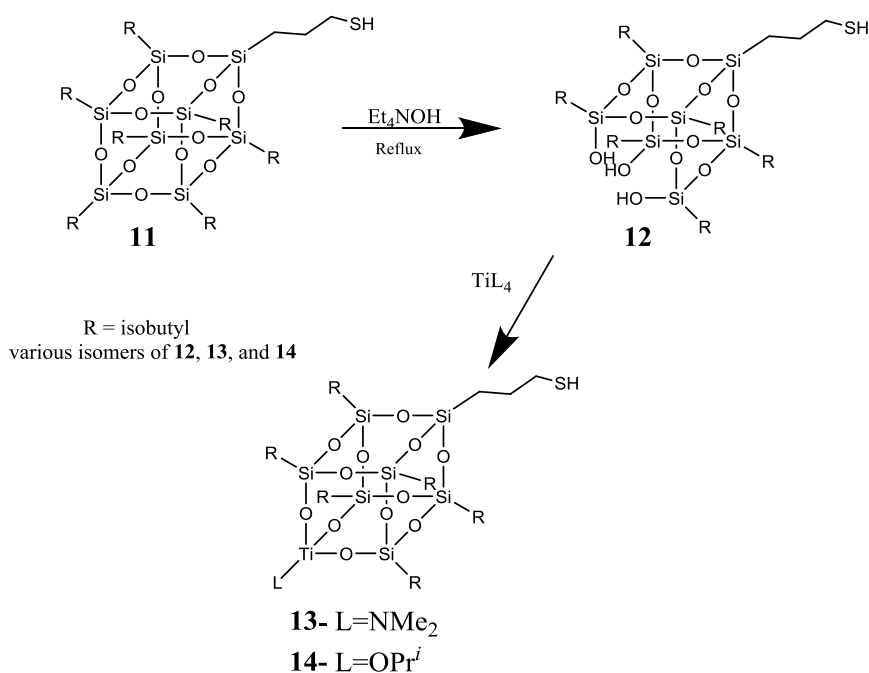
**Figure 5.9**—TEM micrographs of Au/SiO<sub>2</sub> nanoparticles N<sub>2</sub>-cooled after calcination step



After confirming that the Au nanoparticles were in the correct size range, a tripodal titanium POSS complex containing a thiol tail was synthesized; the complex was subsequently tethered to Au nanoparticles. Numerous reports have investigated the strength of Au-thiol bonds. The bond dissociation was determined to be on the order of 50 kcal/mol for Au-thiol while C-C bonds display 83-85 kcal/mol suggesting that Au-thiol bonds display good strength.<sup>26,191-193</sup>

The synthesis of **12** (Scheme 5.6) was accomplished by removing one framework silicon from mercaptaisobutyl POSS (**11**) via base catalyzed excision adapted from Feher.<sup>96-99</sup> Excision of mercaptaisobutyl POSS was accomplished by refluxing Et<sub>4</sub>NOH in THF for four hours to produce (HS(CH<sub>2</sub>)<sub>3</sub>(i-C<sub>4</sub>H<sub>9</sub>)<sub>6</sub>Si<sub>7</sub>O<sub>9</sub>(OH)<sub>3</sub> (**12**) in moderate yield (42%). The structure and formulation of **12** was confirmed by solution (<sup>1</sup>H, <sup>13</sup>C, & <sup>29</sup>Si) NMR and IR. <sup>29</sup>Si NMR spectra showed silanol Si atoms at δ-59.1, consistent with previously reported chemical shift (δ-58.5) for silanol Si atoms for (i-Bu)<sub>7</sub>Si<sub>7</sub>O<sub>9</sub>(OH)<sub>3</sub>.<sup>99</sup> Additionally, the silanol signal displayed the expected 3:4 integral ratio with overlapping resonances for silsesquioxane Si atoms between δ -68.2 and -68.8. Evidence for the retention of the unique thiol tail was observed in the <sup>1</sup>H NMR spectra which showed a resonance at δ 4.10 for the thiol group along with a broad resonance at δ 6.56 for the silanol protons. Further confirmation that both the thiol and silanol groups were present in **12** came from the IR spectrum which showed an OH stretch (3200 cm<sup>-1</sup>) as well as a SH stretch (2580 cm<sup>-1</sup>).

**Scheme 5.6**—Synthesis of tripodal Ti POSS



Ti was inserted into **12** via protonolysis of  $\text{Ti}(\text{NMe}_2)_4$  or  $\text{Ti}(\text{OPr}^i)_4$  with one equivalent of **12** to give **13** and **14** in excellent yields (Figure 5.6). **13** and **14** were confirmed by solution ( $^1\text{H}$ ,  $^{13}\text{C}$ , &  $^{29}\text{Si}$ ) NMR and IR.  $^1\text{H}$  NMR showed the loss of the silanol peaks (6.56 ppm) while retaining the thiol peak around 4.1 for both **13** and **14**. For **13**, some residual  $\text{HNMe}_2$ , by-product of protonolysis, was present and has been shown in chapter 2, to bind to the Ti center. This broadens the Ti- $\text{NMe}_2$  resonances in the  $^1\text{H}$  NMR due to the slow exchange between  $\text{HNMe}_2$  and Ti- $\text{NMe}_2$ . On the other hand, **14** showed characteristic isopropoxide resonances at 4.49 ppm ( $\text{OCH}(\underline{\text{H}})(\text{CH}_3)_2$ ) and 1.27 ppm ( $\text{OCH}(\underline{\text{C}}\text{H}_3)$ ) while not containing any isopropyl alcohol by-product. Further confirmation of the formation of **13** and **14** came from the  $^{29}\text{Si}$  NMR which showed the absence of the silanol resonances around -59 ppm and only showed the framework silsesquioxane Si atoms from -68 to -70 ppm. IR spectra of **13** and **14** showed the loss of the OH stretch ( $3200\text{ cm}^{-1}$ ) while the SH stretch ( $2580\text{ cm}^{-1}$ ) remained.

Tripodal Ti POSS was tethered onto the Au/SiO<sub>2</sub> supports by first dissolving the POSS in Et<sub>2</sub>O followed by the addition of the Au/SiO<sub>2</sub> support into the solution. The mixture was allowed to stir for 30 minutes and then slowly dried under reduced pressure. To remove any free Ti POSS species, the resulting material was washed with copious amounts of ACN.

### 5.3.2 Epoxidation Trials

Epoxidation of propene was first analyzed with gold dispersed on TiO<sub>2</sub> in order to validate the reactor setup. As seen in Table 5.1 entry 1, the catalyst showed high selectivity and a yield of 0.8% at 70°C, which was in line with literature reports.<sup>7,143,155,162,164,170,172,188,194-197</sup> Next, the Au/SiO<sub>2</sub> was tested to see if the support without Ti would show any activity (Table 5.1-entry 2). There was no conversion observed, indicating that without the Ti present, no epoxidation would take place. As a final check of our system before supported tripodal Ti POSS catalysts were tested,  $\text{Ti}(\text{OPr}^i)_4$  was supported on the different Au/SiO<sub>2</sub> samples in order to ensure the Au nanoparticles were in the correct size

range for epoxidation reaction (Table 5.1-entry 3). Indeed, the epoxidation reaction showed high selectivity and an overall yield of 1% after the first cycle.

Verification of our system included validating the reactor setup, ensuring the Au nanoparticles were in the correct range, and showing that Ti was needed for epoxidation to occur. Next, tripodal titanium silsesquioxanes immobilized onto Au/SiO<sub>2</sub> were tested. As can be seen in Table 5.1 entry 4 and 5, there was minimal activity for **13-Au/SiO<sub>2</sub>** (0.05% yield of PO) or **14-Au/SiO<sub>2</sub>** (0.06% yield of PO). We knew that our Au NPs were active so it was postulated that the surface was interacting with the Ti center. It is known that SiO<sub>2</sub> has free silanols on the surface and has the possibility of interacting with the Ti center. In fact, it has been shown in the literature that by silylating the support surface, the activity of the catalyst increased, giving higher PO selectivity (95% vs 90%) as well as higher H<sub>2</sub> efficiency (12% vs 7.5%) albeit the PO conversion decreased. The lower conversion was thought to be due to reaction site blocking by the silylating agent.<sup>144</sup>

**Table 5.1—Epoxidation Results**

Entry No.	Catalyst	Temperature (°C)	Selectivity For PO (%)	Yield (%)
1	Au/TiO <sub>2</sub>	70	100	0.8
2	Au/SiO <sub>2</sub>	70	0	0
3	Ti(OPr <sup>i</sup> ) <sub>4</sub> supported on Au/SiO <sub>2</sub> *	70	85	1
4	5 wt% Ti(NMe <sub>2</sub> ) Thiol Isobutyl POSS supported on Au/SiO <sub>2</sub>	70	Maximum of 6.5	0.05
5	5 wt% Ti(OPr <sup>i</sup> ) Thiol Isobutyl POSS supported on Au/SiO <sub>2</sub>	70	Maximum of 7	0.06
6	5 wt% Ti(OPr <sup>i</sup> ) Thiol Isobutyl POSS supported on silylated Au/SiO <sub>2</sub>	70	Maximum of 2.3	0.06
7	10 wt% Ti(OPr <sup>i</sup> ) Thiol Isobutyl POSS supported on Au/SiO <sub>2</sub> *	70	0	0
8	5 wt% Ti(OPr <sup>i</sup> ) Cyclohexyl POSS supported on silylated Au/SiO <sub>2</sub>	70	5.3	0.13
9	40 wt% Ti(OPr <sup>i</sup> ) Cyclohexyl POSS supported on Au/SiO <sub>2</sub> *	70	Maximum of 7	Maximum of 0.17

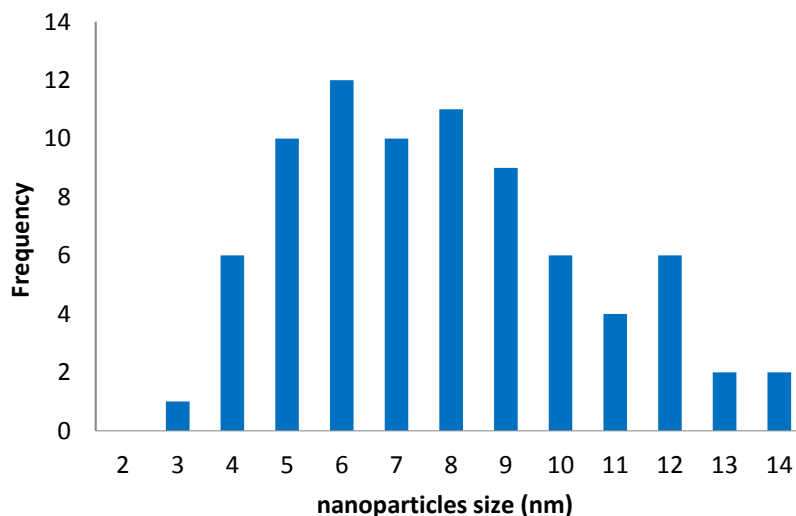
0.4 g catalysts, 1:1:1 O<sub>2</sub>:H<sub>2</sub>:Propene, GHSV = 7000 hr<sup>-1</sup>, Feed flow = 100 sccm, Analyzed by GC-FID

\*Used with both Au/SiO<sub>2</sub> and silylated Au/SiO<sub>2</sub> supports

In order to prevent interactions between the surface silanols and the Ti center, the SiO<sub>2</sub> support was silylated. When the SiO<sub>2</sub> support is silylated, the surface is hydrophobic, which prevents Au deposition via deposition-precipitation method. Thus, we silylated the Au/SiO<sub>2</sub> supports after calcination using BSTFA (Bis(trimethylsilyl)trifluoroacetamide) with 1% TMCS (trimethylchlorosilane) until all the silanol groups present were consumed based on IR analysis, i.e. we made the Au/SiO<sub>2</sub> by deposition-precipitation then silylated after calcination. The Au

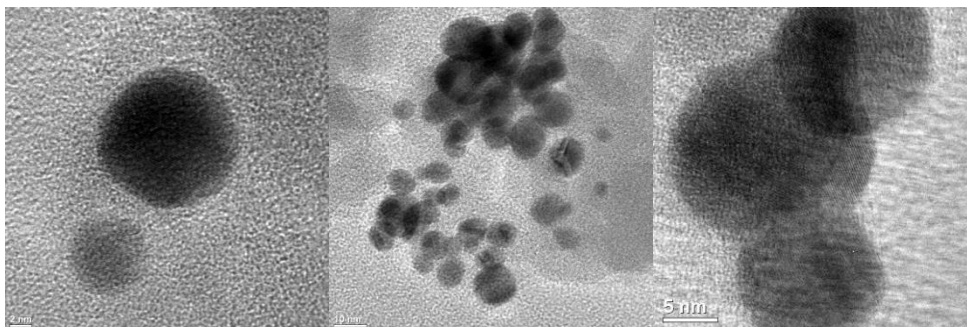
nanoparticle size distribution for silylated supports air-cooled after calcination is shown in Figure 5.10. TEM micrographs (Figure 5.11) show the Au nanoparticles aggregated together and in some cases, multiple nanoparticles are overlapping which, resulted in a wide range of Au nanoparticle size. The observed aggregation is most likely due to greater hydrophobic character of the support, which enhances the ability of nanoparticles to move freely due to attractive forces between the nanoparticles. A second batch of Au/silylated SiO<sub>2</sub> was synthesized as previously described except the material was cooled under a N<sub>2</sub> atmosphere after calcination to prevent water formation on the surface. The Au nanoparticles size distribution can be seen in Figure 5.12. Similar to the silylated Au/SiO<sub>2</sub> catalyst dried under air, the TEM showed the Au nanoparticles overlapped with each other and clustered together when compared to non-silylated Au/SiO<sub>2</sub> (Figure 5.13).

**Figure 5.10**—Size distribution of silylated Au/SiO<sub>2</sub> nanoparticles air-cooled after calcination and silylation step

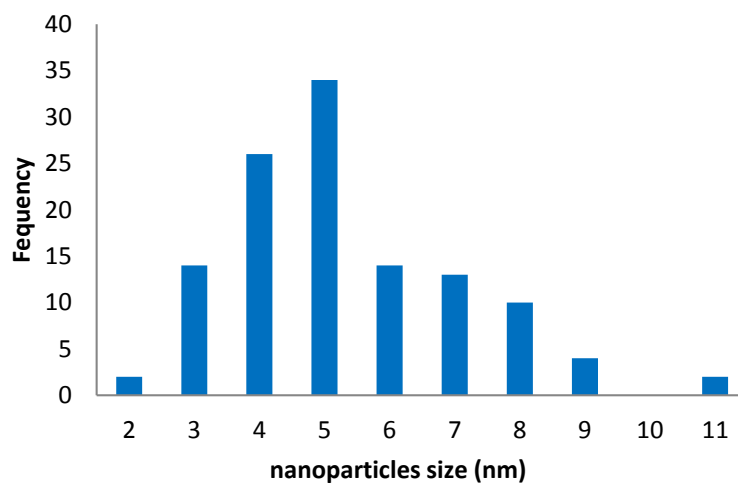




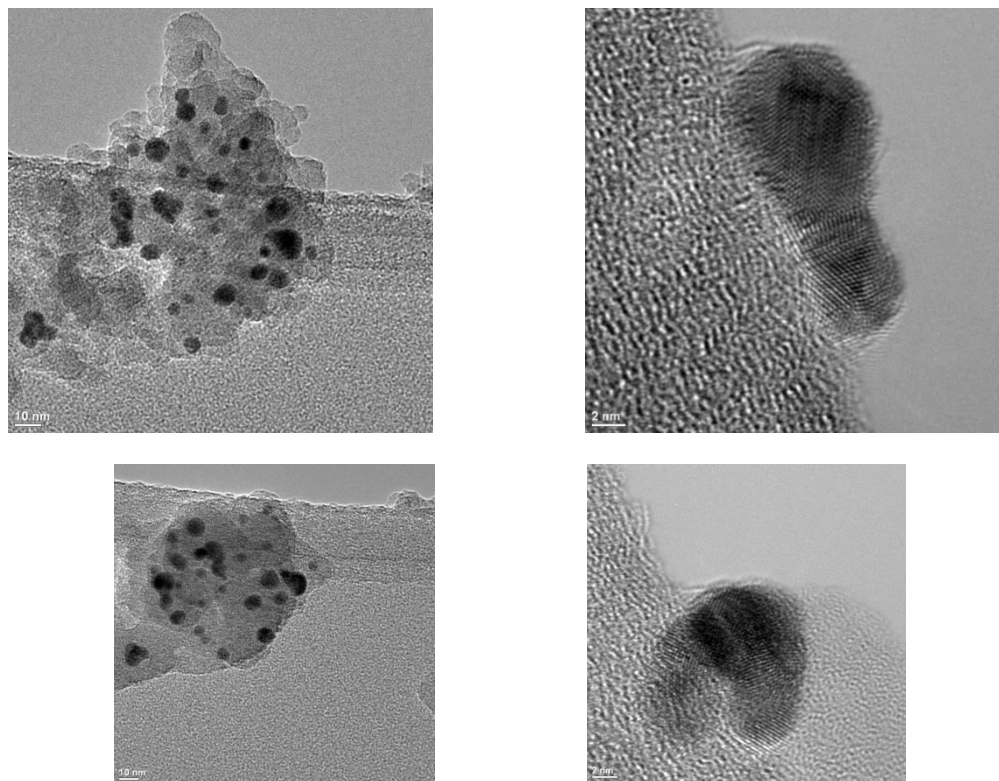
**Figure 5.11**—TEM micrographs of silylated Au/SiO<sub>2</sub> nanoparticles air-cooled after calcination and silylation step



**Figure 5.12**—Size distribution of silylated Au/SiO<sub>2</sub> nanoparticles N<sub>2</sub>-cooled after calcination and silylation step



**Figure 5.13**—TEM micrographs of silylated Au/SiO<sub>2</sub> nanoparticles N<sub>2</sub>-cooled after calcination and silylation step



Analogous to the prep of **14-Au/SiO<sub>2</sub>**, **14-Au/silylated-SiO<sub>2</sub>** was prepared by tethering **14** onto the Au/SiO<sub>2</sub> supports by first dissolving the POSS in Et<sub>2</sub>O followed by the addition of the Au/SiO<sub>2</sub> support into the solution. The mixture was allowed to stir for 30 minutes and then slowly dried under reduced pressure. To remove any free Ti POSS species, the resulting material was washed with ACN. **14-Au/silylated-SiO<sub>2</sub>** catalyzed epoxidation of propene employing H<sub>2</sub> and O<sub>2</sub> (Table 5.1-entry 6 and 7) displayed lower selectivity compared to **14-Au/SiO<sub>2</sub>**. However when compared to Au/TiO<sub>2</sub> or even Ti(OPr<sup>i</sup>)<sub>4</sub> supported on Au/SiO<sub>2</sub> there was essentially minimal amount of activity observed for both **14-Au/silylated-SiO<sub>2</sub>** and **14-Au/SiO<sub>2</sub>**. This suggested that there may not be enough Ti present in the catalysts since the POSS ligand is very bulky compared to Ti. Therefore, the loading of tripodal Ti POSS was increased to 10 wt% (Table 5.1-entry 7) however this also showed no catalytic activity.

Observing that there was essentially no activity for either **13-Au/SiO<sub>2</sub>** or **14-Au/SiO<sub>2</sub>**, it was determined that the thiol tail may not be effectively keeping the Ti in close proximity to the Au nanoparticles. It was thought to test a uniformly substituted POSS which does not contain a thiol tail. Previously, it has been determined that uniformly substituted [Ti(NMe<sub>2</sub>)<sub>2</sub>((i-C<sub>6</sub>H<sub>11</sub>)<sub>7</sub>Si<sub>7</sub>O<sub>12</sub>)] (**10**) has a higher *k*<sub>2</sub> value compared to a regiomeric mixture of tripodal titanium silsesquioxanes (Chapter 2). Therefore, [Ti(OPr<sup>i</sup>)<sub>3</sub>((i-C<sub>6</sub>H<sub>11</sub>)<sub>7</sub>Si<sub>7</sub>O<sub>12</sub>)] (**15**) was prepared via literature method<sup>40</sup> and then impregnated (→) onto Au/SiO<sub>2</sub> support (**15**→Au/SiO<sub>2</sub>). **15**→Au/SiO<sub>2</sub> catalyzed epoxidation of propene (Table 5.1-entry 8) showed a slightly higher yield (0.13%) than **13-Au/SiO<sub>2</sub>** or **14-Au/SiO<sub>2</sub>**. Although the yield was higher, the selectivity remained extremely low (5.3%) and in comparison to Au/TiO<sub>2</sub> or Ti(OPr<sup>i</sup>)<sub>4</sub> supported on Au/SiO<sub>2</sub>, there was essentially no activity seen for these catalysts either.

5 and 10 wt% loading of tripodal Ti silsesquioxanes were inefficient catalysts for the epoxidation of propene. The Ti center is the active site for the epoxidation of propene. Therefore, since POSS ligand is very bulky compared to Ti, catalysts containing 5 wt% of Ti (40 wt% of **15**) were tested for the epoxidation of propene (Table 5.1-entry 9). Indeed we did see the highest selectivity (7%) and yield (0.17%) observed to date for these tripodal Ti catalysts; however they pale in comparison to Au/TiO<sub>2</sub> or Ti(OPr<sup>i</sup>)<sub>4</sub> supported on Au/SiO<sub>2</sub>. For all the catalysts tested, even if some activity was observed for the first cycle, they degraded quickly and no additional yield was obtained.

## 5.4 Conclusion

After observing that all the tripodal Ti POSS catalyst showed almost no activity, we terminated the epoxidation reactions. It was evident that although this was a promising idea, the catalysts are just not active under our reaction conditions for the direct epoxidation of propene using molecular oxygen as the oxidant.

Looking back to the reaction mechanism, there are essentially three steps that have to occur for PO formation. First the Au nanoparticles have to generate  $H_2O_2$  *in situ*. Next the Ti must be in close proximity to the Au nanoparticles in order to form the active Ti-OOH species. Finally, before  $H_2O_2$  decomposes, propene must react with the Ti hydroperoxide species to generate PO. Additionally, after formation, the PO must not decompose before it reaches the GC detector.

Breaking these steps down into different parts we first must determine if the Au nanoparticles are indeed forming  $H_2O_2$ . In order to investigate this, epoxidation trials were conducted using  $Ti(OPr^i)_4$  on Au/SiO<sub>2</sub> supports. These catalysts did show conversion of propene and relatively high yields as compared to the tripodal Ti POSS catalysts suggesting that the Au nanoparticles were forming  $H_2O_2$ . Further evidence is provided by the consumption of  $H_2$  and  $O_2$  gas for all epoxidation trials which contained Au nanoparticles, suggesting that indeed the Au nanoparticles were forming  $H_2O_2$ .

The next step would be to form the Ti-OOH species which is thought to be the rate determining step. This would be accomplished by having the Ti in close proximity to the Au nanoparticles where  $H_2O_2$  was formed. When the Au nanoparticle forms  $H_2O_2$ , there are at least two different routes that can occur. The first is the formation of the Ti-OOH species and the second is the decomposition to water and  $H_2$ . Although we did not analyze for the formation of the Ti-OOH species, this could be accomplished by using *in situ* IR which would show the Ti-OOH species as has been demonstrated by others.<sup>46,137,145,151,154,155,158,161,162,169,194,195,198,199</sup> After the Ti-OOH species is formed, propene is converted to PO. However, the rate of Ti-OOH decomposition can also dominate the reaction if the olefin is not in close proximity to the Ti-OOH species.

In addition to these reaction steps, we can look at deactivation pathways as well: one major pathway would be the loss of Ti via hydrolysis. This occurs

when water is present either on the catalyst surface or in the reaction stream. It has been postulated that indeed  $\text{H}_2\text{O}_2$  is being formed by the Au nanoparticle tested by our system. Therefore, we can assume that some of the  $\text{H}_2\text{O}_2$  is being decomposed to form water as well. Since our support has some degree of polarity, the water formed could stick to the surface causing a loss of any Ti present in our catalysts. To avoid this, we could try to place our catalysts in a hydrophobic medium to use in the reactor which would prevent water from deactivating our catalysts. Another option would be to incorporate our tripodal Ti POSS into a polymer which would then be used as a support for the Au nanoparticles and allow for a higher degree of hydrophobicity.

The size of the POSS could also play a large role in why these catalysts were inactive. It could be that the Ti is positioned away from the Au nanoparticles and as soon as the  $\text{H}_2\text{O}_2$  is produced it does not interact with the Ti center but passed through the  $\text{SiO}_2$  support or decomposes instead. It would be interesting to do a TEM/XRD (transmission electron microscope/X-ray diffraction) and AFM (atomic force microscopy) study to determine if the Ti POSS was in fact tethered to the Au nanoparticles or if they are isolated on the  $\text{SiO}_2$  surface. Additionally, the thiol tail could be tuned in order to achieve the best length and rigidity to hold the Ti close to the Au nanoparticles. Finally, the support could play a major role in the catalytic activity. It would be interesting to study various different supports such as graphite in order to gain a better understanding of the reaction steps occurring.

Vast amount of work can be conducted in order to improve these catalysts, such as *in situ* IR, TEM/XRD and AFM study, alter thiol tail, embed catalysts into a hydrophobic membrane, etc. which could generate an active catalyst or help to better understand that key reactions steps that need to proceed for a successful reaction.

Copyright © Sarah Michelle Peak 2015

## Chapter 6: Conclusions and Future Work

Chapters 2 and 3 demonstrated that homogeneous tripodal titanium silsesquioxanes display excellent catalytic activity using TBHP as the oxidant for the epoxidation of cyclic olefins (cyclohexene and 1-methylcyclohexene), terminal olefins (1-octene), and more demanding olefins such as limonene and  $\alpha$ -pinene. In fact, compared to other titanium catalysts, homogeneous tripodal titanium silsesquioxanes are some of the most active catalysts developed to date. Due to the excellent promise of homogeneous tripodal titanium silsesquioxanes, they were perfect candidates for immobilization in order to generate heterogeneous catalysts that could be reused.

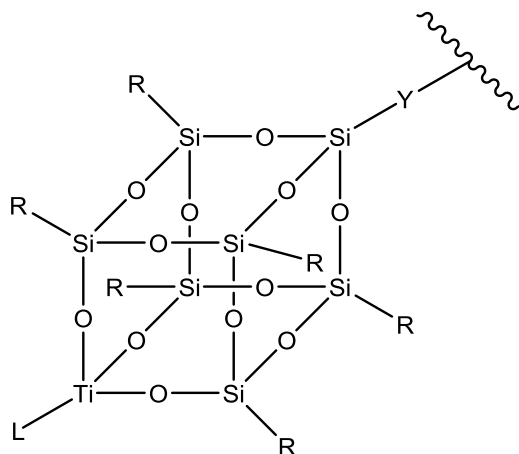
Indeed, Chapter 2 demonstrated the successful immobilization of tripodal titanium silsesquioxane onto hyperbranched polysiloxysilane matrices. The materials displayed similar selectivities compared to the homogeneous analogs for the epoxidation of 1-octene employing TBHP as the oxidant. Additionally, it was shown that the immobilized catalysts can be reused up to five recycles with only a slight loss in activity due to the presence of excess *t*-butanol. However, we were able to successfully repair the catalysts and regain similar activity as the pristine catalysts. Chapter 3 demonstrated the versatility of immobilized titanium catalysts where all of the catalysts explored displayed similar epoxidation selectivities for the olefins tested compared to the homogeneous analogs; the exception being  $\alpha$ -pinene which resulted in slightly lower selectivity. Although selectivity for  $\alpha$ -pinene oxide was lower for the immobilized catalysts versus the homogeneous analogs, the results obtained were either comparable or superior to numerous other catalysts reported.

Employing TBHP as the oxidant generates *t*-butanol as the co-product, which needs to be disposed of or recycled. However, if H<sub>2</sub>O<sub>2</sub> was used instead, this would generate water as a co-product leading to higher atom efficiency and less environmental impacts. Chapter 4 demonstrated that when hydrogen peroxide was employed, the catalysts were less active compared to when TBHP

was used as the oxidant due to degradation of the catalysts from the water present. Reaction conditions were modified in order to remove excess water from the reaction medium. As a result, **c-P1-8** displayed higher catalytic activity compared to runs where water was not removed. In industry, more concentrated H<sub>2</sub>O<sub>2</sub> can be used and will inherently show higher activity compared to the results shown herein.

Even though these results are very promising, there are always improvements that can be made to allow for the development of better catalysts. The catalytic system developed allows for numerous manipulations of the catalyst to tune it for optimal activity. In order to improve the overall rate of the reaction, the ligand on titanium (L in Figure 6.1) can be changed from NMe<sub>2</sub>, which has been shown to autoretard the reaction, to a less basic ligand such as OPr<sup>*i*</sup>, OPh, CH<sub>2</sub>Ph or OSiMe<sub>3</sub> and ideally generate faster catalysts. Additionally, electron withdrawing ligands such as OC<sub>6</sub>H<sub>4</sub>F-*p* or OC<sub>6</sub>H<sub>4</sub>NO<sub>2</sub>-*p* can be employed that have been shown to have a higher *k*<sub>2</sub> value than the ligands mentioned above. Similarly, substituents of the silsesquioxane (R in Figure 6.1) can be changed to smaller cyclohexyl or cyclopentyl groups which have been shown to give faster catalysts when compared to the isobutyl analog. The rigidity and length of the tail (Y in Figure 6.1) can also be explored in order to determine if the orientation of the POSS moiety within the polymer matrix plays a role in the catalytic activity. Additionally, the POSS loading can be altered in order to determine if there is an optimum titanium loading for the epoxidation reactions.

**Figure 6.1**—Tripodal titanium silsesquioxane



Aside from altering the POSS complex, the polymer can also be modified to achieve optimum catalytic activity. Possible modifications include changing the molecular weight of the polymer as well as the degree of crosslinking. By altering the molecular weight of the polymer and/or the degree of crosslinking, there would be a balance between rate of diffusion for the reactant and the protection of the titanium center from degradation due to water, which results in catalyst deactivation. When TBHP is employed as the oxidant, heterogenization is beneficial in order to generate a robust, recyclable, and repairable catalyst that has similar catalytic activity compared to the homogeneous analogs. However when  $\text{H}_2\text{O}_2$  is used as the oxidant, protection of the titanium center from water is the most beneficial aspect of heterogenization. Therefore, the catalyst displaying the highest catalytic activity when TBHP is employed could be different than the catalyst developed for  $\text{H}_2\text{O}_2$  epoxidation reactions.

Chapter 5 focused on the direct epoxidation of propene by tethering tripodal titanium silsesquioxane onto  $\text{Au}/\text{SiO}_2$ . Our results indicate that further improvements need to be made (these were discussed in the conclusion section of Chapter 5).



Tripodal titanium silsesquioxanes, both homogeneous and immobilized catalysts, displayed superior activity for epoxidation reactions employing TBHP for different olefins. Additionally, immobilized tripodal titanium silsesquioxanes were active catalysts when H<sub>2</sub>O<sub>2</sub> was employed as the oxidant and displayed either comparable or superior catalytic activity to numerous other titanium containing catalysts reported. The results discussed in this dissertation show that tripodal titanium silsesquioxanes are excellent catalysts for the epoxidation of olefins and have great potential for use in industry.

**Appendix**  
LIST OF ABBREVIATIONS AND SYMBOLS

General

ACN	Acetonitrile
ROOH	Alkyl hydroperoxide
Å	Angstrom, $10^{-10}$ m
C	Celsius
cm	centimeter
CDCl <sub>3</sub>	Deuterated chloroform
CPPA	<i>cis</i> -1-propenylphosphonic acid
°	Degree
DP	Deposition-precipitation
DMF	Dimethylformamide
EO	Ethylene Oxide
GC-FID	Gas chromatography-flame ionization detector
g	Grams
Hz	Hertz, s <sup>-1</sup>
mCPBA	meta-chlorperoxybenzoic acid
µL	Microliter
mg	Milligrams
mL	Milliliters
mmoles	Millimoles
MCM-41	Mobil composition of matter No. 41
nm	Nanometer
NP	Nanoparticle
ppm	Parts per million
PDMS	Polydimethylsiloxane
POSS	Polyoligomeric silsesquioxanes
PO	Propylene oxide

RGA	Residual gas analyzer
s	Seconds
SSHC	Single-site heterogeneous catalyst
sccm	standard cubic centimeter per minute
T	Temperature
TBHP	<i>Tert</i> -butyl hydroperoxide
THF	Tetrahydrofuran
3-D	Three dimension
t	Time
Ti	Titanium
TS-1	Titanium silicalite-1
TEM	Transmission electron microscopy
UV	Ultraviolet
wt%	Weight percent
XPS	X-ray photoelectron spectroscopy

For nuclear magnetic resonance (NMR) spectra and infrared (IR) spectra

ATR	Attenuated total reflectance
$\delta$	Chemical shift (in parts per million)
d	Doublet
m	Multiplet
NMR	Nuclear magnetic resonance
s	Singlet
t	Triplet
$\text{cm}^{-1}$	Wavenumbers

Figure A1— UV-Vis of  $[\text{Ti}(\text{NMe}_2)\{\text{Et}_3\text{Si}(\text{CH}_2)_3(i\text{-Bu})_6\text{Si}_7\text{O}_{12}\}]$  (**7**)

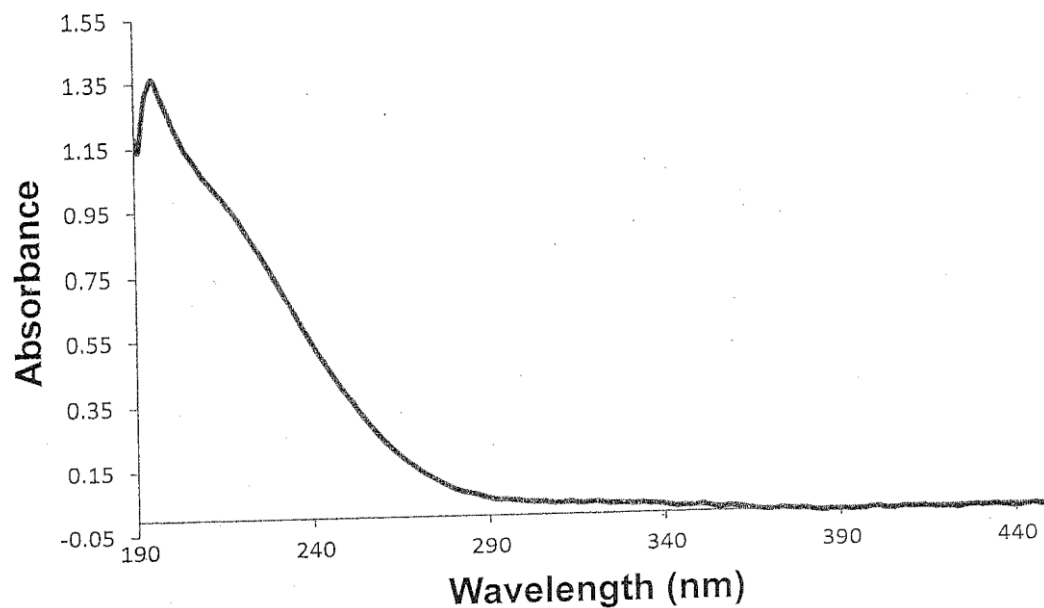


Figure A2—UV-Vis spectrum of  $[\text{Ti}(\text{NMe}_2)\{\text{HMe}_2\text{Si}(\text{CH}_2)_3(i\text{-Bu})_6\text{Si}_7\text{O}_{12}\}]$  (**8**)

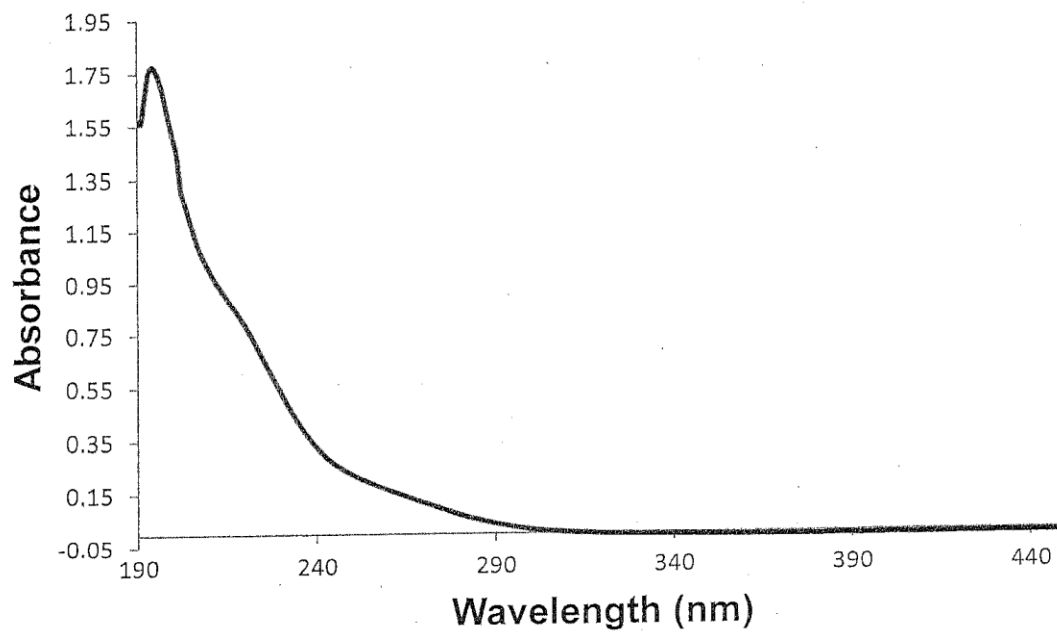


Figure A3—UV- Vis spectrum of (P1-8)

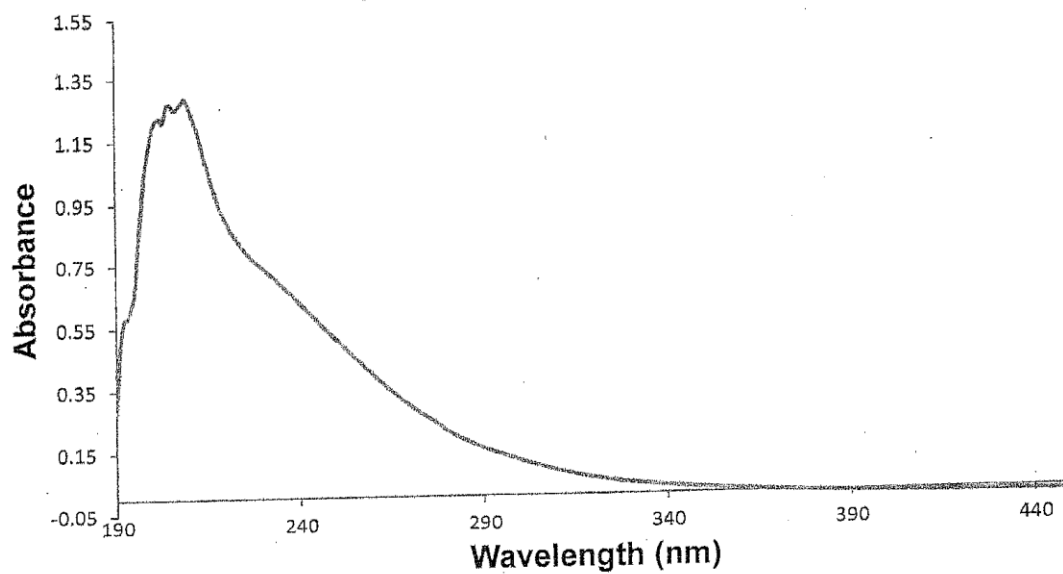


Figure A4—UV- Vis spectrum of (c-P1-8)

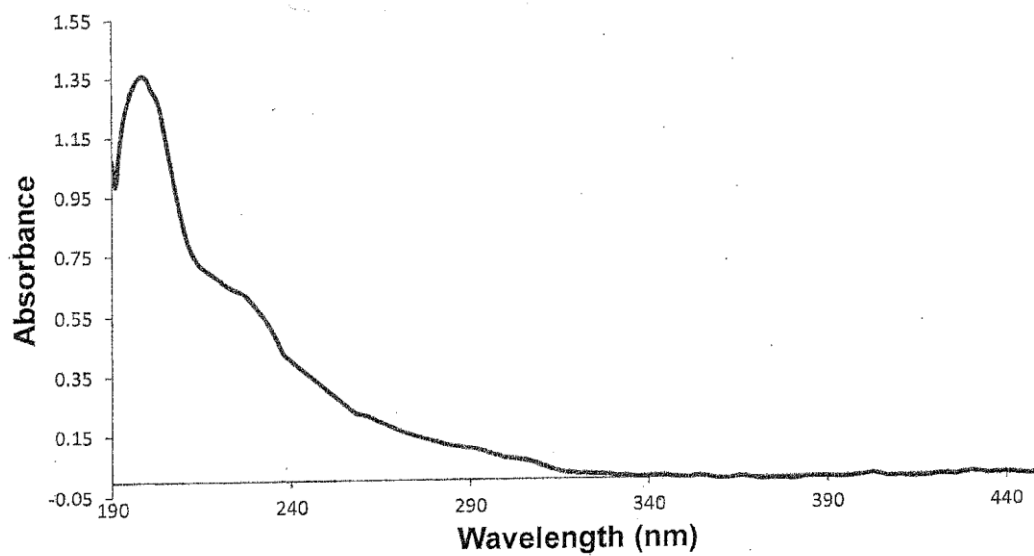
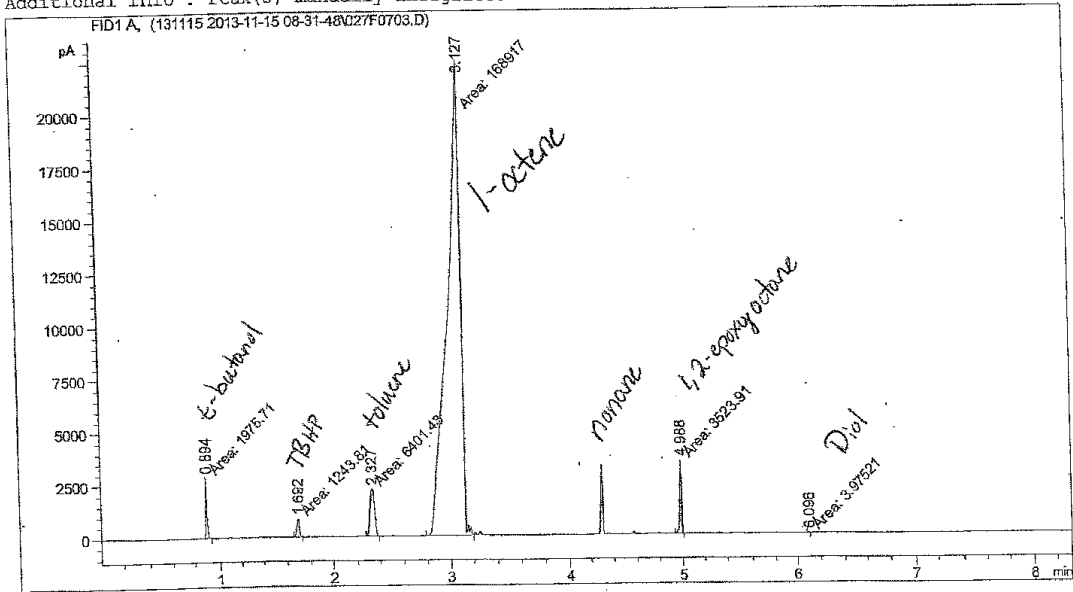


Figure A5. Typical GC chromatograph for epoxidation of 1-octene (73 g) using TBHP (31 mmol) and homogeneous catalysts (**7-10**, 0.2mmol Ti) after 10 minutes (50 % conversion)

Acq. Instrument : 6890 GC  
 Injection Date : 11/15/2013 11:30:08 AM  
 Location : Vial 27  
 Inj : 3  
 Inj Volume : 1 µl  
 Acq. Method : C:\CHEM32\2\DATA\131115 2013-11-15 08-31-48\TBHP.M  
 Last changed : 10/31/2013 8:46:25 AM  
 Analysis Method : C:\CHEM32\2\METHODS\TBHP.M  
 Last changed : 11/4/2013 9:34:49 AM  
 (modified after loading)  
 Additional Info : Peak(s) manually integrated



Area Percent Report

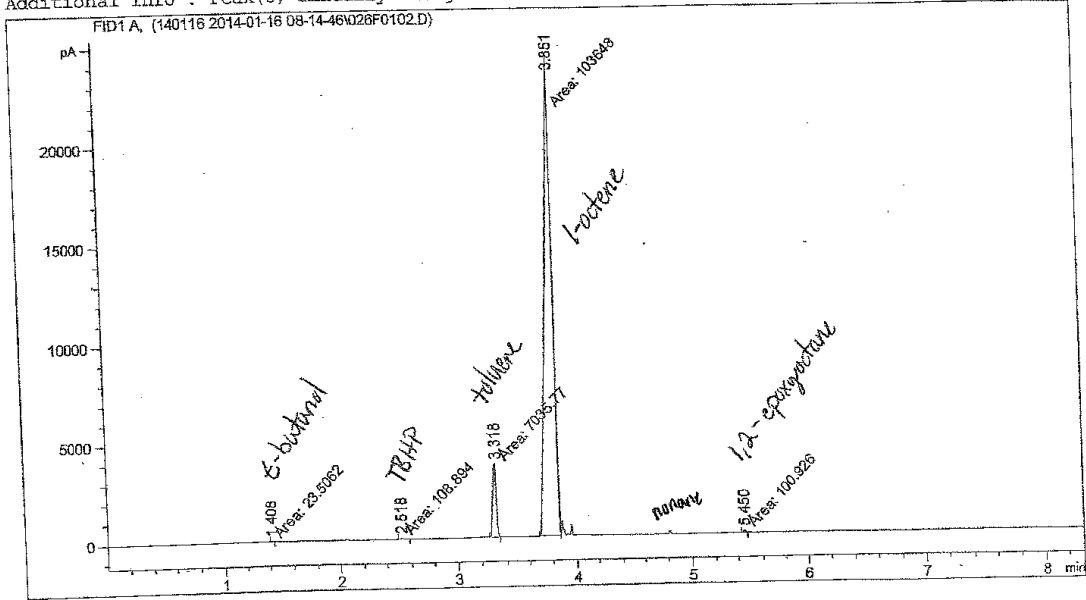
Sorted By : Signal  
 Multiplier: : 1.0000  
 Dilution: : 1.0000  
 Use Multiplier & Dilution Factor with ISTDs

Signal 1: FID1 A,

Peak #	RetTime [min]	Type	Width [min]	Area [pA*s]	Height [pA]	Area %
1	0.894	MM	0.0115	1975.71008	2854.69165	1.08516
2	1.692	MM	0.0246	1243.80823	841.38214	0.68316
3	2.327	MM	0.0480	6401.42725	2222.18237	3.51599
4	3.127	MM	0.1242	1.68917e5	2.26594e4	92.77798
5	4.988	MM	0.0169	3523.90967	3469.61523	1.93551
6	6.096	MM	0.0130	3.97521	5.10472	0.00218

Figure A6. Typical GC chromatograph for epoxidation of 1-octene (20 g) using TBHP (0.55 mmol) and P1-8 (0.06 mmol Ti) as catalyst after 1 hours (50 % conversion)

Acq. Instrument : 6890 GC  
 Injection Date : 1/16/2014 8:37:01 AM  
 Location : Vial 20  
 Inj : 2  
 Inj Volume : 1 µl  
 Acq. Method : C:\CHEM32\2\DATA\140116 2014-01-16 08-14-46\TBHP.M  
 Last changed : 10/31/2013 8:46:25 AM  
 Analysis Method : C:\CHEM32\2\DATA\140114 2014-01-14 08-36-34\TBHP.M  
 Last changed : 10/31/2013 8:46:25 AM  
 Additional Info : Peak(s) manually integrated



Area Percent Report

Sorted By : Signal  
 Multiplier: : 1.0000  
 Dilution: : 1.0000  
 Use Multiplier & Dilution Factor with ISTDs

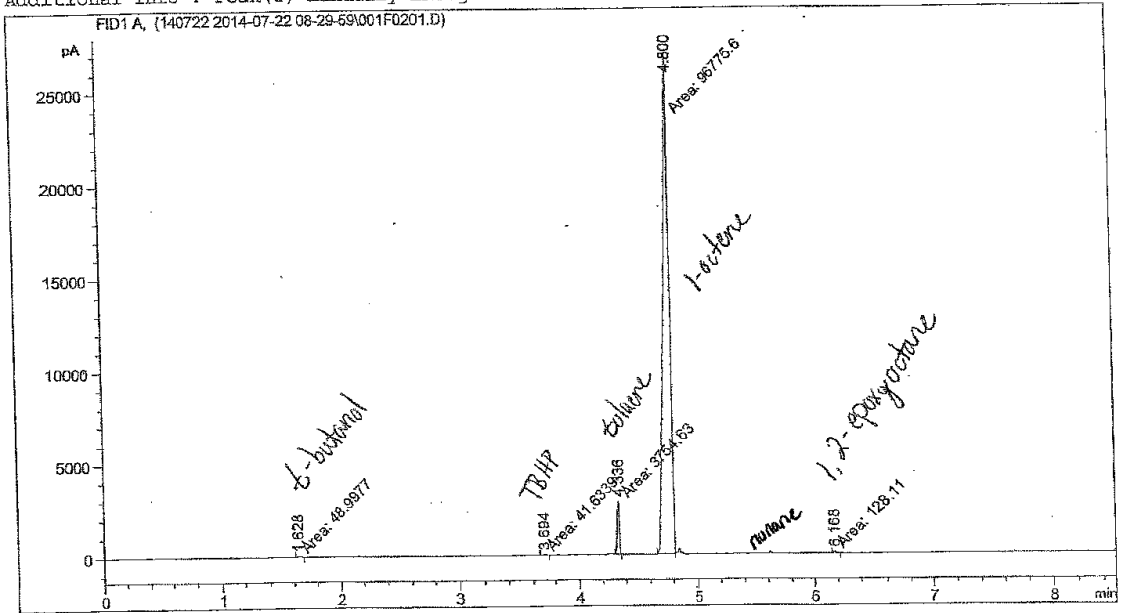
Signal 1: FID1 A,

Peak #	RetTime [min]	Type	Width [min]	Area [pA*s]	Height [pA]	Area %
1	1.408	MM	0.0138	23.50615	28.46376	0.02119
2	2.518	MM	0.0260	108.89423	69.80731	0.09818
3	3.318	MM	0.0313	7035.76563	3740.97241	6.34329
4	3.851	MM	0.0703	1.03648e5	2.45753e4	93.44635
5	5.450	MM	0.0137	100.92631	122.58056	0.09099

Totals : 1.10917e5 2.85371e4

Figure A7. Typical GC chromatograph for epoxidation of 1-octene (20 g) using TBHP (0.55 mmol) and **c-P1-8** (0.02 mmol Ti) as catalyst after 16 hours (50 % conversion)

Acq. Instrument : 6890 GC Location : vial 1  
 Injection Date : 7/22/2014 9:13:30 AM Inj : 1  
 Inj Volume : 1 µl  
 Acq. Method : C:\CHEM32\2\DATA\140722 2014-07-22 08-29-59\TBHP.M  
 Last changed : 7/14/2014 10:04:33 AM  
 Analysis Method : C:\CHEM32\2\METHODS\FAME.M  
 Last changed : 7/14/2014 2:21:25 PM  
 (modified after loading)  
 Additional Info : Peak(s) manually integrated



Area Percent Report

Sorted By : Signal  
 Multiplier: : 1.0000  
 Dilution: : 1.0000  
 Use Multiplier & Dilution Factor with ISTDs

Signal 1: FID1 A,

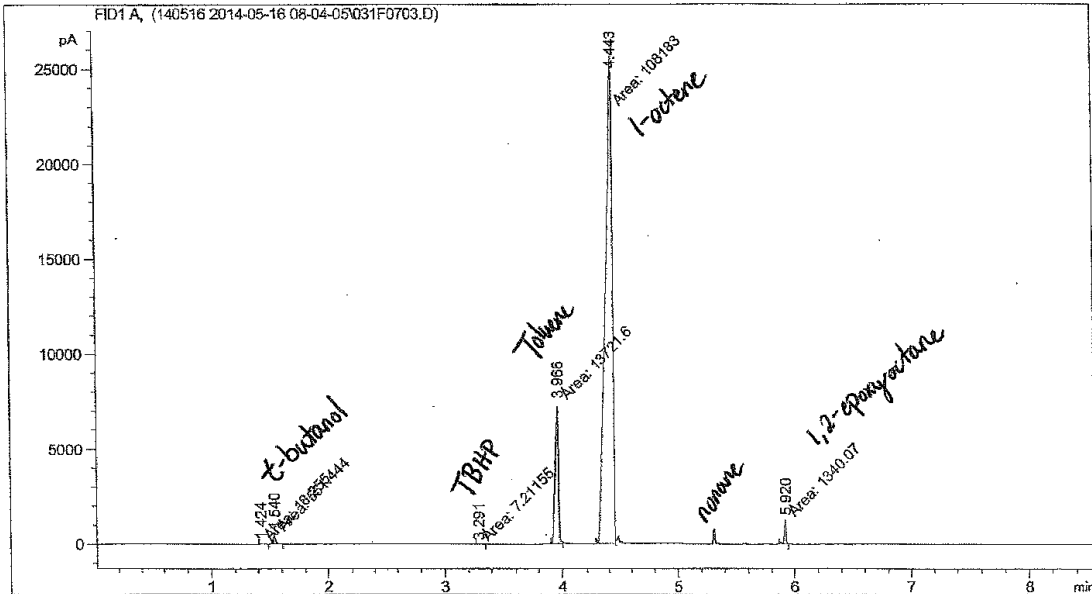
Peak #	RetTime [min]	Type	Width [min]	Area [pA*s]	Height [pA]	Area %
1	1.628	MM	0.0153	48.99767	53.53557	0.04863
2	3.694	MM	0.0197	41.63385	35.17838	0.04132
3	4.336	MM	0.0217	3754.62695	2890.14014	3.72672
4	4.800	MM	0.0610	9.67756e4	2.64200e4	96.05617
5	6.168	MM	0.0186	128.10971	114.62490	0.12716

Totals : 1.00749e5 2.95135e4



Figure A8. Typical GC chromatograph for epoxidation of 1-octene (73 g) using TBHP (31 mmol) and homogeneous catalysts (**7-10**, 0.2mmol Ti) after 30 minutes (100 % conversion)

Acq. Operator : Seq. Line : 7  
 Acq. Instrument : 6890 GC Location : Vial 31  
 Injection Date : 5/16/2014 2:11:50 PM Inj : 3  
 Inj Volume : 1 µl  
 Acq. Method : C:\CHEM32\2\DATA\140516 2014-05-16 08-04-05\TBHP.M  
 Last changed : 3/26/2014 9:01:04 AM  
 Analysis Method : C:\CHEM32\2\DATA\140515 2014-05-15 08-17-08\TBHP.M  
 Last changed : 3/26/2014 9:01:04 AM  
 Additional Info : Peak(s) manually integrated



Area Percent Report

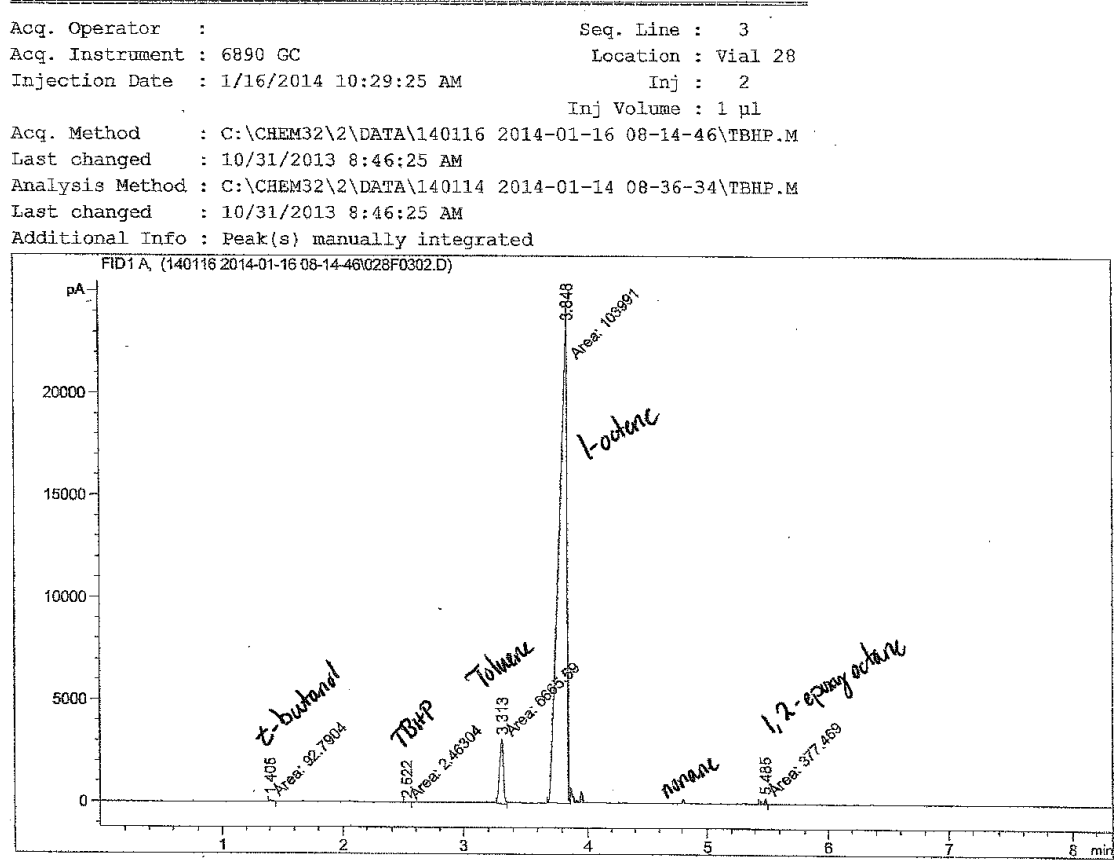
Sorted By : Signal  
 Multiplier: : 1.0000  
 Dilution: : 1.0000  
 Use Multiplier & Dilution Factor with ISTDs

Signal 1: FID1 A,

Peak #	RetTime [min]	Type	Width [min]	Area [pA*s]	Height [pA]	Area %
1	1.424	MM	0.0161	18.25497	18.85500	0.01474
2	1.540	MM	0.0177	551.44360	520.35498	0.44535
3	3.291	MM	0.0298	7.21155	4.03481	0.00582
4	3.966	MM	0.0308	1.37216e4	7418.14355	11.08170
5	4.443	MM	0.0694	1.08183e5	2.59660e4	87.37012
6	5.920	MM	0.0171	1340.06873	1308.43518	1.08225

Totals : 1.23822e5 3.52358e4

Figure A9. Typical GC chromatograph for epoxidation of 1-octene (20 g) using TBHP (0.55 mmol) and **P1-8** (0.06 mmol Ti) as catalyst after 2 hours (100 % conversion)



Area Percent Report

Sorted By : Signal  
 Multiplier: : 1.0000  
 Dilution: : 1.0000  
 Use Multiplier & Dilution Factor with ISTDs

Signal 1: FID1 A,

Peak #	RetTime [min]	Type	Width [min]	Area [pA*s]	Height [pA]	Area %
1	1.405	MM	0.0150	92.79037	103.27884	0.08350
2	2.522	MM	0.0301	2.46304	1.36352	0.00222
3	3.313	MM	0.0352	6665.59033	3159.40503	5.99804
4	3.848	MM	0.0715	1.03991e5	2.42494e4	93.57658
5	5.485	MM	0.0221	377.46872	284.28781	0.33967

Totals : 1.11129e5 2.77977e4

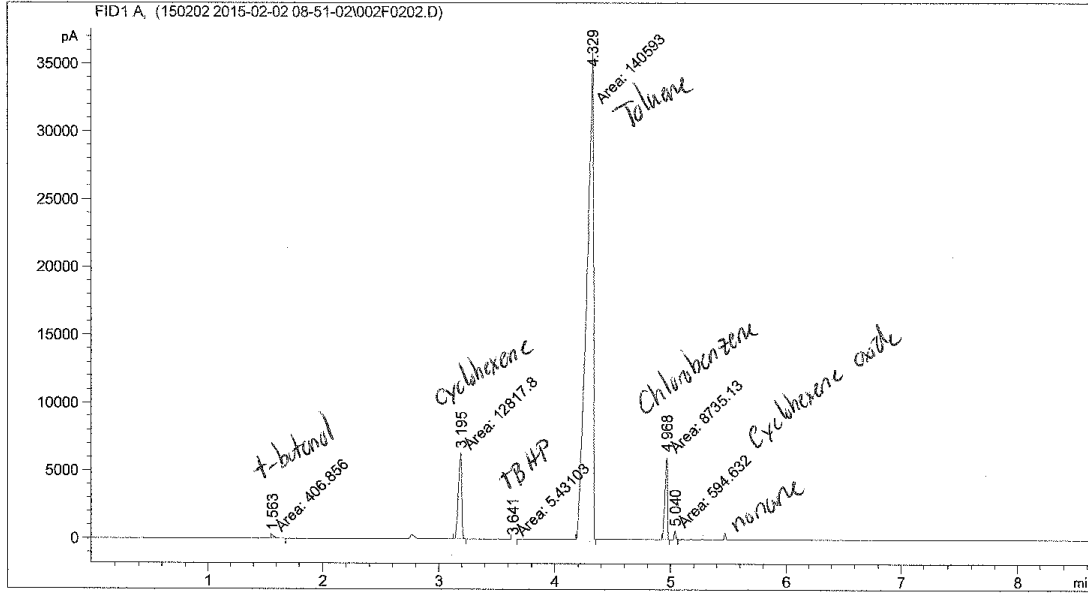


Figure A11. Typical GC chromatograph for epoxidation of cyclohexene (60 mmol) using TBHP (3 mmol) toluene as solvent, and chlorobenzene as internal standard and homogeneous catalysts (**9-10**, 0.02 mmol Ti) after 10 minutes (98 % conversion)

```

=====
Acq. Operator   :                               Seq. Line :    2
Acq. Instrument : 6890 GC                       Location  : Vial 2
Injection Date  : 2/2/2015 10:17:59 AM          Inj       :    2
                                                    Inj Volume: 1 µl
Acq. Method    : C:\CHEM32\2\DATA\150202 2015-02-02 08-51-02\TBHP.M
Last changed   : 12/1/2014 2:57:55 PM
Analysis Method: C:\CHEM32\2\METHODS\TBHP.M
Last changed   : 12/1/2014 2:57:55 PM
Additional Info: Peak(s) manually integrated
=====

```



Area Percent Report

```

=====
Sorted By      :      Signal
Multiplier:    :            1.0000
Dilution:      :            1.0000
Use Multiplier & Dilution Factor with ISTDs
=====

```

Signal 1: FID1 A,

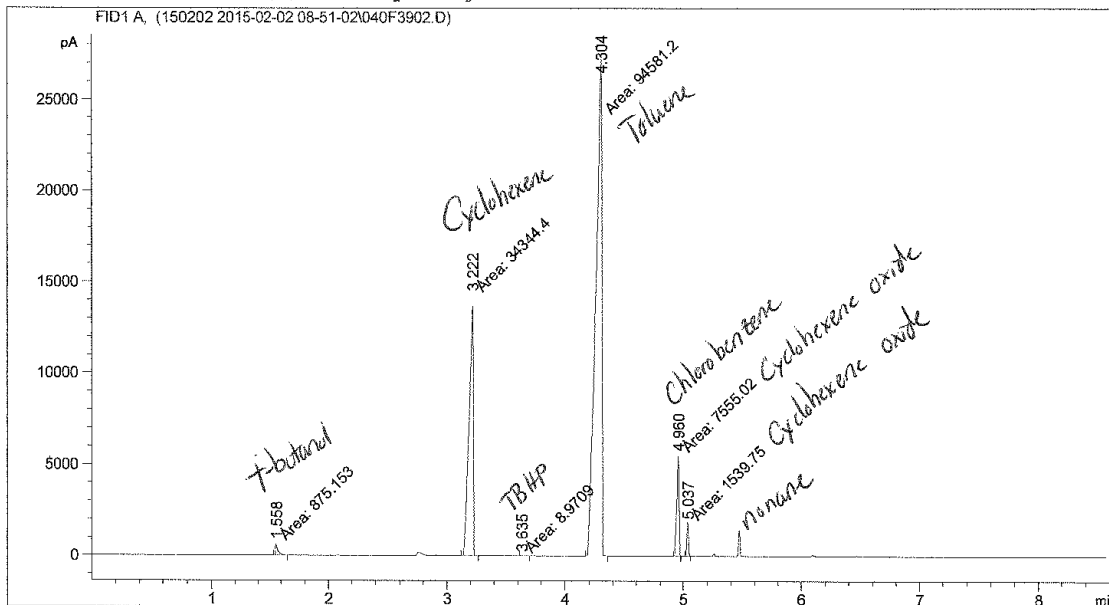
Peak #	RetTime [min]	Type	Width [min]	Area [pA*s]	Height [pA]	Area %
1	1.563	MM	0.0252	406.85599	268.85400	0.24937
2	3.195	MM	0.0336	1.28178e4	6362.04785	7.85635
3	3.641	MM	0.0306	5.43103	2.95645	0.00333
4	4.329	MM	0.0636	1.40593e5	3.68232e4	86.17253
5	4.968	MM	0.0237	8735.12793	6155.21338	5.35396
6	5.040	MM	0.0147	594.63214	673.46381	0.36446

Totals : 1.63153e5 5.02858e4

Figure A12. Typical GC chromatograph for epoxidation of cyclohexene (60 mmol) using TBHP (3 mmol) toluene as solvent, and chlorobenzene as internal standard and heterogeneous catalysts (**P1-8** or **c-P1-8**, 0.02 mmol Ti) after 12 hours (99 % conversion)

```

=====
Acq. Operator   :                               Seq. Line :   39
Acq. Instrument : 6890 GC                       Location  : Vial 40
Injection Date  : 2/3/2015 2:17:55 PM           Inj       :    2
                                                Inj Volume: 1 µl
Acq. Method    : C:\CHEM32\2\DATA\150202 2015-02-02 08-51-02\TBHP.M
Last changed   : 12/1/2014 2:57:55 PM
Analysis Method: C:\CHEM32\2\METHODS\TBHP.M
Last changed   : 12/1/2014 2:57:55 PM
Additional Info : Peak(s) manually integrated
=====
  
```



Area Percent Report

```

Sorted By      :      Signal
Multiplier:    :      1.0000
Dilution:      :      1.0000
Use Multiplier & Dilution Factor with ISTDs
  
```

Signal 1: FID1 A,

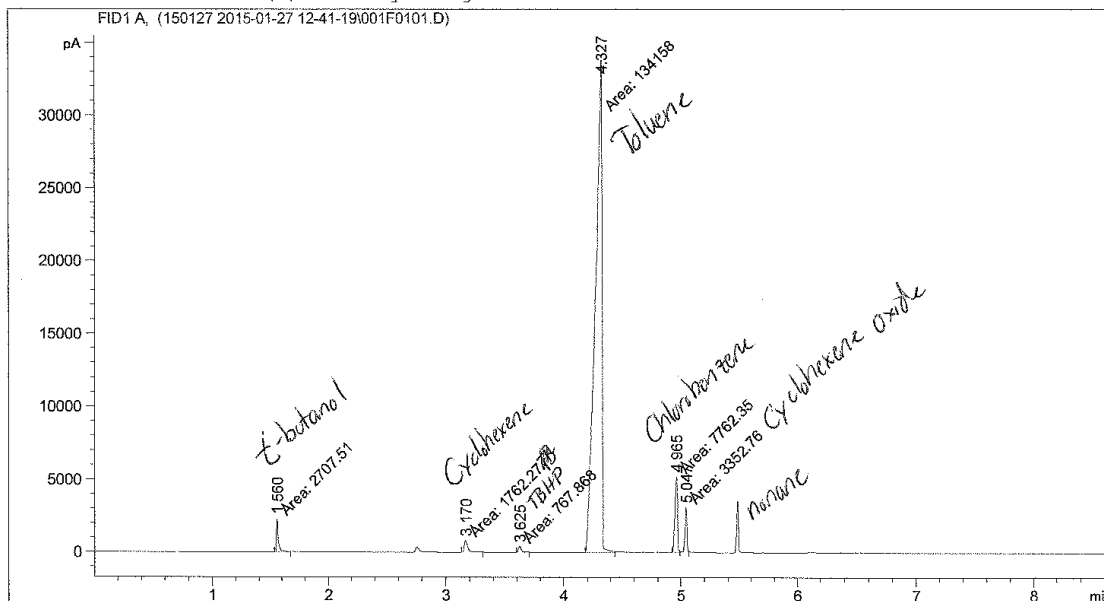
Peak #	RetTime [min]	Type	Width [min]	Area [pA*s]	Height [pA]	Area %
1	1.558	MM	0.0229	875.15338	635.86743	0.63004
2	3.222	MM	0.0401	3.43444e4	1.42757e4	24.72522
3	3.635	MM	0.0369	8.97090	4.04820	0.00646
4	4.304	MM	0.0563	9.45812e4	2.80179e4	68.09079
5	4.960	MM	0.0228	7555.02100	5533.92529	5.43900
6	5.037	MM	0.0143	1539.74915	1793.86768	1.10849

Totals : 1.38905e5 5.02613e4

Figure A13. Typical GC chromatograph for epoxidation of cyclohexene (3 mmol) using TBHP (3 mmol) toluene as solvent, and chlorobenzene as internal standard and heterogeneous catalysts (**9-10**, 0.02 mmol Ti) after 40 minutes (70 % conversion)

```

=====
Acq. Operator   :                               Seq. Line :    1
Acq. Instrument : 6890 GC                       Location  : Vial 1
Injection Date  : 1/27/2015 12:45:12 PM         Inj       :    1
                                                Inj Volume: 1 µl
Acq. Method    : C:\CHEM32\2\DATA\150127 2015-01-27 12-41-19\TBHP.M
Last changed   : 12/1/2014 2:57:55 PM
Analysis Method: C:\CHEM32\2\METHODS\TBHP.M
Last changed   : 12/1/2014 2:57:55 PM
Additional Info: Peak(s) manually integrated
=====
  
```



Area Percent Report

```

Sorted By      :      Signal
Multiplier:    :      1.0000
Dilution:      :      1.0000
Use Multiplier & Dilution Factor with ISTDs
  
```

Signal 1: FID1 A,

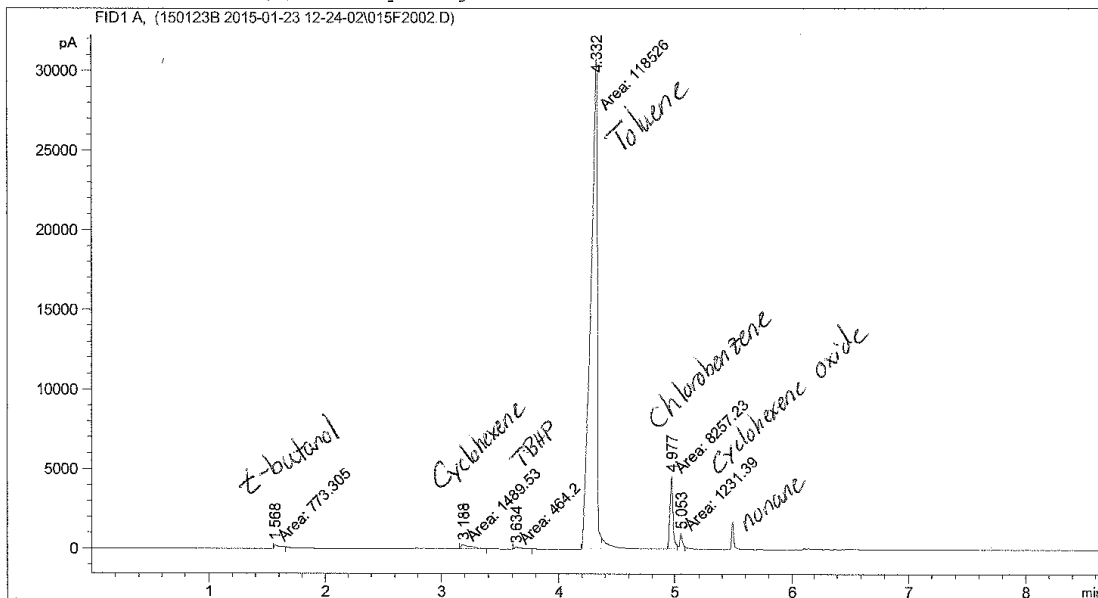
Peak #	RetTime [min]	Type	Width [min]	Area [pA*s]	Height [pA]	Area %
1	1.560	MM	0.0196	2707.51050	2299.04028	1.79888
2	3.170	MM	0.0357	1762.26587	822.81647	1.17085
3	3.625	MM	0.0319	767.86847	401.65683	0.51017
4	4.327	MM	0.0663	1.34158e5	3.37269e4	89.13519
5	4.965	MM	0.0247	7762.35107	5239.89648	5.15733
6	5.047	MM	0.0179	3352.75903	3114.09619	2.22758

Totals : 1.50511e5 4.56044e4

Figure A14. Typical GC chromatograph for epoxidation of cyclohexene (3 mmol) using TBHP (3 mmol) toluene as solvent, and chlorobenzene as internal standard and heterogeneous catalysts (**P1-8**, 0.02 mmol Ti) after 4 hours (70 % conversion)

```

=====
Acq. Operator   :                               Seq. Line :   20
Acq. Instrument : 6890 GC                       Location  : Vial 15
Injection Date  : 1/24/2015 3:16:07 AM          Inj       :    2
                                                    Inj Volume: 1 µl
Acq. Method     : C:\CHEM32\2\DATA\150123B 2015-01-23 12-24-02\TBHP.M
Last changed    : 12/1/2014 2:57:55 PM
Analysis Method : C:\CHEM32\2\DATA\150123 2015-01-23 08-48-07\TBHP.M
Last changed    : 12/1/2014 2:57:55 PM
Additional Info : Peak(s) manually integrated
=====
  
```



Area Percent Report

```

Sorted By      :      Signal
Multiplier:    :      1.0000
Dilution:      :      1.0000
Use Multiplier & Dilution Factor with ISTDs
  
```

Signal 1: FID1 A,

Peak #	RetTime [min]	Type	Width [min]	Area [pA*s]	Height [pA]	Area %
1	1.568	MM	0.0492	773.30542	261.96402	0.59147
2	3.188	MM	0.0901	1489.52856	275.68375	1.13929
3	3.634	MM	0.0699	464.19952	110.62763	0.35505
4	4.332	MM	0.0643	1.18526e5	3.07309e4	90.65667
5	4.977	MM	0.0302	8257.22656	4559.98779	6.31567
6	5.053	MM	0.0224	1231.38794	914.18347	0.94185

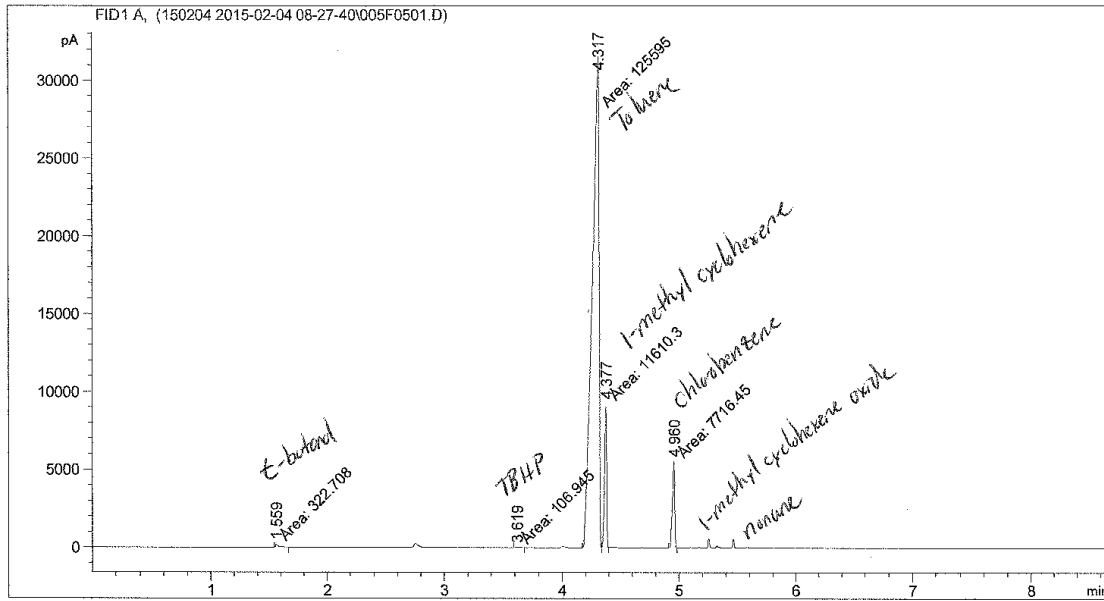
Totals : 1.30742e5 3.68534e4

Figure A15. Typical GC chromatograph for epoxidation of 1-methylcyclohexene (60 mmol) using TBHP (3 mmol) toluene as solvent, and chlorobenzene as internal standard and homogeneous catalysts (**9-10**, 0.02 mmol Ti) after 10 minutes (92 % conversion)

```

=====
Acq. Operator   :                               Seq. Line :    5
Acq. Instrument : 6890 GC                       Location  : Vial 5
Injection Date  : 2/4/2015 10:37:19 AM          Inj       :    1
                                                    Inj Volume: 1 µl

Acq. Method    : C:\CHEM32\2\DATA\150204 2015-02-04 08-27-40\TBHP.M
Last changed   : 12/1/2014 2:57:55 PM
Analysis Method : C:\CHEM32\2\METHODS\TBHP.M
Last changed   : 12/1/2014 2:57:55 PM
Additional Info : Peak(s) manually integrated
=====
  
```



Area Percent Report

```

Sorted By      :      Signal
Multiplier:    :      1.0000
Dilution:      :      1.0000
Use Multiplier & Dilution Factor with ISTDs
  
```

Signal 1: FID1 A,

Peak #	RetTime [min]	Type	Width [min]	Area [pA*s]	Height [pA]	Area %
1	1.559	MM	0.0239	322.70850	225.30055	0.22202
2	3.619	MM	0.0332	106.94548	53.74065	0.07358
3	4.317	MM	0.0643	1.25595e5	3.25673e4	86.40787
4	4.377	MM	0.0208	1.16103e4	9284.09375	7.98772
5	4.960	MM	0.0231	7716.44580	5577.90576	5.30882

Totals : 1.45351e5 4.77084e4

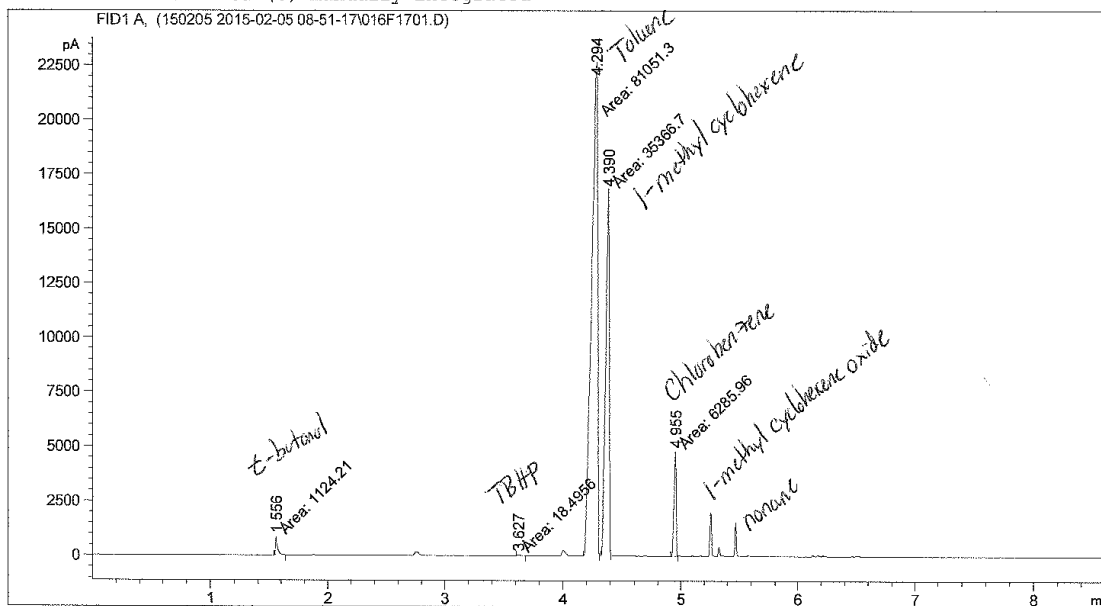


Figure A16. Typical GC chromatograph for epoxidation of 1-methylcyclohexene (60 mmol) using TBHP (3 mmol) toluene as solvent, and chlorobenzene as internal standard and heterogeneous catalysts (**P1-8** or **c-P1-8**, 0.02 mmol Ti) after 4 hours (98 % conversion)

```

=====
Acq. Operator   :                               Seq. Line : 17
Acq. Instrument : 6890 GC                       Location  : Vial 16
Injection Date  : 2/6/2015 12:48:24 AM         Inj       : 1
                                                    Inj Volume: 1 µl
Acq. Method    : C:\CHEM32\2\DATA\150205 2015-02-05 08-51-17\TBHP.M
Last changed   : 12/1/2014 2:57:55 PM
Analysis Method: C:\CHEM32\2\METHODS\TBHP.M
Last changed   : 12/1/2014 2:57:55 PM
Additional Info: Peak(s) manually integrated
=====

```



Area Percent Report

```

=====
Sorted By      :      Signal
Multiplier:    :      1.0000
Dilution:      :      1.0000
Use Multiplier & Dilution Factor with ISTDs
=====

```

Signal 1: FID1 A,

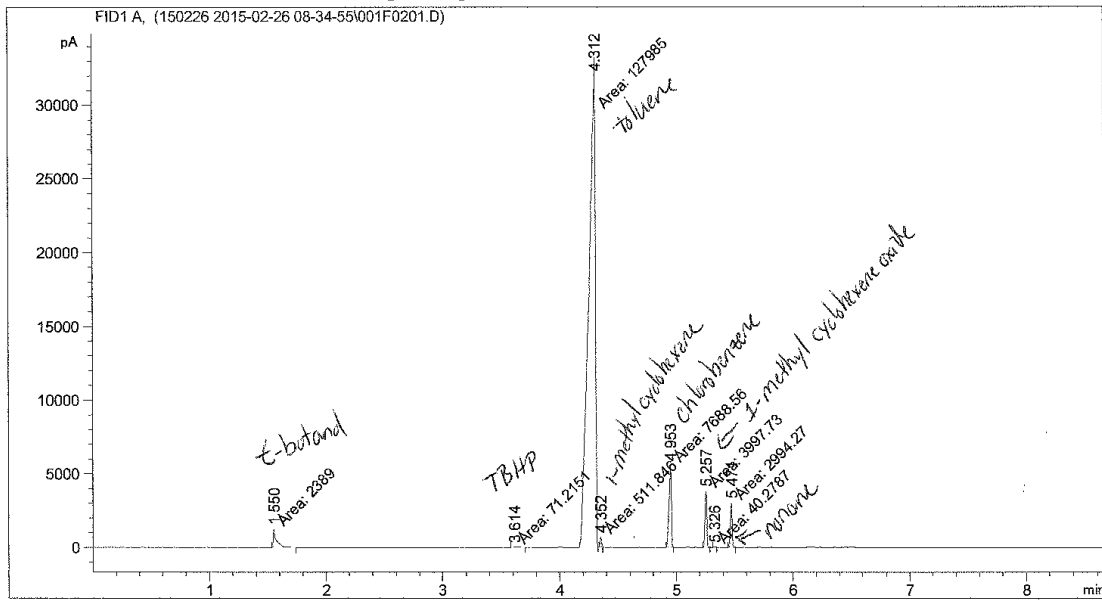
Peak #	RetTime [min]	Type	Width [min]	Area [pA*s]	Height [pA]	Area %
1	1.556	MM	0.0225	1124.21155	831.65948	0.90774
2	3.627	MM	0.0317	18.49557	9.71806	0.01493
3	4.294	MM	0.0598	8.10513e4	2.26045e4	65.44487
4	4.390	MM	0.0352	3.53667e4	1.67484e4	28.55686
5	4.955	MM	0.0218	6285.96045	4815.01416	5.07560

Totals : 1.23847e5 4.50093e4

Figure A17. Typical GC chromatograph for epoxidation of 1-methylcyclohexene (3 mmol) using TBHP (3 mmol) toluene as solvent, and chlorobenzene as internal standard and homogeneous catalysts (**10**, 0.02 mmol Ti) after 14 hours (85 % conversion)

```

=====
Acq. Operator   :                               Seq. Line :    2
Acq. Instrument : 6890 GC                       Location  : Vial 1
Injection Date  : 2/26/2015 9:19:33 AM          Inj       :    1
                                                    Inj Volume: 1 µl
Acq. Method    : C:\CHEM32\2\DATA\150226 2015-02-26 08-34-55\TBHP.M
Last changed   : 12/1/2014 2:57:55 PM
Analysis Method: C:\CHEM32\2\DATA\150224 2015-02-24 08-27-48\TBHP.M
Last changed   : 12/1/2014 2:57:55 PM
Additional Info : Peak(s) manually integrated
=====
  
```



Area Percent Report

```

Sorted By      :      Signal
Multiplier:    :      1.0000
Dilution:      :      1.0000
Use Multiplier & Dilution Factor with ISTDs
  
```

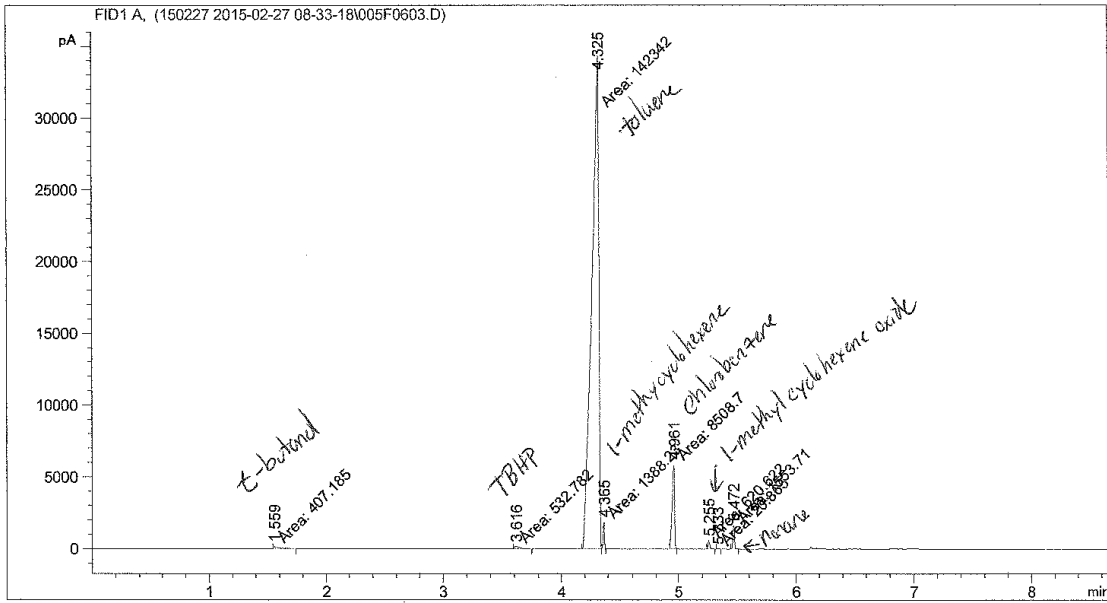
Signal 1: FID1 A,

Peak #	RetTime [min]	Type	Width [min]	Area [pA*s]	Height [pA]	Area %
1	1.550	MM	0.0322	2389.00488	1235.81775	1.63992
2	3.614	MM	0.0486	71.21512	24.41350	0.04889
3	4.312	MM	0.0615	1.27985e5	3.47020e4	87.85481
4	4.352	MM	0.0123	511.84570	695.33081	0.35135
5	4.953	MM	0.0230	7688.56055	5583.46875	5.27777
6	5.257	MM	0.0173	3997.72729	3862.30542	2.74422
7	5.326	MM	0.0152	40.27872	44.02626	0.02765
8	5.471	MM	0.0164	2994.27295	3039.36646	2.05540

Figure A18. Typical GC chromatograph for epoxidation of 1-methylcyclohexene (3 mmol) using TBHP (3 mmol) toluene as solvent, and chlorobenzene as internal standard and heterogeneous catalysts (**P1-8**, 0.02 mmol Ti) after 20 hours (60 % conversion)

```

=====
Acq. Operator   :                               Seq. Line :    6
Acq. Instrument : 6890 GC                       Location  : Vial 5
Injection Date  : 2/27/2015 1:51:55 PM         Inj       :    3
                                                Inj Volume: 1 µl
Acq. Method    : C:\CHEM32\2\DATA\150227 2015-02-27 08-33-18\TBHP.M
Last changed   : 12/1/2014 2:57:55 PM
Analysis Method: C:\CHEM32\2\DATA\150224 2015-02-24 08-27-48\TBHP.M
Last changed   : 12/1/2014 2:57:55 PM
Additional Info: Peak(s) manually integrated
=====
    
```



Area Percent Report

```

Sorted By      :      Signal
Multiplier:    :      1.0000
Dilution:      :      1.0000
Use Multiplier & Dilution Factor with ISTDs
    
```

Signal 1: FID1 A,

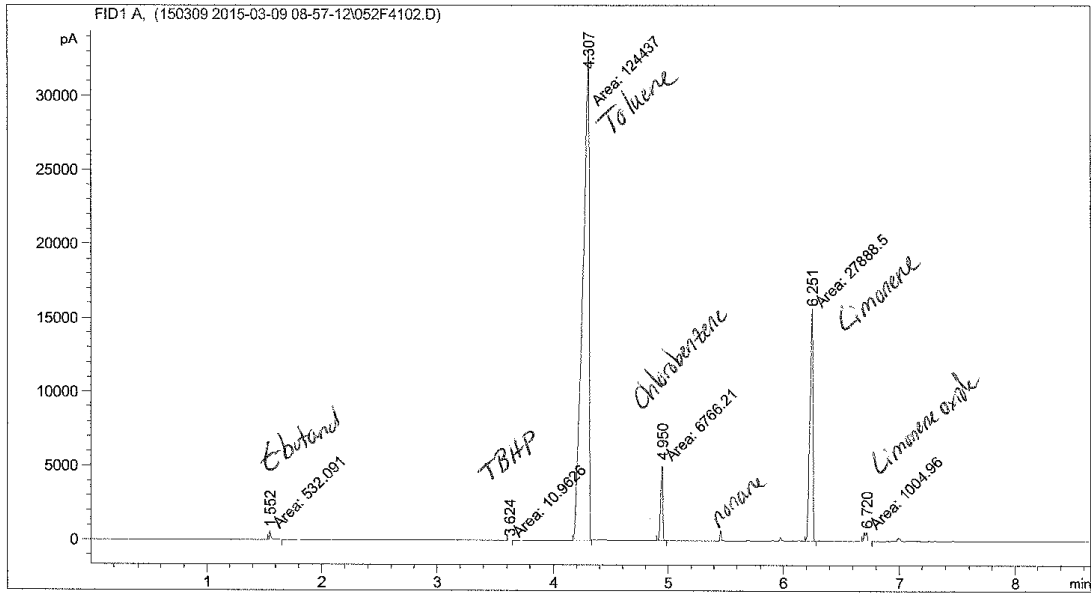
Peak #	RetTime [min]	Type	Width [min]	Area [pA*s]	Height [pA]	Area %
1	1.559	MM	0.0398	407.18518	170.66064	0.26207
2	3.616	MM	0.0485	532.78241	183.08849	0.34290
3	4.325	MM	0.0690	1.42342e5	3.43873e4	91.61247
4	4.365	MM	0.0124	1388.22778	1867.18457	0.89347
5	4.961	MM	0.0238	8508.69629	5958.97949	5.47625
6	5.255	MM	0.0174	620.62183	594.11176	0.39944
7	5.333	MM	0.0174	20.86496	19.94396	0.01343
8	5.472	MM	0.0159	1553.71375	1630.17102	0.99998

Figure A19. Typical GC chromatograph for epoxidation of limonene (60 mmol) using TBHP (3 mmol) toluene as solvent, and chlorobenzene as internal standard and homogeneous catalysts (**9-10**, 0.02 mmol Ti) after 10 minutes (98 % conversion)

```

=====
Acq. Operator   :                               Seq. Line :   41
Acq. Instrument : 6890 GC                       Location  : Vial 52
Injection Date  : 3/10/2015 3:31:36 PM          Inj       :    2
                                                    Inj Volume: 1 µl

Acq. Method    : C:\CHEM32\2\DATA\150309 2015-03-09 08-57-12\TBHP.M
Last changed   : 12/1/2014 2:57:55 PM
Analysis Method: C:\CHEM32\2\DATA\150224 2015-02-24 08-27-48\TBHP.M
Last changed   : 12/1/2014 2:57:55 PM
Additional Info: Peak(s) manually integrated
=====
  
```



Area Percent Report

```

Sorted By      :      Signal
Multiplier:    :      1.0000
Dilution:      :      1.0000
Use Multiplier & Dilution Factor with ISTDs
  
```

Signal 1: FID1 A,

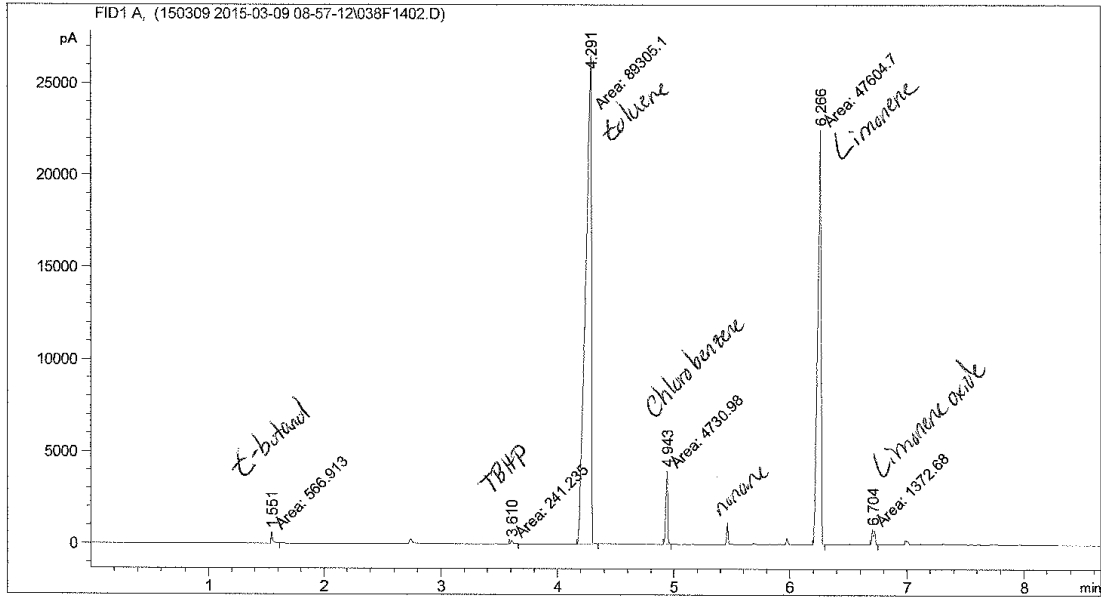
Peak #	RetTime [min]	Type	Width [min]	Area [pA*s]	Height [pA]	Area %
1	1.552	MM	0.0160	532.09076	555.88055	0.33123
2	3.624	MM	0.0296	10.96264	6.16746	0.00682
3	4.307	MM	0.0633	1.24437e5	3.27494e4	77.46342
4	4.950	MM	0.0219	6766.21094	5155.26221	4.21204
5	6.251	MM	0.0299	2.78885e4	1.55612e4	17.36089
6	6.720	MM	0.0284	1004.95746	588.91345	0.62560

Totals : 1.60640e5 5.46168e4

Figure A20. Typical GC chromatograph for epoxidation of limonene (60 mmol) using TBHP (3 mmol) toluene as solvent, and chlorobenzene as internal standard and heterogeneous catalysts (**P1-8** or **c-P1-8**, 0.02 mmol Ti) after 6.5 hours (70 % conversion)

```

=====
Acq. Operator   :                               Seq. Line :   14
Acq. Instrument : 6890 GC                       Location  : Vial 38
Injection Date  : 3/9/2015 10:06:44 PM         Inj       :    2
                                                Inj Volume: 1 µl
Acq. Method    : C:\CHEM32\2\DATA\150309 2015-03-09 08-57-12\TBHP.M
Last changed   : 12/1/2014 2:57:55 PM
Analysis Method: C:\CHEM32\2\DATA\150224 2015-02-24 08-27-48\TBHP.M
Last changed   : 12/1/2014 2:57:55 PM
Additional Info: Peak(s) manually integrated
=====
  
```



Area Percent Report

```

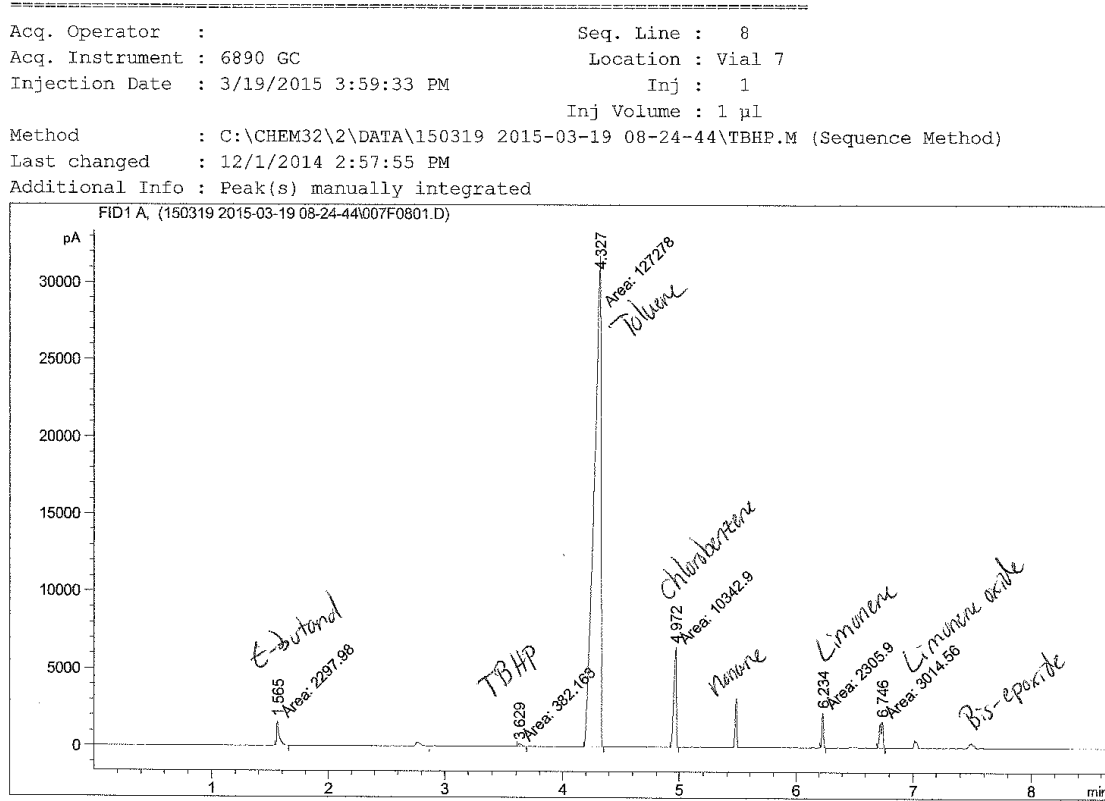
Sorted By      :      Signal
Multiplier:    :      1.0000
Dilution:      :      1.0000
Use Multiplier & Dilution Factor with ISTDs
  
```

Signal 1: FID1 A,

Peak #	RetTime [min]	Type	Width [min]	Area [pA*s]	Height [pA]	Area %
1	1.551	MM	0.0156	566.91339	604.08936	0.39418
2	3.610	MM	0.0233	241.23541	172.76477	0.16773
3	4.291	MM	0.0560	8.93051e4	2.65751e4	62.09437
4	4.943	MM	0.0197	4730.97949	3995.99414	3.28948
5	6.266	MM	0.0352	4.76047e4	2.25096e4	33.09981
6	6.704	MM	0.0276	1372.68359	829.05554	0.95443

Totals : 1.43822e5 5.46866e4

Figure A21. Typical GC chromatograph for epoxidation of limonene (3 mmol) using TBHP (3 mmol) toluene as solvent, and chlorobenzene as internal standard and homogeneous catalysts (**10**, 0.02 mmol Ti) after 10 minutes (71 % conversion)



Area Percent Report

```

Sorted By      :      Signal
Multiplier:    :      1.0000
Dilution:      :      1.0000
Use Multiplier & Dilution Factor with ISTDs

```

Signal 1: FID1 A,

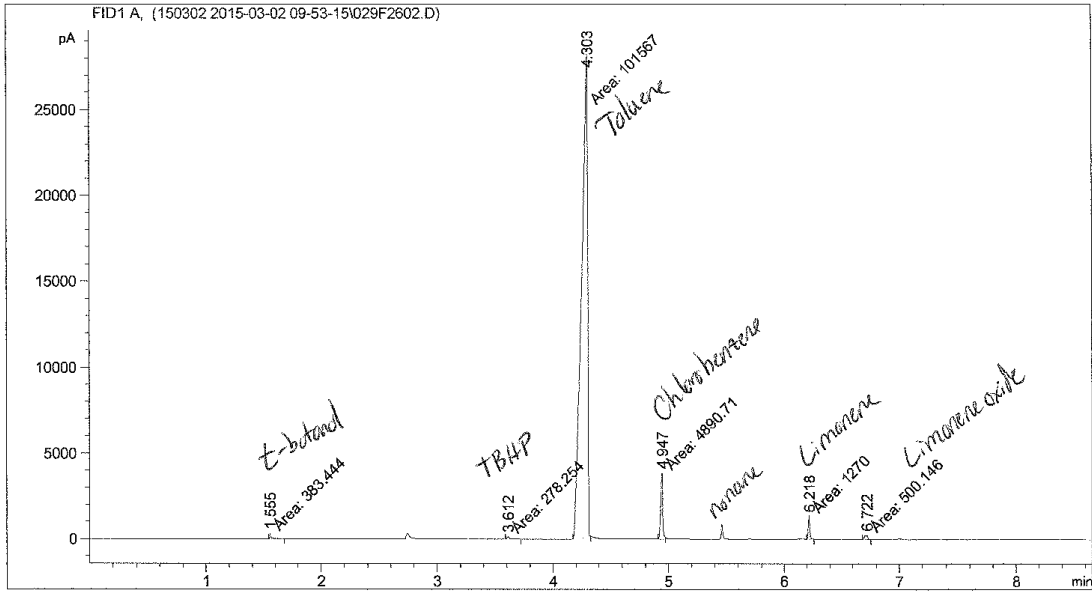
Peak #	RetTime [min]	Type	Width [min]	Area [pA*s]	Height [pA]	Area %
1	1.565	MM	0.0237	2297.97583	1616.13123	1.57804
2	3.629	MM	0.0361	382.16306	176.61072	0.26244
3	4.327	MM	0.0658	1.27278e5	3.22523e4	87.40329
4	4.972	MM	0.0264	1.03429e4	6535.31299	7.10261
5	6.234	MM	0.0162	2305.90332	2368.26929	1.58349
6	6.746	MM	0.0290	3014.56421	1732.97498	2.07013

Totals : 1.45622e5 4.46816e4

Figure A22. Typical GC chromatograph for epoxidation of limonene (3 mmol) using TBHP (3 mmol) toluene as solvent, and chlorobenzene as internal standard and heterogeneous catalysts (**P1-8**, 0.02 mmol Ti) after 30 hours (50 % conversion)

```

=====
Acq. Operator   :                               Seq. Line :   26
Acq. Instrument : 6890 GC                       Location  : Vial 29
Injection Date  : 3/3/2015 2:37:04 AM           Inj       :    2
                                                Inj Volume: 1 µl
Acq. Method    : C:\CHEM32\2\DATA\150302 2015-03-02 09-53-15\TBHP.M
Last changed   : 12/1/2014 2:57:55 PM
Analysis Method: C:\CHEM32\2\DATA\150224 2015-02-24 08-27-48\TBHP.M
Last changed   : 12/1/2014 2:57:55 PM
Additional Info: Peak(s) manually integrated
=====
  
```



Area Percent Report

```

Sorted By      :      Signal
Multiplier:    :      1.0000
Dilution:      :      1.0000
Use Multiplier & Dilution Factor with ISTDs
  
```

Signal 1: FID1 A,

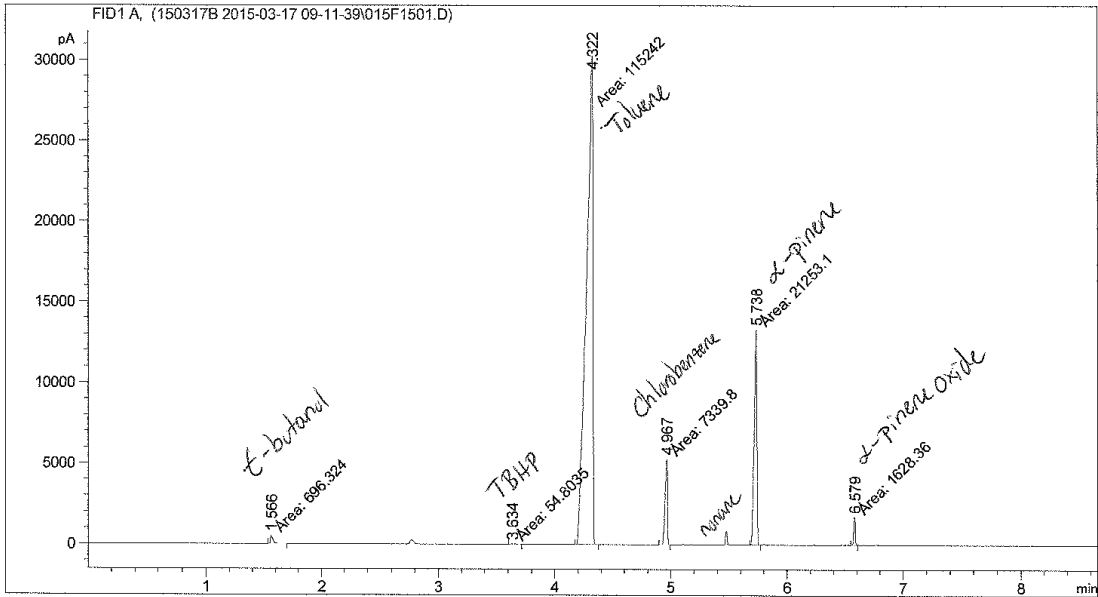
Peak #	RetTime [min]	Type	Width [min]	Area [pA*s]	Height [pA]	Area %
1	1.555	MM	0.0203	383.44434	314.48154	0.35214
2	3.612	MM	0.0326	278.25385	142.38383	0.25554
3	4.303	MM	0.0589	1.01567e5	2.87548e4	93.27526
4	4.947	MM	0.0210	4890.70801	3890.29126	4.49143
5	6.218	MM	0.0155	1270.00012	1363.39795	1.16632
6	6.722	MM	0.0316	500.14587	264.02927	0.45931

Totals : 1.08890e5 3.47293e4

Figure A23. Typical GC chromatograph for epoxidation of  $\alpha$ -pinene (60 mmol) using TBHP (3 mmol) toluene as solvent, and chlorobenzene as internal standard and homogeneous catalysts (**9-10**, 0.02 mmol Ti) after 10 minutes (90 % conversion)

```

=====
Acq. Operator   :                               Seq. Line :   15
Acq. Instrument : 6890 GC                       Location  : Vial 15
Injection Date  : 3/17/2015 3:36:54 PM          Inj       :    1
                                                    Inj Volume: 1  $\mu$ l
Acq. Method    : C:\CHEM32\2\DATA\150317B 2015-03-17 09-11-39\TBHP.M
Last changed   : 12/1/2014 2:57:55 PM
Analysis Method: C:\CHEM32\2\DATA\150224 2015-02-24 08-27-48\TBHP.M
Last changed   : 3/12/2015 2:09:17 PM
                (modified after loading)
Additional Info : Peak(s) manually integrated
=====
  
```



Area Percent Report

```

Sorted By      :      Signal
Multiplier:    :      1.0000
Dilution:      :      1.0000
Use Multiplier & Dilution Factor with ISTDs
  
```

Signal 1: FID1 A,

Peak #	RetTime [min]	Type	Width [min]	Area [pA*s]	Height [pA]	Area %
1	1.566	MM	0.0234	696.32446	494.90964	0.47624
2	3.634	MM	0.0282	54.80348	32.40728	0.03748
3	4.322	MM	0.0634	1.15242e5	3.02720e4	78.81711
4	4.967	MM	0.0230	7339.79639	5309.22949	5.01989
5	5.738	MM	0.0266	2.12531e4	1.33302e4	14.53560
6	6.579	MM	0.0156	1628.36292	1742.57678	1.11368



Figure A24. Typical GC chromatograph for epoxidation of  $\alpha$ -pinene (60 mmol) using TBHP (3 mmol) toluene as solvent, and chlorobenzene as internal standard and homogeneous catalysts (**P1-8** or **c-P1-8**, 0.02 mmol Ti) after 4 hours (76 % conversion)

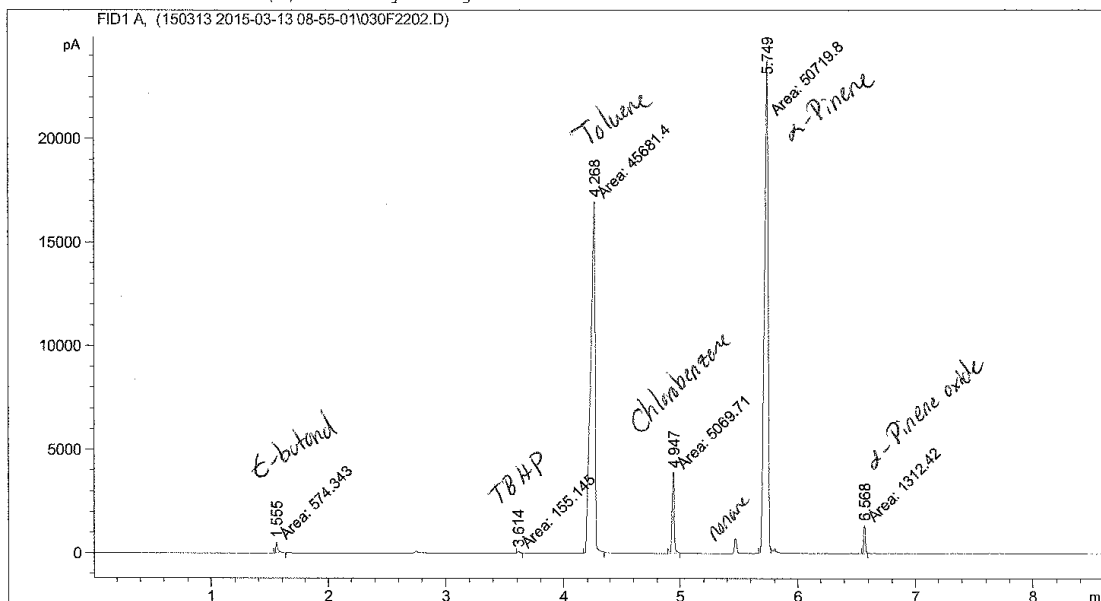
```

=====
Acq. Operator   :                               Seq. Line : 22
Acq. Instrument : 6890 GC                       Location  : Vial 30
Injection Date  : 3/13/2015 11:16:43 PM        Inj       : 2
                                                    Inj Volume: 1  $\mu$ l

Acq. Method    : C:\CHEM32\2\DATA\150313 2015-03-13 08-55-01\TBHP.M
Last changed   : 12/1/2014 2:57:55 PM
Analysis Method: C:\CHEM32\2\DATA\150224 2015-02-24 08-27-48\TBHP.M
Last changed   : 3/12/2015 2:09:17 PM
                (modified after loading)

Additional Info : Peak(s) manually integrated
=====

```



Area Percent Report

```

=====
Sorted By      :      Signal
Multiplier:    :      1.0000
Dilution:      :      1.0000
Use Multiplier & Dilution Factor with ISTDs
=====

```

Signal 1: FID1 A,

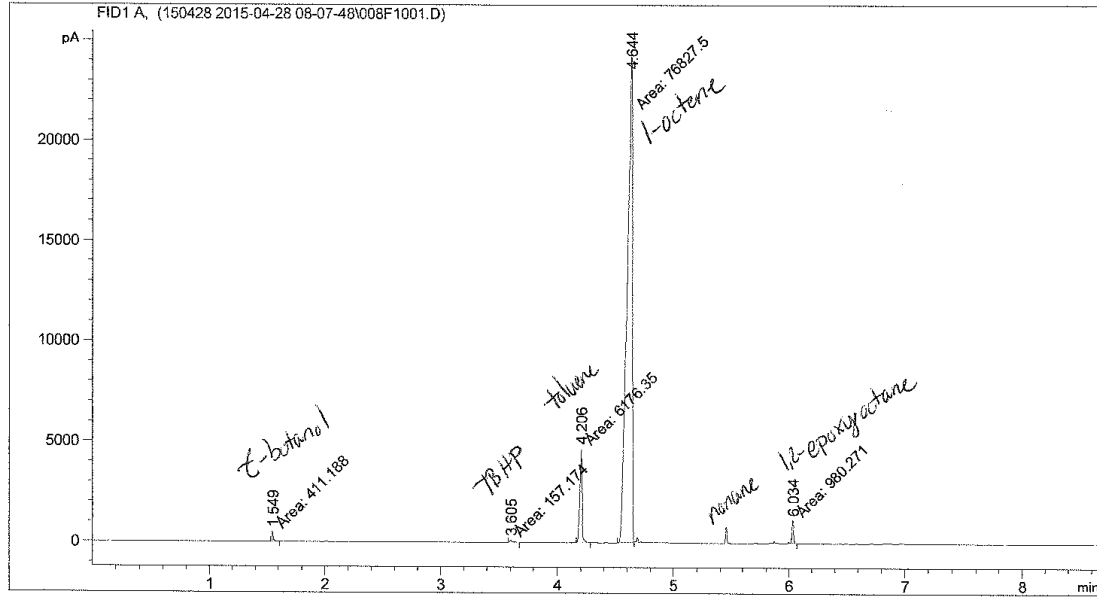
Peak #	RetTime [min]	Type	Width [min]	Area [pA*s]	Height [pA]	Area %
1	1.555	MM	0.0189	574.34326	506.76529	0.55485
2	3.614	MM	0.0261	155.14526	98.97945	0.14988
3	4.268	MM	0.0449	4.56814e4	1.69702e4	44.13118
4	4.947	MM	0.0216	5069.70996	3916.72974	4.89766
5	5.749	MM	0.0356	5.07198e4	2.37235e4	48.99854
6	6.568	MM	0.0156	1312.42224	1397.94324	1.26788



Figure A26. Typical GC chromatograph for epoxidation of 1-octene (60 mmol) using TBHP (3 mmol) toluene as internal standard and heterogeneous catalysts (**P1-8** or **c-P1-8**, 0.02 mmol Ti) after 12 hours (70 % conversion) at 60 °C

```

=====
Acq. Operator   :                               Seq. Line : 10
Acq. Instrument : 6890 GC                       Location  : Vial 8
Injection Date  : 4/28/2015 5:21:26 PM         Inj       : 1
                                                Inj Volume: 1 µl
Acq. Method    : C:\CHEM32\2\DATA\150428 2015-04-28 08-07-48\TBHP.M
Last changed   : 3/30/2015 9:26:59 AM
Analysis Method: C:\CHEM32\2\DATA\150406 2015-04-06 08-54-45\TBHP.M
Last changed   : 3/30/2015 9:26:59 AM
Additional Info: Peak(s) manually integrated
=====
  
```



Area Percent Report

```

Sorted By      :      Signal
Multiplier:    :      1.0000
Dilution:      :      1.0000
Use Multiplier & Dilution Factor with ISTDs
  
```

Signal 1: FID1 A,

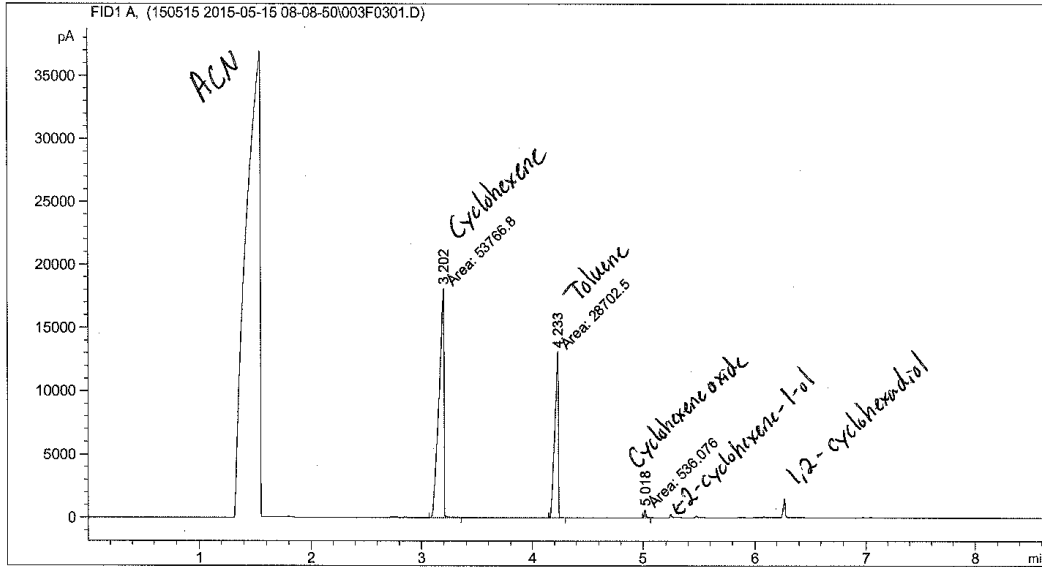
Peak #	RetTime [min]	Type	Width [min]	Area [pA*s]	Height [pA]	Area %
1	1.549	MM	0.0140	411.18768	491.24530	0.48631
2	3.605	MM	0.0208	157.17450	126.15002	0.18589
3	4.206	MM	0.0219	6176.35156	4703.08740	7.30475
4	4.644	MM	0.0512	7.68275e4	2.50212e4	90.86368
5	6.034	MM	0.0141	980.27063	1162.82410	1.15936

Totals : 8.45525e4 3.15045e4

Figure A27. Typical GC chromatograph for epoxidation of cyclohexene (45 mmol) using H<sub>2</sub>O<sub>2</sub> (2 mmol) toluene as internal standard, ACN as solvent and heterogeneous catalyst (c-P1-8, 0.02 mmol Ti) at 12 hours (100 % conversion H<sub>2</sub>O<sub>2</sub>) at 60 °C

```

=====
Acq. Operator   :                               Seq. Line :    3
Acq. Instrument : 6890 GC                       Location  : Vial 3
Injection Date  : 5/15/2015 10:17:19 AM         Inj       :    1
                                                Inj Volume: 1 µl
Acq. Method    : C:\CHEM32\2\DATA\150515 2015-05-15 08-08-50\TBHP.M
Last changed   : 5/13/2015 10:50:36 AM
Analysis Method: C:\CHEM32\2\DATA\150406 2015-04-06 08-54-45\TBHP.M
Last changed   : 5/15/2015 8:41:31 AM
                (modified after loading)
Additional Info : Peak(s) manually integrated
    
```



Area Percent Report

```

Sorted By      :      Signal
Multiplier:    :      1.0000
Dilution:      :      1.0000
Use Multiplier & Dilution Factor with ISTDs
    
```

Signal 1: FID1 A,

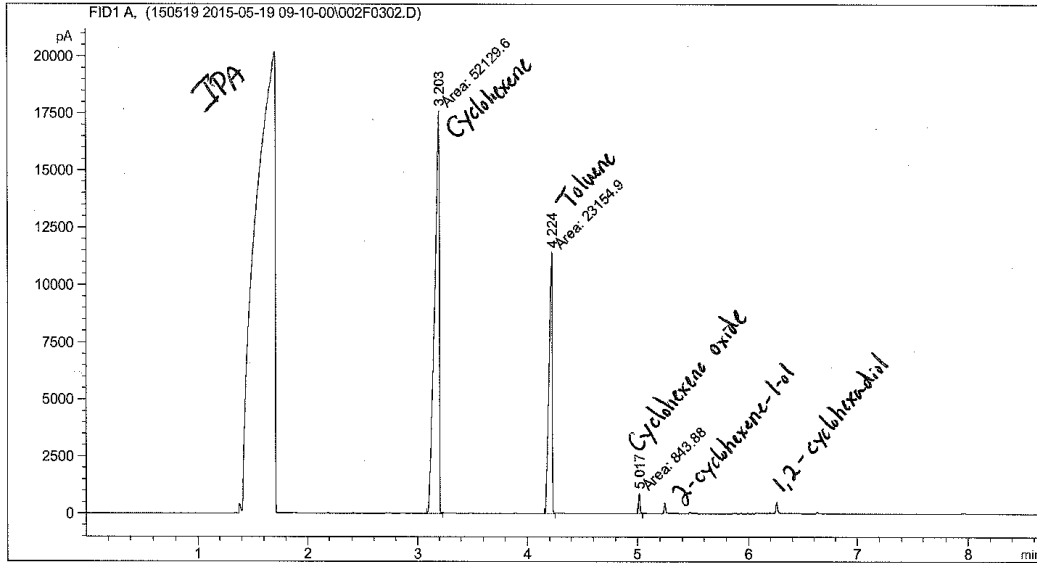
Peak #	RetTime [min]	Type	Width [min]	Area [pA*s]	Height [pA]	Area %
1	3.202	MM	0.0495	5.37668e4	1.80990e4	64.77505
2	4.233	MM	0.0365	2.87025e4	1.31104e4	34.57912
3	5.018	MM	0.0158	536.07574	566.22382	0.64583

Totals : 8.30054e4 3.17757e4

Figure A28. Typical GC chromatograph for epoxidation of cyclohexene (45 mmol) using H<sub>2</sub>O<sub>2</sub> (2 mmol) toluene as internal standard, IPA as solvent and heterogeneous catalyst (c-P1-8, 0.02 mmol Ti) at 12 hours (100 % conversion H<sub>2</sub>O<sub>2</sub>) at 60 °C

```

=====
Acq. Operator   :                               Seq. Line :    3
Acq. Instrument : 6890 GC                       Location  : Vial 2
Injection Date  : 5/19/2015 10:37:06 AM         Inj       :    2
                                                Inj Volume: 1 µl
Acq. Method    : C:\CHEM32\2\DATA\150519 2015-05-19 09-10-00\TBHP.M
Last changed   : 5/13/2015 10:50:36 AM
Analysis Method: C:\CHEM32\2\DATA\150406 2015-04-06 08-54-45\TBHP.M
Last changed   : 5/15/2015 8:41:31 AM
                (modified after loading)
Additional Info : Peak(s) manually integrated
    
```



Area Percent Report

```

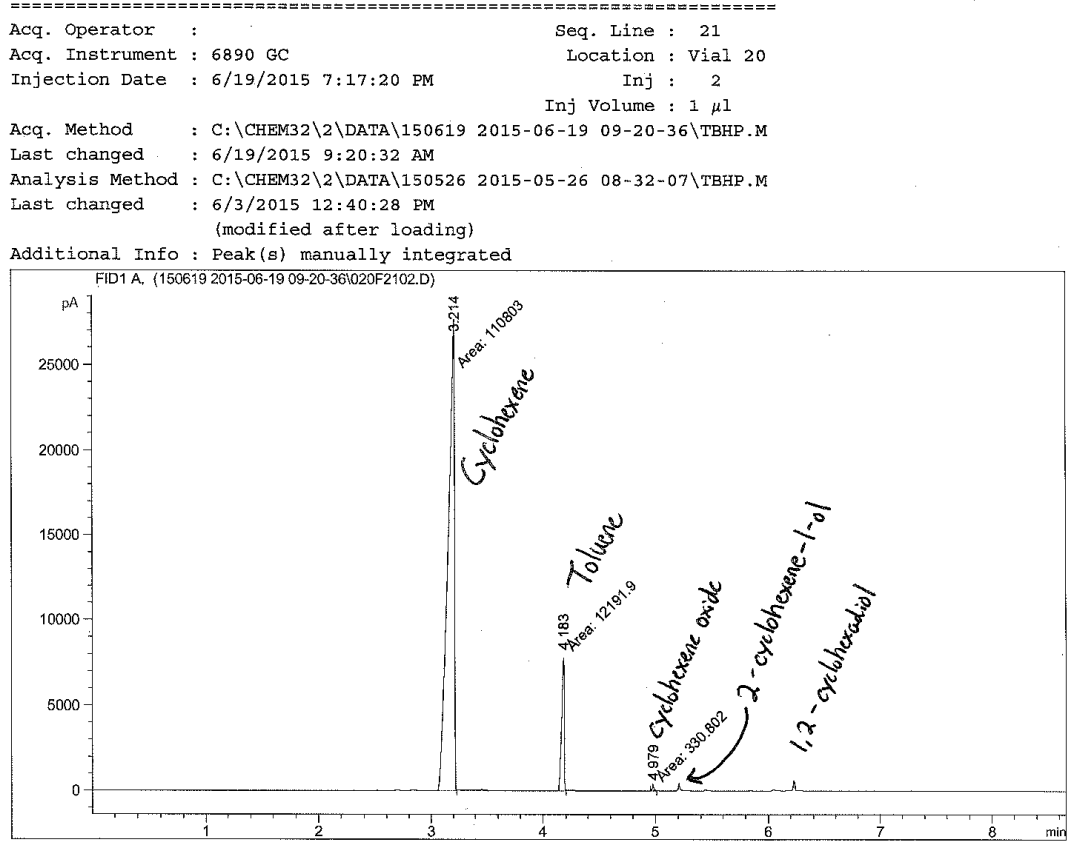
Sorted By      :      Signal
Multiplier:    :      1.0000
Dilution:      :      1.0000
Use Multiplier & Dilution Factor with ISTDs
    
```

Signal 1: FID1 A,

Peak #	RetTime [min]	Type	Width [min]	Area [pA*s]	Height [pA]	Area %
1	3.203	MM	0.0492	5.21296e4	1.76418e4	68.47589
2	4.224	MM	0.0337	2.31549e4	1.14520e4	30.41561
3	5.017	MM	0.0157	843.88037	896.00861	1.10850

Totals : 7.61284e4 2.99898e4

Figure A29. Typical GC chromatograph for epoxidation of cyclohexene (>45 mmol) using H<sub>2</sub>O<sub>2</sub> (2 mmol) toluene as internal standard, and heterogeneous catalyst (**c-P1-8**, 0.02 mmol Ti) at 5 hours (60 % conversion H<sub>2</sub>O<sub>2</sub>) at 60 °C



Area Percent Report

```

Sorted By      :      Signal
Multiplier:    :      1.0000
Dilution:      :      1.0000
Use Multiplier & Dilution Factor with ISTDs
    
```

Signal 1: FID1 A,

Peak #	RetTime [min]	Type	Width [min]	Area [pA*s]	Height [pA]	Area %
1	3.214	MM	0.0645	1.10803e5	2.86435e4	89.84585
2	4.183	MM	0.0253	1.21919e4	8028.92627	9.88592
3	4.979	MM	0.0156	330.80206	353.03146	0.26823

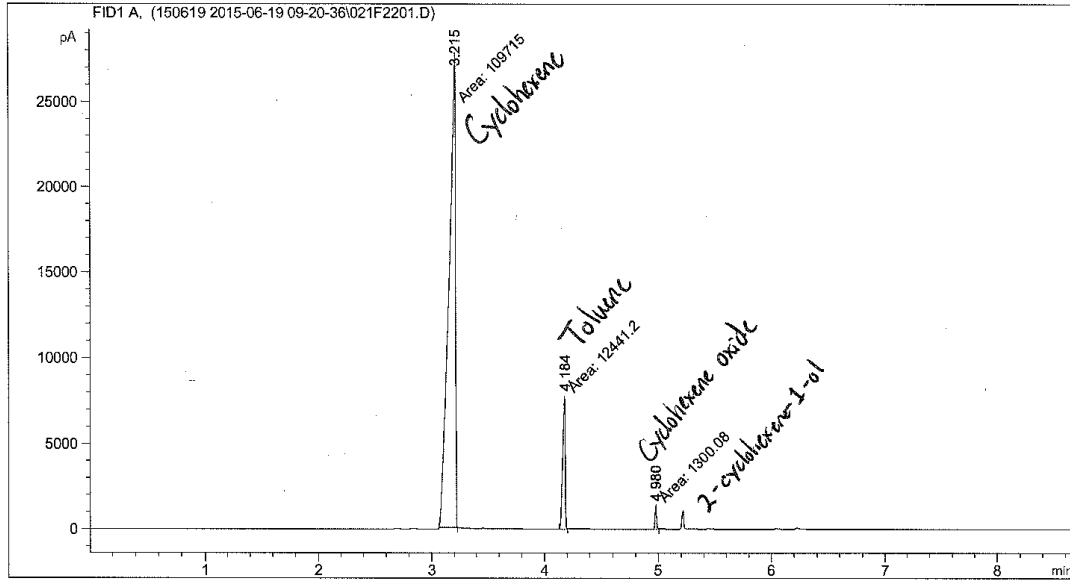
Totals :                    1.23326e5  3.70254e4

Figure A30. Typical GC chromatograph for epoxidation of cyclohexene (>45 mmol) using H<sub>2</sub>O<sub>2</sub> (2 mmol) toluene as internal standard, and heterogeneous catalyst (**c-P1-8**, 0.02 mmol Ti) at 12 hours (100 % conversion H<sub>2</sub>O<sub>2</sub>) at 60 °C

```

=====
Acq. Operator   :                               Seq. Line : 22
Acq. Instrument : 6890 GC                       Location  : Vial 21
Injection Date  : 6/19/2015 8:00:02 PM          Inj       : 1
                                                Inj Volume: 1 µl

Acq. Method    : C:\CHEM32\2\DATA\150619 2015-06-19 09-20-36\TBHP.M
Last changed   : 6/19/2015 9:20:32 AM
Analysis Method: C:\CHEM32\2\DATA\150526 2015-05-26 08-32-07\TBHP.M
Last changed   : 6/3/2015 12:40:28 PM
                (modified after loading)
Additional Info : Peak(s) manually integrated
    
```



=====  
 Area Percent Report  
 =====

```

Sorted By      :      Signal
Multiplier:    :      1.0000
Dilution:      :      1.0000
Use Multiplier & Dilution Factor with ISTDs
    
```

Signal 1: FID1 A,

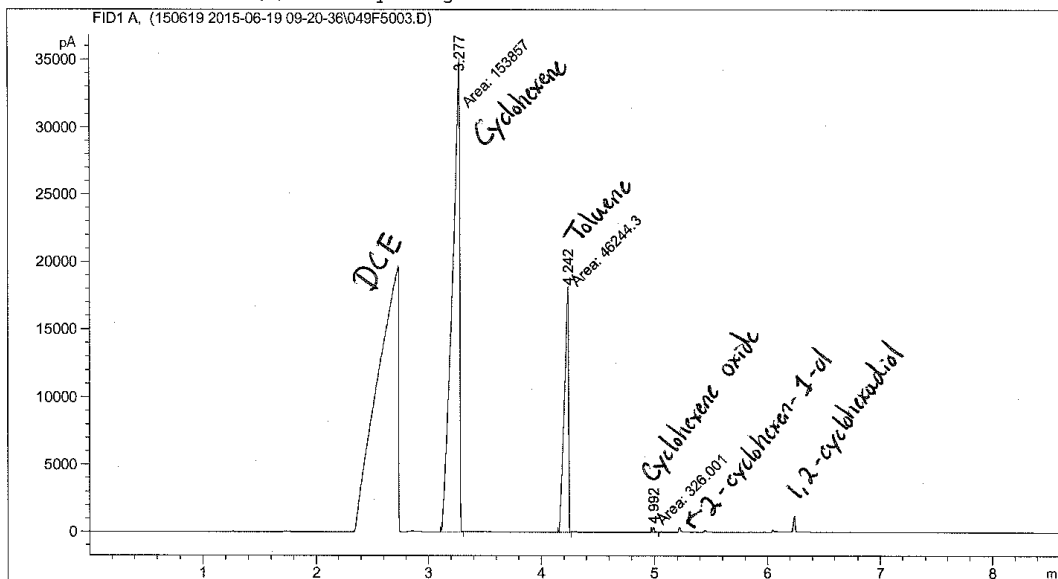
Peak #	RetTime [min]	Type	Width [min]	Area [pA*s]	Height [pA]	Area %
1	3.215	MM	0.0662	1.09715e5	2.76254e4	88.86957
2	4.184	MM	0.0264	1.24412e4	7857.39795	10.07737
3	4.980	MM	0.0153	1300.07788	1412.40259	1.05307
Totals :				1.23456e5	3.68952e4	

Figure A31. Typical GC chromatograph for epoxidation of cyclohexene (>45 mmol) using H<sub>2</sub>O<sub>2</sub> (2 mmol) toluene as internal standard, DCE as solvent and heterogeneous catalyst (**c-P1-8**, 0.02 mmol Ti) at 6 hours (60 % conversion H<sub>2</sub>O<sub>2</sub>) at 60 °C

```

=====
Acq. Operator   :                               Seq. Line :   50
Acq. Instrument : 6890 GC                       Location  : Vial 49
Injection Date  : 6/21/2015 2:18:50 AM          Inj       :    3
                                                Inj Volume: 1 µl

Acq. Method    : C:\CHEM32\2\DATA\150619 2015-06-19 09-20-36\TBHP.M
Last changed   : 6/19/2015 9:20:32 AM
Analysis Method: C:\CHEM32\2\DATA\150526 2015-05-26 08-32-07\TBHP.M
Last changed   : 6/3/2015 12:40:28 PM
                (modified after loading)
Additional Info : Peak(s) manually integrated
    
```



=====  
 Area Percent Report  
 =====

```

Sorted By      :      Signal
Multiplier:    :      1.0000
Dilution:      :      1.0000
Use Multiplier & Dilution Factor with ISTDs
    
```

Signal 1: FID1 A,

Peak #	RetTime [min]	Type	Width [min]	Area [pA*s]	Height [pA]	Area %
1	3.277	MM	0.0735	1.53857e5	3.48794e4	76.76449
2	4.242	MM	0.0429	4.62443e4	1.79830e4	23.07285
3	4.992	MM	0.0160	326.00113	340.42172	0.16265

Totals :                                    2.00427e5  5.32028e4

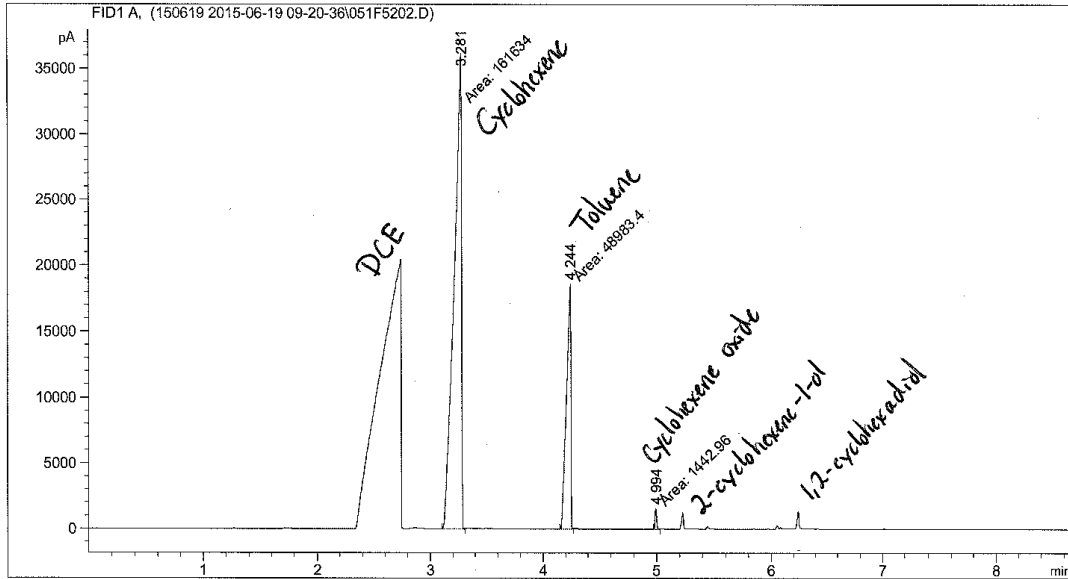


Figure A32. Typical GC chromatograph for epoxidation of cyclohexene (>45 mmol) using H<sub>2</sub>O<sub>2</sub> (2 mmol) toluene as internal standard, DCE as solvent and heterogeneous catalyst (**c-P1-8**, 0.02 mmol Ti) at 12 hours (100 % conversion H<sub>2</sub>O<sub>2</sub>) at 60 °C

```

=====
Acq. Operator   :                               Seq. Line : 52
Acq. Instrument : 6890 GC                       Location  : Vial 51
Injection Date  : 6/21/2015 4:03:43 AM          Inj       : 2
                                                    Inj Volume: 1 µl

Acq. Method     : C:\CHEM32\2\DATA\150619 2015-06-19 09-20-36\TBHP.M
Last changed    : 6/19/2015 9:20:32 AM
Analysis Method : C:\CHEM32\2\DATA\150526 2015-05-26 08-32-07\TBHP.M
Last changed    : 6/3/2015 12:40:28 PM
                (modified after loading)
Additional Info : Peak(s) manually integrated
    
```



Area Percent Report

```

Sorted By      :      Signal
Multiplier:    :      1.0000
Dilution:      :      1.0000
Use Multiplier & Dilution Factor with ISTDs
    
```

Signal 1: FID1 A,

Peak #	RetTime [min]	Type	Width [min]	Area [pA*s]	Height [pA]	Area %
1	3.281	MM	0.0735	1.61634e5	3.66336e4	76.22074
2	4.244	MM	0.0439	4.89834e4	1.85974e4	23.09881
3	4.994	MM	0.0158	1442.96216	1519.52661	0.68045

Totals : 2.12060e5 5.67506e4

## References:

- (1) Wada, K.; Hirabayashi, K.; Watanabe, N.; Yamamoto, S.; Kondo, T.; Mitsudo, T.-a.; Inoue, M. *Topics in Catalysis* **2009**, *52*, 693.
- (2) Chanda, M.; Roy, S. K. *Industrial Polymers, Specialty Polymers and Their Applications*; Taylor and Francis Group, 2007.
- (3) Dever, J. P.; George, K. F.; Hoffman, W. C.; Soo, H. *Kirk-Ottmer Encyclopedia of Chemical Technology*; 4th ed.
- (4) Solomons, T. W. G.; Fryhle, C. B. *Organic Chemistry*. ; 9th ed.; John Wiley & Sons, 2008.
- (5) Klein, D. *Organic Chemistry*; 2nd ed.; Wiley & Sons.
- (6) Smith, M. B.; March, J. *Advanced Organic Chemistry, Reaction, Mechanisms, and Structure*; 5th ed.; John Wiley & Sons, 2001.
- (7) Oyama, S. T. *Mechanisms in Homogeneous and Heterogeneous Epoxidation Catalysis* **2008**, *3*.
- (8) Schaus, S. E.; Brandes, B. D.; Larrow, J. F.; Tokumaga, M.; Hansen, K. B.; Gould, A. E.; Furrow, M. E.; Jacobsen, E. N. *Journal of the American Chemical Society* **2002**, *124*, 1307.
- (9) Udagawa, T.; Yuan, J.; Panigrahy, D.; Chang, Y.-H.; Shah, J.; D'Amato, R. J. *THE JOURNAL OF PHARMACOLOGY AND EXPERIMENTAL THERAPEUTICS* **2000**, *294*, 421.
- (10) Rowe, D. *Chemistry and Technology of Flavours and Fragrances*; Blackwell Publishing, 2005.
- (11) Organization, W. H. *Safety Evaluation of Certain Food Additives*; World Health Organization, 2006; Vol. 65.
- (12) Vicevic, M.; Boodhoo, K. V. K.; Scott, K. *Chemical Engineering Journal* **2007**, *133*, 43.
- (13) Denver, J. P.; George, K. F.; Hoffman, W. C.; Soo, H. In *Kirk-Othmer Encyclopedia of Chemical Technology*; Sons, J. W., Ed.; John Wiley & Sons: 2000.
- (14) Dever, J. P.; George, K. F.; Hoffman, W. C.; Soo, H. *Kirk-Ottmer Encyclopedia of Chemical Technology*; 4th ed.; John Wiley & Sons; Vol. 10.
- (15) Kollar, J.; to Halcon: 1967.
- (16) Adolfsson, H. *Modern Oxidation Methods*; Wiley and Sons, 2010.
- (17) Hauser, S. A.; Cokoja, M.; Kühn, F. E. *Catalysis Science & Technology* **2013**, *3*, 552.
- (18) Huber, S.; Cokoja, M.; Kühn, F. E. *Journal of Organometallic Chemistry* **2014**, *751*, 25.
- (19) Jorgensen, K. A. *Chemical Reviews* **1989**, *89*, 431.
- (20) Terfassa, B.; Schachner, J. A.; Traar, P.; Belaj, F.; Mösch Zanetti, N. C. *Polyhedron* **2014**, *75*, 141.
- (21) Xia, Q.-H.; Ge, H.-Q.; Ye, C.-P.; Liu, Z.-M.; Su, K.-X. *Chemical Reviews* **2005**, *105*, 1603.
- (22) Arnold, U. *Mechanisms in Homogeneous and Heterogeneous Epoxidation Catalysis* **2008**, 387.
- (23) Dinoi, C.; Ciclosi, M.; Manoury, E.; Maron, L.; Perrin, L.; Poli, R. *Chemistry* **2010**, *16*, 9572.
- (24) Rezaeifard, A.; Haddad, R.; Jafarpour, M.; Hakimi, M. *Journal of the American Chemical Society* **2013**, *135*, 10036.
- (25) Sousa, J. L. C.; Santos, I. C. M. S.; Simões, M. M. Q.; Cavaleiro, J. A. S.; Nogueira, H. I. S.; Cavaleiro, A. M. V. *Catalysis Communications* **2011**, *12*, 459.

- (26) Zhu, Y.; Wang, Q.; Cornwall, R. G.; Shi, Y. *Chem Rev* **2014**, *114*, 8199.
- (27) Chong, A. O.; Sharpless, K. B. *Journal of Organic Chemistry* **1977**, *42*, 1587.
- (28) Jarrais, B.; Pereira, C.; Silva, A. R.; Carvalho, A. P.; Pires, J.; Freire, C. *Polyhedron* **2009**, *28*, 994.
- (29) Pereira, C.; Leite, A.; Nunes, A.; Rebelo, S. L. H.; Rangel, M.; Freire, C. *Catalysis Letters* **2010**, *135*, 98.
- (30) Pereira, C.; Silva, J. F.; Pereira, A. M.; Araújo, J. P.; Blanco, G.; Pintado, J. M.; Freire, C. *Catalysis Science & Technology* **2011**, *1*, 784.
- (31) Abbenhuis, H. C. L.; Krijnen, S.; van Santen, R. A. *Chemical Communications* **1997**, 331.
- (32) Aish, E. H.; Crocker, M.; Ladipo, F. T. *Journal of Catalysis* **2010**, *273*, 66.
- (33) Antonova, N. S.; Carbo, J. J.; Kortz, U.; Kholdeeva, O. A.; Poblet, J. M. *J. AM. CHEM. SOC.* **2010**, *132*, 7488.
- (34) Beck, C.; Mallat, T.; Baiker, A. *Catalysis Letters* **2003**, *88*, 203.
- (35) Carmalt, C. J.; Peters, E. S.; Parkin, I. P.; Tocher, D. A. *New Journal of Chemistry* **2005**, *29*, 620.
- (36) Carniato, F.; Boccaleri, E.; Marchese, L. *Dalton transactions* **2008**, 36.
- (37) Cativiela, C.; Fraile, J. M.; Garcia, J. I.; Mayoral, J. A. *Journal of Molecular Catalysis A: Chemical* **1996**, *112*, 259.
- (38) Clerici, M. G.; Ingallina, P. *Journal of Catalysis* **1993**, *140*, 71.
- (39) Crocker, M.; Herold, R. H. M.; Orpen, A. G. *Chemical Communications* **1997**, 2411.
- (40) Crocker, M.; Herold, R. H. M.; Orpen, A. G.; Overgaag, M. T. A. *Journal of the Chemical Society, Dalton Transactions* **1999**, 3791.
- (41) do Carmo, D. R.; Filho, N. L. D.; Stradiotto, N. R. *Materials Research Bulletin* **2007**, *42*, 1811.
- (42) Fandos, R.; Gallego, B.; Otero, A.; Rodriguez, A.; Ruiz, M. J.; Terreros, P. *Dalton transactions* **2007**, 871.
- (43) Fraile, J.; Garcia, J.; Mayoral, J.; Vispe, E. *Journal of Catalysis* **2005**, *233*, 90.
- (44) Fraile, J. M.; García, J. I.; Mayoral, J. A.; Vispe, E.; Brown, D. R.; Naderi, M. *Chemical Communications* **2001**, 1510.
- (45) Giovenzana, T.; Guidotti, M.; Lucenti, E.; Orbelli Biroli, A.; Sordelli, L.; Sironi, A.; Ugo, R. *Organometallics* **2010**, *29*, 6687.
- (46) Gleeson, D.; Sankar, G.; Catlow, C. R. A.; Thomas, J. M.; Spanó, G.; Bordiga, S.; Zecchina, A.; Lamberti, C. *Physical Chemistry Chemical Physics* **2000**, *2*, 4812.
- (47) Jin, F.; Chen, S.-Y.; Jang, L.-Y.; Lee, J.-F.; Cheng, S. *Journal of Catalysis* **2014**, *319*, 247.
- (48) Katsuki, T.; Sharpless, K. B. *Journal of the American Chemical Society* **1980**, *102*, 5974.
- (49) Kumar, R.; Pais, G. C. G.; Pandey, B.; Kumar, P. *J. CHEM. SOC., CHEM. COMMUN.* **1995**, 1315.
- (50) Maschmeyer, T.; Klunduk, M. C.; Martin, C. M.; Shephard, D. S.; Johnson, B. F. G.; Maschmeyer, T.; Thomas, J. M. *Chemical Communications* **1997**, 1847.
- (51) Oldroyd, R. D.; Thomas, J. M.; Maschmeyer, T.; MacFaul, P. A.; Snelgrove, D. W.; Ingold, K. U.; Wayner, D. D. M. *Agnew. Chem. Int. Ed. Engl.* **1996**, *35*, 2787.
- (52) Pérez, Y.; Quintanilla, D. P.; Fajardo, M.; Sierra, I.; del Hierro, I. *Journal of Molecular Catalysis A: Chemical* **2007**, *271*, 227.

- (53) Pescarmona, P. P.; van der Waal, J. C.; Maschmeyer, T. *Catalysis Today* **2003**, *81*, 347.
- (54) Sakugawa, S.; Wada, K.; Inoue, M. *Journal of Catalysis* **2010**, *275*, 280.
- (55) Skowronska-Ptasinska, M. D.; Vorstenbosch, M. L. W.; van Santen, R. A.; Abbenhuis, H. C. L. *Angew. Chem. Int. Ed.* **2002**, *41*, 437.
- (56) Smet, P.; Riondato, J.; Pauwels, T.; Moens, L.; Verdonck, L. *Inorganic Chemistry Communications* **2000**, *3*, 557.
- (57) Urabe, H.; Sato, F. *Lewis Acids in Organic Synthesis* **2000**, 653.
- (58) Viotti, O.; Seisenbaeva, G. A.; Kessler, V. G. *Inorganic chemistry* **2009**, *48*, 9063.
- (59) Wada, K.; Watanabe, N.; Kondo, T.; Mitsudo, T.-a. *Chemical Engineering Science* **2008**, *63*, 4917.
- (60) Wang, Q.; Neudorfl, J. M.; Berkessel, A. *Chemistry* **2014**.
- (61) YAMAMOTO, Z. L. A. H. *Acc. Chem. Res.* **2013**, *46*, 506.
- (62) Zhang, L.; Abbenhuis, H. C.; Gerritsen, G.; Bhriain, N. N.; Magusin, P. C.; Mezari, B.; Han, W.; van Santen, R. A.; Yang, Q.; Li, C. *Chemistry* **2007**, *13*, 1210.
- (63) Grivani, G.; Tangestaninejad, S.; Habibi, M. H.; Mirkhani, V.; Moghadam, M. *Applied Catalysis A: General* **2006**, *299*, 131.
- (64) Kholdeeva, O. A. *European Journal of Inorganic Chemistry* **2013**, *2013*, 1595.
- (65) Nur, H.; Prasetyoko, D.; Ramli, Z.; Endud, S. *Catalysis Communications* **2004**, *5*, 725.
- (66) To, J.; Sherwood, P.; Sokol, A. A.; Bush, I. J.; Catlow, C. R. A.; van Dam, H. J. J.; French, S. A.; Guest, M. F. *Journal of Materials Chemistry* **2006**, *16*, 1919.
- (67) Xu, L.; Ren, Y.; Wu, H.; Liu, Y.; Wang, Z.; Zhang, Y.; Xu, J.; Peng, H.; Wu, P. *Journal of Materials Chemistry* **2011**, *21*, 10852.
- (68) Zhan, G.; Du, M.; Huang, J.; Li, Q. *Catalysis Communications* **2011**, *12*, 830.
- (69) R. Hutter, T. M., D. Dutoit and A. Baiker *Topics in Catalysis* **1996**, *3*, 421.
- (70) Muller, C. A.; Maciejewski, M.; Mallat, T.; Baiker, A. *Journal of Catalysis* **1999**, *184*, 280.
- (71) Nishimura, N.; Tanikawa, J.; Fujii, M.; Kawahara, T.; Ino, J.; Akita, T.; Fujino, T.; Tada, H. *Chemical Communications* **2008**, 3564.
- (72) Srour, H.; Le Maux, P.; Simonneaux, G. *Inorganic chemistry* **2012**, *51*, 5850.
- (73) Wortmann, R.; Flörke, U.; Sarkar, B.; Umamaheshwari, V.; Gescheidt, G.; Herres-Pawlis, S.; Henkel, G. *European Journal of Inorganic Chemistry* **2011**, *2011*, 121.
- (74) Lane, B. S.; Burgess, K. *Chemical Reviews* **2003**, *103*, 2457.
- (75) Trach, Y. B.; Makota, O. I. *International Journal of Chemical Kinetics* **2009**, *41*, 623.
- (76) Schmidt, A.; Grover, N.; Zimmermann, T. K.; Graser, L.; Cokoja, M.; Pöthig, A.; Kühn, F. E. *Journal of Catalysis* **2014**, *319*, 119.
- (77) Trach, Y. B.; Nikipanchuk, M. V.; Komarenskaya, Z. M. *Kinetics and Catalysis* **2004**, *45*, 504.
- (78) Trach, Y. B.; Makota, O. I. *Theoretical and Experimental Chemistry* **2002**, *38*, 250.
- (79) Burke, A. J. *Coordination Chemistry Reviews* **2008**, *252*, 1770.
- (80) Kanai, H.; Okumurab, Y.; Utani, K.; Hamadac, K.; Imamurab, S. *Catalysis Letters* **2001**, *76*, 207.
- (81) Cusso, O.; Garcia-Bosch, I.; Ribas, X.; Lloret-Fillol, J.; Costas, M. *Journal of the American Chemical Society* **2013**, *135*, 14871.
- (82) Rose, E.; Andrioletti, B.; Zrig, S.; Quelquejeu-Etheve, M. *Chemical Society reviews* **2005**, *34*, 573.

- (83) Ghorbanloo, M.; Monfared, H. H.; Janiak, C. *Journal of Molecular Catalysis A: Chemical* **2011**, *345*, 12.
- (84) Buijink, J. F. K.; van Vlaanderen, J. J. M.; Crocker, M.; Niele, F. G. M. *Catalysis Today* **2004**, 93.
- (85) Prasetyokoa, D.; Ramli, Z.; Enduda, S.; Nur, H. *React. Kinet. Catal. Lett.* **2005**, *86*, 83.
- (86) Prasetyoko, D.; Fansuri, H.; Ramli, Z.; Endud, S.; Nur, H. *Catalysis Letters* **2008**, *128*, 177.
- (87) Donoeva, B. G.; Trubitsina, T. A.; Antonova, N. S.; Carbó, J. J.; Poblet, J. M.; Al-Kadamany, G.; Kortz, U.; Kholdeeva, O. A. *European Journal of Inorganic Chemistry* **2010**, *2010*, 5312.
- (88) Dusi, M.; Mallat, T.; Baiker, A. *Journal of Molecular Catalysis A: Chemical* **1999**, *138*, 15.
- (89) Beck, C.; Mallat, T.; Baiker, A. *Catalysis Letters* **2001**, *75*, 131.
- (90) Murugavel, R.; Roesky, H. W. *Angew. Chem. Int. Ed. Engl.* **1997**, *36*, 477.
- (91) Melero, J. A.; Iglesias, J.; Arsuaga, J. M.; Sainz-Pardo, J.; de Frutos, P.; Blazquez, S. *Journal of Materials Chemistry* **2007**, *17*, 377.
- (92) Adam, W.; Corma, A.; García, H.; Weichold, O. *Journal of Catalysis* **2000**, *196*, 339.
- (93) Mostafa, S. I.; Ikeda, S.; Ohtani, B. *Journal of Molecular Catalysis A: Chemical* **2005**, *225*, 181.
- (94) Haddad, T. S.; Viers, B. D.; Phillips, S. H. *Journal of Inorganic and Organometallic Polymers* **2001**, *11*, 155.
- (95) Kudo, T.; Gordon, M. S. *J. Phys. Chem. A* **2001**, *105*, 11276.
- (96) Feher, F. J.; Soulivong, D.; Lewis, G. T. *Journal of the American Chemical Society* **1997**, *119*, 11323.
- (97) Feher, F. J.; Soulivong, D.; Eklund, A. G. *Chem. Commun.* **1998**, 399.
- (98) Feher, F. J.; Terroba, R.; Ziller, J. W. *Chem. Commun.* **1999**, 2153.
- (99) Feher, F. J.; Terroba, R.; Ziller, J. W. *Chem. Commun.* **1999**, 2309.
- (100) Guo, X.; Wang, W.; Liu, L. *Polymer Bulletin* **2009**, *64*, 15.
- (101) Pescarmona, P. P.; van der Waal, J. C.; Maschmeyer, T. *Chemistry* **2004**, *10*, 1657.
- (102) Feher, F. J.; Budzichowski, T. A. *Polyhedron* **1995**, *14*, 3239.
- (103) Wang, Y.; Magusin, P.; Vansanten, R.; Abbenhuis, H. *Journal of Catalysis* **2007**, *251*, 453.
- (104) Carniato, F.; Bisio, C.; Sordelli, L.; Gavrilova, E.; Guidotti, M. *Inorganica Chimica Acta* **2012**, *380*, 244.
- (105) Mwangi, M. T.; Runge, M. B.; Bowden, N. B. *J. AM. CHEM. SOC. COMM.* **2006**, *128*, 14434.
- (106) Rubinsztajn, S. *Journal of Inorganic and Organometallic Polymers* **1994**, *4*, 61.
- (107) Si, Q.-F.; Wang, X.; Fan, X.-D.; Wang, S.-J. *Journal of Polymer Science Part A: Polymer Chemistry* **2005**, *43*, 1883.
- (108) Waddams, A. L. *Chemicals from Petroleum: an Introductory Survey. 4th Ed* **1978**, 101.
- (109) Denver, J. P.; George, K. F.; Hoffman, W. C.; Soo, H. *Kirk-Othmer Encycl. Chem. Technol. (5th Ed.)* **2005**, 632.
- (110) Sheldon, R. A.; Van Vliet, M. C. *Fine Chem. Heterog. Catal.* **2001**, 473.
- (111) Bradley, C. A.; McMurdo, M. J.; Tilley, T. D. *J. Phys. Chem. C* **2007**, *111*, 17570.

- (112) Raboin, L.; Yano, J.; Tilley, T. D. *Journal of Catalysis* **2012**, *285*, 168.
- (113) Boudjema, S.; vispe, E.; Choukchou-Brahm, A.; Mayoral, J. A.; Bachir, R.; Fraile, J. M. *RSC Adv.* **2015**, 6853.
- (114) Linic, S.; Barteau, M. A. *Handb. Heterog. Catal. (2nd Ed.)* **2008**, 3448.
- (115) Taramasso, M.; Perego, G.; Notari, B.; Enichem, Ed. 1983; Vol. 4,410,501.
- (116) Millini, R.; Massara, E. P.; Perego, G.; Bellussi, G. *Journal of Catalysis* **1992**, *137*, 497.
- (117) Wattimena, F.; Wulff, H. P.; Oil, S., Ed. Britan, 1971; Vol. 1,249,079.
- (118) Tuel, A.; Hubert-Pfalzgraf, L. G. *Journal of Catalysis* **2003**, 343.
- (119) Yuan, Q.; Hagen, A.; Rossner, F. *Applied Catalysis A: General* **2006**, *303*, 81.
- (120) Capel-Sanchez, M. C.; Campos-Martin, J. M.; Fierro, J. L. G.; de Frutos, M. P.; Polo, A. P. *Chemical Communications* **2000**, 855.
- (121) Krijnen, S.; Abbenhuis, H. C. L.; Hanssen, R. W. J. M.; Van Hooff, J. H. C.; Van Santen, R. A. *Agnew. Chem. Int. Ed. Engl.* **1998**, *37*, 356.
- (122) Muzafarov, A. M.; Golly, M.; Moeller, M. *Macromolecules* **1995**, *28*, 8444.
- (123) Herzig, C.; Deubzer, B. *Polym. Prepr. (Am. Chem. Soc., Div. Polym. Chem.)* **1998**, *39*, 477.
- (124) Lang, H.; Luhmann, B. *Adv. Mater. (Weinheim, Ger.)* **2001**, *13*, 1523.
- (125) Interrante, L. V.; Li, J.; Lu, N. *Polym. Prepr. (Am. Chem. Soc., Div. Polym. Chem.)* **2004**, *45*, 589.
- (126) Armarego, W. L. F.; Perrin, D. D. *Purification of Laboratory Chemicals, Fourth Edition*, 1997.
- (127) Feher, F. J.; Budzichowski, T. A.; Rahimian, K.; Ziller, J. W. *J. Am. Chem. Soc.* **1992**, *114*, 3859.
- (128) Buys, I. E.; Hambley, T. W.; Houlton, D. J.; Maschmeyer, T.; Masters, A. F.; Smith, A. K. *J. Mol. Catal.* **1994**, *86*, 309.
- (129) Fan, W.; Wu, P.; Tatsumi, T. *J. Catal.* **2008**, *256*, 62.
- (130) Buijink, J. K. F.; van Vlaanderen, J. J. M.; Crocker, M.; Niele, F. G. M. *Catal. Today* **2004**, *93-95*, 199.
- (131) Wattimena, F.; Wulff, H. P.; (Shell Internationale Research Maatschappij N. V.). Application: DE  
DE, 1970, p 44 pp.
- (132) Adam, W.; Corma, A.; Garcia, H.; Weichold, O. *J. Catal.* **2000**, *196*, 339.
- (133) Sheldon, R. A.; Van Doorn, J. A. *J. Catal.* **1973**, *31*, 427.
- (134) Arends, I. W. *Angewandte Chemie* **2006**, *45*, 6250.
- (135) Davis, P.; Murugavel, R. *Synthesis and Reactivity in Inorganic, Metal-Organic, and Nano-Metal Chemistry* **2005**, *35*, 591.
- (136) Chiker, F.; Launay, F.; Nogier, J. P.; Bonardet, J. L. *Green Chemistry* **2003**, *5*, 318.
- (137) Guidotti, M.; Batonneau-Gener, I.; Gianotti, E.; Marchese, L.; Mignard, S.; Psaro, R.; Sgobba, M.; Ravasio, N. *Microporous and Mesoporous Materials* **2008**, *111*, 39.
- (138) D.H. Wells, J.; Delgass, W. N.; Thomson, K. T. *Journal of the American Chemical Society* **2004**, *126*, 2956.
- (139) Limberg, C. *Angewandte Chemie* **2003**, *42*, 5932.
- (140) Lousada, C. M.; Johansson, A. J.; Brinck, T.; Jonsson, M. *The Journal of Physical Chemistry C* **2012**, *116*, 9533.
- (141) Teshima, N.; Genfa, Z.; Dasgupta, P. K. *Analytica Chimica Acta* **2004**, *510*, 9.
- (142) Plotkin, J. S. *Propylene Oxide. Process Technology*, Nexant, 2009.

- (143) Huang, J.; Haruta, M. *Research on Chemical Intermediates* **2011**, *38*, 1.
- (144) Joshi, A. M.; Taylor, B.; Cumararatunge, L.; Thomson, K. T.; Nicholas Delgass, W. **2008**, 315.
- (145) Nijhuis, T.; Gardner, T.; Weckhuysen, B. *Journal of Catalysis* **2005**, *236*, 153.
- (146) Rocha, T. C. R.; Hävecker, M.; Knop-Gericke, A.; Schlögl, R. *Journal of Catalysis* **2014**, *312*, 12.
- (147) Stangland, E. E.; Stavens, K. B.; Andres, R. P.; Delgass, W. N. *Journal of Catalysis* **2000**, *191*, 332.
- (148) Stangland, E. E.; Taylor, B.; Andres, R. P.; Delgass, W. N. *J. Phys. Chem. B* **2005**, *109*, 2321.
- (149) Smart, L. E.; Moore, E. A. *Solid State Chemistry*, 2005.
- (150) Sanchez, A.; Abbet, S.; Heiz, U.; Schneider, W. D.; Hakkinen, H.; Barnett, R. N.; Landman, U. *J. Phys. Chem. A* **1999**, *103*, 9573.
- (151) Boronat, M.; Concepcion, P.; Corma, A. *J. Phys. Chem. C* **2009**, *113*, 16772.
- (152) Pina, C. D.; Falletta, E.; Prati, L.; Rossi, M. *Chemical Society reviews* **2008**, *37*, 2077.
- (153) Edwards, J. K.; Solsona, B.; Landon, P.; Carley, A. F.; Herzing, A.; Watanabe, M.; Kiely, C. J.; Hutchings, G. J. *Journal of Materials Chemistry* **2005**, *15*, 4595.
- (154) Gaudet, J.; Bando, K. K.; Song, Z.; Fujitani, T.; Zhang, W.; Su, D. S.; Oyama, S. T. *Journal of Catalysis* **2011**, *280*, 40.
- (155) Huang, J.; Lima, E.; Akita, T.; Guzmán, A.; Qi, C.; Takei, T.; Haruta, M. *Journal of Catalysis* **2011**, *278*, 8.
- (156) Landon, P.; Collier, P. J.; Papworth, A. J.; Kiely, C. J.; Hutchings, G. J. *Chemical Communications* **2002**, 2058.
- (157) Laursen, A. B.; Man, I. C.; Trinhammer, O. L.; Rossmeisl, J.; Dahl, S. *Journal of Chemical Education* **2011**, *88*, 1711.
- (158) Ojeda, M.; Iglesia, E. *Chemical Communications* **2009**, 352.
- (159) Wang, Y.-g.; Wang, J.-g. *Catalysis Letters* **2012**, *142*, 601.
- (160) Pritchard, J. C.; He, Q.; Ntainjua, E. N.; Piccinini, M.; Edwards, J. K.; Herzing, A. A.; Carley, A. F.; Moulijn, J. A.; Kiely, C. J.; Hutchings, G. J. *Green Chemistry* **2010**, *12*, 915.
- (161) Nijhuis, T.; Sacaliuc, E.; Beale, A.; Vandereerden, A.; Schouten, J.; Weckhuysen, B. *Journal of Catalysis* **2008**, *258*, 256.
- (162) Haruta, M.; Kawahara, J. *Mechanisms in Homogeneous and Heterogeneous Epoxidation Catalysis* **2008**, 297.
- (163) D.H. Wells, J.; Delgass, W. N.; Thomson, K. T. *Journal of Catalysis* **2004**, *225*, 69.
- (164) Nijhuis, T.; Weckhuysen, B. *Catalysis Today* **2006**, *117*, 84.
- (165) Sacaliucparvulescu, E.; Friedrich, H.; Palkovits, R.; Weckhuysen, B.; Nijhuis, T. *Journal of Catalysis* **2008**, *259*, 43.
- (166) Uphade, B. S.; Okumura, M.; Tsubota, S.; Haruta, M. *Applied Catalysis A: General* **2000**, *190*, 43.
- (167) Bowker, M. *The Basis and Applications of Heterogeneous Catalysis*; Oxford University Press Inc.: New York, 1998.
- (168) Sinhaa, A. K.; Seelana, S.; Tsubotaa, S.; Harutab, M. *Topics in Catalysis* **2004**, *29*, 95.
- (169) Lee, W.-S.; Cem Akatay, M.; Stach, E. A.; Ribeiro, F. H.; Nicholas Delgass, W. *Journal of Catalysis* **2014**, *313*, 104.
- (170) Nijhuis, T. A.; Sacaliuc-Parvulescu, E.; Govender, N. S.; Schouten, J. C.; Weckhuysen, B. M. *Journal of Catalysis* **2009**, *265*, 161.

- (171) Qi, C.; Akita, T.; Okumura, M.; Haruta, M. *Applied Catalysis A: General* **2001**, *218*, 81.
- (172) Mul, G.; Zwijnenburg, A.; van der Linden, B.; Makkee, M.; Moulijn, J. A. *Journal of Catalysis* **2001**, *201*, 128.
- (173) Nijhuis, T. A.; Huizinga, B. J.; Makkee, M.; Moulijn, J. A. *Ind. Eng. Chem. Res.* **1999**, *38*, 884.
- (174) Taylor, B.; Lauterbach, J.; Blau, G.; Delgass, W. *Journal of Catalysis* **2006**, *242*, 142.
- (175) Liu, T.; Hacıoğlu, P.; Oyama, S. T.; Luo, M.-F.; Pan, X.-R.; Lu, J.-Q. *Journal of Catalysis* **2009**, *267*, 202.
- (176) Wells, J., David H.; Joshi, A. M.; Delgass, W. N.; Thomson, K. T. *J. Phys. Chem. B* **2006**, *110*, 14627.
- (177) Sacaliuc, E.; Beale, A.; Weckhuysen, B.; Nijhuis, T. *Journal of Catalysis* **2007**, *248*, 235.
- (178) Kapoor, M. P.; Sinha, A. K.; Seelan, S.; Inagaki, S.; Tsubota, S.; Yoshida, H.; Haruta, M. *Chemical Communications* **2002**, 2902.
- (179) Uphade, B. *Journal of Catalysis* **2002**, *209*, 331.
- (180) Qi, C.; Huang, J.; Bao, S.; Su, H.; Akita, T.; Haruta, M. *Journal of Catalysis* **2011**, *281*, 12.
- (181) Chen, J.; Halin, S. J. A.; Ferrandez, D. M. P.; Schouten, J. C.; Nijhuis, T. A. *Journal of Catalysis* **2012**, *285*, 324.
- (182) Lee, W.-S.; Zhang, R.; Akatay, M. C.; Baertsch, C. D.; Stach, E. A.; Ribeiro, F. H.; Delgass, W. N. *ACS Catalysis* **2011**, *1*, 1327.
- (183) Chowdhury, B.; Bravo-Suarez, J. J.; Date, M.; Tsubota, S.; Haruta, M. *Angewandte Chemie* **2006**, *45*, 412.
- (184) Sinha, A. K.; Seelan, S.; Tsubota, S.; Haruta, M. *Angewandte Chemie* **2004**, *43*, 1546.
- (185) Mennemann, C.; Claus, P. *Catalysis Letters* **2009**, *134*, 31.
- (186) Lu, J.; Zhang, X.; Bravo-Suárez, J. J.; Fujitani, T.; Oyama, S. T. *Catalysis Today* **2009**, *147*, 186.
- (187) Nijhuis, T. A.; Weckhuysen, B. M. *Chemical Communications* **2005**, 6002.
- (188) Huang, J.; Akita, T.; Faye, J.; Fujitani, T.; Takei, T.; Haruta, M. *Angewandte Chemie* **2009**, *48*, 7862.
- (189) Llorca, J.; Dominguez, M.; Ledesma, C.; Chimentao, R. J.; Medina, F.; Jesus, S.; Angurell, I.; Seco, M.; Rossell, O. *Journal of Catalysis* **2008**, *258*, 187.
- (190) T. Alexander Nijhuis, T. V., and Bert M. Weckhuysen *J. Phys. Chem. B* **2005**, *109*, 19309.
- (191) Love, J. C.; Estroff, L. A.; Kriebel, J. K.; Nuzzo, R. G.; Whitesides, G. M. *Chemical Society reviews* **2005**, *105*, 1103.
- (192) Xue, Y.; Li, X.; Li, H.; Zhang, W. *Nature communications* **2014**, *5*, 4348.
- (193) Hakkinen, H. *Nature Chemistry* **2010**, *4*, 443.
- (194) Choudhary, T. V.; Goodman, D. W. *Topics in Catalysis* **2002**, *21*, 25.
- (195) Nijhuis, T. A.; Visser, T.; Weckhuysen, B. M. *Journal of Physical Chemistry, B* **2005**, *109*, 19309.
- (196) Ruiz, A.; van der Linden, B.; Makkee, M.; Mul, G. *Journal of Catalysis* **2009**, *266*, 286.
- (197) Zwijnenburg, A.; Goossens, A.; Sloof, W. G.; Craje, M. W. J.; van der Kraan, A. M.; de Jongh, L. J.; Makkee, M.; Moulijn, J. A. *J. Phys. Chem. B* **2002**, *106*, 9853.



(198) Chowdhury, B.; Bando, K. K.; Bravo-Suárez, J. J.; Tsubota, S.; Haruta, M. *Journal of Molecular Catalysis A: Chemical* **2012**, *359*, 21.

(199) Joshi, A. M.; Delgass, W. N.; Thomson, K. T. *Journal of Physical Chemistry Letters, C* **2007**, *111*, 7841.

## **Vita**

**Sarah Michelle Peak**

### **Personal Information**

Place of Birth: Frankfort, KY U.S.A.

### **Education**

Georgetown College

Georgetown, KY U.S.A.

Bachelor of Science Degree in Chemistry (2008)

Eastern Kentucky University

Richmond, KY U.S.A.

Master of Science Degree in Chemistry (2010)

Thesis—"Synthesis of fused ring thiophens for the use in electronic devices"

University of Kentucky

Lexington, KY U.S.A.

Doctoral studies (2010-2015)

Advisor: Dr. Folami Ladipo

### **Awards and Scholarships**

Outstanding Thesis for Eastern Kentucky University (2010)

University of Kentucky Teaching Assistantship (2010-2011 & 2014-2015)

University of Kentucky Research Assistantship (2011-2014)

Eastern Kentucky Teaching Assistantship (2008-2010)

Tutor, University of Kentucky (2010-2015)

## **Publications**

Sarah M. Peak, Mark Crocker, Folami T. Ladipo. *ACS Catalysis*, Submitted.

Nathan C. Tice, Sarah M. Peak, Benjamin T. Cannon, Ethan S. Laha, Eli G. Estes, Chad A. Snyder & Sean Parkin. The synthesis, characterization, and structure of a series of 4*H*-thieno[3,4-*c*]pyrroles and their corresponding pyrrolium cyanoborohydride salts. *Journal of Sulfur Chemistry*, **2014**, 35, 596-605

Nathan C. Tice, Sarah M. Peak, & Sean Parkin. The unexpected formation and structure of 4,6-dimethylthieno[3,4-*c*]thiophene-1(3*H*)-thione. *Heterocycles*, **2010**, 81, 2229-2237

Nathan C. Tice, Sarah M. Peak, & Sean Parkin. Synthesis and structure of 5,7-dimethylthieno[3,4-*d*]pyridazine. *Heterocycles*, **2010**, 81, 1631-1639

## **Conference Proceedings**

“Tripodal titanium silsesquioxanes: Selective catalysts for alkene epoxidation using hydrogen peroxide.” ACS National Conference. Denver, CO March 26, 2015

“Tripodal titanium silsesquioxanes: Selective catalysts for alkene epoxidation.” SERMACS Conference, Nashville, TN October 16, 2014

“Tripodal titanium silsesquioxanes: Selective catalysts for alkene epoxidation.” Tri-State Catalysis Symposium. Louisville, KY September 15, 2014

“Tripodal titanium silsesquioxanes: Selective catalysts for alkene epoxidation using hydrogen peroxide.” ACS National Conference. Dallas, TX March 19, 2014